

**Electrochemical Noise Monitoring of AISI Type 304L  
Stainless Steel for Nuclear Reprocessing and Waste  
Storage Applications**

*By*

**Girija Suresh**

**(Enrollment No: ENGG02200804018)  
Indira Gandhi Centre for Atomic Research,  
Kalpakkam 603 102, INDIA**

*A thesis submitted to the*  
**Board of Studies in Engineering Sciences**

*In partial fulfillment of requirements  
For the Degree of*

**DOCTOR OF PHILOSOPHY**

*of*

**Homi Bhabha National Institute**



April, 2014

**Electrochemical Noise Monitoring of AISI Type 304L  
Stainless Steel for Nuclear Reprocessing and Waste  
Storage Applications**

*A thesis submitted to the  
Board of Studies in Engineering Sciences  
Homi Bhabha National Institute (HBNI)  
In partial fulfillment of requirement  
for the Degree of*

**DOCTOR OF PHILOSOPHY**

**in**

**Engineering Sciences**

*By*

**Girija Suresh**

**Enrollment No: ENGG02200804018**

**Indira Gandhi Centre for Atomic Research**

**Research Supervisor**

**Prof. Dr. U. Kamachi Mudali**

**Associate Director, Corrosion Science and Technology Group,**

**Head, Reprocessing Research and Development Division,**

**Indira Gandhi Centre for Atomic Research**

**Kalpakkam-603102, India**

# Homi Bhabha National Institute

## Recommendations of the Viva Voce Board

As members of the Viva Voce Board, we certify that we have read the dissertation prepared by **Mrs. GIRIJA SURESH** entitled “**Electrochemical Noise Monitoring of AISI Type 304L Stainless Steel for Nuclear Reprocessing and Waste Storage Applications**” and recommend that it may be accepted as fulfilling the dissertation requirement for the Degree of Doctor of Philosophy.



Date: 20.2.2015

Chairman – **Dr. B.P.C. Rao**



Date: 20.2.2015

Guide / Convener – **Prof. U. Kamachi Mudali**



Date : 20.2.2015

Member 1 – **Dr. S. Rangarajan**



Date: 20.2.2015

Member 2 – **Dr. C. Mallika**




Date: 20.2.2015

Examiner - **Prof. V.S. Raja**

Final approval and acceptance of this dissertation is contingent upon the candidate's submission of the final copies of the dissertation to HBNI.

I hereby certify that I have read this dissertation prepared under my direction and recommend that it may be accepted as fulfilling the dissertation requirement.



Date : 20-2-2015

**Prof. U. Kamachi Mudali**

Place: Kalpakkam

**Supervisor and Convener**

## STATEMENT BY AUTHOR

---

This dissertation has been submitted in partial fulfillment of requirements for an advanced degree at Homi Bhabha National Institute (HBNI) and is deposited in the Library to be made available to borrowers under rules of the HBNI.

Brief quotations from this dissertation are allowable without special permission, provided that accurate acknowledgement of source is made. Requests for permission for extended quotation from or reproduction of this manuscript in whole or in part may be granted by the Competent Authority of HBNI when in his or her judgment the proposed use of the material is in the interests of scholarship. In all other instances, however, permission must be obtained from the author.



**(Girija Suresh)**



## DECLARATION

---

I, hereby declare that the investigation presented in this thesis entitled “**Electrochemical Noise Monitoring of AISI Type 304L Stainless Steel for Nuclear Reprocessing and Waste Storage Applications**” submitted to **Homi Bhabha National Institute (HBNI)**, Mumbai, India, for the award of **Doctor of Philosophy in Engineering Sciences** is the record of work carried out by me under the guidance of **Prof. U. Kamachi Mudali**. The work is original and has not been submitted earlier as a whole or in part for a degree /diploma at this or any other Institution/ University.



**(Girija Suresh)**

*Dedicated To...*

*My Sons*

*S.Ashish & S.Anish*

## ACKNOWLEDGEMENT

---

Foremost, I would like to express my sincere gratitude and thanks to my mentor and research guide, **Prof. Dr. U.Kamachi Mudali**, Associate Director, Corrosion Science and Technology Group, Indira Gandhi Centre for Atomic Research, for his valuable guidance, scholarly inputs, unconditional support and consistent encouragement throughout the research work. I consider it as a great opportunity to do my doctoral programme under his guidance and to learn from his research expertise.

I acknowledge with sincere thanks **Dr. P.R. Vasudeva Rao**, Director, IGCAR for the academic support, direction, and the facilities provided to carry out the research work. Words of gratitude are due for **Dr. T. Jayakumar**, Dean, HBNI-IGCAR and Director, Metallurgy & Materials Group for the immense support, positive disposition, valuable suggestions and encouragement especially during the course work and at various phases of the research work, which has made this feat possible.

I take this opportunity to express my sincere thanks to the doctoral committee members **Dr.B.P.C.Rao** (Chairman), **Dr. S.Rangarajan** (Member) and **Dr.C.Mallika** (Member) for the valuable evaluation, inspiration and timely suggestions which helped to improvise the research work. My sincere thanks are also due to **Dr. M. Sai Baba**, Associate Director, Resources Management Group and Convener, Engineering Sciences Standing Committee and all the faculty members of Homi Bhabha National Institute, for the informative lectures and support rendered during the course work.

My sincere and heartfelt gratitude is extended to **Dr.G.Sasikala**, Head, MMS, MTD, Dean, Academic, Engineering Sciences, HBNI for all the support rendered.

I would like to pay my high regards and gratitude to **Dr.N.Parvathavarthini, CSTG** for the valuable scientific discussions, affection, moral support, blessings and encouragement that helped in successful and timely completion of the thesis.

I wish to extend my sincere thanks to **Dr.M.G.Pujar, CSTG**, for the valuable discussions, timely help and words of encouragement and support during the course of my research work.

I am grateful to **Dr.S.Ningshen, CSTG**, for the help, direction and encouragement rendered for the successful presentation of the thesis. I take this opportunity to extend a special thanks to **Mr.A.Ravishankar, CSTG**, for the valuable discussions, kind help and support during the period of course work, comprehensive viva, synopsis and thesis presentation.

I wish to extend my deep sense of thanks and gratitude to **Mr.T.Nandakumar, CSTG**, for all the support rendered throughout the period of research work.

I acknowledge **all colleagues of CSTG** and all my good friends and well wishers, for the encouragement and help at various phases of the research work. Words are short to express my deep sense of gratitude to my friends, **Mr.Marriappan (MTD), Mrs.B.Sasi (NDED), Mr.Sivakumar (MPD), Mrs.Prasanthi (PMG), Mrs.S.Kalavathi (CMPD), Mrs.S.Sumathi (WSCD)** for the valuable discussions during course work and research work.

I am indebted to my husband, **Dr. A.Suresh**, and my two sons, **S.Ashish and S.Anish**, whose prayers, patience, sacrifice, perseverance and support helped me sail through challenging tasks, especially during the course work, and made my dream come true. I'm indebted to my sons for sacrificing their precious time of care and guidance I should have

given, during their crucial stages of education. I sincerely thank lord almighty for blessing me with an excellent family. My thanks are due to my **late father-in-law**, my **mother-in-law**, **sisters-in-law**, **brother-in-law** and their spouses for their prayers and support. I take this opportunity to thank my **brothers** and my **sister** for the care, affection and prayers that helped me get going. Not the least, I thank their spouses for all their help and care.

Most importantly, I would extend my deepest debt of gratitude to my late mother, **Mrs.P.N.Malathy** and my late father, **Mr. I.R.Narayanan Pillai** for being with me all through. Above all, I thank Lord almighty, for the all time blessings that has helped me accomplish my goal.

# **CONTENTS**

	<b>Page Number</b>
I Synopsis	i
II List of figures	xvii
III List of tables	xxv
IV List of abbreviation	xxvii

1

## **CHAPTER 1**

### **Introduction and Literature Review**

1.1 Indian Nuclear Energy Programme: The three stage	1
1.2 Backend of the nuclear fuel cycle	3
1.3 Materials for reprocessing	6
1.4 Materials for storage of high level liquid waste	8
1.4.1 Development of materials for high level liquid waste storage	9
1.5 Corrosion monitoring	11
1.5.1 Limitations of conventional techniques	15
1.5.2 Advantage of electrochemical noise technique	16
1.6 Electrochemical noise monitoring in nuclear waste storage tanks - International experience	17
1.6.1 Hanford Site	18
1.6.2 Savannah river site (SRS)	19
1.6.3 Oak Ridge National Laboratory (ORNL)	20
1.6.4 Idaho National Engineering & Environmental Laboratory (INEEL)	20
1.7 Types of Noise	20
1.8 Electrochemical noise : defenitions & literature review	22
1.8.1 Random process	22
1.8.2 Electrochemical noise – Definition	23

1.8.2.1	Electrochemical potential noise	23
1.8.2.2	Electrochemical current noise	24
1.8.3	How potential and current noises emerge ?	24
1.8.4	Sources of electrochemical noise	24
1.8.5	Cell Configuration	26
1.8.6	Measurement of Electrochemical Noise	28
1.8.6.1	Individual measurement of current or potential noise	28
1.8.6.2	Simultaneous measurement of potential and current noise	29
1.8.7	Data Collection	29
1.8.7.1	Sampling and aliasing	29
1.8.7.2	Antialiasing Filtering	30
1.8.8	Data treatment	31
1.8.9	Data Analysis	33
1.8.9.1	Visual examination of the time record	33
1.8.9.2	Data analysis in the time domain (statistical analysis)	34
1.8.9.3	Data analysis in the frequency domain (spectral analysis)	38
1.8.9.4	Autocorrelation function (ACF)	45
1.8.9.5	Chaos methods	45
1.8.9.6	Shot noise analysis	46
1.8.9.7	Wavelets to study electrochemical noise transients	47
1.9	Electrochemical noise investigations – a brief review	51

## 2. **CHAPTER 2**

### **Materials and experimental details**

2.1	Chemical composition of the materials used	63
2.2	Solution preparation	64
2.3	Heat treatments	67
2.3.1	Solution annealing and sensitization	67
2.3.2	Forging and rolling heat treatments	68

2.4 Specimen preparation	68
2.4.1 Specimen preparation for electrochemical potentiodynamic polarization Studies	68
2.4.2 Specimen preparation for electrochemical noise studies in nitric acid and Simulated high level waste medium	69
2.4.3 Specimen preparation for electrochemical noise studies in chloride medium	70
2.5 Oxalic acid etching and microstructural evaluation	71
2.6 Potentiodynamic anodic polarization experiments	71
2.6.1 Potentiodynamic anodic polarization in nitric acid medium and simulated HLW	74
2.6.2 Pitting corrosion studies in 0.5 M NaCl	74
2.6.3 Double loop electrochemical potentiokinetic reactivation (DL-EPR) test	75
2.7 Passive film analysis by Laser Raman Spectroscopy	75
2.7.1 Potentiostatic anodic polarization	75
2.7.2 Laser Raman Spectroscopy (LRS)	76
2.8 Electrochemical noise measurements	76
2.8.1 Data treatment and analysis	79
2.8.1.1 Correction for potential noise from pseudoreference Electrode	80
2.8.1.2 Data Analysis	81



**Electrochemical noise monitoring during pitting corrosion of 304L SS**

3.1	Introduction	87
3.2	Electrochemical noise monitoring during pitting corrosion of 304L stainless steel	88
3.2.1	Time domain and power spectra	88
3.2.2	Statistical analysis	93
3.2.3	Wavelet analysis	98
3.3	Conclusions	103

**Electrochemical noise monitoring of 304L SS in nitric acid and simulated nuclear high level waste medium**

4.1	Introduction	106
4.2	Microstructure evaluation and DL-EPR test	107
4.3	Electrochemical noise monitoring of 304L SS in nitric acid medium	109
4.3.1	Electrochemical noise time record	109
4.3.2	Electrochemical noise resistance	114
4.4	Electrochemical noise monitoring of 304L SS in simulated high level waste	119
4.4.1	Electrochemical noise time record	119
4.4.2	Electrochemical noise resistance	127
4.5	Post experimental optical microstructures	130
4.6	Conclusions	132

**Effect of nitrogen on corrosion behavior of nitrogen****Containing 304L SS in nitric acid and simulated high level waste medium**

5.1	Introduction	136
5.2	Effect of nitrogen on corrosion behavior of nitrogen containing 304L SS in nitric acid and chloride medium by potentiodynamic anodic polarization	137
5.2.1	Microstructure	137
5.2.2	Energy dispersive spectra of the nitrogen containing 304L SS	140
5.2.3	Potentiodynamic anodic polarization behavior of forged nitrogen containing 304L SS in nitric acid medium	142
5.2.4	Effect of concentration and temperature of nitric acid on corrosion behavior of the stainless steels	149
5.2.5	Effect of nitrogen on corrosion behavior of the nitrogen-containing stainless steel alloys in nitric acid	151
5.2.6	Effect of nitrogen on pitting corrosion of high-nitrogen stainless steel alloys in 0.5 M NaCl	152
5.3	Effect of nitrogen on corrosion behavior of nitrogen containing 304L SS in nitric acid and simulated HLW by electrochemical noise	157
5.3.1	Evaluation of Stern - Geary coefficient	157
5.3.2	Time record and noise resistance	159
5.3.3	Spectral noise resistance	164
5.3.4	Shot noise analysis	168
5.3.4.1	Characteristic frequency plots	168

5.3.4.2 Cumulative probability plots	171
5.3.5 Wavelet analysis	173
5.4 Passive film analysis by laser Raman spectroscopy	177
5.5 Conclusions	180

## **6**

## **CHAPTER 6**

### **Summary and conclusions**

6.1 Summary and conclusions from the study on electrochemical noise monitoring during pitting corrosion of 304L SS	183
6.2 Summary and conclusions from the studies on electrochemical noise monitoring of 304L SS in nitric acid and simulated nuclear high level waste medium	185
6.3 Summary and conclusions from studies on the effect of nitrogen on corrosion behavior of nitrogen containing 304L SS in nitric acid medium	186
6.4 Scope for future work	188
V References	189
VI List of Publications	210

## **SYNOPSIS**

To secure the energy demands of the growing Indian economy, Department of Atomic Energy (DAE) in India has evolved a three-stage nuclear power program based on closed fuel cycle [1]. This calls for adopting spent fuel reprocessing, conditioning and recycle as an important option. With total protection of the environment as an overriding consideration, management of the radioactive waste generated in the fuel cycle has received high priority in India's nuclear programme right from its inception and it covers the entire range of activities from handling, treatment, conditioning, transport, storage and finally disposal [2]. In the backend of the nuclear fuel cycle, Austenitic stainless steel of AISI (American Iron and Steel Institute) type 304L SS is the major construction material in Indian nuclear reprocessing plants [3, 4], where nitric acid is the process medium used from low to high concentration and from room temperature to boiling conditions and in high level liquid waste storage plants [2], where the acidity ranges from 1-6M depending on the type of nuclear waste and the process conditions.

AISI type 304L SS is characterized by excellent corrosion resistance in nitric acid medium owing to the spontaneous formation of protective, self healing, tenacious  $\text{Cr}_2\text{O}_3$  passive film. But at concentrations greater than 8M acid and elevated temperatures ( $> 80^\circ \text{C}$ ), the passive film is damaged, rendering the steel to corrosion in the acidic environment. The presence of oxidizing ions in high level liquid waste, in combination with the radioactive heat, ennoble the corrosion potential of the stainless steel close to transpassive region and, in addition, the ions that gets adsorbed on the passive film surface weakens it, leading to breakdown during long term exposure. Thus, corrosion monitoring is an essential requirement in nuclear

reprocessing and waste storage plants in order to achieve an extended service life. Conventional corrosion monitoring techniques [5] such as coupon tests, electrical resistance and linear polarization resistance methods, though provide reliable corrosion rates, are based on the assumption that corrosion is uniform, and hence, are not suitable for localized corrosion monitoring and also do not provide a real time online information. Most of the electrochemical techniques for corrosion monitoring require an external perturbation that disturbs the very system that is being measured. Electrochemical noise [6, 7, 8, 9, 10] (EN) has emerged as a powerful corrosion monitoring tool as it stands unique in its credentials over other techniques. Electrochemical noise describes the spontaneous fluctuation of current and potential that occurs during an electrochemical process and corrosion being predominantly electrochemical in nature, these fluctuations can be tapped to map the corrosion event. Electrochemical noise gives an instantaneous and online indication of the corrosion events as and when it occurs and the signals represent distinct fingerprints for various types of corrosion. The technique requires no external perturbation and therefore, measurements can be made from naturally corroding systems and hence, can be applied to real structures. The technique is unique in its unprecedented ability to detect online as it happens and discern localized corrosion events. The application of electrochemical noise includes corrosion monitoring [8, 9, 11], investigating various types of corrosion like uniform and localized corrosion [9, 12], monitoring crack propagation in stress corrosion cracking [13, 14], evaluation of corrosion inhibitors [15], monitoring microbiologically induced corrosion, acid dew point corrosion in exhaust systems [17], coating evaluation [18] and many others.

The international experience in corrosion monitoring of nuclear high level waste storage plant includes, the Department of Energy (DOE) sites such as Hanford,

Savannah River Site (SRS), Oak ridge Reservation (ORR), Idaho National Engineering and Environmental Laboratory (INEEL) implementing corrosion coupons, linear polarization resistance (LPR) and electrical resistance (ER) probes for monitoring the corrosivity of underground nuclear waste storage tanks made of carbon steel and stainless steels, holding caustic and acidic waste [19]. These probes though detected uniform corrosion, failed to provide any indication of pitting and stress corrosion cracking, which were the primary modes of degradation in these plants. In 1995, DOE's Tanks Focus Area (TFA) launched the development and deployment of EN probes in these nuclear installations and achieved good degree of success in indicating uniform and localized corrosion events (pitting and SCC) as well.

Toward developing EN probes for corrosion monitoring application in reprocessing and waste storage medium, a three identical electrode probe made of 304L SS was designed. The objective of this thesis is to demonstrate the capability of the three identical electrode probe to monitor the corrosion activity of 304L SS in reprocessing and waste management environments. The studies presented in the thesis thus, can be categorized into three parts.

1. The first part comprised electrochemical noise monitoring of 304L SS during pitting corrosion. Presence of chloride ions in reprocessing medium or high level waste, by ingress of chloride from the water or acid, is detrimental. Chloride ions get adsorbed on the passive film and penetrate through the protective passive film causing local breakdown of passive film and leading to the formation of pits. The propagation and growth of these pits in reprocessing and waste storage plants cause radioactive leaks, which are highly catastrophic, and hence, there is a need for monitoring pitting corrosion. This aims to obtain electrochemical noise data using the three identical

electrode probe made of 304L SS, and derive mechanistic information of the processes occurring on the material surface exposed to environments conducive for pitting to occur.

2. AISI type 304L SS exhibits good passivation properties in nitric acid though, uniform dissolution from the film surface on long term exposure to the acid could contribute to low corrosion activity. The objective of the second study was to establish electrochemical noise resistance, a parameter derived from statistical analysis of electrochemical noise-time record, to determine the corrosion activity during the monitoring of 304L SS exposed to nitric acid and simulated high level waste, by using the three electrode probe. Electrochemical noise resistance is known to be equivalent to polarization resistance and hence, can replace the latter in the well known Stern Geary equation to determine the corrosion rates. Though this parameter is applied to obtain uniform corrosion rates, few attempts have been made by researchers to use this parameter to estimate the corrosion activity of low active systems, such as those for passive systems.

3. Towards developing materials for reprocessing and high level waste storage, nitrogen containing 304L SS are being considered as potential candidates for structural materials. Though nitrogen additions provide well balanced combination of excellent mechanical properties and corrosion resistance, their corrosion property in nitric acid environments is an important concern. Studies were thus taken up to investigate the effect of nitrogen on the corrosion property of three nitrogen containing (0.132 %N, 0.193 %N, 0.406 %N) 304L SS by potentiodynamic anodic polarization technique in these media. Another objective was to establish the three electrode electrochemical noise probe made of these materials to monitor the corrosion activity in reprocessing and waste storage medium and also to obtain

information on the effect of nitrogen on the corrosion property by electrochemical noise.

The thesis presents six chapters which are organized in the following sequence.

Chapter 1: Introduction and literature review

Chapter 2: Materials and experimental methods

Chapter 3: Results and discussion

Electrochemical noise monitoring during pitting corrosion of 304L SS

Chapter 4: Results and discussion

Electrochemical noise monitoring of 304L SS in nitric acid and simulated nuclear high level waste medium

Chapter 5: Results and discussion

Effect of nitrogen on the corrosion behaviour of nitrogen containing 304L SS in nitric acid medium

Chapter 6: Summary and conclusions

## ***Chapter 1***

### ***Introduction and literature review***

The chapter commences with the introduction of the three stages of Indian nuclear programme and backend of the nuclear fuel cycle, followed by a description of the materials for nuclear reprocessing and high level liquid waste storage. A brief discussion on corrosion monitoring and the conventionally used methods to accomplish the same with international experience in corrosion monitoring in nuclear waste storage tanks is presented in the subsequent section. This chapter introduces the electrochemical noise technique and describes the definitions of electrochemical noise, measurement procedures and the different analysis methods of the acquired noise signals. The introduction follows a brief literature review of electrochemical



noise starting from the time of its inception till the current scenario, and the need / importance of the current study presented in the thesis.

## ***Chapter 2***

### ***Materials and experimental methods***

This chapter presents the chemical composition of the materials used for the various studies reported in the thesis, the heat treatments, specimen preparation, electrolyte preparation, etching procedure and microstructural evaluation, and passive film study by laser Raman spectroscopy. This chapter also describes the experimental procedures which include potentiodynamic anodic polarization, electrochemical noise measurements and the analysis methods associated with these studies.

## ***Chapter 3***

### ***Electrochemical noise monitoring during pitting corrosion of 304L SS***

Chapter 3 presents the results of electrochemical noise monitoring of 304L SS during pitting corrosion in ferric chloride medium, under freely corroding conditions.

Electrochemical current and potential noises were simultaneously acquired from 304L SS in 0.05M ferric chloride ( $\text{FeCl}_3$ ) using three identical electrode configuration. The acquired data were visually examined and analyzed by statistical, spectral and wavelet analysis. The results of potential and current time records indicated high amplitude fluctuations during the initial stages of immersion. The random high amplitude fluctuations became more defined as corrosion progressed, and distinct potential and current spikes were obtained, which were indicative of pitting attack. The corresponding power spectral plots [20] exhibited  $1/f^n$  variation and the roll off slope corroborated with pitting attack. Statistical evaluation of the time record was carried out and parameters such as localization index [21], standard deviation of potential noise as well as the kurtosis [7, 22] of potential and current noise corroborated with

pitting attack. However, useful information on the corrosion mechanism could not be obtained from the skewness [7, 22]. Energy distribution plots obtained from wavelet analysis [23, 24] were found to provide useful information on the progress of corrosion. During initial stages of immersion, metastable pitting, propagation and repassivation of pits and stable pitting occurred on the specimen surface, the dominant process being propagation and repassivation of pits. With time of immersion, metastable pitting was suppressed and the corrosion mechanism comprised propagation and repassivation of pits and stable pitting, the latter being the most predominant. Although electrochemical noise time domain and power spectral analysis provided an insight on the corrosion mechanism as a whole, wavelet analysis provided intrinsic details on the processes occurring on the specimen surface as corrosion progressed.

#### ***Chapter 4***

##### ***Electrochemical noise monitoring of 304L SS in nitric acid and simulated nuclear high level waste medium***

In the interest to develop electrochemical noise probes for corrosion monitoring in nuclear reprocessing and waste storage applications, laboratory scale electrochemical noise monitoring experiments were carried out on AISI 304L SS in nitric acid and simulated high level waste (HLW) environments by simulating plant conditions. In nuclear waste tank infrastructure, problems related to sensitization can occur in the heat affected zones near welds as a result of thermal cycling during welding of thick components. This could lead to corrosion problems during long term exposure to nitric acid and HLW and hence, demands monitoring. The objective of the study was to acquire electrochemical noise signals from AISI type 304L SS under various microstructural conditions (solution annealed and sensitized) in nitric acid medium of

varying concentration ( 4M, 8M, 12M ) and temperature (298K, 323K), and in simulated HLW, under naturally corroding conditions, with respect to time of immersion, and derive information on the corrosion processes as well as on the corrosion activity, so as to understand similar phenomenon likely to occur in reprocessing and waste storage plants during monitoring. This chapter demonstrates the application of electrochemical noise resistance [7, 25, 26] (a parameter derived from the EN time records) as a monitoring tool to reflect the corrosion activity of 304L SS in various environments, simulating reprocessing and waste storage conditions during the monitoring period. EN records revealed passivation process during the monitoring period, under all conditions studied, except for the sensitized specimen in 4M nitric acid (323K) which showed localized attack. Optical micrograph confirmed localized attack for sensitized 304L SS in 4M nitric acid at the electrolyte temperature of 323K. No surface attack was observed in other specimens. The time records of the solution annealed 304L SS in simulated HLW under ambient conditions showed regions of depassivation by the ions present in the waste solution. The results revealed decrease of noise resistance with increase in concentration of nitric acid for solution annealed 304L SS at 298 K and 323 K electrolyte temperature implying higher corrosion activity at higher concentration. Increase in temperature did not appreciably increase the corrosion activity. For the sensitized 304L SS, the corrosion activity was found to be comparable in 4M, 8M and 12M nitric acid at 298K. An appreciable increase in corrosion activity occurred in 8M nitric acid when the electrolyte temperature was increased to 323K. The corrosion activity was found to be higher for sensitized specimen compared to solution annealed 304L SS. The decrease in noise resistance for the sensitized specimen in simulated HLW (323K) was found to be marginal when compared to that of the solution annealed specimens

implying comparable corrosion activity for the solution annealed and sensitized specimen during the period of measurement. The high noise resistance for these systems could be attributed to the passive state, which the system exhibited throughout the monitoring period. Nevertheless, the variations in the noise resistance in the environments are because of differences in the dissolution rates from the passive film surface. Electrochemical noise resistance was found to be useful in discerning the differences in the corrosion activity even for systems that exhibited low corrosion activity. An inverse relation between EN resistance and corrosion activity could be established for 304L SS in nitric acid and simulated HLW from the results of the present study.

## ***Chapter 5***

### ***Effect of nitrogen on corrosion behavior of nitrogen containing 304L SS in nitric acid medium***

This chapter describes the studies carried out on the corrosion behavior of three nitrogen containing 304L SS (0.132 %N, 0.193 %N, 0.406 %N) in nitric acid and simulated HLW by potentiodynamic anodic polarization and electrochemical noise techniques. Potentiodynamic anodic polarization experiments were carried out on the three nitrogen containing 304L SS under forged and rolled microstructural conditions, in nitric acid and chloride medium. The effect of concentration (1M, 4M, 6M) and temperature (298K, 323K) of nitric acid and the effect of nitrogen content in acid and chloride medium, on the corrosion resistance is discussed. Scanning electron micrographs, optical micrographs and energy dispersive spectra were used for microstructural evaluation.

The three nitrogen containing stainless steels in the forged and rolled conditions were found to possess good corrosion resistance in nitric acid medium (1M, 4M, 6M) and

simulated HLW medium. Increase of concentration and temperature of the acid increased the corrosion potential of the forged and rolled alloys, which could be attributed to global reduction of nitric acid. Yet, a well defined passive range was maintained. Increase in nitrogen content of the alloys showed no discernable difference in the corrosion property in nitric acid and simulated HLW which could be attributed to the spontaneous formation of chromium oxide passive film in these media. The presence of oxidizing ions in simulated HLW ennobled the corrosion potential though, no detrimental effect was found on the passive film stability of the nitrogen containing stainless steel alloys. All the hot rolled nitrogen containing stainless steel alloys exhibited a marginal improvement in corrosion resistance in nitric acid medium when compared to the forged stainless steel alloys of the same composition. The results from the pitting corrosion studies showed that an increase in the nitrogen content from 0.132 wt% N to 0.193 wt% N in the forged alloy increased the pitting corrosion resistance. Further increase in nitrogen to 0.406% decreased the pitting resistance due to the presence of continuous network of chromium and manganese rich precipitates along the grain boundary, as inferred from SEM and EDS analysis. In the rolled stainless steel alloys, an increase up to 0.406% N was found to be beneficial in enhancing the pitting resistance. The improvement in the pitting resistance of the hot rolled high nitrogen stainless steel could be attributed to various aspects. Hot rolling and annealing had resulted in partial dissolution of both carbide and nitride precipitates, leading to a more homogeneous matrix, consequently reducing the number of pit initiation sites. In addition, dissolution of chromium nitride precipitates resulted in enrichment of the stainless steel matrix with nitrogen. Nitrogen in solid solution is known to enhance the corrosion property of stainless steel, in particular pitting corrosion resistance. Beneficial role of nitrogen in enhancing the

pitting resistance could be attributed to the well known theories of ammonia formation, surface enrichment, anodic segregation and local inhibition.

Electrochemical current and potential noise was acquired from the three nitrogen containing AISI type 304L SS in 1M, 4M, 8M nitric acid and simulated high level waste under ambient conditions. Statistical, spectral, shot noise and wavelet analysis were performed on the acquired signals from all the above mentioned environments. The results showed that the stainless steels exhibited good corrosion resistance in nitric acid and simulated high level waste medium, as evidenced by the high noise resistance and spectral noise resistance [27] and the two parameters showed good equivalence. In addition, the two parameters were found to show an inverse relation with corrosion activity and an increase in nitrogen content of the stainless steels was found to decrease the corrosion activity in nitric acid and simulated HLW medium as well. From shot noise analysis [7, 28, 29], it was found that the characteristic frequency decreased with increase in nitrogen content and the frequency of distribution shifted towards lower frequency as nitrogen content increased. Except for a couple of disagreements, a direct correlation between nitrogen content and corrosion activity was established by shot noise analysis. In addition, the frequency of distribution was found to shift towards higher frequency with increase in concentration implying higher corrosion activity at higher concentration. Electrochemical noise analysis indicated better passive film stability in 4M nitric acid compared to 1M and 8M nitric acid. The energy distribution plots [23, 24] of current noise were found to be useful in deriving mechanistic information about the processes happening on the electrode surface. Laser Raman spectra (LRS) for passive film analysis inferred a stable passive film in 4M nitric acid when compared to 1M and 8M nitric acid and an unstable film structure in simulated HLW. LRS results were in tandem with electrochemical noise results.

## ***Chapter 6***

### ***Summary and conclusions***

Chapter 6 presents a summary and conclusion of the various studies presented in the thesis towards establishing electrochemical noise and a three identical electrode probe to monitor the EN activities on the surface of 304L SS exposed to various environments simulating nuclear reprocessing and waste storage medium.

1. Electrochemical noise monitoring of 304L SS in 0.05M FeCl<sub>3</sub> using the three electrode probe gave distinct features of pitting attack. Parameters such as standard deviation, localization index, kurtosis from statistical analysis and roll off slope from power spectral analysis gave time average information that the surface was undergoing pitting attack. The energy distribution plots from wavelet analysis were useful in reflecting the predominant processes occurring on the metal surface as corrosion progressed. The change in mechanism from metastable / stable pitting to purely stable pitting was well depicted.

2. It was aimed to demonstrate the three identical electrode noise probe to monitor the corrosion activity of 304L SS in reprocessing and waste storage medium by simulating the conditions in the laboratory and to establish electrochemical noise resistance as a parameter which reflects the corrosion activity. The results inferred that electrochemical noise resistance monitoring using three identical electrode probe of 304L SS (sensitized and solution annealed) in varying concentrations and temperature of nitric acid and simulated HLW was found to be useful in discerning the variations in the corrosion activity even for systems that exhibited low corrosion activity. The time records depicted passivation process in all conditions studied except for the sensitized specimen at elevated temperature of 4M acid which showed localized attack, as also evidenced by post experimental microstructures. The high

noise resistance for these systems could be attributed to passive state which the system exhibited throughout the monitoring period, nevertheless, the variations in the noise resistance in the environments are because of variations in the dissolution rates from the passive film surface. Hence, noise resistance which is applicable to delineate uniform corrosion rates was established to reflect the corrosion activity of 304L SS undergoing passivation process in reprocessing and waste storage medium. An inverse relationship was established between noise resistance and corrosion activity.

3. Corrosion studies on three nitrogen containing stainless steels (under forged and rolled conditions) in nitric acid and simulated HLW medium inferred superior resistance of the rolled steels compared to the forged steel in acid and chloride media, but no inferior influence of nitrogen on the corrosion property was noticed from potentiodynamic anodic polarization studies in acid medium.

It was possible to establish the three identical electrode noise probe to monitor the surface activity of the nitrogen containing 304L SS in nitric acid and simulated HLW medium. The positive effect of nitrogen in acid medium was evidenced by electrochemical noise analysis. Electrochemical noise-time record reflected passivation process for these steels in these environments, which was substantiated by statistical, spectral, wavelet and shot noise analysis. Noise resistance and spectral noise resistance increased while the frequency of events decreased with increase in nitrogen content. The energy distribution plots from wavelet analysis were useful in determining the corrosion mechanism.

## ***References***

1. J Homi Bhabha, N B Prasad, "A Study of the Contribution of Atomic Energy to a Power Programme in India," Proceedings of the Second United Nations



- International Conference on the Peaceful Uses of Atomic Energy, Geneva, pp 89-101, September 1958.
2. K. Raj, K.K. Prasad, N.K. Bansal, Nuclear Engineering and Design 236 (2006) 914.
  3. Baldev Raj, U.Kamachi Mudali, Progress in Nuclear Energy 48 (2006) 283.
  4. U.Kamachi Mudali, R.K. Dayal, J.B. Gnanamoorthy, Journal of Nuclear Materials 203 (1993) 73.
  5. Xu, Recent Patents on Corrosion Science 2 (2010) 34.
  6. W.P.Iverson, Journal of Electrochemical Society 115 (6) (1968) 617.
  7. R. A. Cottis, Corrosion 57 (2001) 265.
  8. S.Girija, U.Kamachi Mudali, V.R. Raju, Baldev Raj, Corrosion Reviews 23 (2-3) (2005) 107.
  9. S.Girija, U.Kamachi Mudali, V.R.Raju, R.K.Dayal, H.S.Khatak, Baldev Raj, Material Science and Engineering A 407 (2005) 188.
  10. S.Girija, U.Kamachi Mudali, H.S.Khatak, Baldev Raj, Corrosion Science 49 (11) (2007) 4051.
  11. D.A.Eden, A.N.Rothwell, J.L.Dawson, in Corrosion/91, paper 444, National Association of Corrosion Engineers, Houston 1991.
  12. M.G.Pujar, U.Kamachi Mudali, Sudhansu Sekhar Singh, Corrosion Science, 53 (2011) 4178-4186.
  13. T.Anita, M.G.Pujar, H.Shaikh, R.K.Dayal, H.S.Khatak, Corrosion Science 48 (2006) 2689-2710.
  14. T.Anita, M.G.Pujar, C.Mallika, U.Kamachi Mudali, R.K.Dayal, Evaluation of the effect of nitrogen on stress corrosion cracking of austenitic stainless steels using electrochemical noise technique, in : Proceedings, of the eleventh International

- Conference on High Nitrogen Steels and Interstitial Alloys, Chennai, India, September 27-29, 2012, pp. 213-220.
15. C.Monticelli, G.Brunoro, A.Frignani, G.Trabanelli, *Journal of the Electrochemical Society*, 139 (1992) 706.
  16. M.G.Pujar, R.P.George, P.Muralidharan, U.Kamachi Mudali, 67 (11) *Corrosion* (2011) 115004-1 - 115004-11.
  17. W.M.Cox, D.Gearey, J.L.Dawson, "Corrosion – Industrial problems Treatment and Control Techniques, in: *Proceedings of the Kuwait Conference*, Pergamon Press, Oxford, 1987, p.83.
  18. D.A.Eden, M.Hoffman, B.S.Skerry, *Polymer Material Science Engineering*, 53 (1985) 388.
  19. Michael T. Terry, Glenn L. Edgemon, Ronald E. Mizia, *Development and Deployment of Advanced Corrosion Monitoring Systems for High-Level Waste Tanks*, WM'02 Conference, February 24-28, 2002, Tucson, AZ- pg. 1
  20. J. L. Dawson, "Electrochemical Noise Measurement: The Definitive In-Situ Technique for Corrosion Applications," *Electrochemical Noise Measurement for Corrosion Applications*, eds. J.R. Kearns, J. R. Scully, P. R. Roberge, D. L. Reichert, J. L. Dawson (ASTM, Philadelphia, 1996), p. 3.
  21. D.G.John, J.L.Dawson, *International Patent WO 87/07022*, World intellectual property Organization, 1987.
  22. D. Eden, "Electrochemical Noise - The first two octaves" *CORROSION / 98* (Houston, TX: NACE, 1998) paper 386
  23. J.A.Wharton, R.J.K.Wood, B.G.Mellor, *Corrosion Science* 45 (2003) 97.
  24. A.Abelle, M.Bethencourt, F.J.Botana, M.Marcos, J.M.Sanchez-Amaya, *Electrochimica Acta* 46 (2001) 2353.

25. D.A.Eden, K.Hladky, D.G. John, J.L.Dawson, Proceedings of the Corrosion/86, Houston, T, NACE, paper no. 274, 1986.
26. J.L. Dawson, D. M. Farrell, P.J.Aylott and K. Hladky., NACE CORROSION / 89 Conference, NACE, New Orleans, LA, 198.
27. F.Mansfeld, L.T.Han, C.C.Lee, Journal of Electrochemical Society 143 (12) (1996) L286.
28. R.A.Cottis, M.A.A.Al-Awadhi, H.Al-Mazeedi, S.Turgoose, Electrochimica Acta 46 (2001) 3665.
29. J.M.Sanchez-Amaya, R.A.Cottis, F.J.Botana, Corrosion Science 47 (2005) 3280.

# **LIST OF FIGURES**

<b>S.No</b>	<b>Figure Caption</b>	<b>Page Number</b>
1.	Figure 1.1 Indian nuclear energy programme: The three stage	2
2.	Figure 1.2 The backend comprises of reprocessing and waste management	3
3.	Figure 1.3 The classification of physical process	22
4.	Figure 1.4 General scheme of FWT algorithm	50
5.	Figure 1.5 Daubechies wavelets	51
6.	Figure 2.1 Photos of mounted Specimen for polarization studies	28
7.	Figure 2.2 Photos of teflon mounted three electrode probe for EN studies in nitric acid and simulated high level waste	69
8.	Figure 2.3 Figure 2.3 photos of bare electrodes for EN studies in chloride medium	70
9.	Figure 2.4 Potentiodynamic anodic polarization curve in nitric acid medium depicting various conditions in reprocessing plant	72
10.	Figure 2.5 Schematic representation of polarization cell (ASTM G5)	73
11.	Figure 2.6 Schematic representation of the EN cell using three identical electrode configuration	77
12.	Figure 2.7 Schematic of the connections between EN cell and instrument , WE-1: working electrode 1, WE-2 : working electrode 2	78

13.	Figure 2.8	Photograph of the experimental set up for the electrochemical studies	79
14.	Figure 2.9	Typical plots of potential noise before and after trend removal	80
15.	Figure 2.10	A scheme of the data analysis methods used for the various electrochemical noise studies	82
16.	Figure 3.1	Electrochemical current and potential noise-time records taken after a) 1 h b) 10 h c) 14 h d) 23 h e) 25 h of immersion	89
17.	Figure 3.2	PSD of potential and current noise with time of immersion a & c) 1 h, b & d) 25 h	91
18.	Figure 3.3	Optical micrograph of 304L SS after electrochemical noise experiment showing pitting attack (after 25 h of immersion)	92
19.	Figure 3.4	Standard deviation of potential noise as a function of time of immersion, for 304L SS in 0.05 M FeCl <sub>3</sub>	94
20.	Figure 3.5	Localization index for 304L SS in 0.05 M FeCl <sub>3</sub> as a function of time of immersion	94
21.	Figure 3.6	Kurtosis of potential and current noise for 304L SS in 0.05 M FeCl <sub>3</sub> with time of immersion	96
22.	Figure 3.7	Skewness of potential and current noise for 304L SS in 0.05 M FeCl <sub>3</sub> with time of immersion	97
23.	Figure 3.8	Typical representations of coefficients obtained by wavelet transform of the current noise time record taken 14 h	

	after immersion	98
24.	Figure 3.9 a) EDP of current noise after 1 h of immersion	100
	b) EDP of current noise after 10 h of immersion	101
	c) EDP of current noise after 14 h of immersion	101
	d) EDP of current noise after 23 h of immersion	102
	e) EDP of current noise after 25 h of immersion	103
25.	Figure 4.1 Optical micrograph of 304 L SS used for EN measurements	
	after oxalic acid etching a) solution annealed	
	b) sensitized	108
26.	Figure 4.2 DL-EPR test plot for 304L SS, a) solution annealed,	
	b) sensitized	108
27.	Figure 4.3 EN-time records taken after 150 h of immersion of solution	
	annealed 304L SS in a) 4 M nitric acid (298 K) b) 8 M	
	nitric acid (298 K), c) 12 M nitric acid (298 K)	110
28.	Figure 4.4 EN-time records taken after 150 h of immersion of solution	
	annealed 304L SS in a) 8 M nitric acid (323 K) b) 4 M nitric	
	acid (323 K)	111
29.	Figure 4.5 EN-time records taken after 150 h of immersion of sensitized	
	304L SS in a) 4 M nitric acid (298 K), b) 8 M nitric acid	
	(298 K), c) 4 M nitric acid (323 K), d) 8 M nitric acid (323 K)	112
30.	Figure 4.6 Electrochemical noise resistance Vs Time plots for a) solution	
	annealed 304L SS at 298 K electrolyte Temperature, b) sensitized	
	304L SS at 298 K electrolyte temperature, c) solution annealed	

	304L SS at 323 K electrolyte temperature, d) sensitized	
	304L SS at 323 K.	116
31.	Figure 4.7 EN-time record for 304L SS in 3 M nitric acid (298K) taken after a) 85 h, b) 125 h of immersion.	120
32.	Figure 4.8 EN-time record for 304L SS in simulated HLW (in 3M nitric acid) (298 K) taken after a) 85 h, b) 125 h of immersion.	121
33.	Figure 4.9 Passivation in 3 M nitric acid.	
34.	Figure 4.10 Passivation by 3 M nitric acid and decrease in passive film stability by oxidizing ions present in simulated HLW	123
35.	Figure 4.11 Schematic representation of cation adsorption into passive film	125
36.	Figure 4.12 EN-time record taken 150 h of immersion of 304L SS in simulated HLW (323 K) a) solution annealed, b) sensitized.	126
37.	Figure 4.13 Electrochemical noise resistance Vs Time plots for solution annealed 304L SS in 3 M nitric acid and simulated HLW at 298 K	129
38.	Figure 4.14 Electrochemical noise resistance Vs Time plots for solution annealed and sensitized 304L SS in simulated HLW at 323 K	129
39.	Figure 4.15 Typical micrographs taken after EN experiments for 304 L SS at 298 K electrolyte temperature, showing no corrosion attack for solution annealed specimen in	

	4 M HNO <sub>3</sub> , b) solution annealed specimen in 8 M HNO <sub>3</sub> , c) solution annealed specimen in 12 M HNO <sub>3</sub> d) sensitized specimen in 4 M HNO <sub>3</sub> , e) sensitized specimen in 8 M HNO <sub>3</sub> , f) sensitized specimen in 12 M HNO <sub>3</sub>	131
40.	Figure 4.16 Typical micrographs taken after EN experiments for 304 L SS at 323 K electrolyte temperature, showing no corrosion attack for a) solution annealed specimen in 4 M HNO <sub>3</sub> , b) solution annealed specimen in 8 M HNO <sub>3</sub> , c) sensitized specimen in 8M HNO <sub>3</sub> , d) Localized attack seen in sensitized 304L SS in 4 M HNO <sub>3</sub>	132
41.	Figure 5.1 Optical micrographs of the forged a) 304LN1F SS, b) 304LN2F SS c) 304LN3F SS	138
44.	Figure 5.2 SEM of the forged a) 304LN1F SS, b) 304LN2F SS c) 304LN3F SS	138
45.	Figure 5.3 Optical micrographs of the rolled a) 304LN1R SS b) 304LN2R SS c) 304LN3R SS	139
46.	Figure 5.4 SEM of the rolled a) 304LN1R SS b) 304LN2R SS c) 304LN3R SS	139
47.	Figure 5.5 EDS of the matrix and precipitate of the forged and rolled nitrogen containing 304LN1 stainless steel, showing chromium and manganese enrichment in the precipitate compared to matrix.	141
48.	Figure 5.6 EDS of the matrix and precipitate of the forged and rolled	



- nitrogen containing 304LN2 stainless steel, showing chromium and manganese enrichment in the precipitate compared to matrix, and a decline in Fe content in the precipitate compared to matrix. 141
49. Figure 5.7 EDS of the matrix and precipitate of the forged and rolled nitrogen containing 304LN3 stainless steel, showing chromium and maximum manganese enrichment in the precipitate compared to matrix, and a substantial decline in Fe content in the precipitate compared to matrix. 142
50. Figure 5.8 Potentiodynamic anodic polarization curves in 1 M, 4 M, and 6 M HNO<sub>3</sub> (298 K) for the forged nitrogen containing stainless steels 143
51. Figure 5.9 Potentiodynamic anodic polarization curves in 1 M, 4 M, and 6 M HNO<sub>3</sub> (298 K) for the rolled nitrogen containing stainless steels 144
52. Figure 5.10 Potentiodynamic anodic polarization curves in 1M, 4M, and 6M HNO<sub>3</sub> (323K) for the as forged nitrogen containing stainless steels 145
53. Figure 5.11 Potentiodynamic anodic polarization curves in 1 M, 4 M, and 6 M HNO<sub>3</sub> (323 K) for the rolled nitrogen containing stainless steels 146
54. Figure 5.12 Potentiodynamic anodic polarization curves for the a) forged and b) rolled nitrogen containing stainless steels containing

	three different nitrogen contents in 0.5 M NaCl	153
55.	Figure 5.13 Typical Polarization curves for the nitrogen containing stainless steels in 1 M and 8 M HNO <sub>3</sub>	158
56.	Figure 5.14 Typical representation of electrochemical current and potential noise time record for 304L SS containing a) 0.132% N b) 0.193% N in 4 M HNO <sub>3</sub> taken b) after 8 h of immersion	160
57.	Figure 5.15 Electrochemical noise resistance of the three nitrogen containing 304L SS in 1 M, 4 M, 8 M HNO <sub>3</sub> and simulated HLW	162
58.	Figure 5.16 Spectral noise resistance of the three nitrogen containing 304L SS in 1 M, 4 M, 8 M HNO <sub>3</sub> and simulated HLW medium.	165
59.	Figure 5.17 Plots showing correlations between noise resistance and spectral noise resistance for the nitrogen containing stainless steels in HNO <sub>3</sub> and simulated HLW medium.  $R_{sn}^o$ is found to track $R_n$	168
60.	Figure 5.18 characteristic frequencies as a function of time of immersion for the three nitrogen containing stainless steels in HNO <sub>3</sub> acid and simulated HLW medium.	170
61.	Figure 5.19 Cumulative probability plots representing the distribution of frequencies for the three nitrogen containing stainless steels in HNO <sub>3</sub> and simulated HLW medium.	172

62. Figure 5.20 Typical representation of eight level decomposition using Daubechies 4 wavelet, of the current noise time record of the stainless steel containing 0.406% N in 1 M  $\text{HNO}_3$ , taken 20 h after immersion 174
63. Figure 5.21 Typical representation of energy distribution plots of current noise for the nitrogen containing stainless steel in 1 M  $\text{HNO}_3$ , showing maximum deposition of energy at D1 crystal, which is attributed to rapid current transients during passivation. 176
64. Figure 5.22 Laser Raman spectra of passive films formed on the three nitrogen containing 304L SS in 1 M, 4 M, 8 M  $\text{HNO}_3$  and simulated HLW. excitation wavelength = 488 nm, laser power = 10 mw, laser exposure time = 5s, Acquisitions = 20. 178

## **LIST OF TABLES**

<b>S.No</b>	<b>Table Caption</b>	<b>Page Number</b>
1.	Table 1.1 Range of PI for various corrosion processes.	36
2.	Table 1.2 Reid and Eden's table of skewness and kurtosis values for various corrosion processes.	38
3.	Table 2.1 Chemical composition of 304L SS (in wt %) used for the studies.	64
4.	Table 2.2 Chemical composition (in wt %) of the three nitrogen containing 304L SS used for the studies.	64
5.	Table 2.3 Composition of simulated high level waste solution prepared in 3 M nitric acid.	66
6.	Table 3.1 PSD roll off slopes derived from power spectral density plots	92
7.	Table 3.2 Scale range for $j=8$ , $\Delta t = 0.5s$ .	99
8.	Table 4.1 Average electrochemical noise resistance of 304L SS in nitric acid medium for 250 h of immersion.	117
9.	Table 4.2 Average electrochemical noise resistance of 304L SS in simulated HLW.	128
10.	Table 5.1 Electrochemical parameters for the forged nitrogen containing stainless steels in nitric acid medium.	148

11.	Table 5.2	Electrochemical parameters for the rolled nitrogen containing stainless steels in nitric acid medium.	148
12.	Table 5.3	Pitting Potential of the as-forged and hot rolled nitrogen containing stainless steel alloy in 0.5 M NaCl.	154
13.	Table 5.4	Stern Geary coefficients in V/decade, for the nitrogen containing stainless steels	160
14.	Table 5.5	The average noise resistance for 24 h of immersion.	164
15.	Table 5.6	Raman assignments corresponding to the various peak	180

## **LIST OF ABBREVIATIONS**

<b>BARC</b>	Bhabha Atomic Research Centre
<b>PHWR</b>	Pressurized Heavy Water Reactor
<b>PUREX</b>	Plutonium Uranium Reduction Extraction
<b>CORAL</b>	Compact Reprocessing of Advance Fuels in Lead Shielded Cells
<b>AIISI</b>	American Iron and Steel Institute
<b>ASTM</b>	American Society for Testing and Materials
<b>EN</b>	Electrochemical noise
<b>LPR</b>	Linear Polarization Resistance
<b>SEM</b>	Scanning electron microscopy
<b>EDS</b>	Energy dispersive X-ray spectroscopy
<b>LRS</b>	Laser Raman Spectroscopy
<b>ZRA</b>	Zero resistance Ammeter
<b>EDP</b>	Energy distribution plots
<b>FFT</b>	Fast Fourier Transform
<b>PSD</b>	Power Spectral Density
<b>WE</b>	Working electrode
<b>RE</b>	Reference Electrode
<b>U</b>	Uranium
<b>Pu</b>	Plutonium
<b>Th</b>	Thorium
<b>HLW</b>	High level liquid waste
<b>HNO<sub>3</sub></b>	Nitric acid
<b>HCl</b>	Hydrochloric acid

<b>HNS</b>	High nitrogen steel
<b>SS</b>	Stainless Steel
<b>OCP</b>	Open circuit potential

The chapter presents a brief introduction on the three stages of Indian nuclear programme and the backend of nuclear fuel cycle. The materials for nuclear reprocessing and high level liquid waste storage are discussed. A brief discussion on corrosion monitoring and international experience in corrosion monitoring in nuclear waste storage tanks is presented in the subsequent section. The chapter describes the electrochemical noise technique, measurement procedures and the different analysis methods. The introduction follows a brief literature review of electrochemical noise starting from the time of its inception till the current scenario, and the need for the current study presented in the thesis.

---

### ***1.1 Indian Nuclear Energy Programme: The three stage***

To secure the energy demands of the growing Indian economy, Department of Atomic Energy (DAE) in India has evolved a three-stage nuclear power program based on closed fuel cycle [1]. The path to India's nuclear energy self-sufficiency was outlined by Drs. H. J. Bhabha with a three stage plan for a sustainable nuclear energy program considering India's limited uranium, but abundant thorium natural resources. The first stage envisages the use of natural uranium to fuel pressurized heavy water moderated reactors and to generate plutonium for fueling the second stage of fast breeder reactors for power production. In the second stage, plutonium reprocessed from the spent fuel of the first stage is fueled in fast breeder reactors that would contain thorium blankets for breeding



uranium-233. The objective of the second stage is to breed uranium-233 as well as additional plutonium for second and third stage reactors and to produce power to support India's future economic expansion. The fissile content of the natural uranium reserves will be depleted by the first stage pressurized heavy water reactors (PHWR). Hence, it is necessary for India to close the nuclear fuel cycle – that is, to reprocess the spent PHWR fuel and recycle the fissile and fertile materials in the fast breeder reactors. These reactors will increase the fissile material inventory of both plutonium and U-233 and also expand India's nuclear power capacity. The objective of stage three is to achieve a sustainable nuclear fuel cycle by developing Th–U-233 based systems that utilize India's vast thorium reserves to provide long-term energy security with nuclear power. A summary of the three stage Indian nuclear energy programme is presented in Figure.1.1.

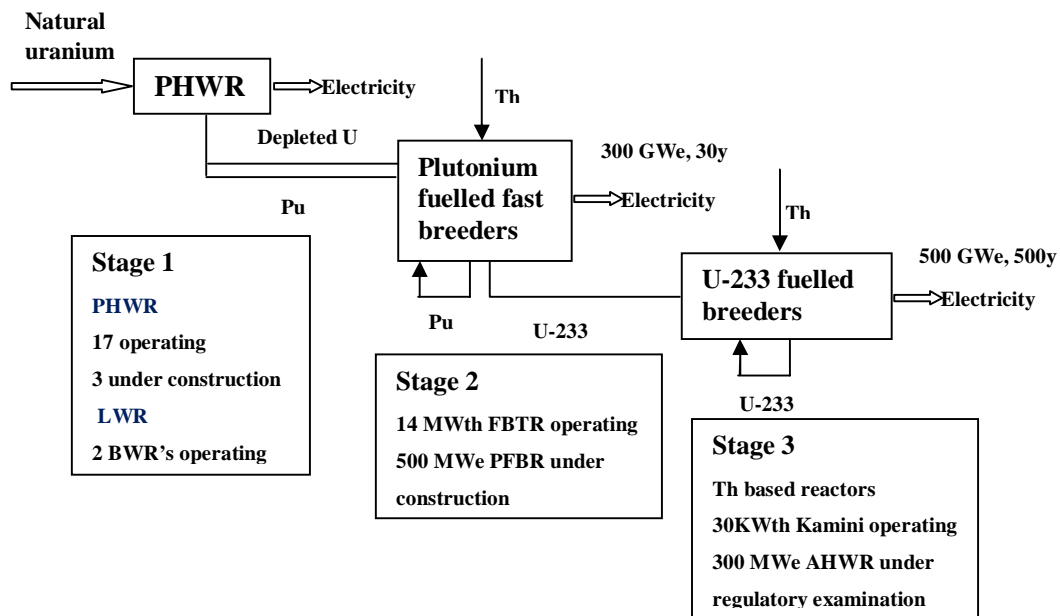


*Figure 1.1 Indian nuclear energy programme: The three stage*

Thus, Thorium utilization is the long term core objective of India's nuclear power program. Kalpakkam, India, is the unique nuclear site in the world housing all three Stages and closed fuel cycle facilities.

### ***1.2 Backend of the nuclear fuel cycle***

While mining of uranium, its fabrication into nuclear fuel and its subsequent utilization in a nuclear reactor for the extraction of electrical power, constitute the front-end of the nuclear fuel cycle, fuel reprocessing and high level waste management are the two major back-end activities [2,3,4,5] (Figure 1.2).

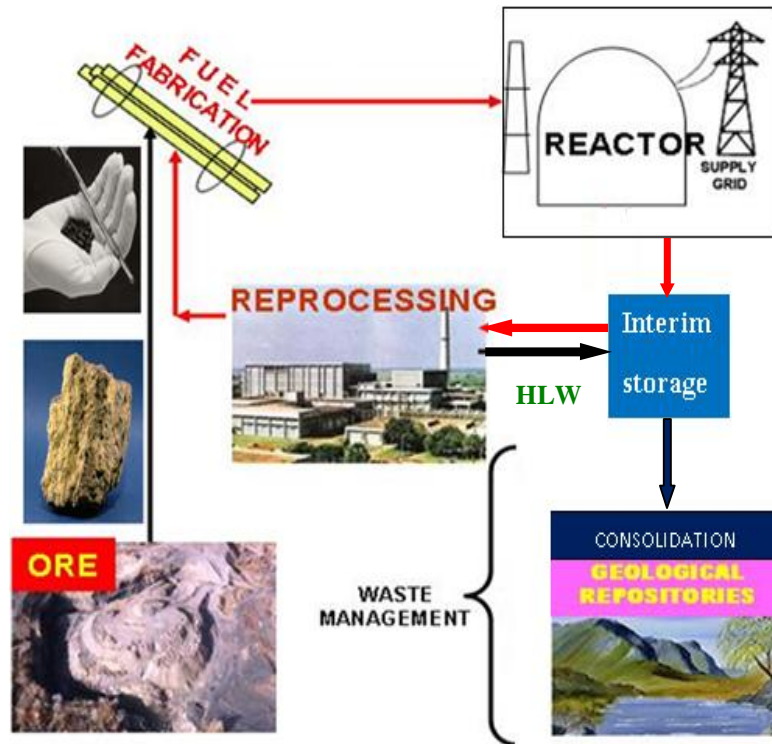


***Figure 1.2 The backend comprises of reprocessing and waste management***

Fuel reprocessing aims at recovering the reusable fissile and fertile component of the spent fuel, while high level waste management consists of treatment and safe disposal of those components of spent fuel that have no immediate and ready use and which also contain high levels of radioactivity. Reprocessing forms an integral part of the Indian Nuclear Energy Programme which is based on the optimum resource utilization. India has chosen to follow a closed fuel cycle policy to ensure long term energy security. This calls for adopting reprocessing, conditioning and recycle option. Having low reserves of uranium and high reserves of thorium, this strategy of reprocessing and recycle of uranium and plutonium would lead to optimum resource utilization. Thus, in the Indian context, spent fuel is a vital resource material and not a waste to be disposed off. Currently, India has three operating reprocessing plants based on Plutonium Uranium Extraction (PUREX) technology [6, 7] one each at Trombay, Tarapur and Kalpakkam . While the Trombay facility reprocesses spent fuel from research reactors, the plants at Tarapur and Kalpakkam processes the oxide fuels from PHWRs. As compared to the reprocessing of spent fuel from PHWR's containing low Pu content, the reprocessing of FBR fuels with high Pu content poses tough challenges. The ions of Pu, fission products and transuranics increases the solution potential and oxidizing power of the nitric acid process medium and enhance the corrosion rate and failure probability of the vessels and equipment [3] made mostly of austenitic stainless steels. Based on the country's experience on thermal reactor fuel reprocessing, a compact reprocessing facility for advanced fuels in lead shielded cells (CORAL) [2] has been commissioned in Kalpakkam for reprocessing of fast reactor carbide fuels. The facility has now successfully reprocessed the 2.5-years cooled 165 GWd/t burnup MC fuel with 70% Pu discharged

from fast breeder test reactor. The PUREX would be the workhorse of fast reactor fuel reprocessing for the forthcoming decades [2, 8]. With total protection of the environment as an overriding consideration, management of the radioactive waste generated in the fuel cycle has received high priority in India's nuclear programme right from its inception and it covers the entire range of activities from handling, treatment, conditioning, transport, storage and finally disposal [4]. Based on indigenous materials and capabilities, technology has been developed and is in routine application for the management of low and intermediate level wastes meeting the stringent regulatory requirements and standards.

Treatments of reprocessed wastes have received considerable attention because they contain nearly 99% of the activity generated in the nuclear fuel cycle. Indian waste management facilities are co-located with waste generating facilities, i.e., nuclear reactor, reprocessing plant and fuel fabrication facility, so as to avoid any undue radiation exposure during transportation of waste from one place to another. Effective management involves segregation, characterization, handling, treatment, conditioning and monitoring, prior to final disposal. The long term action plan formulated for the management of these wastes consists of solidification of the medium level wastes in a suitable matrix in reliable containers and burying them in totally water-proof concrete tile holes with protective barriers. High level waste includes uranium, plutonium, and other highly radioactive elements formed during fission. Most of the radioactive isotopes in high level waste emit large amounts of radiation and have extremely long half-lives (some longer than 100,000 years) creating long time periods before the waste will settle to safe levels of radioactivity. High-level liquid waste (HLW) generated during reprocessing of spent

nuclear fuels is concentrated by evaporation and stored in stainless steel tanks. These storage tanks require cooling and continuous surveillance. Liquid storage [4] in stainless steel tanks is at best an interim step and a three-step strategy for management of HLW has been adopted in India. This involves: (i) Immobilization of waste oxides by vitrification in glass matrix and doubly encapsulating the solidified mass in corrosion resistant containers called canisters. (ii) Interim retrievable storage of the sealed waste canisters under continuous cooling and surveillance in an engineered storage facility for 20 to 30 years; (iii) Ultimate disposal of the cooled solidified waste in deep geological formations with added protection barriers. The first Indian vitrification facility for high level waste was commissioned at WIP, (Tarapur interim storage facility at Solid Storage and Surveillance Facility (SSSF), Tarapur. The second vitrification facility has been commissioned at BARC, Trombay to manage HLW generated during reprocessing of spent nuclear fuel from research reactors at site [4, 9]. The third vitrification facility is commissioned at Kalpakkam.

### ***1.3 Materials for reprocessing***

In Indian reprocessing plants, the various operations involving aqueous reprocessing employs nitric acid as the main process medium, which is used from room temperature to boiling point, and from dilute to concentrated solutions (up to 12M) [10,11]. Among the materials for reprocessing plant equipment, type 304L stainless steels (SS) and some valve metals like titanium, zirconium, etc are being used depending on the concentration and temperature of nitric acid employed [11, 12]. Apart from dissolvers and evaporators where high concentration (8-12M) of nitric acid at temperatures up to 400 K are used, austenitic stainless steels of AISI (American Iron and Steel Institute) type 304L SS are

extensively used for all other unit processes in the plant. The most widely used grades for nitric acid type are the low carbon type 304L or stabilized austenite grades – type 321 and type 347 [11]. These alloys resist corrosion up to a temperature of 353 K and concentrations up to 60%  $\text{HNO}_3$ . Stainless steels with higher levels of carbon, such as type 304 SS that are not stabilized with titanium or niobium, are subjected to intergranular attack in nitric acid at the heat-affected zone of the welds. This is a result of sensitization process, which is due to the precipitation of chromium carbides at the grain boundaries. The molybdenum grades (type 316, 316L, 317, 317L) are not preferred for nitric acid applications because molybdenum tends to promote the formation of sigma phase, which is less resistant to nitric acid. AISI type 304L SS is found to be a satisfactory material of construction for application in nuclear fuel reprocessing plant components such as pipelines, vessels and tanks [10-12]. At higher concentration than 8M nitric acid, at higher temperatures, and in the presence of oxidizing ions, the chromium oxide passive film becomes unstable leading to transpassive dissolution thus exposing the material to the corrosive acid [13, 14]. Under these circumstances, 304LSS is susceptible to uniform corrosion, intergranular corrosion, end grain attack, and galvanic corrosion. Such conducive conditions for corrosion are found in equipments such as acid dissolver, acid recovery evaporator, intercycle U+Pu evaporator, final plutonium nitrate concentrator, oxalic acid mother liquor evaporator, vitrification off gas treatment. The advanced nitric acid grade (NAG) SS with controlled chemical composition of impurities like S, B, P etc., and with higher Si, Cr etc. have also been found to undergo IGC under such aggressive nitric acid conditions [1,3]. Valve metals such as Ti, Zr, Hf, Nb, Ta and their alloys such as Ti–5% Ta, Ti–5% Ta–1.8%Nb etc have

been found to be alternative materials in such critical applications. The formation of  $\text{Ti}^{4+}$  in nitric acid medium facilitates the formation of a highly stable  $\text{TiO}_2$  which imparts a superior corrosion resistance to titanium. The presence of oxidizing species ( $\text{Fe}^{3+}$ ,  $\text{Cr}^{6+}$ ,  $\text{Ti}^{4+}$ ,  $\text{Si}^{4+}$ , etc) and fission products do not affect the corrosion performance of titanium as  $\text{Ti}^{4+}$  formed is highly inhibitive making Ti suitable in recycled nitric acid streams and reboiler loops. Despite these credentials, failures in acid condensers and evaporators have been reported due to the formation of semi protective oxide film. In these arenas, Ti-5% Ta-1.8%Nb and Zr have been found to be highly resistant. Zirconium extends an outstanding corrosion resistance due to the formation of dense, self healing and strongly adherent protective stable  $\text{ZrO}_2$  film and it does not form non-adherent oxide with poor corrosion resistance under condensing conditions as in the case of titanium [3]. However, zirconium is more expensive than titanium and has been reported to be susceptible to stress corrosion cracking in concentrated acidic conditions, particularly above 30% at boiling point.

#### ***1.4 Materials for storage of high level liquid waste***

In India, the high-level liquid waste generated from the reprocessing of reactor fuels are kept in the acidic condition in high-integrity stainless steel tanks. Neutralizing the acidic waste with caustic and storing it in carbon steel tanks increases the volume considerably and also forms precipitates and sludge which limits the flexibility in subsequent treatment of the waste. The waste tanks are in thick-walled concrete cells or underground vaults for appropriate shielding and are either double-walled or have a steel-lined vault to retain any leakage from the primary holding containers. The capacity of this outer container should be capable of retaining the entire contents of a holding tank. Stainless steel tanks in use

range from 70 to as much as 1000 m<sup>3</sup> capacity. Cooling systems (water) are provided to remove decay heat, to keep the temperature of the solution below 65°C in order to reduce the corrosion of the stainless steel. Storage tank systems should also provide for in-tank agitation, ventilation, monitoring, solution transfer from both inner and outer containers, vapor condensation, removal of gases produced by radiolysis, and off-gas filtration. Austenitic stainless steel of type 304L SS are being used as major construction material for these storage tanks and 304 SS is being used as underground vaults. Though stainless steels exhibit excellent corrosion resistance in nitric acid medium, the presence of oxidizing ions in combination with the radioactive heat elevates the corrosion potential to transpassive region rendering the steel to corrosive attack during long term storage.

#### ***1.4.1 Development of materials for high level liquid waste storage***

Toward development of materials for high level waste storage tanks, nitrogen containing austenitic stainless steels [15, 16, 17] and nickel based superalloys [18-20] are being explored as candidate materials. Nickel based super alloys have been found to possess good corrosion resistance in studies carried out in simulated high level waste medium [18-20], nevertheless, they are almost comparable to 304L SS in this medium [21].

Nitrogen containing, high nitrogen stainless steels are drawing attention as structural materials because of the well balanced combination of good mechanical properties and corrosion resistance [22]. The term “high nitrogen” steels (HNS) is used, if the steels contain more than 0.08 wt % nitrogen in a martensitic matrix or more than 0.4 wt % nitrogen with an austenitic matrix [23]. For austenitic stainless steels, even nitrogen levels higher than 0.06 wt% give significant improvement in corrosion properties. Nitrogen represents an economically and environmentally versatile alloying element [24].



The combination of a wide spectrum of properties of HNS has offered innumerable applications today in many industries. High nitrogen stainless steels containing nitrogen around 0.4 wt % are preferred for applications in chemical industry, marine environments, desalination plants, pulp and paper and for specific applications in nuclear industry. The beneficial effect of nitrogen on the mechanical property was first studied by Andrew [25] and the positive effect of nitrogen on the corrosion resistance was first reported by Uhlig [26]. Nitrogen dissolves interstitially in austenitic structures in relatively high quantities and produce significant solution hardening. Low nitrogen content can lead to the formation of sigma phase thus reducing corrosion resistance and high nitrogen content may lead to precipitation of  $\text{Cr}_2\text{N}$ , hence deteriorating localized corrosion resistance. Therefore, nitrogen content should be optimum to obtain a homogeneous microstructure. The credentials of nitrogen as an alloying element in austenitic stainless steels have been dealt with by many investigators [27, 28, 29]. Nitrogen is reported to enhance resistance to pitting corrosion, intergranular corrosion and stress corrosion cracking in certain environment [30, 31]. Nitrogen imparts grain size strengthening and is a better solid solution strengthener than carbon. Nitrogen being an austenite stabilizer reduces the amount of nickel required for stabilization. The role of nitrogen in enhancing passivity and pitting corrosion resistance is a well discussed subject [32].

Addition of nitrogen to 304L SS to improve the corrosion properties in nitric acid medium was considered for developing such materials for nitric acid applications (both reprocessing and high level liquid waste storage). In collaboration with Bulgarian Academy of Sciences, Bulgaria, type 304L SS with known amounts of alloying elements

like V, S, P, Si, Mn and different amounts of nitrogen ( 0.132%, 0.193%, 0.406%N) were manufactured in Bulgaria and tested in India for its corrosion property by ASTM A262 practice A, E, C, potentiodynamic polarization in nitric acid medium and chloride medium [33,34] and the cumulative results have shown improved corrosion resistance of the stainless steel alloys, with nitrogen addition. Nitrogen addition also showed enhanced mechanical properties with significant increase in yield strength with very good elongation [22]. Nitrogen addition has been reported to improve the sliding wear resistance and cavitation erosion resistance of austenitic stainless steels [22]. Based on the studies, the nitrogen added stainless steels have been found to be suitable for nitric acid applications where combined corrosion and wear resistances with improved mechanical properties are necessary.

### ***1.5 Corrosion monitoring***

Corrosion is one of the most important ageing mechanisms impacting the assets of plant component and equipments. Uncontrolled corrosion can cause leaks and component failures, bringing about a reduction in both the performance and reliability of important equipments, unplanned shutdowns, environmental contamination, contamination of products and loss of consumer confidence and not the last to mention is the potential harm to humans and costly in terms of repair. For this reason considerable effort must be made in corrosion control at all stages of a system's life, from the design table to the last stage of operation. Current corrosion inspection and monitoring typically requires planned periodic shutdowns to inspect the equipment. Scheduled shutdowns are costly in terms of productivity losses, restart energy and material costs. Unscheduled shutdowns are disruptive and often quite expensive. Inspection refers to short-term “one-off”

measurements taken in accordance with maintenance and inspection schedules. Corrosion monitoring describes the measurement of corrosion damage over a longer time period and often involves an attempt to gain a deeper understanding of how and why the corrosion rate fluctuates over time. Corrosion inspection and monitoring are most beneficial and cost-effective when they are utilized in an integrated manner. They are complementary and should not be viewed as substitutes for each other. In its simplest form, corrosion monitoring may be described as acquiring data on the rate of material degradation. The data need to be converted to information for effective decision making in the management of corrosion. This requirement has led to the expansion of corrosion monitoring into the domains of real-time data acquisition, process control, knowledge-based systems, smart structures, and condition-based maintenance. The desire for excellence in plant operation and safety demands for effective implementation of corrosion monitoring which helps mitigate corrosion:

- by providing an early warning of the damaging process conditions which may result in a corrosion-induced failure.
- by studying the correlation of changes in process parameters and their effect on system corrosivity.
- by diagnosing a particular corrosion problem, identifying its cause and the rate controlling parameters, such as pressure, temperature, pH, flow rate.
- by evaluating the effectiveness of a corrosion control/prevention technique such as chemical inhibition and the determination of optimal applications.
- by providing management information relating to the maintenance requirements and ongoing condition of plant.

Corrosion monitoring is the practice of measuring the corrosivity of process stream conditions by the use of “probes” which are inserted into the process stream and which are continuously exposed to the process stream condition. Corrosion monitoring “probes” can be mechanical, electrical, or electrochemical devices [35, 36]. Corrosion monitoring techniques could be direct or indirect. Direct techniques measure parameters that are directly associated with corrosion processes and indirect techniques measure parameters that are only indirectly related to corrosion damage. A second categorization scheme is into intrusive and nonintrusive forms. Intrusive techniques require direct access to the corrosive environment through a structure. Sensors and test specimens typify this approach. Nonintrusive methods require no additional hardware to perform a corrosion measurement. A further distinction is possible between on-line and off-line techniques. On-line techniques are those with continuous monitoring capabilities during operation, whereas off-line methods require periodic sampling and separate analysis. Based on the classifications, there are various corrosion monitoring techniques [37].

### ***Direct Techniques***

1. Corrosion Coupons (intrusive)
2. Electrical resistance (ER) (intrusive)
3. Linear Polarisation Resistance (LPR) (intrusive)
4. Electrochemical Impedance Spectroscopy (EIS) (intrusive)
5. Electrochemical Noise (EN) (intrusive)
5. Zero Resistance Ammetry (ZRA) (intrusive)
6. Potentiodynamic Polarisation (intrusive)
7. Thin Layer Activation and Gamma Radiography (intrusive / non-intrusive)
8. Electrical Field Signature Method (EFSM) (non-intrusive)
9. Acoustic Emission (AE) (intrusive)

### ***Indirect Techniques***

1. Corrosion Potential (non-intrusive)
2. Hydrogen Monitoring (non-intrusive)
3. Chemical Analyses

The most commonly used or the core of the industrial monitoring techniques range from non electrochemical methods such as coupon testing and electrical resistance measurements, to electrochemical techniques such as linear polarization resistance, electrochemical potential measurements, electrochemical impedance measurements [38, 39].

***Coupon tests*** are the most widely used for corrosion monitoring. In these tests, racks of coupons are immersed in the process fluid and are removed after planned intervals to measure the weight change and the corresponding corrosion rates are calculated. They may be used to quantify the severity of the corrosion attack and can be employed to identify some forms of localized corrosion. However, they provide only cumulative and retrospective information. Also, this method uses large number of coupons over a period.

***Electrical resistance methods*** are based on the gradual increase in the resistance of a conductor as its cross sectional area is reduced by corrosion. This technique can give reasonable indication of cumulative corrosion rate. However, it is incapable of recording instantaneous or short term changes in corrosion rate and it is not appropriate for use in systems, which are susceptible to localized corrosion. This method is sensitive to conductive deposits of corrosion products and it is also difficult or impossible to compensate adequately for temperature fluctuations typical of operating process streams.

***Polarization resistance measurement***, also known as linear polarization resistance is a direct current (DC) electrochemical method of corrosion rate estimation. It is primarily

useful in moderate or high conductivity systems where it can provide an excellent indication of uniform corrosion rate. This method is not useful where the conductivity of the solution is low and also in inhibited systems where absorbed layer of inhibitors interfere with the measurements.

***Electrochemical impedance spectroscopy*** (EIS) involves applying frequencies and low amplitude sinusoidal voltage wave to produce perturbation signals on the working electrode. The corrosion state can be predicted by analyzing the current response of the voltage or the frequencies. An important advantage of EIS is the possibility of using very small amplitude signals without disturbing the property being measured. The equivalent resistance and capacitance values are interpreted in terms of interfacial phenomena. Equivalent electrical circuits can be developed from this and used to provide information regarding the corrosion mechanism. Many researchers have established the application of EIS [40-42] in corrosion over the last 20 years, the most important application of EIS is in the coating area and for evaluating corrosion inhibitors.

#### ***1.5.1 Limitations of conventional techniques***

The greatest limitation of the conventional methods is the assumption that corrosion attack is predominantly uniform. In the majority of the situations, this assumption is not justified adequately. Most corrosion damage is due to localized corrosion such as pitting, crevice and stress corrosion cracking, and cavitation damage (erosion corrosion). Conventional technology, as well known techniques, in many cases is unable to provide a reliable indication for the estimation of corrosion rate. These limitations have severely constrained the use of corrosion monitoring technology for process control, in the past. The real corrosion monitoring or surveillance system should have a real time sensitive

indication and a link to the operating parameters. The former is achieved by modern electrochemical methods and the latter by having sensors to record the operating conditions.

**Electrochemical noise** [43-50] has gained popularity in the current scenario as a potentially corrosion monitoring tool because of the unique credentials the technique has over other conventional techniques.

### ***1.5.2 Advantage of electrochemical noise technique***

- *Among the techniques reported for studying the corrosion processes, it has been said that only electrochemical noise measurement method gives an instantaneous on-line indication of the corrosion events as these occur, and robust methodology to detect onset of a corrosion process like pitting, crevice corrosion, stress corrosion cracking etc.*
- *The technique is unique in that the ‘signatures’ from electrochemical noise sensors can be used to derive not only corrosion rates, but also mechanistic information about the corrosion type (general or localized).*
- *Localized corrosion processes which are difficult to monitor by other techniques, give particularly strong electrochemical noise signals, and hence electrochemical noise can detect and discern localized corrosion.*
- *The most attractive credential of this technique is that it does not polarize the corroding specimen and hence can be applied to real structures and is also not affected by conductive deposits. Whereas, most electrochemical methods for corrosion analysis use an external current or voltage source, and therefore the very corrosion signals, which need to be investigated, are disturbed.*

- *Because of the simplicity of the testing appliances, electrochemical noise method has attracted much attention in the field of electrochemistry. The instrument needed to make the measurements is simple, particularly with modern computer based data acquisition techniques.*
- *Electrochemical noise can be measured in potentiostatically-polarized conditions and in freely corroding systems. The first technique is suitable for the study of corrosion processes while the second technique is more appropriate for corrosion monitoring.*
- *Of particular interest is the fact that the electrochemical noise technique has application in low conductivity environment (solution resistance  $> 100,000$  ohms), where other electrochemical techniques fail to function, in such environments.*

However, due to the non-stationary nature of electrochemical noise signal, the data analysis has been an active area of research for its wide applications. Some of the limitation is also while dealing with electrochemical noise when many redox reactions are involved, such as stainless steel in alkaline permanganate solution. Another limitation is that electrochemical noise over-estimates very low corrosion rates. The data generated is enormous making data handling a tedious process, and variance still persists on the interpretations of electrochemical noise data.

### ***1.6 Electrochemical noise monitoring in nuclear waste storage tanks - International experience***

The Department of Energy (DOE) sites, USA, uses underground storage tanks made of carbon or stainless steel to store radioactive liquid waste generated from weapon



production and nuclear fuel reprocessing sites [51-53]. Historically, corrosion monitoring and control in nuclear waste tanks of DOE's site were accomplished through waste chemistry sampling and analysis, coupon measurement, linear polarization and electrical resistance, but with limited degrees of success. These techniques were highly expensive, time consuming and lacked real time corrosion information. In addition, these techniques indicated uniform corrosion occurring in the plant, but provided no indication of localized corrosion, though pitting and stress corrosion cracking were the primary modes of degradation in these materials. In 1995, the development and deployment of electrochemical noise probes in carbon and stainless steel waste tanks of Hanford, Savannah River Site (SRS), Oak ridge Reservation (ORR), Idaho National Engineering and Environmental Laboratory (INEEL) resulted in monitoring of corrosion in caustic and acidic waste produced from their nuclear installations. A brief summary of the development and deployment of the probes is described in the forthcoming sections.

#### ***1.6.1 Hanford Site***

The Lockheed-Martin Hanford Site has 177 underground carbon steel, single shelled and double shelled waste tanks that store caustic radioactive waste of variable composition, but generally containing nitrite/nitrate/hydroxide of sodium [51, 54]. Leaks were detected in one of the single shelled tanks in the 1950's and in many more single shelled tanks at later instances. The probable mode of failure was reported to be as a result of nitrate stress corrosion cracking and pitting. Based on several studies carried by the DOE sites toward development of EN probes, a prototype system was constructed and deployed in Hanford site in 1996. Subsequently, five additional systems were deployed in successive years, with improved design based on the experiences in the previous system, and the

fifth probe was installed in August 2001. The electrochemical noise probe comprised of three identical electrodes made of stainless steel immersed in the waste and automated data collection system. Eight channels of electrodes were used, of which four channels comprised of C-ring (stressed, notched, pre-cracked) and four bullet electrodes for detecting SCC and pitting / uniform corrosion respectively. Individual radiation-resistant insulated conductors are attached to each electrode and lead up through the stainless steel probe body to the probe top, from where cables are used to transmit signal from the probe electrodes to the data collection hardware. Most of the data showed that the tanks primarily underwent uniform corrosion at very low rates and few EN transients indicative of unknown electrochemical events also were recorded.

#### ***1.6.2 Savannah river site (SRS)***

The alkaline waste generated from Savannah river site in Aiken, South Carolina, is being stored and handled in fifty-one underground carbon steel tanks for the last few decades. SRS initiated development of a remote, real time monitoring probe integrating laser Raman spectroscopy for chemical analysis and electrochemical noise for corrosion monitoring [51]. A height adjustable probe was designed to make measurements at various heights due to the dynamic waste composition resulting from frequent additions and removal. A moveable probe head mounted on a flexible cable deployed from a reel mechanism housed in a confinement chamber has EN electrodes attached to the exterior while the Raman laser probe is housed inside. The sample for Raman chemical analysis is drawn into a sample chamber through a filter. The probe head is attached to stainless steel cable that houses and protects the cables and tubes associated with each of the technologies. Laboratory testing, which was performed with electrodes similar to those

for the actual probe, showed that the cable type and length and the use of an intrinsic safety barrier did not alter or affect the acquired signal.

#### ***1.6.3 Oak Ridge National Laboratory (ORNL)***

Low level liquid waste produced at ORNL is stored in waste tanks fabricated from 304L stainless steel pipes with a capacity to store 50,000 gallons of waste [51]. Prior to the deployment of the system in 2001, laboratory testing were carried to characterize the behavior of 304L SS in simulated waste to support field data interpretation. The system for ORNL was deployed in 2001 and has been successfully collecting data on a full time basis and produced EN data for uniform and pitting corrosion.

#### ***1.6.4 Idaho National Engineering & Environmental Laboratory (INEEL)***

High level acidic waste containing high concentration of chloride and fluorides produced from reprocessing of spent nuclear at INEEL was stored in 347 and 304L stainless steel tanks [51, 52]. Corrosion monitoring in these tanks consisted of remote visual inspection using video cameras and coupon measurements. At INEEL, a preliminary programme was initiated to show the applicability of EN on 304L in nitric acid and simulated waste solution [51, 52]. These testing demonstrate that EN measurements can be made with austenitic stainless steel used in construction of INEEL HLW tanks with the ultimate goal of implementing the deployment of the probes in the HLW tanks.

### ***1.7 Types of Noise***

Noise is generally understood as any unwanted disturbance that interferes with a desired signal. They are also called interferences. To name a few of the noises,

Fluctuations in fluid flow (Hydrodynamic noise) (ii) meteorological variations (scintillation noise) (iii) errors in computation (round off noise) (iv) quantization noise in analog to digital conversion (v) interference in the outer space (cosmic noise) (vi) vibrations from the earth ground (seismic noise) (vii) background noise are the environmental noise, mechanical noise from refrigerators, air conditioning, motors etc., (viii) The variability in gene activity between cells in genetically identical populations (Transcriptional noise). etc.

(ix) Since electric current is considered to originate from procession of electrons or particles which have thermal kinetic energies and random components of velocity, the procession is not perfectly regular, rather random producing noise which necessarily appears in electrical communications as fundamental noise which are the thermal, shot and flicker noise.

Thermal noise (Johnson - Nyquist noise) is caused by random movement of charge carriers by virtue of its thermal energy and causes random variation of current or voltage. This noise can be reduced by reducing temperature of the circuit. It was first observed by Johnson of Bell telephone Laboratories in 1927, and a theoretical analysis was given by H.Nyquist in 1928 and hence this noise is also called the Johnson noise or Nyquist noise.

Shot noise occurs due to discrete nature of charge carriers in any device by virtue of their kinetic energy. It occurs in the emission current of thermionic valves, semiconductor junction devices. In many ways, shot noise and thermal noise are similar as they occur due to random fluctuations of a large number of electrons and the power spectral density of shot noise and thermal noise is uniform.

Flicker noise (or  $1/f$  noise, pink noise, semiconductor noise) is associated with conduction process in semiconductor devices and occurs in transistors, diodes, resistors etc.. The power spectral density of flicker noise increases as frequency decreases.

In general, noise is a random signal consisting of frequency components that are random in both amplitude and phase.

## **1.8 Electrochemical noise : definitions & literature review**

### **1.8.1 Random process**

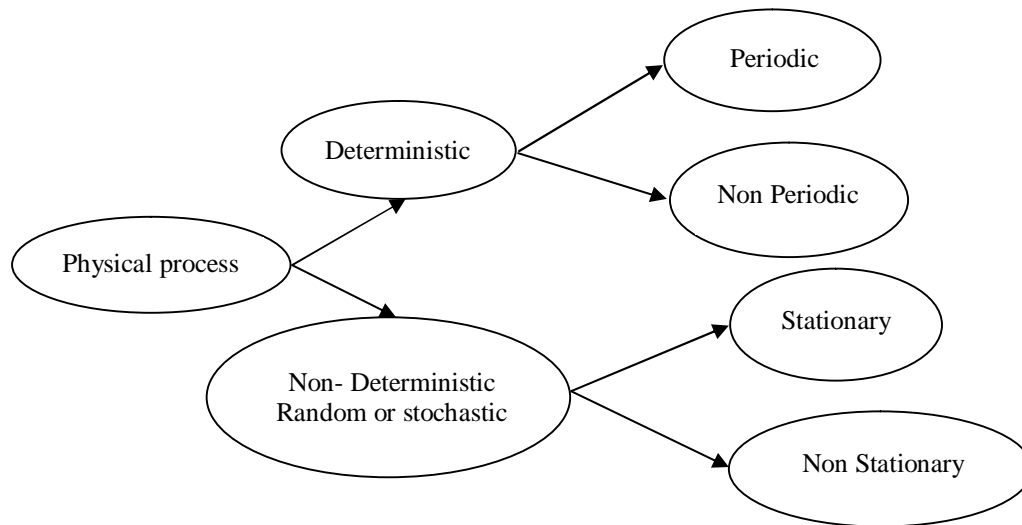


**Figure 1.3 The classification of physical process**

All physical processes are classified into deterministic or non deterministic [44, 55] (random or stochastic). Deterministic processes may be periodic or non periodic

(transient) and can be mathematically defined by time varying functions. Sawtooth and step functions used in polarization and sinusoidal and pseudorandom perturbations used in electrochemical impedance studies belong to the deterministic processes. Fluctuations of corrosion potential are random and are thus non deterministic and should be analysed by statistics or probability rather than algebraic equations. Electrochemical noise (EN) is a random low frequency process which can be stationary or nonstationary. They are described by probability density functions or statistical terms. For a stationary process, the first moments or mean and the statistical properties are invariant with time, such as those with low rates of uniform corrosion. Whereas, a non stationary random process have time varying functions that are determined by obtaining instantaneous averages over the set of time records forming the process. EN produced during passivity breakdown and pitting initiation is an example of a deterministic process [56] and thermal noise that results from electron vibration is classified as non-deterministic.

### ***1.8.2 Electrochemical noise - Definition***

The term electrochemical noise [43-50, 57, 58] is a generic term used to describe the low level, low frequency spontaneous fluctuations of potentials or current that occurs during an electrochemical process. It manifests itself in two guises, as potential noise or current noise, depending on the mode of measurement.

#### ***1.8.2.1 Electrochemical potential noise***

Electrochemical potential noise describes time dependant fluctuations in corrosion potential, and is usually in the range of mV. Electrochemical potential noise is measured between a working electrode or between two working electrodes coupled through a ZRA

and a noise free reference electrode or a pseudoreference electrode. Pseudoreference electrode is made from the same material as that of the working electrode.

#### ***1.8.2.2 Electrochemical current noise***

Electrochemical current noise describes the time dependant fluctuations in corrosion current, usually in the range of  $\mu\text{A}$ . Electrochemical current noise is measured between a pair of identical working electrodes, with the current being measured using a zero resistance ammeter (ZRA) to ensure that the two electrodes are at the same electrode potential. Electrochemical current noise may also be measured as the current from a single electrode that is held at a fixed potential.

#### ***1.8.3 How potential and current noises emerge?***

The reason cited, for the change in potential is a minute transient change in the electrical charges on the electrode produced as a result of cathodic and anodic reactions during the corrosion processes [43, 44, 49]. These spontaneous fluctuations in the electrical quantities manifest in the form of potential noise and current noise signals during different corrosion processes such as uniform corrosion, localized corrosion and passivation of electrochemical system. The electrochemical noise fluctuations appear to be connected to local variations in the rates of anodic and cathodic reactions as a consequence of both stochastic processes (breakdown and repassivation of the passive film) and deterministic processes (film formation and pit propagation). The frequency of current and potential fluctuations is in the range of 1Hz or less. Since the electrochemical noise of a freely corroding system is a low frequency signal, it usually has maximum amplitude at frequencies  $< 10^{-5}$  Hz.

#### ***1.8.4 Sources of electrochemical noise***

The sources of electrochemical noise may be classified into three categories [44, 46, 49] Charge transfer effects contribute to noise, whose spectral density, the amount of noise present in a given bandwidth, is essentially constant over a wide range of frequencies and is of low amplitude. This category covers noise originating from thermal agitation of charge carriers; noise caused by charge being transferred in discrete amounts and by other such phenomena.

A second source of noise relates to surface processes occurring on the electrode and specifically to their inhomogeneties. These give rise to fluctuations at frequencies of approximately 1Hz and below. The observed spectral density of these fluctuations in general varies with frequency and the amplitude can be much higher than that caused by charge carrier effects.

At very low frequencies, environmental changes, such as variations of physical and chemical parameters of the observed system, result in low fluctuations of the electrode potential or current. These often have the appearance of drift of the electrode potential and can sometimes be accounted for by existing theories of electrode thermodynamics and kinetics.

The other sources of electrochemical noise are as listed below:

***(i) Uniform Corrosion:*** Uniform corrosion might be expected to be free of noise, with atoms leaving the metal surface at a uniform rate. However, even a perfectly homogeneous dissolution process gives rise to some fluctuations in rate akin to Brownian motion. Furthermore, there are a number of mechanisms by which it is expected that even a uniform dissolution process will occur as a series of bursts.



*ii) Pitting Corrosion:* The pitting process is often found to result in metastable pit nucleation and propagation, giving rise to current transients lasting for a time of the order of one second, and involving a charge of the order of  $10^{-6}$  C (corresponding to around  $10^{12}$  atoms). Thus, the noise associated with pitting corrosion is much larger than that observed for uniform corrosion.

*iii) Mass Transport fluctuations:* Fluctuations in the boundary layer thickness for a mass transport will give rise to fluctuations in the current. This will be observed most strongly in turbulent conditions, although even in nominally laminar conditions, it is expected that some fluctuations will occur.

*iv) Bubble nucleation, growth and detachment:* When hydrogen evolution is the predominant cathodic reaction, it is clear that the growth and detachment of hydrogen bubbles gives rise to fluctuations in the flowing current.

*(v) Corrosion processes* such as crevice corrosion, stress corrosion cracking, intergranular corrosion, erosion corrosion, microbially induced corrosion and corrosion fatigue also generate electrochemical noise, which are characteristic of these processes.

### ***1.8.5 Cell Configuration***

American Standard for Testing and Materials (ASTM) [44] has recommended a three electrode configuration for electrochemical noise measurements. Two types of configurations are described.

***Configuration 1:*** The configuration involves two of the three electrodes as working electrodes prepared from the same alloy, so as to be nominally identical. These two electrodes are referred to as the working electrode pair (WE). The third electrode may be

either a low impedance, low noise reference electrode or identical to the other two electrodes (pseudoreference electrode). The use of identical working electrodes ensures that any observed fluctuations originate from the test electrodes. Also environmental changes tend to affect both electrodes equally, reducing the amplitude of the resultant drifts. A low impedance, low noise reference electrode is recommended, as high impedance reference electrode tends to be more susceptible to electrostatic pickup. It is desirable to minimize the bias caused by such environmental noise. Hladky and Dawson [59] used platinum reference electrode as compared to a calomel electrode, to study the localized corrosion of mild steel in chloride solution inhibited by nitrate. The authors opined that Pt electrode with low impedance is ideally suitable for the measurements despite lacking a well-defined half-cell potential. A saturated silver/silver chloride electrode with a low rate of leakage has also been found to be suitable. To the contrary, calomel reference electrodes are unsuitable for low-level signal measurements because of their extreme susceptibility to electromagnetic and acoustic pick up. A pseudoreference electrode may be used instead of a conventional reference electrode to measure electrochemical potential noise. It is best to use a material identical to the electrode pair that has either the same area of one working electrode or the sum of the two areas of the working electrodes. When an identical material is not used, it is recommended that the pseudoreference electrode have noise signal characteristics, such that, their amplitudes are not greater than the magnitude of the potential noise signal to be measured. The characteristic potential noise of the pseudoelectrode in the electrolyte should be measured and subtracted as background noise from the noise measured from the working electrode

pair, or alternatively correction factors [44] could be applied to negate the noise contribution from the pseudoreference electrode.

**Configuration 2:** The configuration involves a conventional three-electrode arrangement similar to that described in the ASTM Test Method G5 [60] to conduct the experiment.

The configuration comprises of a working electrode, two counter electrodes, and a luggin capillary with salt bridge connection to the reference electrode. The luggin-probe salt bridge separates the bulk solution from the saturated calomel reference electrode. The potential of the working electrode is measured relative to the reference electrode and the current is measured between the working electrode and counter electrode.

### ***1.8.6 Measurement of Electrochemical Noise***

There are two related, but distinctly different approaches to the measurement of electrochemical noise.

#### ***1.8.6.1 Individual measurement of current or potential noise***

Electrochemical noise measurements can be done by individually measuring the electrochemical potential noise or electrochemical current noise. These measurements are made at open circuit potentials or by potentiostatic and galvanostatic [44, 46, 49] methods to measure electrochemical current and potential noise respectively. Under galvanostatic/potentiostatic control, the cell configuration 2 is followed. Here, the current is measured between the working electrode and an inert counter electrode, whereas the potential of the working electrode is measured against a reference electrode. Most commercial potentiostats/galvanostats measure current more accurately than potential,

making the potentiostatic electrochemical noise measurement the more accurate of the two options.

#### ***1.8.6.2 Simultaneous measurement of potential and current noise***

For analysis it is of great value to measure both current and potential noise simultaneously. The measurement of current noise essentially requires a short circuit condition, whereas potential noise must be measured with a high impedance load. A common experimental arrangement uses three identical electrodes, where one pair acts as a current noise source under short – circuit conditions, the second as a potential noise source under open circuit condition. One electrode acts as a common electrode.

All the measurements based on simultaneous acquisition of potential and current noise, can be made on a system at open circuit potential using the cell configuration<sup>1</sup> for arrangements.

#### ***1.8.7 Data Collection***

Data collection involves sampling of the measured parameter, potential or current, at predetermined intervals for a required number of samples.

***1.8.7.1 Sampling and aliasing:*** The frequency resolution that is obtained when the data is processed depends on the sampling interval chosen to record the data. Thus the potential and current should be recorded in a systematic way. If the sampling interval ' $\delta t$ ' were chosen too close, then the result would be an increase in computation time. On the other hand, if the interval is chosen too far, the problem of aliasing will occur. If we take regular samples of a signal above the Nyquist frequency (If the sample period is  $\delta t$ , the frequency of  $\frac{1}{2} \delta t$  is known as Nyquist frequency), the results are exactly the same as if

we had taken samples from a signal of the same amplitude, but at frequencies below Nyquist frequency. This phenomenon is called aliasing [46, 49]. It is essential to avoid aliasing by filtering out frequencies above the Nyquist limit before sampling. The power values of the high frequency and low frequency components will overlap resulting in flattening of the high end of spectrum. Thus the sampling interval is decided by the frequency resolution required.

From the sampling theorems, for a time interval  $\delta t$ , the maximum frequency definition that can be obtained without aliasing is  $F_c$ , and both are related by

$$F_c = 1/2\delta t \quad (1.1)$$

and minimum frequency resolution that can be obtained is

$$F_{\min} = 1/N\delta t \quad (1.2)$$

Where  $N$  = Total number of samples in the data record.

#### ***1.8.7.2 Antialiasing Filtering***

To avoid aliasing, components of frequency greater than Nyquist frequency ( $f_s / 2$ ), has to be eliminated before analog to digital (A/D) conversion, using low pass filter [46, 49, 61, 62]. The cut off frequency ( $f_c$ ) of the low pass filter has to be fixed at a value marginally lower than  $f_{\max}$ , about 0.7 to 0.8  $f_{\max}$  (0.35 to 0.4  $f_s$ ) depending on the slope of the filter roll off, where  $f_{\max}$  is the upper limit of Nyquist interval that can be correctly analyzed. The frequency range that is analyzed is limited to  $[0, f_c]$ . As  $f_c$  is related to sampling rate  $f_s$ , EN measurements in a large frequency range requires the use of low pass filters also varying in a large frequency range. As these filters are highly expensive, some manufacturers of EN acquisition have adopted filtering technique based on digital processing which has been discussed by Bastos et al [62]. One method involves data

sampling at a fixed high frequency and using low pass filter at a fixed cut off frequency, and the average over 'n' points is retained, where  $n = (f_{\text{hfs}} / f_s)$  and  $f_{\text{hfs}}$  represents the fixed high frequency sampling and  $f_s$  is the desired sampling frequency.

#### ***1.8.8 Data treatment : Trend removal***

The potential and current noise raw data contains noise component superimposed on a Direct Current (DC) trend. The DC drift or trend is defined as the variation of the mean current or potential divided by time and is not useful for the corrosion phenomenon. Since the noise signals are measured between two nominally identical electrodes, the mean value of the difference of potential and current flowing between them is expected to be zero. The electrochemical noise signals should appear as quasi-random fluctuations around zero. Since the calculation of the power spectral density (PSD) and the standard deviation presupposes a stationary process, it is necessary to apply some procedure to the incoming signal in order to eliminate its drift. The reasons for this behavior may be diverse and difficult to understand. The signal though may be stationary, it may yet contain frequency components lower than  $1/T$  (where  $T$  is the sampling period), or there may be some slow alteration of the system under study that causes the drift. In corrosion studies, progressive deterioration of the electrodes can occur resulting in lack of stationarity. Many of the natural processes could be non stationary and non linear. The former may introduce a DC drift since its statistical parameters change over time. The effects of drift in the noise data on the analysis is well discussed in literature. Any DC drift can introduce new, false frequency components. The presence of drift implies that the signal is non stationary and all standard analysis procedures become invalid. Bertocci et al [63, 64] have shown that a linear drift in the potential/current noise produces  $1/f^2$

slopes in the power spectral density plots at low frequencies and affects the standard deviations of current and potential noise used for computation of noise resistance. The choice of the method is again one of the most difficult problems in electrochemical noise measurements. The procedure must be simple and straightforward, must effectively attenuate the low frequency components without eliminating useful information or create artifacts. To effectively remove the trend leaving a valid signal is yet a challenging task. Some of the procedures [65] include moving average removal (MAR), linear detrending, polynomial fitting, analog or digital high-pass filtering. Wavelets [66, 67] and artificial neural networks [68] have also been used for trend removal. As it is beyond the purview of this thesis to elaborate on all the methods, some of the frequently used methods are briefed. Polynomial fitting [69] is performed using squares regression, and then noise is obtained as the difference between experimental and predicted data. MAR [70] uses moving average to compute noise. Butterworth [71], uses analogical filters and is a part of the Matlab Signal Processing Toolbox©. Mansfeld et al [72] have pointed out considerable drawbacks on the recently proposed moving average removal method and hence has not recommended this method for trend removal. However, Ashassi et al [73] obtained good correlation between noise resistance and polarization resistance using the MAR method for detrending, in their studies on inhibition effect of new Fuchsin dye on the corrosion of mild steel in 1 M HCl. An increased order of polynomial results in more trend removal and also leading to loss of valuable data. Literature study reveals varied opinions on the credentials and limitations of the various trend removal methods. Among these methods for trend removal, the linear fit was found to be most commonly used by researchers [46, 65, 74-76, 77]. This method is based on the assumption that the drift

follows a linear relationship. In this method, the experimental raw data is fit by linear method and the linear regression functions generated for the potential-time and current-time records are subtracted from the raw data.

### ***1.8.9 Data Analysis***

#### ***1.8.9.1 Visual examination of the time record***

The time records present the instantaneous potential or current fluctuations as a function of time and are considered to be a standard method to record and view data. EN data can be interpreted by investigating and analysing the shape, size and distributions of potential or current transients observed during the corrosion processes. The potential–time record or current-time record gives typical fingerprints for various corrosion processes like pitting, crevice and stress corrosion cracking (SCC) [43, 46, 57, 59, 78-81]. This is a very effective method of detecting specific transients such as those generated during pit initiation or SCC. It is also possible to see clear-cut signals, which may be generated during crevice or pitting corrosion and the standard deviation of the signal can be estimated simply by observing the ‘width’ of the signal trace. It is recommended that a visual examination of the time record should always be the first part of a data analysis procedure. With experience, it should be possible to identify different corrosion mechanisms from raw noise data.

Nevertheless, the time records cannot be considered as conclusive evidence of the processes and hence, the acquired electrochemical noise time records should be further analysed in the time domain (statistical) or alternatively, data is converted to the frequency domain (spectral) using mathematical algorithms such as FFT or maximum entropy method (MEM).



### ***1.8.9.2 Data analysis in the time domain (statistical analysis)***

In the time domain, the voltage or current noise signal is plotted as a function of time. A number of statistical parameters can be derived from the noise-time record.

#### ***i) Mean***

The mean [46, 48, 49] is not a part of the noise measurement, especially for measurement made between two nominally identical electrodes, where expected value of the mean is zero. However, the actual value of the mean has been of significance in some of the parameters used to detect localized corrosion and it clearly does not contain information about the behavior of the electrodes.

#### ***ii) Standard deviation or variance***

This is described as the root mean square (rms) voltage after having subtracted the DC component and is a measure of the AC power of the signal. The standard deviation of current ( $\sigma_i$ ) and voltage ( $\sigma_v$ ) can represent the corrosion status of the metal and permit the identification of the nature of the attack.

The standard deviation can be evaluated as

$$\sigma = \sqrt{\frac{\sum_{i=1}^n (x_i - \bar{x})^2}{n}} \quad (1.3)$$

### **iii) Localized corrosion parameter**

#### **a) Coefficient of Variation of Current (CVC)**

This is defined as standard deviation divided by mean. A large CVC of the current is associated with large events and hence with localized corrosion [46, 49]. However, this parameter might not be useful in cases where coupling of two nominally identical electrodes would give mean current to be almost zero.

#### **b) Localization Index (LI) or Pitting Index (PI)**

It is defined as the rms current divided by the standard deviation.

$$PI = i_{rms}/\sigma_i \quad (1.4)$$

$$\sigma_i = \sqrt{\frac{\sum_{i=1}^n (x_i - \bar{x}_i)^2}{n}} \quad \text{and} \quad i_{rms} = \sqrt{\frac{\sum_{i=1}^n x_i^2}{n}}, \text{ n being the number of data points.}$$

Where,  $\bar{x}_i$  = Mean of the detrended noise data,

$\sigma_i$  = standard deviation of current noise

and  $i_{rms}$  = root mean square current noise

A range of values of (pitting index) PI has been reported for different corrosion mechanism under the name-pitting index (PI) [82].

Type of corrosion	pitting index
Uniform	0.001 < P.I. < 0.01
Mixed	0.01 < P.I. < 0.1
Localized	0.1 < P.I. < 1

***Table 1.1 Range of PI for various corrosion processes [82]***

Table 1 shows the correlation between pitting index (PI) and type of corrosion.

***iv) Charge in transient (CIT)***

CIT has been shown to give a reasonable estimate of the magnitude of pitting events. Charge in the elementary transients making up noise signals can be estimated from a combination of the current and potential noise as,

$$q_a = \frac{\sqrt{(E_n^2) \times (I_n^2)}}{2Bb} \quad (1.5)$$

Where,  $q_a$  is the charge in transient,  $\overline{E_n^2}$  is the potential noise power,  $\overline{I_n^2}$  is the current noise power,  $B$  is the Stern-Geary coefficient, and  $b$  is the bandwidth.

***(v) Noise resistance ( $R_n$ )***

Electrochemical noise resistance ( $R_n$ ), a parameter first proposed by Eden [83] is obtained by statistical evaluation of time records and is defined as the ratio of the

standard deviations of potential noise ( $\sigma_v$ ) to the standard deviation of current noise ( $\sigma_i$ ) [83, 84]. Noise resistance is represented in equation (1) as:

$$R_n = \sigma_v / \sigma_i \quad (1.6)$$

Several researchers claim noise resistance to be equivalent to polarization resistance ( $R_p$ ) [85-90]. This allows the potential noise to be modeled as the action of the current noise on the metal solution impedance, with the latter usually treated as  $R_p$ .

Enormous efforts have been made by researchers to find the physical meaning of  $R_n$  and its similarities with  $R_p$ . Kelly et al [91] have studied electrochemical noise in stainless steel and mild steel in solutions ranging from pH 1 to pH 7 and concluded that  $R_n$  generally tracks  $R_p$ .

#### *(vi) Skewness and Kurtosis*

Skewness and kurtosis indicate the shape character of distribution of the noise data [46, 92, 93]. The skew is a dimensionless description of the extent to which the distributions of values are skewed about the mean, or in simple terms skewness characterizes the asymmetry of distribution of the data set around the mean value of the data set. Kurtosis gives a measure if the data is peaked or flat compared to Gaussian distribution. Kurtosis of a normal (Gaussian) distribution is 3 and higher values indicate more sharply peaked distribution than a normal distribution and kurtosis less than 3 indicates flat topped distribution. Skewness and kurtosis of electrochemical noise is defined using the second, third and fourth moments, by the following equations [92].

$$\text{Kurtosis} = m_4 / m_2^2 \quad (1.7)$$

$$\text{Skewness} = \frac{m_3}{m_2^{2/3}} \quad (1.8)$$

Where  $m_2, m_3, m_4$  are second third and fourth moments respectively

$m_2 = 1/N \sum_{l=1}^N (i - \bar{i})^2$  ,  $m_3 = 1/N \sum_{l=1}^N (i - \bar{i})^3$  ,  $m_4 = 1/N \sum_{l=1}^N (i - \bar{i})^4$  and  $i$  represents potential or current noise.

Skewness and kurtosis have been used by several investigators [46, 50, 94] to identify corrosion mechanism. Reid and Eden [95] have patented values of kurtosis and skewness parameters derived from statistical evaluation of time records to identify corrosion mechanism.

Mechanism	Potential		Current	
	skewness	kurtosis	skewness	kurtosis
General	< ±1	< 3	< ± 1	< 3
Pitting	< -2	>> 3	> ± 2	>> 3
Transgranular SCC	+ 4	20	- 4	20
Intergranular SCC ≠1	- 6.6	18 to 114	1.5 to 3.2	6.4 to 15.6
Intergranular SCC ≠2	- 2 to -6	5 to 45	3 to 6	10 to 60

***Table 1.2 Reid and Eden's table of skewness and kurtosis values for various corrosion processes [95]***

### ***1.8.9.3 Data analysis in the frequency domain (spectral analysis)***

Noise spectra in the frequency domain are represented either as

(i) amplitude (decibel, dB) plots

(ii) noise power or PSD plots

In both cases, log of frequency (Hz) is plotted against log spectral power density ( $V^2/\text{Hz}$  or  $A^2/\text{Hz}$ ) or against the amplitude ( $V/\sqrt{\text{Hz}}$  or  $A/\sqrt{\text{Hz}}$ ). Noise amplitude is square root of noise power, given by  $\text{dB} = 20 \log (\text{voltage ratio})$  [44, 49].

A common feature of the PSD plot is that the white noise (which is independent of frequency) for uniform corrosion appears in the lower frequency region, and the  $1/f^n$  noise for localized corrosion appears in the higher frequency range. Several parameters can be evaluated from the power spectral plots which are related to corrosion mechanism and the extent of corrosion. The slope of the  $1/f^n$  noise is called the roll off slope which is related to the type of corrosion. The frequency at the cross point between the white noise and the  $1/f^n$  noise is defined as the roll off frequency. The area under the power spectrum curve contains the total power in the signal, and is identical to the standard deviation calculated from the time record. Thus as the frequency spectrum moves to higher power spectral densities, the rate of reaction may be expected to increase. Periodic signals will clearly give rise to a peak in the power spectrum, and these may be related to crevice or pitting corrosion. Hladky and Dawson [96] have studied the crevice attack of 'shape memory' alloy (Ti-Ni) in 0.3M HCl. Different types of corrosion generate different shapes of electrochemical voltage and current signals, which is reflected in the PSD values. Since the noise signals in certain time interval can be expressed by only one PSD curve in the frequency domain, there exist some argument on how the shapes of PSD plots, the roll off slope and roll off frequency are related to the corrosion processes. Bertocci and Yang-Xiang [97] believed that the roll off

frequency of PSD is related to the time constant of repassivation and reflects the degree of aggressiveness of the local environment inside the pits. Fakuda and Mizuno [98] have studied the current transients for pure iron and stainless steel and have shown that, in the passive state, the roll off slope is zero, which meant ‘white’ noise in both low and high frequency ranges, while the slope value steeply decreased to below  $-1$  before pit generation. There are many controversial points about the experimental results and explanations about the noise spectrum. Pujar et al [99] in their studies on pitting corrosion of 316 SS in chloride medium, have found that roll off slope are not true indicators of corrosion mechanism. Bagley [100] found that different corrosion types cannot be distinguished reliably on roll off slope values. Mansfeld and Xiao [101] opined that the conclusion made by Searson and Dawson [102] that a slop of  $-20$  dB is characteristic of localized corrosion was not always true. The physical meaning of roll off slope and the type of corrosion is still a subject under debate.

Analysis by Gabrielli et al [79] has indicated that when the current transient shows a sudden death, the high frequency limit of PSD varies like  $f^2$  whatever the shape of the transient. A slow rise followed by a slow death gave rise to an  $f^4$  trend. Therefore, it seems probable, a definite relationship can be established between the noise transient and the noise spectrum.

Shi et al [94] from their studies on pitting corrosion of stainless steels and pure aluminum in sodium chloride medium proposed new indices,  $S_E$  and  $S_G$  to evaluate pitting corrosion by dimensional analysis of three parameters of PSD,

$$S_E = f_c^2 \cdot \sqrt{k} \quad \text{and} \quad S_G = \frac{w}{f_c \cdot k} \quad (1.9)$$

Where,  $k$  is the roll off slope,  $f_c$  is the critical frequency or roll off frequency, and  $w$  is the low-frequency plateau level.  $S_E$  was found to be proportional to the rapid potential oscillations and higher amplitude fluctuation and can be used as an index to characterize pitting corrosion.  $S_E$  depicts the distribution behavior of electrochemical noise, while  $S_G$  could be used to depict the slower corrosion processes (adsorption, desorption, diffusion etc).

Legat and Dolecek [103] in their investigation on corrosion of various metal solution combinations have established a correlation between corrosion current density obtained from Tafel extrapolation and the PSD values. It was established that the average PSD of measured current noise, PSD [I] at higher frequency intervals (10 mHz to 250 mHz) correlates with the corrosion current density as:

$$\overline{PSD(I)}(\omega_2 - \omega_1) = \frac{1}{(\omega_2 - \omega_1)} \sum_{\omega_1}^{\omega_2} F(\omega)^2 \Delta\omega \quad (1.10)$$

Where  $\omega_2 - \omega_1$  is the frequency interval on a log scale,  $F(\omega^2)$  is the PSD value of the electrochemical current in decibels, and  $\omega$  is the frequency step on a log scale.

The authors opined that a good correlation between the PSD (I) and corrosion current density confirms that, PSD (I) at higher frequencies could be used as an exact measure of general corrosion. Although some investigators argued that features of the PSD curves such as the slope of the decaying power with frequencies, can be related to corrosion rates, it remained that much useful information is lost when real time data is converted into frequency domain [104]. Since PSD is based on a signal averaging method (such as FFT), it represents an average of system behavior during the selected data acquisition period rather than discrete or localized events. For this reason, PSD is not particularly



useful for corrosion monitoring in comparison to electrochemical noise measurement-time plot. However, PSD plot is useful for determining and visualizing how the amplitude of an electrochemical noise measurement varied as a function of frequency.

**(i) *Fast Fourier Transform***

The most commonly used mathematical function for converting signals in a time domain to frequency domain is the Fast Fourier Transform (FFT) and Maximum Entropy Method (MEM).

FFT performs a spectral analysis of the random transient of the electrochemical noise signal in a frequency range dependent upon the sampling time and the length of the data recording. It provides an exact description of the frequency content of the signal analyzed, if it is assumed that the signal is one cycle of a periodic waveform with all the cycles before and after the measurement period being exactly the same. This assumption leads to a number of complications. Firstly, if the mean value of a signal is drifting with time, this is interpreted as a saw-tooth waveform, and creates frequency components. Second, the implied ‘joining-up’ of the start and the end of the time record is liable to create sharp transitions, which are not representative of the signal. These two problems are overcome by pre-processing (drift removal and windowing) of the signal before undertaking the Fourier transformation. The FFT produces noisy spectra and is appropriate for repetitive signals and the data sets with a reasonable number of sample points [44] (> 1040, 2080 S .. so on).

**(ii) *Windowing***

It is a common practice to perform a trend removal before analyzing electrochemical noise signals. This also serves to set the signal mean to zero. This may still leave sharp

transitions at the end of the signal, and these are eliminated by multiplying the signal by a windowing function, which are zero at the ends of the time record and one in the center. It is important to conduct trend removal before windowing. If the windowing is done first, the subsequent trend removal will destroy the benefits of the windowing process. The modified time record is transformed to the frequency domain, usually using the Fast Fourier Transform (FFT). The resultant frequency spectrum must then be normalized to relate the power present in the spectrum to that present in the signal.

*(iii) Maximum Entropy Method (MEM)*

MEM was developed by Burg [105] to analyze a limited number of sample points in geophysical studies. While Fourier transform directly calculates the frequencies actually present in the time record being analyzed, the maximum entropy method (also known as the all-poles or autoregressive model) calculates the coefficients of a series of filters that would have to be applied to white noise to obtain the observed time record [44, 46, 49]. An advantage of MEM is that it gives continuous and smooth curves and hence roll – off slopes and frequency cut off can be easily evaluated. MEM is preferable in many respects when the time data is only weakly stationary. MEM gives a set of coefficients, to calculate the power spectral density for any frequency. As FFT and MEM produces identical spectra from electrochemical noise except that the former is noisy, the selection of the method and display as either PSD or amplitude would be a choice left to the investigator [44].

*(iv) Spectral noise resistance ( $R_{sn}$ )*

Mansfeld and co-workers [106] introduced a parameter called the spectral noise response,  $R_{sn}(f)$ , which has the unit of resistance and allows evaluation of the frequency

dependence of electrochemical noise data similar to the analysis of power spectral density plots.

$$R_{sn}(f) = \left| \frac{V_{PSD}(f)}{I_{PSD}(f)} \right|^{1/2} \quad (1.11)$$

Where  $V_{PSD}(f)$ ,  $I_{PSD}(f)$  are the power spectrum density functions of voltage and current signals. This ratio of the PSD of the potential to that of the current is termed as the electrochemical noise impedance.

At very low frequencies, the spectral noise resistance  $R_{sn}^o$  is determined as the DC limit of these plots as,

$$R_{sn}^o = \lim_{f \rightarrow 0} \{R_{SN}(f)\} \quad (1.12)$$

A good agreement between  $R_{sn}^o$ ,  $R_n$ ,  $R_p$  has been observed for various systems [50,107,108].

#### ***(iv) Relationship between PSD and variance***

If narrow range of frequencies is selected by suitable filtering, the variance observed would be the PSD multiplied by the bandwidth of the filter. The variance observed for a given signal is the integral divided by frequency of the PSD. PSD and variance divided by bandwidth may be interchanged in many of the theoretical results, such as the shot noise formula [46], provided the frequency range included in the measurement of the variance is taken into account. Some parameters, such as the  $R_n$ , are ideally measured at a low frequency. These will typically be estimated better by taking the PSD at a suitable frequency than by using the variance or standard deviation measured over an arbitrary

range of frequencies. If the PSD attains a valid low-frequency limit, then this is usually an appropriate value to use.

#### ***1.8.9.4 Autocorrelation function (ACF)***

The ACF is the expected value of the product of the time series at one time and at certain later times [46, 49]. Consequently, the ACF is a function of the lag time, the time difference between two samples. For Gaussian white noise, where each sample in the time record is an independent sample from a normal distribution, the ACF is zero for all lags except zero. This method has generally been superseded by power spectra, which presents the same information in a more intuitive way.

#### ***1.8.9.5 Chaos methods***

Chaos analysis attempts to characterize behavior that is deterministic but highly unstable [46]. The analysis of electrochemical noise by mathematical tools from the theory of Chaos has been confirmed as a rich source of information about corrosion processes. It has been ascertained that different types of electrochemical noise have different attractors. The Chaotic analysis of the electrochemical noise has indicated that the correlation dimension increases from passivation to localized, mixed, and uniform corrosion. The results of chaotic analysis indicated that localized corrosion is a low-dimensional chaotic process, whereas uniform corrosion is a random process. The Lyapunov exponent (LE) that describes the approach rate of trajectory of dynamic systems is considered the most useful dynamical diagnostic for chaotic systems. A positive value of LE indicates that there is at least one direction in phase space along

which an attractor exhibits unstable behavior. A system with positive LE is considered chaotic. Spectral analysis enables the indication of corrosion rate, whereas chaotic analysis provides more data about the type of corrosion. Hence, spectral and chaotic treatments are, in some way, complimentary methods for the study of electrochemical noise.

#### ***1.8.9.6 Shot noise analysis***

Shot noise theory for electrochemical noise [46,109-111] has gained popularity in the recent years for providing mechanistic information about the nature of corrosion process and the extent as well. According to shot noise theory, signals are composed of packets of data departing from the base line. In corrosion systems, current noise signals could be considered as a series of statistically independent packets of charge having a short duration and shot noise is produced by current being carried by discrete charge carriers. The theory assumes some restrictions [46, 74, 75, 111, 112] on the noise generating process when applied to electrochemical noise analysis:

The current is generated by pulses of the same charge and shape, although both positive - going and negative-going pulses may occur

- These pulses are statistically independent (this is a necessary condition for the analysis).
- The cathodic reaction is considered to be noiseless, so only the anodic reactions are treated as a noise source (this is not a necessary condition, but simplifies the analysis, and is necessary to invert the analysis).

- The two working electrodes have equal corrosion rate (this is not a necessary condition, but simplifies the analysis, and is necessary to invert the analysis).
- The solution resistance is assumed to be zero (this is not a necessary condition for the calculation of the expected behavior, but it is necessary to invert the analysis).

Based on these assumptions of shot noise described by Cottis [109, 111] it is possible to determine the charge in each event ( $q$ ), the frequency of appearance of each event ( $f_n$ ) which could be related to corrosion mechanism.

$$q = \sqrt{(PSD_v \times PSD_i)} / B \quad (1.13)$$

$$f_n = B^2 / (A \times PSD_v) \quad (1.14)$$

Where,  $PSD_v$  and  $PSD_i$  are the power spectral density values at low frequency,  $B$  is the Stearn-Geary coefficient. To accommodate systems where the assumptions may not be valid, the term characteristic charge and characteristic frequency has been proposed for  $q$  and  $f_n$  respectively. The characteristic charge,  $q$  is the charge in individual transient and is related to the mass of metal lost in the corrosion events and  $f_n$  gives information about the rate at which these events are happening or frequency of the events. As the characteristic frequency is believed to be proportional to the specimen area for a shot noise process, it is presented as frequency per unit area [109, 111].

The cumulative probability,  $F(f_n)$ , at each  $f_n$  is derived from the set of  $f_n$  values for a particular experiment. The  $f_n$  values are initially arranged in the ascending order for  $N$  data sets. The cumulative probability is evaluated as  $M / (N+1)$ , where  $M$  is the rank in the data set.

#### ***1.8.9.7 Wavelets to study electrochemical noise transients***

The main disadvantage of the statistical and spectral method is that they analyze signals by averaging the features across the whole time record. These methods are devised for stationary signals (all its statistical properties such as mean and variance do not change with time) that do not show distinctive transients. Wavelet transforms avoid these limitations. Wavelet transform has been proposed to study both stationary and non-stationary electrochemical noise time record [113, 114]. Since electrochemical noise signals are frequently nonstationary, the wavelet analysis is an attractive tool. The technique of wavelet analysis may be regarded as a variant of Fourier analysis in which the continuous sine waves used in the Fourier transform are replaced by transients with a finite duration, known as wavelets [46, 113-117]. Unlike FFT, the wavelet analysis can retain time domain information and can analyze non-stationary time series without the requirement for detrending and windowing [118]. The wavelets are small waves that grow and decay in a limited time period and have an average value of zero. A set of wavelets of varying amplitude, duration, and location can then be constructed such that their sum reproduces the signal of interest. There are two types of wavelet transforms, the continuous wavelet transform (CWT) and the discrete wavelet transform (DWT).

In DWT [115, 116], an electrochemical noise signal (time record),  $X_n$  ( $n = 1 \dots N$ ) can be represented as a linear combination of basis functions  $\Phi_{j,k}$  and  $\psi_{j,k}$  which are formed from the mother wavelet  $\psi(t)$  and father wavelet  $\Phi(t)$  by translating in time and dilating in scale [46, 113-117].

$$\varphi_{j,k}(t) = 2^{-j/2} \psi(2^{-j}t - k) \quad (1.15)$$

$$\phi_{j,k}(t) = 2^{-j/2} \phi(2^{-j}t - k), \quad (1.16)$$

$j, k \in \mathbb{Z}$  where  $k = 1, 2, \dots, N/2$ ,  $N$  is the number of data record,  $\mathbb{Z}$  is set of integers,  $j = 1, 2, \dots, j$ ,  $j$  is a small natural number that depends on  $N$ . For full decomposition of a finite length signal,  $2^j = N$ .

The time record  $x(t)$  can be represented as

$$x(t) = \sum_k s_{j,k} \phi_{j,k}(t) + \sum_k d_{j,k} \psi_{j,k}(t) + \sum_k d_{j-1,k} \psi_{j-1,k}(t) + \dots + \sum_k d_{1,k} \psi_{1,k}(t) \quad (1.17)$$

Where  $s_{j,k}$ ,  $d_{j,k}$ ,  $\dots, d_{1,k}$  are the wavelet coefficients,  $j$  is a small natural number which depends on  $N$  and the basis function,  $k$  takes a value from 1 to the number of coefficient in the specified component,  $s$  and  $d$  are the approximation or smooth coefficient and detailed coefficient respectively.

There are three operations involved in the FWT algorithm, which includes a low pass filter, a high pass filter and a down sampler. Each filter has a down sampler after it. At the first stage, the low frequencies of the signal passes through the low pass filter and high frequencies passes through high pass filter producing the smooth coefficient set  $S_1 = (s_{1,1}, s_{1,2}, \dots, s_{1,N/2})$  and detailed coefficients,  $D_1(d_{1,1}, d_{1,2}, \dots, d_{1,N/2})$ . The detail is kept aside for analysis and the smooth signal is further filtered in the second stage to produce  $S_2$  and  $D_2$ . This process is iterated successively  $j$  times to decompose the signal into  $D_1, D_2, \dots, D_j$  and  $S_j$  coefficients. A typical schematic the FWT algorithm [115, 119] is shown in Figure 1.4. Each set of coefficients,  $D_1, D_2, \dots, D_j$  is called a crystal. The set of approximation coefficients,  $S$  carries information about the general trend of the signal. The set of detailed coefficients,  $D$ , carries information about the local fluctuations in the signal. Each new set of crystal has half the resolution and contains half the number of coefficients and is designated with a successive higher number.

The scale range [117, 120] and frequency range of each crystal is given by



$$(c_1^j, c_2^j) = (2^{-j} \Delta t, 2^{j-1} \Delta t) \quad (1.18)$$

$$(f_1, f_2) = (2^{-j} f_s, 2^{j-1} f_s) \quad (1.19)$$

Where,  $\Delta t$  is the sampling interval.  $f_s$  is the sampling frequency and  $j$  is the number of the crystal. Each of the  $j+1$  signals is called the partial signal which resembles the fluctuations of the original signal at a particular interval of frequency. The unit of the partial signal is same as that of the EN signal. The plot of standard deviation of partial signal (SDPS) as a function of crystal name (SDPS plots) [117] could be used to indicate the extent of corrosion and the plot of the energy of the partial signals against crystal numbers (EDP) [113-117] gives information about the corrosion mechanism.

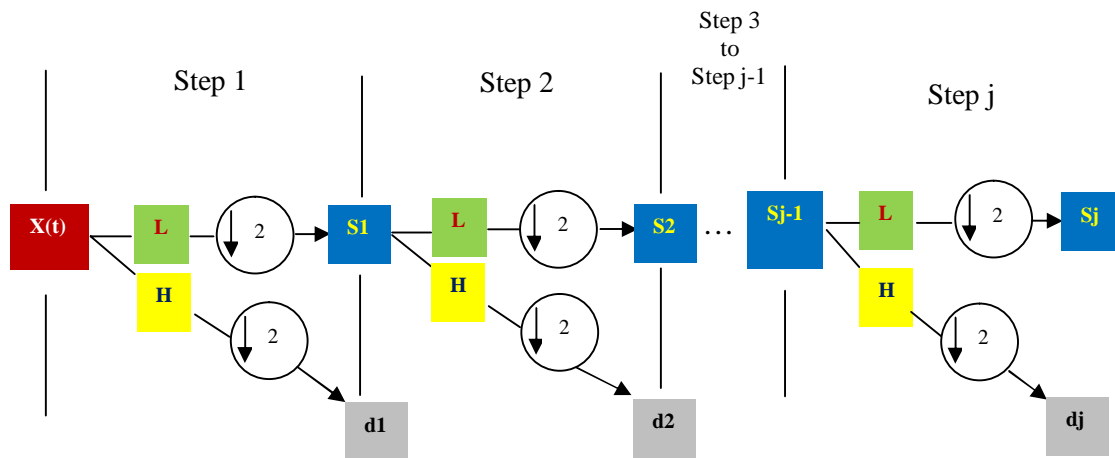


**Figure 1.4 General scheme of FWT algorithm [115, 119]**

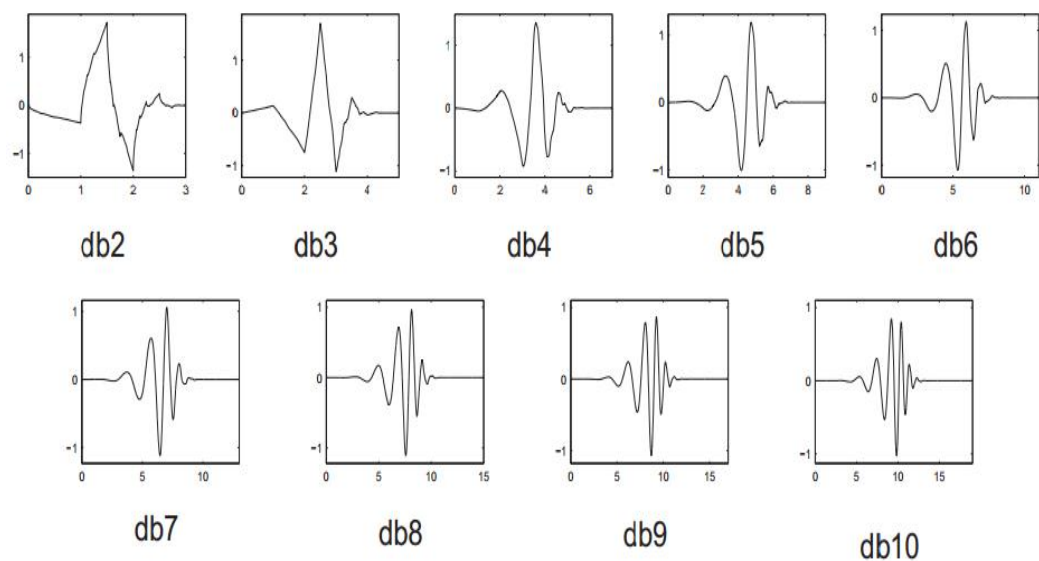


***Figure 1.5 Daubechies wavelets***

It has been reported [121] that among different families of wavelets such as Daubechies, Haar, Coiflets, Symlet etc., the Daubechies 4 or "db4" is highly localized in time and is useful EN studies. Figure 1.5 represents the Daubechies wavelets [122].

### ***1.9 Electrochemical noise investigations – a brief review***

Tyagi et al [123-125], Barker [126, 127] and Fleischmann and Oldham [128] defined electrochemical noise as fluctuations of current or that of potential passing through an interface, under potentiostatic or galvanostatic control. The authors used electrochemical noise measurements to study the equilibrium properties of redox reactions and homogeneous processes in solution. It was pointed out by Barker that electrochemical noise in redox systems is small, and there is no particular advantage of noise

measurements compared to deterministic methods such as impedance measurements for these systems. The measurement of electrochemical noise for corrosion studies was first described by Iverson in 1968 [43]. Iverson found that the frequency and amplitude of potential noise emerging from corroding magnesium, aluminium, aluminium alloys, iron and mild steel depended on the metal being studied. The study of passivity and its breakdown using electrochemical noise measurements was reported by Japanese researchers Okama et al [129] in the mid 1970's. Initial studies by researchers on electrochemical noise were based on potential fluctuations [59, 130, 131]. Work sponsored at UMIST by United Kingdom Ministry of Defence and ICI between 1979 and 1985 was focused at using potential noise measurements for monitoring and detecting localized corrosion [132]. The significance of current fluctuations [133-135] was subsequently understood. Later, it was realized that the combination of electrochemical potential and current noise was more powerful than the individual measurements and Eden [83] first introduced, electrochemical noise resistance method, and then, the electrochemical noise impedance in a patent, based on simultaneous acquisition, which was later adopted by many researchers. Since then, electrochemical noise technique has been practically applied to study a wide variety of corrosion processes from the 1980's. These include corrosion monitoring, investigating various types of corrosion like uniform and localized corrosion, monitoring crack propagation in stress corrosion cracking, evaluation of corrosion inhibitors, monitoring microbiologically induced corrosion in buried pipelines, acid dew point corrosion in exhaust systems, on-line monitoring of raw water corrosiveness, biocide efficacy, and many others. In 1991, a task force was formed by members of ASTM Committee G-1, to develop standards that describe instruments

and methods for making and analyzing electrochemical noise measurements. The task force organized the first international symposium on Electrochemical Noise Measurements for Corrosion Applications which was held in Montreal, Quebec, Canada, 1994 and the approved papers were compiled into ASTM Special Technical Publication [45] (STP) which provides a snapshot portrait of the state of the art for electrochemical noise measurements in the early 1990s.

Though extensive research has since then progressed in the field of electrochemical noise, a brief review of the literature on the research works is at the best presented in the forthcoming section.

Hladky and Dawson [59] obtained distinct noise signatures for pitting and crevice corrosion of mild steel in chloride medium inhibited by sodium nitrate. The change from pitting to crevice attack was first observed as a change in the pattern of the electrode potential behavior. The cyclic movement of the DC potential was replaced by a general random drift interspersed with short periods of the cyclic activity, which became less frequent and the noise output of the electrode undergoing crevice corrosion appeared to be characterized by relatively long bursts of regular peaks occurring at regular interval. The authors also established an inverse relation between slope of high frequency roll off slope and nature of corrosion attack by using  $1/f$  noise from corrosion of copper, aluminum and mild steel [96]. Montesperelli et al [136] reported that electrochemical noise from crevice corrosion of AISI 430 stainless steel in 3% sodium chloride medium could detect the four stage mechanism of crevice corrosion. The electrochemical noise resistance parameter correlated well with polarization resistance from impedance measurements in reflecting the initiation and propagation of the attack. The roll off slopes

from power spectral evaluation indicated the mode of attack. Girija et al [137] reported that the crevice noise time record for 304L SS in 0.05M  $\text{FeCl}_3$  medium comprised of large events with the potential and current noise rising and falling in cycles resulting in humps and wells and the onset of crevice was indicated by a rapid fall of potential noise corresponding to an increase in current noise and a large drop in noise resistance.

Cheng and Rairdan [138] investigated the features of electrochemical noise generated during pitting of A516-70 carbon steel in chloride solutions containing  $\text{Na}_2\text{CrO}_4$ . The critical concentration of chloride to initiate pitting was determined from the current noise time record. The PSD roll off slope was monitored to observe the mechanism changing from pitting to passivity.

Legat and Dolecek [139] studied the mechanism of different types of corrosion of stainless steel (SS) in different electrolytes. The stainless steel in the chosen environment corroded uniformly or locally, or not at all. The electrochemical noise time records generated by localized corrosion and uniform corrosion showed distinct patterns. Further, they reported that the PSD values of voltage and current noise generated by uniform corrosion appeared nearly constant over the whole frequency domain, while the PSD values of voltage and current noise of localized corrosion showed  $1/f$  variation in the higher frequency range.

Stewart et al [140] reported that the potential and current transients generated during the stress corrosion cracking (SCC) of steel in dilute thiosulphate solution were associated with nucleation, temporary growth and arrest of short microcracks and further showed that correlation existed between the number of transients and the number of microcracks seen. Anita et al [141] have obtained widely spaced and high amplitude current transients

during SCC of 316 in boiling acidified NaCl solution. Cottis and Loto [61] have studied the electrochemical noise generated during SCC of high strength carbon steel freely corroding in deaerated, acidified NaCl solution, and the noise emitted correlated with the progress of the stress corrosion test. They showed that the average noise power, measured over a time comparable to the duration of a typical transient, is an effective method for the detection of transients associated with crack propagation. The authors used FFT and MEM method to analyse EN during SCC of alpha brass, high strength aluminum alloy and austenitic stainless steel [61,141,142]. In general, the results showed that SCC was characterized by increase in standard deviation of power spectrum. The cracking failure was indicated by highest standard deviation peak and the power spectra indicated 1/f noise.

Gusmano et al [143] studied the corrosion rate of AISI 1040 'C' steel using Linear Polarization Resistance (LPR) method and electrochemical noise (EN) techniques in  $\text{Na}_3\text{PO}_4$  (passivating solution) and NaCl containing solutions. A good agreement was seen between  $R_n$  by electrochemical technique and  $R_p$  by LPR.

Metikis-Hukovic et al [144] studied the protective qualities of phenol-formaldehyde based and coumarone-indene resin based coatings on low alloy steel under stimulated conditions of marine atmospheric environment using potential noise measurements. The power spectral slopes indicated onset of pitting in Coumarone-indene polymer coated steel and unprotected steel surface after 6 h of exposure, whereas, pitting occurred in phenol formaldehyde coated steel only after 30 h of exposure, as determined from the power spectral slopes.

Bertocci et al [47] have studied the breakdown of passive film by electrochemical noise measurements. The study of random fluctuations in the passive current of electrodes under potentiostatic conditions have shown different noise levels in amorphous and crystalline Fe-Cr-Ni alloy indicating that the breakdown of the passive film differs in two conditions.

Iverson and Heverly [145] exploited the noise produced by anaerobic bacterial corrosion, probably due to breaking of iron-sulfide films, to locate and detect microbial corrosion in underground pipeline structures.

Shinichi Magaino and Ryuichi Yamazaki [146] have recorded the rest potential noise during chemical etching of mild steel in sulphuric acid. They have observed the rest potential noise characteristic of pitting corrosion, when pitting corrosion was proceeding and very smooth noise at a frequency lower than 1 Hz, while uniform dissolution was proceeding.

Mansfeld and Xiao [85] have used the power spectra of potential and current noise for the investigation of the corrosion of pure iron and Al/SiC composites in NaCl solution. Monticelli and coworkers [147, 148] examined the corrosion of aluminum and aluminum composites by the power spectrum of potential noise. The authors illustrated the use of electrochemical noise method to evaluate corrosion inhibitors by studying the corrosion potential fluctuations of aluminum alloy in chloride solutions in presence and absence of inhibitors.

Martinet et al [149] have reported the use of electrochemical noise for different types of batteries under galvanic corrosion. The authors illustrated that the noise level was found to give an estimate of the state of charge of small capacity sealed Ni-MH batteries.

Several tests on Ni-Cd and Ni-MH electric vehicle modules demonstrated the applicability of this technique for overcharge detection.

Intergranular corrosion may be expected to give electrochemical noise characteristics similar to stress corrosion occurring by a continuous process [150]. As with stress corrosion cracking, the shielding of the growing tip of the corrosion penetration by the passive walls may be expected to cause a reduction in the measured electrochemical noise as the depth of penetration increases and this has been observed by Stephenson [151]. This technique has been used to monitor the intergranular corrosion of lead acid battery electrodes.

Cappeln et al [152] analyzed the electrochemical noise obtained from AISI 347, 10CrMo910, X20CrMoV21 steels in molten NaCl-K<sub>2</sub>SO<sub>4</sub> at 630°C. Different types of current noise were identified for pitting, intergranular and peeling corrosion. A distinction between general and intergranular corrosion was made using kurtosis from statistical analysis, and an average value above 6 was inferred to indicate intergranular corrosion and a value below 6 was associated with general corrosion.

Hladky et al [153] have demonstrated feasibility of a multielement probe based on impedance, galvanic coupling and electrochemical noise to monitor corrosion of stainless steel under condensing nitric acid and found good correlation from the three techniques in the indication of uniform and localized corrosion during different periods of monitoring.

Wang et al [154] and Van Nieuwenhove [155] have demonstrated feasibility of electrochemical noise measurements in nuclear fission reactors. Boiling Water Reactor (BWR) core components generally suffer from irradiation assisted stress corrosion



cracking (IASCC). The authors studied the effect of irradiation induced segregation (RIS) on IASCC through a series of stress corrosion tests in simulated BWR environment using an electrochemical noise set up with three electrodes. The coupling current increased in irradiated sensitized type 304SS, only during the initial test period and subsequently leveled off at a later stage. The current rise was attributed to the dissolution current generated by IASCC at the crack tip. For the SEN 304 SS (not irradiated), the level of current increase was significantly lower, suggesting the absence of cracking. After test, hairline cracks were observed on the notch surface of the irradiated sensitized type 304 SS and no cracking occurred on the 304 SS specimen.

Reid et al [156] have described a computer controlled corrosion surveillance system using electrochemical noise technique to identify localized corrosion in a plant. The electrochemical noise technique was successfully employed on a real-time basis in several sour gas plants to get very reliable information about localized corrosion attack.

Wood et al [157] reported electrochemical noise measurements during erosion- corrosion of austenitic stainless steels and thermally sprayed coatings. Passive, general, localized corrosion (metastable and propagating pitting) events were identified in various flow conditions of sodium chloride. EN measurements showed responses to electrolyte permeation of the coating erosion penetration and substrate activity under erosion-corrosion conditions.

Eden et al [158] has presented the state of the art review of electrochemical noise sensors, where, EN sensor configurations for applications in uniform and pitting corrosion detection, for coating and linings applications, and those used in flowing condition, and in low conductivity environments are discussed. Sensors for field applications such as

that for hydrocarbon pipelines, sour gas processing plant, nuclear waste storage tanks, fresh water cooled heat exchangers are also discussed.

In recent years, shot noise and wavelet analysis have gained popularity in electrochemical noise analysis. Al-Mazeedi and Cottis et al [110] have presented parameter maps distinguishing regions of uniform, localized corrosion and inhibition using standard deviation pair and EN resistance-frequency of events pair. Sanchez - Amaya et al [159] used noise resistance and shot noise parameters to study the degree of intergranular corrosion in aluminum alloys. Kyung-Hwan [160] reported the susceptibility of aluminum alloys to pitting corrosion in neutral sodium chloride medium by shot noise method using Weibull distribution function. Frequency of events from shot noise analysis was used to distinguish uniform corrosion and pitting corrosion.

Pujar et al [161] have evaluated the degree of sensitization from standard deviation of current noise and shot noise parameters for 316(N) SS aged at 923 K for different time durations and a good correlation was obtained with DOS from DLEPR studies. Pujar et al [162] applied the shot noise analysis to monitor the progress of microbiologically influenced corrosion (MIC) on 316 stainless steel in natural reservoir water containing biofilm forming microbes and sodium chloride. The initiation and propagation of MIC was detected by significant changes in the shot noise parameters Weibull distribution function from shot noise theory is one of the widely used cumulative probability functions for predicting life time in reliability test [163].

Kyung-Hwan Na et al [164] analysed electrochemical noise obtained from pure aluminum during breakdown of the oxide film in aqueous neutral chloride medium and hydrogen evolution in alkaline medium. According to them, the Weibull probability plot

could clearly distinguish between uniform corrosion and break down of oxide film and hydrogen evolution.

Sung-Woo Kim et al [165] investigated the electrochemical noise from stress corrosion cracking of Alloy 600 material in a simulated environment of a steam generator sludge pile at high temperatures. They found that the shape parameter of the Weibull distribution of the mean time-to-failure for the initiation of SCC is clearly distinguishable from that parameter for the propagation of SCC as well as for the general corrosion.

Tao Zhang et al in their study on pit corrosion susceptibilities of magnesium alloys found that the Weibull distribution function from stochastic analysis or shot noise theory was useful to indicate pit initiation process, while pit growth probability could be determined from Gumbel distribution function from extreme value statistics [166].

Wharton et al [113] used wavelet variance exponent to discriminate various corrosion processes of stainless steels in sodium chloride medium. Kim et al [167] in their studies on potentiostatic critical pitting temperature test for superduplex stainless steel, used wavelet analysis based on fractional energy contribution of smoothed crystals and the lowest frequency detail crystal, to provide information on the type and onset of corrosion (general corrosion, metastable pitting, stable pitting). Muniandy et al [168] found that the multifractal spectra obtained from electrochemical current and potential noise analysis of corrosion of carbon steel in distilled water, were found to be qualitatively different for different temporal stages of the corrosion process.

Chao et al [169] in their study on pitting corrosion of pure aluminium in sodium chloride solution showed that energy distribution plots from wavelet analysis can be used as “fingerprints” of EN signals. Zhao et al [170] demonstrated the use of wavelets to study

the corrosion processes of reinforcing steel in concrete. The energy distribution plots from wavelet analysis have been used as a powerful tool to provide useful information about the dominant process and mechanism during different stages of corrosion [113-117]. Lafront et al [120] used energy distribution plots from wavelet analysis to study copper anode passivation in sulphuric acid industrial electrolyte. Legat et al [171] have reported that chaotic analysis of electrochemical noise from various corrosion process such as metastable pitting, initiation/ repassivation for carbon steel in calcium hydroxide containing additions of chloride and organic inhibitors can be used to determine the different types of corrosion. The correlation dimension and the largest Lyapunov exponent from chaotic analysis confirmed that the unstable corrosion process is driven by low dimensional chaos. Other researchers [172-176] too found that chaotic analysis of EN is useful in determining corrosion types. D.Bahena et al [177] have demonstrated that a positive value of Lyapunov exponent during localized corrosion of NiCoAg alloy in Hank solution indicated that the fluctuations during localized process are chaotic in nature. Chen et al [178] used chaotic analysis to study the metastable pitting of mild steel under wet-dry cycles in NaCl and Na<sub>2</sub>SO<sub>4</sub>. The positive fraction of the largest Lyapunov exponent was found to represent the number and isolation degree of pits in the two environments. Leban and co-workers [179] applied spectral and chaos analysis methods to ECN data from stress corrosion cracking of 304 SS , they concluded that it was impossible to distinguish between the non-active and active cracking periods.

The artificial neural network (ANN) based on Back Propagation and Support Vector Machine is a recent development in the analysis methods for electrochemical noise. ANN

is a mathematical model of simulating human neurons to process information. Though ANN has been established for pattern recognition, forecasting etc. since many years, the application in electrochemical noise has been initiated in the recent past to differentiate corrosion types by using multiple parameters [67].

Literature review shows that extensive work has gone in the field of electrochemical noise in the past three decades. However, except for a couple of reports such as that of Hladky et al [153], DOE sites, Cottis et al [110], electrochemical noise applications for corrosion monitoring of austenitic stainless steels in general, or in specific, about 304L SS in nitric acid and nuclear high level liquid waste environment is not reported.

This chapter presents the chemical composition of the materials used for the various studies presented in the thesis. The specimen preparation, heat treatments, electrolyte preparation, etching procedure and microstructural evaluation and laser Raman spectroscopy for passive film analysis are described. The electrochemical experimental techniques including potentiodynamic anodic polarization and electrochemical noise measurements and the analysis methods associated with these studies are also explained in detail.

---

### ***2.1 Chemical composition of the materials used***

Austenitic stainless steel of AISI (American Iron and Steel Institute) type 304L SS and three nitrogen containing 304L SS were used for the studies presented in this thesis. Under Indo-Bulgarian collaboration programme, stainless steels containing nitrogen content of 0.132 wt % , 0.193 wt % , and 0.406 wt % was manufactured at Institute of Metal Science, Bulgarian Academy of Science and was received in as forged and rolled conditions. For convenience, the three nitrogen containing stainless steels have been designated as 304LN1, 304LN2, 304LN3 representing nitrogen contents of 0.132%, 0.193% and 0.406% respectively. The suffix F and R are included in the designation to represent forged and rolled specimens. For instance, 304LN1F and 304LN1R represents 304L SS containing 0.132%N under forged and rolled conditions, respectively.

The chemical compositions of AISI type 304L SS and the nitrogen containing 304L SS are given in Table 2.1.and Table 2.2.

Element	C	Si	Mn	Cr	Ni	Mo	S	P	Fe
Wt %	0.029	0.41	1.66	17.45	8.97	0.46	0.028	0.031	bal

***Table 2.1 Chemical composition of 304L SS (in wt %) used for the studies***

Material	C	Mn	Si	Cr	Mo	Ni	V	N	S	P	Al	Fe
304LN1	0.03	1.5	0.45	19	0.18	10.7	0.15	0.132	0.005	0.022	0.007	Bal
304LN2	0.032	1.5	0.42	19	0.18	10.3	0.216	0.193	0.004	0.012	0.008	Bal
304LN3	0.033	1.4	0.45	19	0.17	10.8	0.147	0.406	0.004	0.018	0.006	Bal

***Table 2.2 Chemical composition (in wt %) of the three nitrogen containing 304L SS used for the studies***

## ***2.2 Solution preparation***

(i) ***Electrolyte for etching:*** American Society for Testing and Materials (ASTM) A262 Practice A [180] was used for studying the microstructure of specimens. For this purpose, 10 % oxalic acid was prepared for etching of specimen for microstructural investigations.

(ii) ***Elelctrolyte for electrochemical investigations by potentiodynamic anodic polarization and electrochemical noise:***

a) ***Nitric acid:*** 1 M, 4 M, 6 M, 8 M, 12 M concentrations of nitric acid were prepared using AR grade nitric acid in double distilled water. The concentrations of nitric acid were chosen according to the experiment.

Electrochemical noise investigations of 304L SS under solution annealed and sensitized microstructural conditions in nitric acid were carried out in 1 M, 4 M, 8 M, 12 M nitric acid medium at 298 K and in 1 M, 4 M, 8 M at 323 K. EN investigations in 12 M nitric acid (323 K) were not carried out owing to severe release of acid fumes.

Potentiodynamic anodic polarization experiments using the three nitrogen containing stainless steels (304LN1, 304LN2, 304LN3) under forged and rolled microstructural conditions were carried out in 1 M, 4 M, 6 M nitric acid. As the aim of the investigation was to study the effect of nitrogen content on corrosion behavior of the materials in nitric acid medium, only three concentrations of acid was used. As the mechanism of reduction of nitric acid changes above 6 M concentration, potentiodynamic polarization experiments were not carried out above 6 M acid concentration.

Electrochemical noise investigations of the nitrogen containing stainless steel were carried out at two lower concentrations (1 M, 4 M) of nitric acid and one higher concentration (8 M) of nitric acid. Apart from investigating the effect of nitrogen on the corrosion behavior of the alloys in nitric acid medium, the objective was also to demonstrate the three identical electrode probe in reprocessing medium, hence a higher concentration of nitric acid (8 M) was used instead of 6M nitric acid.

***b) Simulated high level waste:*** The composition of simulated high level waste solution used for the studies is given in Table 2.3. This composition represents one of the stored nuclear waste solutions of natural uranium oxide ( $\text{UO}_2$ ) fuel used in pressurized heavy water reactors in India. Nitrates of the corresponding ions represented in Table 2.3 were taken in the required stoichiometric ratio and were dissolved in 3 M  $\text{HNO}_3$ . The



dissolution process in nitric acid was carried out in a laboratory fume hood for safe handling of chemicals and nitric acid fumes.

Elements	Concentration of elements (g/L)	Corresponding Salts taken
Fe	0.72	Fe(NO <sub>3</sub> ) <sub>3</sub>
Cr	0.119	CrO <sub>3</sub>
Ni	0.107	Ni(NO <sub>3</sub> ) <sub>3</sub>
Na	5.5	NaNO <sub>2</sub>
K	0.224	KNO <sub>3</sub>
U	6.34	UO <sub>2</sub> (natural U)
Sr	0.031	Sr(NO <sub>3</sub> ) <sub>3</sub>
Zr	0.004	ZrO(NO <sub>3</sub> ) <sub>2</sub>
Ba	0.064	Ba(NO <sub>3</sub> ) <sub>2</sub>
La	0.18	La <sub>2</sub> O <sub>3</sub>
Ce	0.06	Ce(NO <sub>3</sub> ) <sub>2</sub>
Pr	0.09	Pr <sub>6</sub> O <sub>11</sub>
Nd	0.12	Nd <sub>2</sub> O <sub>3</sub>
Sm	0.0855	Sm <sub>2</sub> O <sub>3</sub>
Y	0.06	Y <sub>2</sub> O <sub>3</sub>
Cs	0.315	CsNO <sub>3</sub>

***Table 2.3 Composition of simulated high level waste solution prepared in 3 M nitric acid***

***c) Electrolyte for pitting corrosion studies by potentiodynamic anodic polarization:***

0.5 M NaCl was used for pitting corrosion studies of the nitrogen containing 304L SS (forged and hot rolled) using potentiodynamic polarization technique. Kalpakkam being a

coastal area, stainless steels are prone to pitting corrosion during storage, as a result of salt deposition on stainless steel surface by condensation and atmospheric evaporation, that can lead to more corrosion. As sea water contains approximately 28 g/l of NaCl (~ 0.5 M), investigations on pitting corrosion of the alloys in 0.5 M NaCl is of significance to understand the corrosion property. Hence pitting corrosion studies of the alloys were carried out in 0.5 M NaCl medium.

***d) Electrolyte for pitting corrosion studies by electrochemical noise:***

A low concentration of ferric chloride solution (0.05 M  $\text{FeCl}_3$ ) was used for pitting corrosion studies of 304L SS by electrochemical noise measurements. As electrochemical noise experiments were carried out at open circuit conditions, austenitic stainless steels would necessarily remain resistant in aqueous sodium chloride solutions even for long exposure period. In order to accelerate the pitting process for measurement that could be plausible in shorter time period, the chemical potential of the electrolyte was ennobled using  $\text{Fe}^{3+}$  ions and hence ferric chloride was preferred for electrochemical noise investigations at open circuit potentials.

***2.3 Heat treatments***

***2.3.1 Solution annealing and sensitization***

In the studies presented in the thesis, AISI type 304L SS was used under solution annealed and sensitized conditions for various electrochemical noise investigations in nitric acid and simulated HLW medium. Solution annealing was carried out at 1373 K for one hour, in order to obtain a homogenized microstructure. After this, the material was quickly cooled in water to prevent any carbide precipitate. For preparation of sensitized specimens, the solution annealed specimens were subjected to sensitization heat

treatment at 948 K for one hour, followed by air cooling, as described in ASTM practice A 262 [180].

### ***2.3.2 Forging and rolling heat treatment***

The forged and rolled nitrogen containing 304L SS were used under as received condition from the Institute of Metal Science, Bulgarian Academy of Science. The process of forging was carried out with two transitions warming, a) 1473 K at the beginning of forging and b) 1243 K – 1273 K at the end of forging. Cooling was carried out in air. The temperatures at the beginning and end of rolling were 1423 K and 1173 K respectively, following which air cooling was done. Consequently, solutionising annealing of the alloys were carried out at 1323 K for 1 h and subsequently water quenched.

## ***2.4 Specimen preparation***

### ***2.4.1 Specimen preparation for electrochemical potentiodynamic polarization studies***

The 304L SS and the nitrogen containing 304 L SS alloys were cut into 10 mm x 10mm x 10mm size, and mounted in an araldite resin, mechanically ground till 1200 grit SiC emery paper and polished till diamond finish. After this, the samples were cleaned in soap solution, acetone, and distilled water.

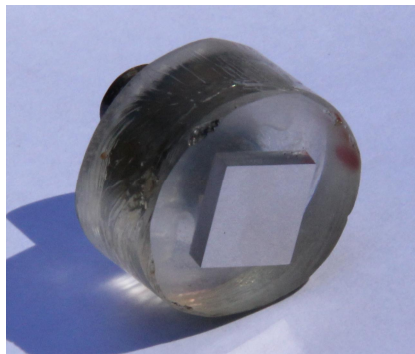


***Figure 2.1 Photos of mounted Specimen for polarization studies***

Care was taken during mounting to avoid gaps between specimen and mount in order to prevent crevice attack during experiments. Figure 2.1 shows the specimen configuration used for polarization studies. These specimens were used for potentiodynamic anodic polarization experiments.

#### ***2.4.2 Specimen preparation for electrochemical noise studies in nitric acid and simulated high level waste medium***

The photographs of the three electrode probe used for electrochemical noise studies in nitric acid and simulated high level waste medium are shown in Figure 2.2.



***Figure 2.2 Photos of teflon mounted three electrode probe for EN studies in nitric acid and simulated high level waste***

The stainless steel alloys were lathe finished into a cylindrical shape with diameter 8mm and length 15 mm-25 mm. The specimens were shrink fit into a teflon mount to avoid gaps between mount and specimen, exposing a surface area of 0.5 cm<sup>2</sup>. The specimens were then mechanically ground till 1200 grit emery and further diamond polished. The prepared specimens were subsequently used for electrochemical noise studies in nitric acid, simulated HLW.

#### ***2.4.3 Specimen preparation for electrochemical noise studies in chloride medium***

Electrochemical noise studies in chloride medium were carried out using bare electrodes, typical photograph is shown in Figure 2.3. The dimensions of the cylindrical specimens were maintained as mentioned above. The specimens were mechanically ground till 1200 grit SiC emery papers and further polished till diamond finish on the flat surface and up to a height of 8 mm on the circumference.

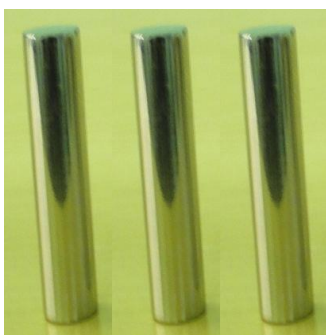


***Figure 2.3 photos of bare electrodes for EN studies in chloride medium***

Since bare specimens were used, the surfaces above a certain height of the immersed area were sealed using teflon tape to prevent exposure to the fumes from the solution.

## ***2.5 Oxalic acid etching and microstructural evaluation***

Etching involves subjecting the surface of a metal to preferential chemical or electrolytic attack in order to reveal microstructural details. The austenitic stainless steel alloys used for various studies presented in the thesis were electrolytically etched in oxalic acid as per ASTM A262 [180]. Etching was carried out by immersing the specimen in 10 % oxalic acid under an impressed current of ( $1\text{ A} / \text{cm}^2$ ) for 90 seconds. The specimens were subsequently investigated for microstructure using optical and scanning electron microscopy (SEM). SEM analysis was carried out using XL30 ESEM, Philips, Holland and elemental analysis was carried out using energy-dispersive spectroscopy (EDS) attached to it. Energy dispersive spectra were taken for elemental analysis on the matrix using selected area of  $50\mu\text{m} \times 50\mu\text{m}$  and spot analysis on the precipitate.

## ***2.6 Potentiodynamic anodic polarization experiments***

Electrochemical polarization techniques provide a relatively rapid means to experimentally determine the corrosion behavior of a metal in a given environment. Polarization [39,181,182] is the variation in electrode potential from the steady-state potential which the electrode exhibits in the absence of an external current. In potentiodynamic anodic polarization, the potential is changed in the anodic (or more positive direction) causing the working electrode to become the anode. For potentiodynamic experiments, the applied potential is increased with time while the current is constantly monitored. The current (or current density) is plotted versus the potential. In the active region, the current increase with applied potential until  $i_{\text{crit}}$  is reached with the maximum critical current. Following the primary passive potential where anodic current is minimum, corrosion current density drops to  $i_{\text{pass}}$  and the material

is in the passive state. After passive region, transpassive region is reached where the protective anodic film is damaged and may break down completely. In the presence of chloride ions, the breakdown occurs at a lower potential called the pitting potential. For spontaneously passivating systems such as for austenitic stainless steels in nitric acid medium, the active-passive transition region doesn't appear as the material corrosion potential being in the passive region. A typical potentiodynamic anodic polarization diagram depicting various regions for austenitic stainless steels, and, in particular for AISI type 304L SS in various conditions of nitric acid medium in a reprocessing plant, is given in Figure 2.4.

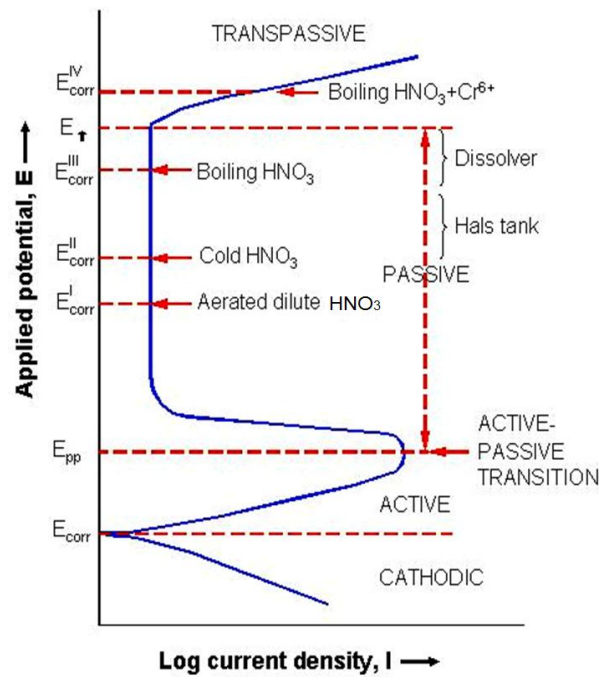


**Figure 2.4 Potentiodynamic anodic polarization curve in nitric acid medium depicting various conditions in reprocessing plant**

In the present study, potentiodynamic anodic polarization experiments were carried out according to the procedure described in ASTM G5 [60].

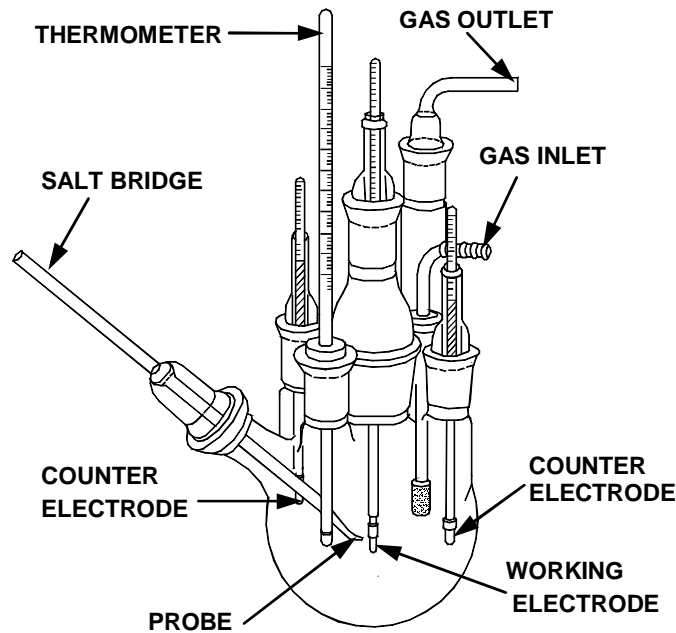


**Figure 2.5** *Schematic representation of polarization cell (ASTM G5) [ 60]*

The polarization cell is a standard round bottom borosilicate flask which holds the electrolyte solution, and is provided with necks that can be used to insert a reference electrode, two platinum auxillary (or counter electrodes), and the specimen (or working electrode) of interest, gas inlet and outlet, thermometer. A representation of the cell is shown in Figure 2.5. Autolab PGSTAT 30 (Ecochemie make, The Netherlands) was used to carry out the potentiodynamic anodic polarization studies. For the measurements, the working electrode was connected to the working electrode cable of Autolab PGSTAT 30, two platinum auxillary electrodes were shorted and connected to the counter electrode



cable of the potentiostat. A calomel reference electrode was connected to the reference electrode of the potentiostat. A luggin probe and salt bridge was used to connect the reference electrode to the electrochemical cell. The luggin probe-salt bridge separates the bulk solution from the saturated calomel reference electrode, and the probe tip can be easily adjusted to bring it in close proximity with the working electrode.

#### ***2.6.1 Potentiodynamic anodic polarization in nitric acid medium and simulated HLW***

The prepared specimens were immersed in the appropriate electrolyte for 30 minutes at open circuit potential (OCP) and subsequently subjected to potentiodynamic anodic polarization from a potential of 250 mV(SCE) below OCP, at ambient temperature (298K) and elevated temperatures (323K), where required. The potential was measured with respect to saturated calomel electrode (SCE) and applied at a scan rate of 10 mV/min. The anodic polarization was carried out until the transpassive potential was reached. The experiments were repeated three times to check for reproducibility. From the polarization curves, electrochemical parameters such as corrosion potential ( $E_{\text{corr}}$ ), passivation current density ( $i_{\text{pas}}$ ), passive range, transpassive potential were determined. The passive range was taken from a potential noble to OCP, till transpassive potential. The potential at which current monotonically increased beyond passive range was inferred as transpassive potential [39].

#### ***2.6.2 Pitting corrosion studies in 0.5 M NaCl***

For pitting corrosion studies, the specimens were immersed in 0.5 M NaCl, which was continuously purged with purified Argon gas for 30 minutes. Subsequently, potentiodynamic anodic polarization experiments was conducted under continuous argon gas purging from a potential of 250 mV(SCE) below open circuit potential at a scan rate

of 10 mV/min. The anodic polarization was carried out until the potential was reached, where monotonic increase in current beyond 25  $\mu\text{A}$  was attained, after a stable passive region. Potential at which the anodic current monotonically increased beyond the passive region was inferred as pitting potential [28, 39, 181, 182].

### ***2.6.3 Double loop electrochemical potentiokinetic reactivation (DL-EPR) test***

Double loop electrochemical potentiokinetic reactivation [30, 183,184,185,186] (DL-EPR) tests were conducted to measure the degree of sensitization (DOS) in 304L SS which was given sensitization heat treatment. DL-EPR test was conducted in 0.5M  $\text{H}_2\text{SO}_4$  + 0.01M KSCN, and solution temperature was maintained at 30° C. Dry, oxygen free argon gas was purged for one hour. The mounted specimen was immersed in the solution and the OCP was observed for 1h of immersion. Subsequently, the electrochemical potential was varied from open circuit potential to +300 mV (SCE) and then back to the open circuit potential at a scan rate of 1.67 mV/s. The degree of sensitization (DOS) was calculated as

$$DOS \ \% = \frac{i_r}{i_a} \times 100 \quad (1)$$

where  $i_r$  is the reactivation current and  $i_a$  is the activation current.

## ***2.7 Passive film analysis by Laser Raman Spectroscopy***

### ***2.7.1 Potentiostatic anodic polarization***

Potentiostatic anodic polarization experiments were carried out on the three nitrogen containing stainless steels in 1M, 4M, 8M nitric acid and simulated HLW for one hour of immersion, at passivation potentials derived from the potentiodynamic anodic

polarization curves, in order to grow the passive film. The specimens were used for passive film analysis by laser Raman spectroscopy [187].

### ***2.7.2 Laser Raman Spectroscopy (LRS)***

LRS experiments were performed on the passive films formed on the surface of the three nitrogen containing type 304L SS specimens using a HR 800 (Jobin Yvon) Raman spectrometer equipped with 1800 grooves/mm holographic grating. For all the Raman measurements at room temperature, the specimens were placed under an Olympus BXFM-ILHS optical microscope mounted at the entrance of the Raman spectrograph. Ar<sup>+</sup> laser of 488 nm was used as an excitation source. The laser spot size of 3  $\mu\text{m}$  diameter was focused tightly on the sample surface using a diffraction limited 10x (NA = 0.25) long distance objective. The laser power at the sample was  $\approx 10$  mW. The slit width of the monochromator was 400  $\mu\text{m}$ . The back scattered Raman spectra were recorded using super cooled ( $< -110^\circ\text{C}$ ) 1024 x 256 pixels charge-coupled device (CCD) detector, over the range 80  $\text{cm}^{-1}$  to 2000  $\text{cm}^{-1}$  with 5s exposure time and 20 CCD accumulations. All the spectra were baseline corrected and normalized.

### ***2.8 Electrochemical noise measurements***

The electrochemical noise measurements were carried out using three nominally identical electrode (identical in composition, dimension, surface finish, microstructure) configurations made of the material under investigation and designed as mentioned in the specimen preparation section 2.4.2 and 2.4.3, for carrying out studies in nitric acid, simulated HLW and ferric chloride medium . Figure 2.6 represents the three identical electrode configuration used for EN measurements. A multichannel electrochemical noise system, Autolab PGSTAT 30 custom built with a low noise module and a data

management system (Ecochemie make, The Netherlands), was used for carrying out the experiments. The three identical electrodes, two of them that served as working electrodes (WE1 and WE2) and one as reference electrode (RE), were immersed in the electrolyte of interest.

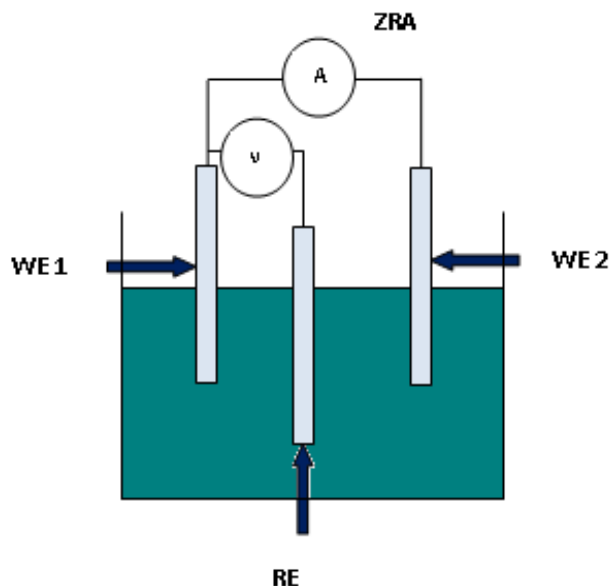


*Figure 2.6 Schematic representation of the EN cell using three identical electrode configuration*

The cell assembly was placed in a Faraday cage to minimize any external influences such as electromagnetic and instrumental noise. The connections from the electrodes of the cell to the Autolab instrument were made as given in Figure 2.7. The Autolab instrument measurement circuit measures the current noise between two identical working electrodes which are coupled through a zero resistance ammeter (ZRA) that keeps the working electrodes at the same corrosion potential. The potential noise of the coupled working electrodes is measured against the reference electrode (RE). As the reference electrode

used is made of the same material as that of the working electrodes, it is called a pseudoreference electrode [49].

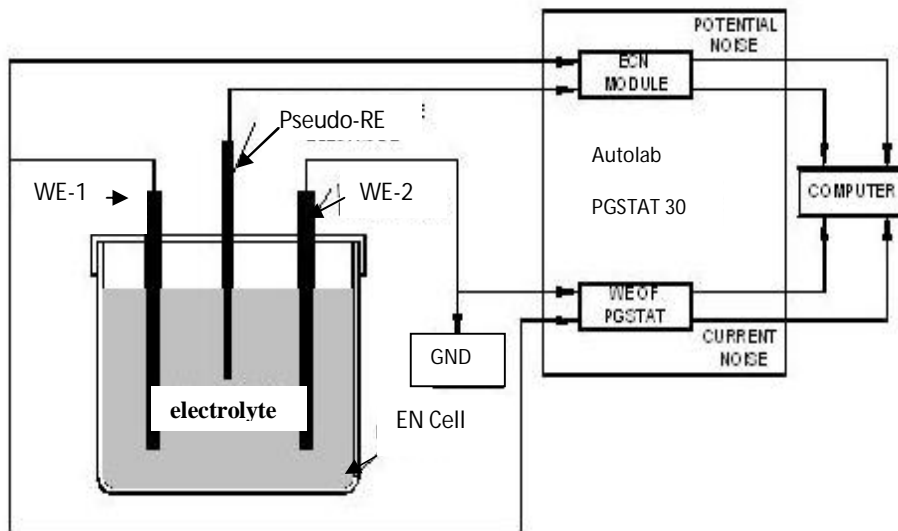


**Figure 2.7 Schematic of the connections between EN cell and instrument**

**WE-1 : working electrode 1 WE-2 : working electrode 2**

Simultaneous acquisition of current and potential noise was carried out with respect to time, under freely corroding condition. A sampling interval of 0.5s was chosen over 8192 consecutive data points. The frequency domain corresponding to the sampling conditions (0.5s) was evaluated to be between 1Hz ( $f_{\max}$ ) and 0.2 mHz ( $f_{\min}$ ), from  $f_{\max} = 1/2\Delta t$  where  $\Delta t$  is the sampling interval and  $f_{\min} = 1/N\Delta t$  where  $N$  is the total number of data points. To avoid aliasing [46], Autolab PGSTAT 30 (built in with a noise module) uses a low pass filter with a cut off of 1 kHz at the input stage. Further, the ADC module samples the signals with the highest possible sampling rate, which is typically about 50 kHz.

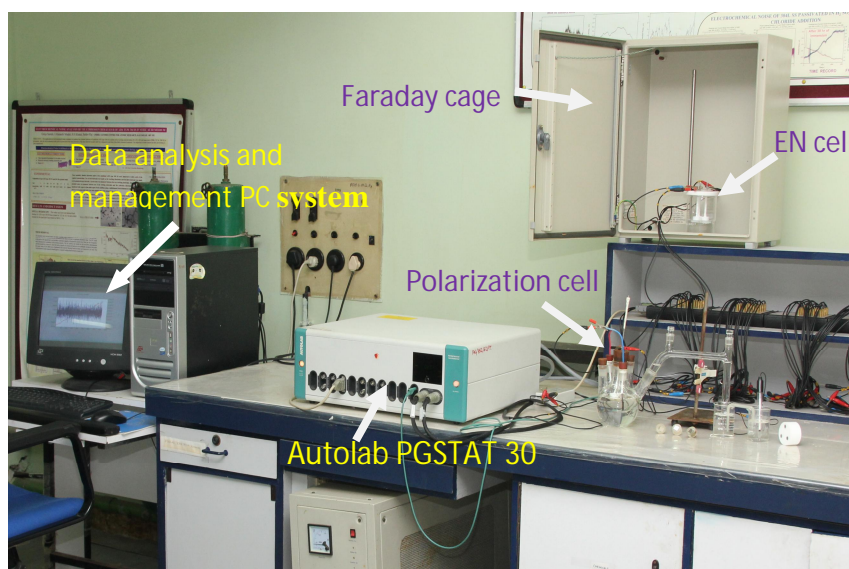


***Figure 2.8 Photograph of the experimental set up for the electrochemical studies***

While the data is being acquired, the A/D values obtained are averaged and an average value is provided in the data at each time interval. As frequencies above Nyquist frequency is cut off before the A/D conversion, aliasing is avoided. Similar procedure has been explained by Bastos et al [62] as an effective method to avoid aliasing. Figure 2.8 shows the photograph of the experimental set up used for the electrochemical studies.

### ***2.8.1 Data treatment and analysis***

In the various studies presented in the thesis, the acquired current and potential noises were detrended by linear fit method [46, 65, 74, 110] in order to remove the DC drift.

Typical plots of potential noise before and after trend removal is represented in Figure 2.9.

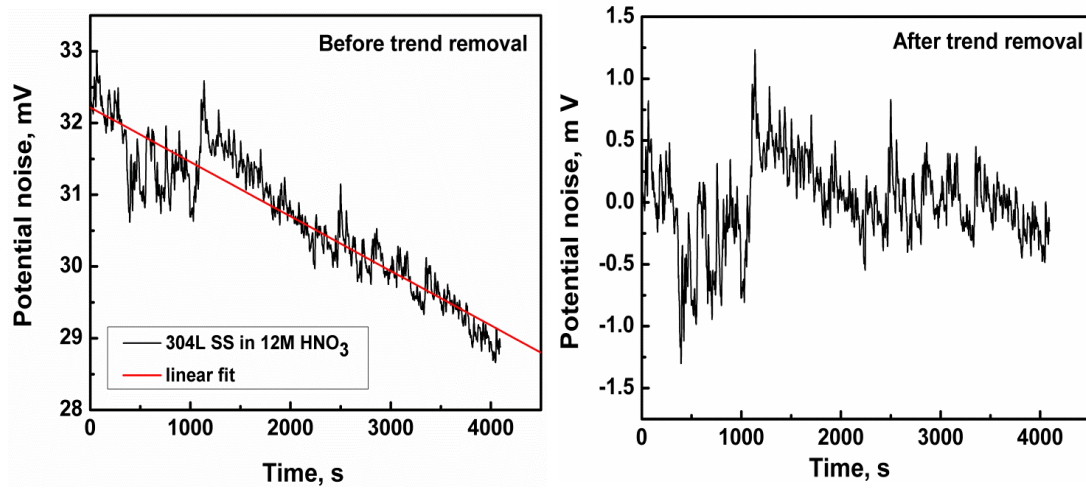


**Figure 2.9** Typical plots of potential noise before and after trend removal

Trend removal was carried out for every time record of the potential and current noise. It was found that the data after trend removal had the mean of potential and current noise around zero. Detrended EN data was subsequently used for all analysis.

#### **2.8.1.1 Correction for potential noise from pseudoreference electrode**

Since the reference electrode used is also identical to the working electrodes (WE1 and WE2, maintained at the same corrosion potential), there are two sources contributing to the potential noise signal, say  $v_1$  and  $v_2$ , where  $v_1$  is the potential noise signal from the working electrode pair and  $v_2$  is the potential noise signal from the reference electrode. Since they are identical electrodes in the same environment, the measured potential noise

signal was divided by  $\sqrt{2}$  to correct for the noise generated by the pseudoreference electrode. The corrected potential noise was used for all analysis.

$$V(measured) = \sqrt{(v_1^2 + v_2^2)}$$

and as  $v_1 = v_2$ ,

$$V(measured) = \sqrt{2v_1^2}$$

$$V_1 = v_{(measured)} / \sqrt{2}$$

The correction factor is applied based on the assumption that the noise contribution from the reference electrode is similar to the coupled electrodes, for identical electrodes in identical environment. This method has been discussed by Dawson [44] and Reichert [188] for potential noise corrections for three identical electrode systems. However, in practical situations, microscopic differences in the electrodes (microstructure, surface finish etc) may result in variations in the noise contributions. This aspect has not been considered in the studies presented in the thesis. In recent literature, Bertocci et al [189] have introduced correction for potential noise taking into consideration the variation in the noise generated by the reference electrode. Such variations in potential noise contributions from the pseudo-reference electrode will be considered in future studies.

### **2.8.1.2 Data Analysis**

A scheme of the data analysis methods used in the various studies presented in the thesis is summarized in Figure 2.10. The corrected EN time records after trend removal and potential noise corrections were visually examined to look for distinct signatures of



various corrosion processes. Further, the corrected data was analysed by statistical [49, 46], spectral [49, 44, 96], wavelet [113-117] and shot noise [109-111] methods to derive parameters which were used to correlate corrosion mechanism and the extent of corrosion.

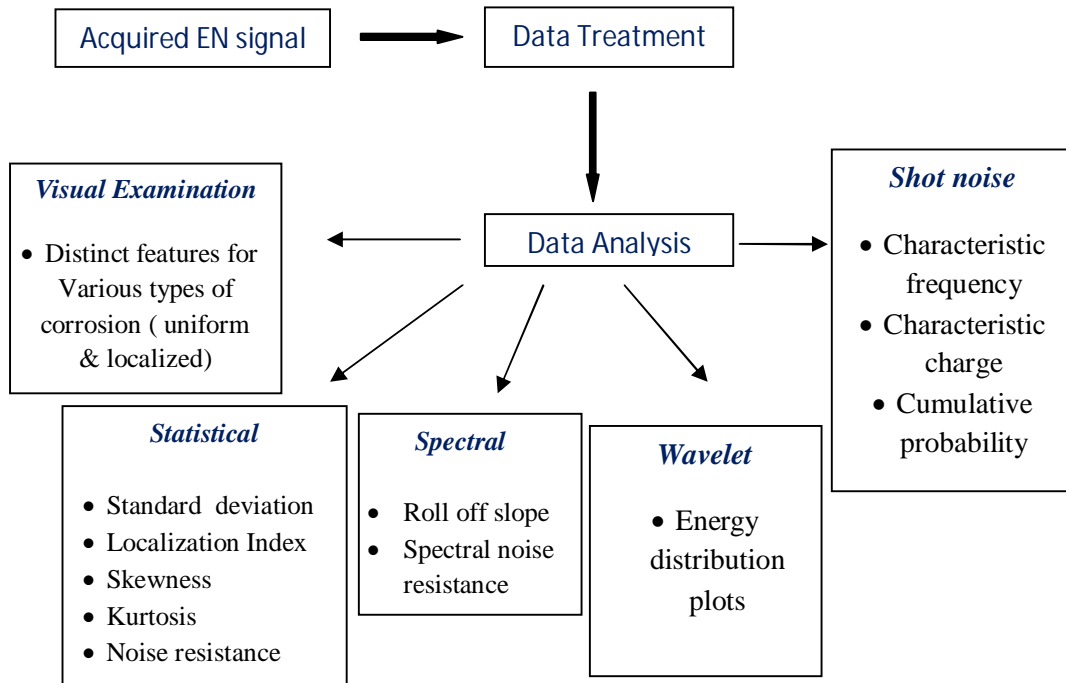


**Figure 2.10 A scheme of the data analysis methods used for the various electrochemical noise studies**

➤ **Statistical evaluation of the time records** were carried out to derive parameters such as (i) standard deviation, (ii) localization index, (iii) skewness, (iv) kurtosis, which were used to derive information on the corrosion mechanism while (v) noise resistance was used to obtain the extent of corrosion or corrosion activity.

➤ ***Power spectral density plots*** The EN time records were converted into power spectral plots by using FFT method, prior to which a hanning windowing function was used. Power spectral density plots (PSD) were obtained from the detrended time records by initially applying a Hann window and subsequently performing an FFT. Since the quantity of interest is the noise content, the mean of the data was subtracted from all the data points. The mean-subtracted data were subjected to windowing. For the windowing purpose, Hann function has been used. The smooth variation of the window function ensures that there are no abrupt spikes in the frequency domain after performing the FFT of the windowed data. The FFT of the resultant data was used to construct the PSD. The power spectral density of the data was obtained as the absolute square of the amplitudes in the frequency-representation given by the FFT.

The following parameters were evaluated from the power spectral density plots.

- i. Roll off slopes for deriving mechanistic information.

The power spectral density (PSD) plots show the following frequency dependency

$\log \text{PSD} = m + n \log f$ , where  $m$  is the magnitude of PSD expressed as  $\log \text{V}^2\text{Hz}^{-1}$  and  $\log \text{A}^2\text{Hz}^{-1}$  for the potential and current noise respectively, it is the intercept of potential or current PSD plot at frequency = 1Hz, and  $n$  is the slope of the PSD plot called the roll - off slope.

- ii. Power spectral density values of current and potential noise were used for computing spectral noise impedance data. The low frequency values were used for computing spectral noise resistance, which were used to derive information on the corrosion activity.

- Parameters such as characteristic frequency, cumulative probability were derived from the shot noise theory for deriving mechanistic information.
- Energy distribution plots [113-117] (EDP) were obtained from wavelet analysis to understand the various processes occurring on the material surface as corrosion progressed. In the studies presented in the thesis, orthogonal wavelet transform (OWT) which is a classical version of DWT, was used to analyze current noise. In this work, the decomposition of the signal was carried out at level eight by orthogonal Daubechies wavelet of the fourth order (db4). The results of the wavelet transform can be represented using the energy distribution (ED) of the crystals.

The energy  $E$  of a signal (time record),  $x_n$ , containing  $N$  number of data points, is given

by 
$$E = \sum_{n=1}^N x_n^2$$

The fraction of energy of each crystal is given by

$$ED_j^d = \frac{1}{E} \sum_{n=1}^N d_{j,n}^2$$

$$ED_j^s = \frac{1}{E} \sum_{n=1}^N s_{j,n}^2$$

The property of the orthogonal is that the energy of the analyzed signal  $X_n$  is equal to the sum of the energies of all the components obtained by the wavelet transform. As the wavelet chosen is orthogonal, the following equation is satisfied.

$$E = ED_j^s + \sum_{j=1}^J ED_j^d$$

ED is a function of the energy of the crystal and does not have unit. The plot of ED Vs corresponding crystal name is called energy distribution plots or EDP. It gives the contribution of every crystal to the original signal.

The chapter presents the results of the investigations carried out on the electrochemical noise monitoring during pitting corrosion of 304L SS in 0.05 M FeCl<sub>3</sub>. Electrochemical current and potential noise was simultaneously acquired from 304L SS in 0.05 M FeCl<sub>3</sub> using a three electrode configuration. Power spectral, statistical and wavelet analysis have been used to know the uniqueness of the parameters proposed for the identification of various types of corrosion process. The results indicated that the roll off slopes derived from power spectral analysis and statistical parameters such as standard deviation, localization index and kurtosis corroborated with pitting as the corrosion mechanism. Energy distribution plots (EDP) obtained from wavelet analysis of current noise was found to be useful to derive mechanistic information on the progress of corrosion. Discrete wavelet transform was used to decompose the signals into D<sub>1</sub>, D<sub>2</sub>, D<sub>3</sub>...D<sub>8</sub>, S<sub>8</sub> set of coefficients. The EDP showed that the contribution from the medium time scale crystal, D<sub>5</sub> prevailed over the smaller time scale crystals and larger time scale crystals during the initial stages of immersion. With increase in time of immersion, the energy deposition on the larger time scale crystals increased and the maximum energy was concentrated on the D<sub>8</sub> crystals indicating that the dominant process occurring on the specimen surface was stable pitting. The results of the investigation are detailed in the chapter.

---

### ***3.1 Introduction***

Pitting is a form of localized attack that results in cavities or holes in the metal surface with diameter about the same or less than the depth. It is one of the most destructive forms of corrosion and causes equipment failure because of perforation, with only a small percent weight loss of the entire structure, and failures occur with extreme suddenness. The detection and quantitative estimation of pitting is difficult and sometimes it may take several months or years to show up in actual service. Conventional corrosion monitoring techniques has been successfully applied to monitor uniform corrosion, but, localized corrosion detection remains a challenge. Electrochemical noise signals emerging from corrosion process gives instantaneous response to localized attacks and hence could be exploited to detect and map the event. The time dependant fluctuation of current and potential during corrosion process have been used to indicate the type of attack and the rate. For uniform corrosion, the methods of noise analysis using noise resistance and impedance are quite well established, however their application is limited for localized corrosion. Electrochemical noise parameters have been deduced by various investigators to understand localized corrosion [49]. Some of the methods that are proposed in literature for monitoring pitting corrosion utilize power spectrum [44, 49, 50, 74, 96, 148] statistical parameters such as skewness, kurtosis [190, 191, 192] localization index [49, 82] estimation of the intensity of characteristic transient occurrence in voltage or current records [193] , shot noise parameters [109] , wavelet [113, 115,116,194] and chaotic analysis.

The presence of chloride ions in reprocessing medium or high level waste, by ingress of chloride from the water or acid used for the preparation of the process medium, is

detrimental. This is mainly because the adsorption and penetration of these ions through the protective passive film on the surface of 304L SS, could lead to local breakdown of passive film, promoting the formation of pits, the propagation and growth of which is catastrophic. The objective of the study is to obtain electrochemical noise data using the three identical electrode probe made of 304L SS, and derive mechanistic information of the processes occurring on the material surface exposed to environments, conducive for pitting to occur. Three identical cylindrical 304L SS bare electrodes were immersed in 0.05 M  $\text{FeCl}_3$  under ambient conditions and electrochemical current and potential noise were acquired under freely corroding conditions for 25 h of immersion. The acquired current and potential noise time records were analyzed by visual examination, statistical, spectral and wavelet methods to derive parameters that could be correlated to corrosion mechanism. The chapter presents the results of electrochemical noise monitoring of 304L SS during pitting corrosion in 0.05 M  $\text{FeCl}_3$  medium, under freely corroding conditions.

---

### ***3.2 Electrochemical noise monitoring during pitting corrosion of 304L stainless steel***

#### ***3.2.1 Time domain and power spectra***

The electrochemical current and potential noise – time records for AISI type 304L SS in 0.05 M  $\text{FeCl}_3$  is given in Figure 3.1 (a-e). It was observed that during the initial stages of immersion, the current and potential noise showed random high amplitude fluctuations which are generally indicative of localized corrosion [110, 195]. With further immersion time, the random potential and current fluctuations started becoming more distinct. After 25 h of immersion, distinct current and potential fluctuation appeared in the time record. For almost every potential drop, a corresponding current spike was observed.

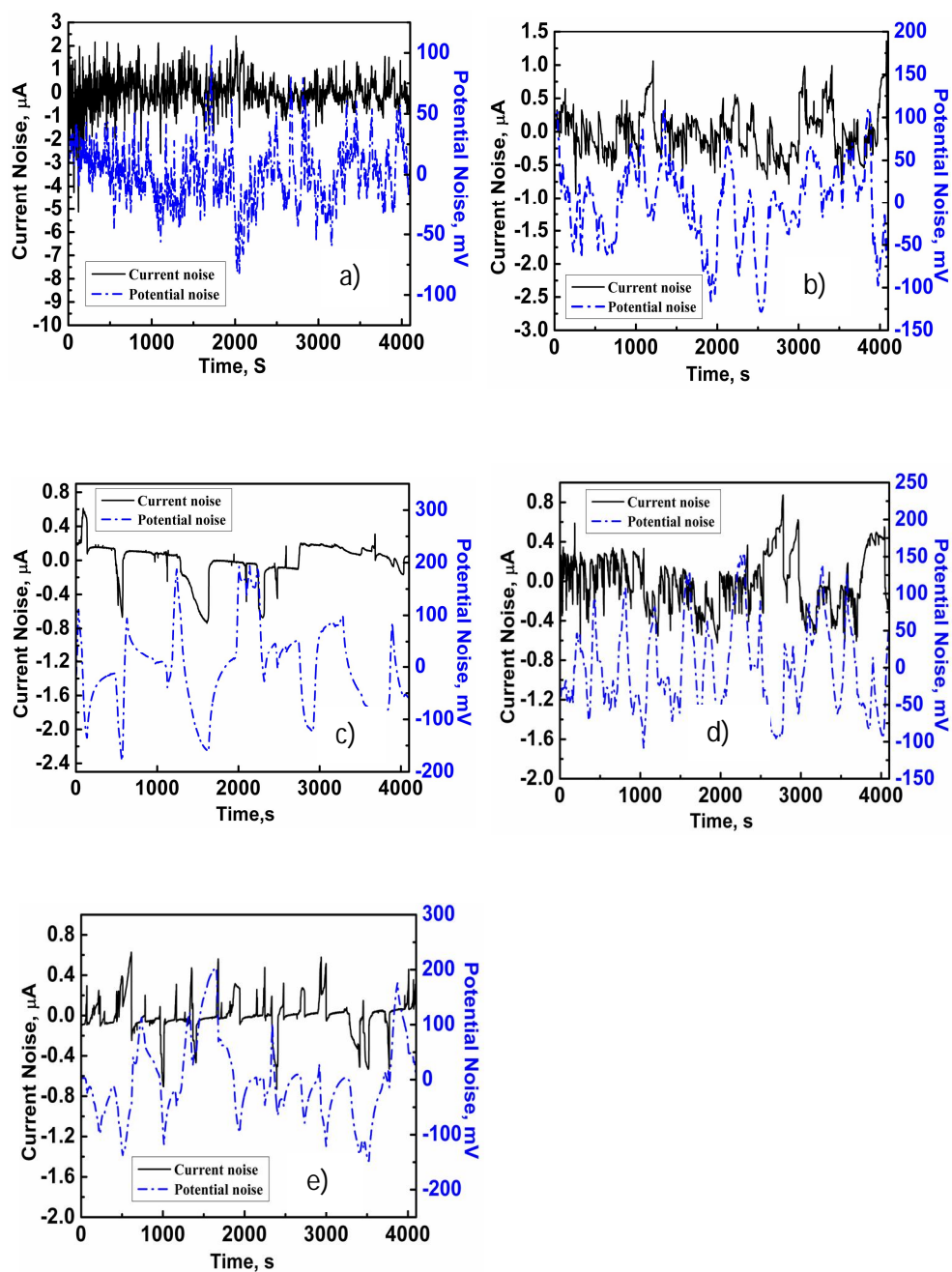


Figure 3.1 Electrochemical current and potential noise-time records taken after a) 1 h b) 10 h c) 14 h d) 23 h e) 25 h of immersion



The potential fluctuations were characterized by a sudden fall and a sudden exponential rise and the current transients showed a sudden rise and fall. The current rise was accompanied by a drop in potential till a local minimum was attained, which corresponds to the repassivation point, after which the potential recovery occurred. The potential recovery does not result from repassivation, as no current flows to the pitted surface during potential recovery. The exponential recovery could be attributed to recharging of double layer [44, 196, 197, 198]. During initiation and propagation of pitting corrosion, metal dissolution and hence electron flow occurs from the pit site to the external metal surface, and these electrons get charged within the passive film and double layer. Subsequently, cathodic consumption of these electrons occurs over the entire surface giving rise to the exponential recovery [198]. These transients showed typical features of pitting attack. It has been reported that potential noise associated with pitting corrosion initiation is characterized by a series of sharp decrease of the electrode potential followed by potential recovery [59, 199].

Typical power spectral density (PSD) plots of potential and current noise taken after 1 h, 25 h of immersion of 304L SS in 0.05 M  $\text{FeCl}_3$  are represented in Figure 3.2 (a-d). The PSD of potential and current noise is found to exhibit  $1/f^n$  variation. The power spectral density decreased with increase in frequency, which could be attributed to localized corrosion. Many investigators have fitted PSD of electrochemical noise during localized corrosion on a logarithmic scale by a  $1/f^n$  function, and used PSD roll-off slope to determine the type of corrosion [56, 57, 102, 103, 200]. Roll off slopes in the range of -2 to -4 has been associated with pitting corrosion [108, 138, 201]. However, discrepancy exists among some researchers on the use of roll of slope for deriving corrosion

mechanism. Dawson et al. [56, 202] have reported small roll-off slope for pitting (-2 and less) and steep slopes of - 4 for general corrosion.

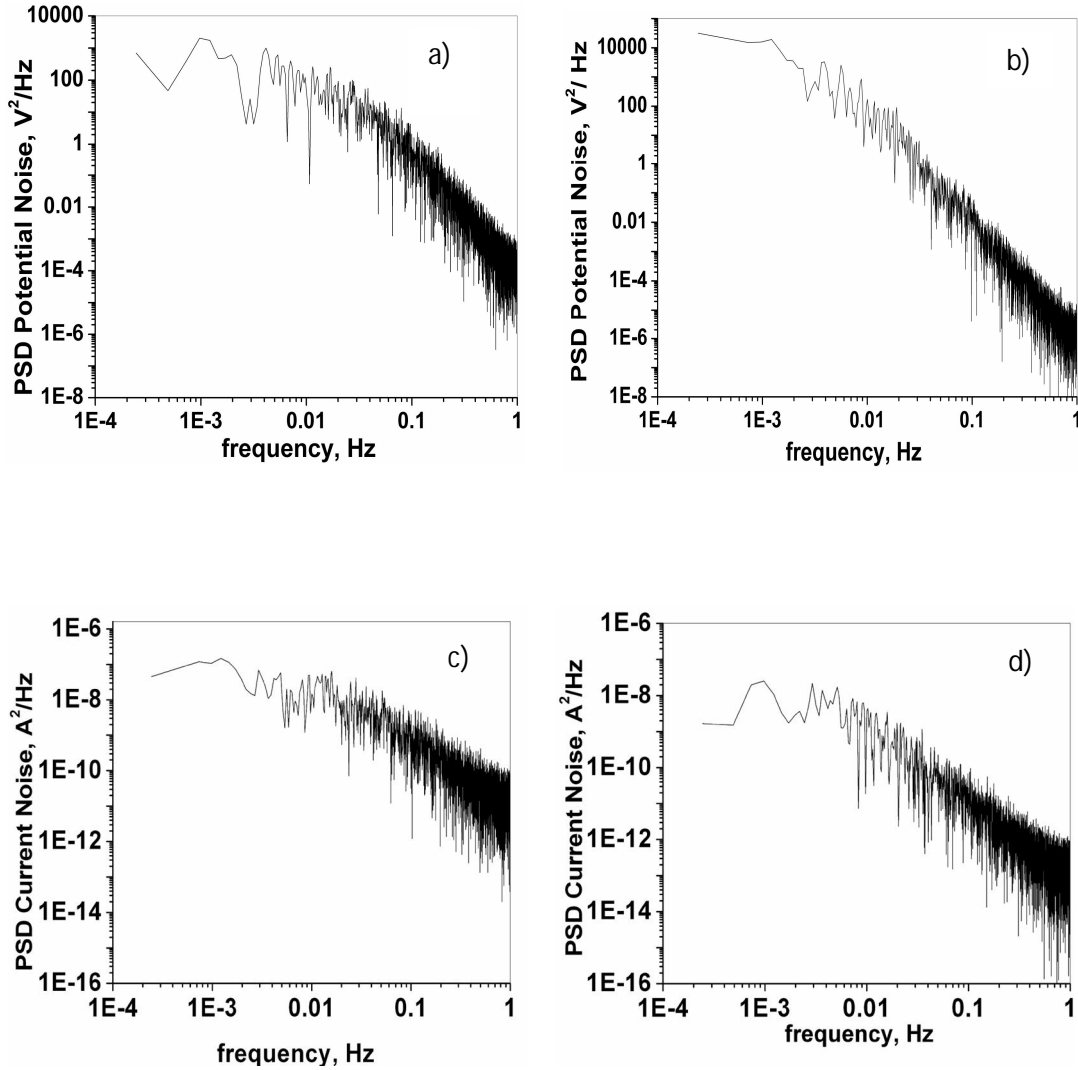


Figure 3.2 PSD of potential and current noise with time of immersion a & c) 1 h, b & d) 25 h

The PSD roll off slope derived from these plots, as the slope of the  $1 / f^n$  noise, is given in Table 3.1.

S No	Number of hours of immersion of 304L SS in 0.05 M FeCl <sub>3</sub>	Roll of slope of PSD of potential noise	Roll off slope of PSD of current noise
1	1	-3.6	-1.8
2	6	-4	-2.0
3	10	-4	-2.2
4	14	-4	-2.7
5	23	-4	-2.1
6	25	-4	-2

***Table 3.1 PSD roll off slopes derived from power spectral density plots***

The PSD roll off slopes of potential noise was found to be around -4, and that for current noise was around -2, which could be attributed to pitting as the mode of attack, throughout the immersion period. Optical micrograph as represented in Figure 3.3 which was taken after electrochemical noise experiment, showed pitting attack.



***Figure 3.3 Optical micrograph of 304L SS after electrochemical noise experiment showing pitting attack (after 25 h of immersion)***

### 3.2.2 Statistical analysis

The standard deviation of potential noise was evaluated from the electrochemical noise – time record using Equation (1.3). Figure 3.4 shows the standard deviation of potential noise as a function of time of immersion. The standard deviation of potential noise was found to be increasing with time of immersion showing increase in the rate of pitting attack as corrosion progressed. The localization index (LI) for 304L SS in 0.05 M FeCl<sub>3</sub> was evaluated from the acquired electrochemical noise data (without detrending) using Equation (1.4) and was found to be in the range of 0.7 and 1 throughout the course of immersion. Localization index of 0.1 to 1 has been attributed to pitting corrosion [108] and hence the mechanism of corrosion of 304L SS in 0.05 M FeCl<sub>3</sub> could be attributed to pitting attack. A graph of LI vs time of immersion is shown in Figure 3.5. LI has been used by several investigators for determining corrosion types [82, 21, 203, 204, 205, 206]. These investigators have used raw noise data to determine LI and arrived at corrosion mechanisms. However, discrepancy exists between various investigators on the data treatment and interpretations using LI. Since the mean of the detrended noise data ( $\overline{x_i}$ ), would be negligible, the standard deviation ( $\sigma_i$ ) and root mean square current noise ( $i_{rms}$ ) would converge to the same value and hence, mathematically, the localization index evaluated from detrended data would be unity, irrespective of the corrosion type. Cottis [46] opined that LI for identification of localization of corrosion is unduly influenced by the mean current and hence less reliable. Mansfeld [72] obtained extreme values of LI of 0 and 1 for uniform corrosion of mild steel and passive behavior of titanium respectively. The author demonstrated that LI = 0 for systems for which the individual data shows only small deviation from the mean and LI=1 for large deviations

and concluded that LI should be used to define the distribution of data around mean and not as an indicator of corrosion mechanism. The author further demonstrated that for trend removed data, LI is unity.

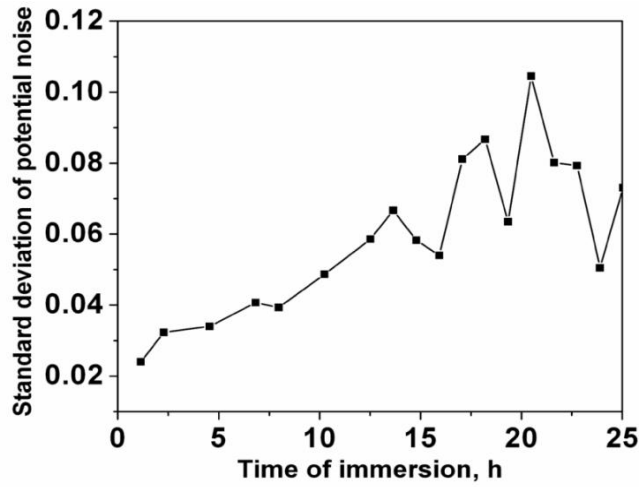


*Figure 3.4 Standard deviation of potential noise as a function of time of immersion, for 304L SS in 0.05 M FeCl<sub>3</sub>*

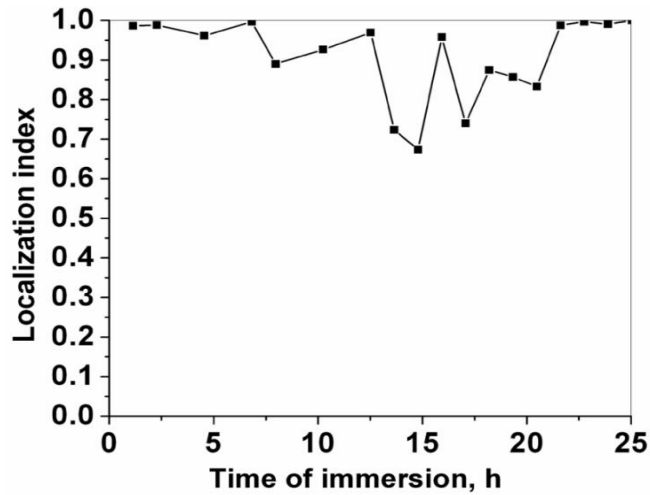


*Figure 3.5 Localization index for 304L SS in 0.05 M FeCl<sub>3</sub> as a function of time of immersion*

Statistical parameters such as kurtosis and skewness have also been reported to indicate corrosion mechanism [46, 92, 95, 195, 207]. Skewness of a Gaussian distribution is zero. A positive value of skewness indicates a tail in the positive direction and negative value indicates a tail in the negative direction. Kurtosis gives a measure if the data is peaked or flat compared to Gaussian distribution. Kurtosis of a Gaussian or normal distribution is 3 and higher values indicate more sharply peaked distribution than a normal distribution and kurtosis less than 3 indicates flat topped distribution. Noise generated from uniform corrosion follows a Gaussian or normal distribution and localized corrosion leads to deviation from a normal distribution and can be determined from kurtosis and skewness. Eden and Reid et al [92, 95, 192] have reported skewness and kurtosis analysis of potential and current signals for identifying corrosion mechanism and values have been tabulated for general and localized (pitting, stress corrosion cracking) corrosion. Values of kurtosis greater than 3 have been associated with pitting corrosion. In the present investigation, the kurtosis and skewness of the acquired current and potential noise were computed over 8192 samples. The standard errors of kurtosis for 8192 samples is  $\sqrt{(24/N)} = 0.054$  and that for skewness is  $\sqrt{(6/N)} = 0.027$ . The kurtosis of potential noise for 304L SS in 0.05 M  $\text{FeCl}_3$ , computed from Equation (1.7), was evaluated to be ranging from 3 to 4, and that for current noise was between 2 to 8. Hence, it could be attributed to pitting as the mode of corrosion attack. The kurtosis of potential and current noise is found to be significantly larger than the standard error and is clearly positive and depicts a peaked distribution. A graph of kurtosis of potential and current noise as a function of time of immersion is shown in Figure 3.6. From the kurtosis values, it has been observed that the material surface is undergoing pitting attack throughout the immersion period.

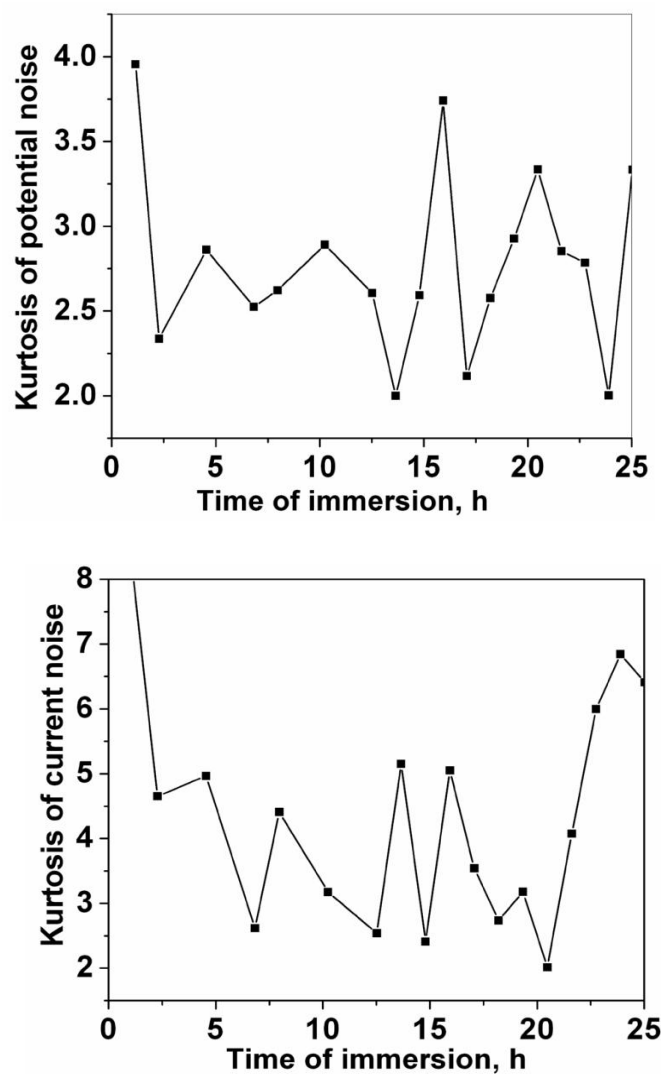


***Figure 3.6 Kurtosis of potential and current noise for 304L SS in 0.05 M FeCl<sub>3</sub> with time of immersion***

The skewness of current and potential noise evaluated from Equation (1.8) was found to be close to zero. The skewness values are not significant to derive useful information about the mode of localized attack. It is reported that unidirectional transients will

produce a skewed distribution, together with a positive kurtosis and bidirectional transients, tend to give zero skew, but the kurtosis will remain positive [117]. In addition, the distribution of current and potential values will tend toward a normal distribution for larger number of transients in which case skew and normalized kurtosis will tend toward zero. Figure 3.7 represents graph of skewness of the noise data as a function of time of immersion.

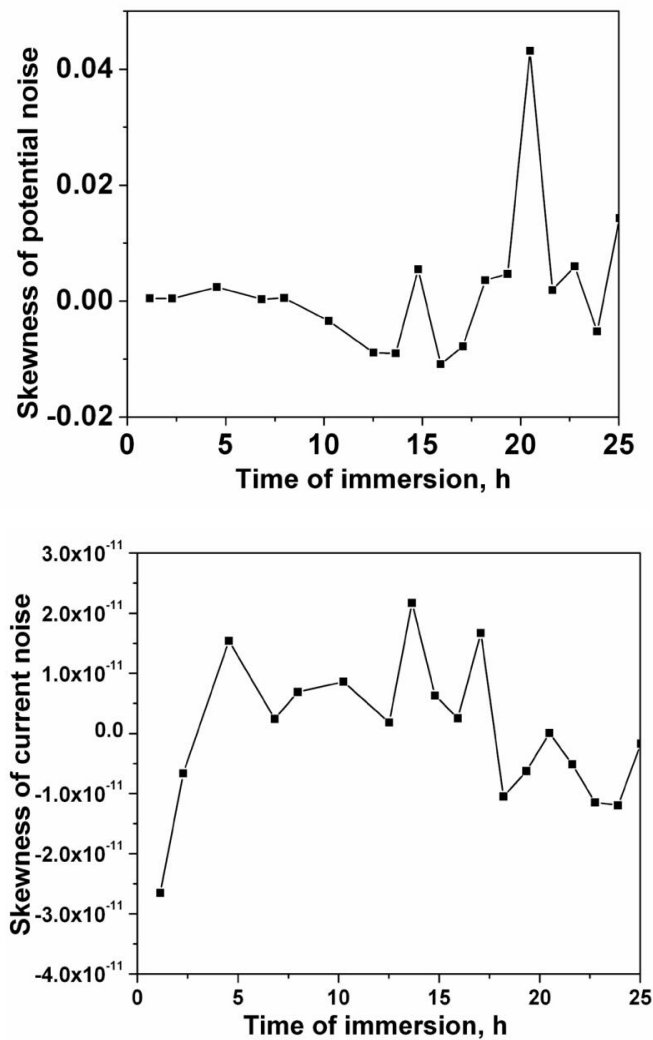


*Figure 3.7 Skewness of potential and current noise for 304L SS in 0.05 M FeCl<sub>3</sub> with time of immersion*



### 3.2.3 Wavelet analysis

A typical representation of an eight level decomposition of the electrochemical current noise - time record taken 14 h after immersion using orthogonal wavelet transform is shown in Figure 3.8.

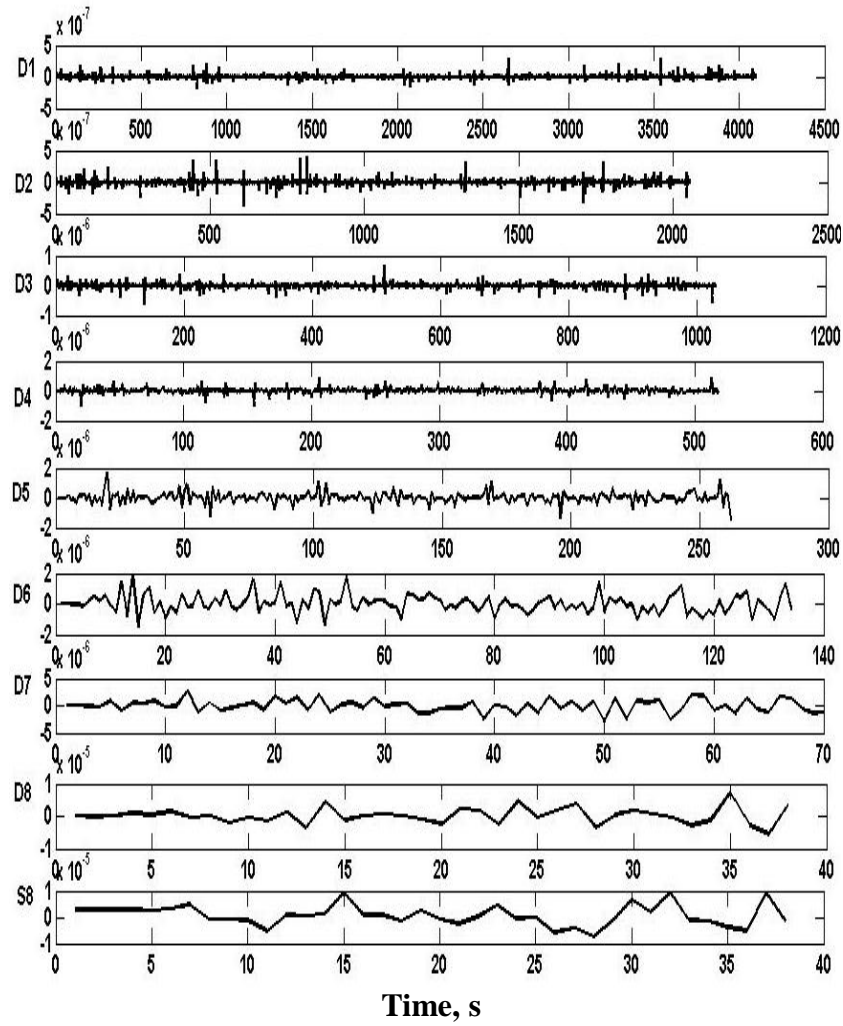


*Figure 3.8 Typical representation of coefficients obtained by wavelet transform of the current noise time record taken 14 h after immersion.*

The scale range calculated using Equation (1.18) for an eight level decomposition is given in Table 3.2.

<b>Crystal name</b>	<b>D1</b>	<b>D2</b>	<b>D3</b>	<b>D4</b>	<b>D5</b>	<b>D6</b>	<b>D7</b>	<b>D8</b>
<b>Scale range(s)</b>	0.5-1	1-2	2-4	4-8	8-16	16-32	32-64	64-128

*Table 3.2 Scale range for  $j=8$ ,  $\Delta t = 0.5$*

The energy distribution plots (EDP) are shown in Figure 3.9 (a-e). According to literature reports [115, 116, 194] the position of the maximum relative energy distribution of a crystal corresponds to dominant process contributing to the signal. The time scale of crystal is ranked as  $D1 < D2 < D3 < D4 < D5 < D6 < D7 < D8$  (as shown in Table 3.2). For an eight level decomposition, EDP can be divided into three zones. The relative energy distribution concentrated on smaller time scale crystals, D1-D3, gives information about rapid events such as metastable pitting, D3-D6 of medium time scale is associated with repassivation / propagation of pits and the large time scale D6-D8 crystal, gives information on diffusion or growth of pits [170, 208, 209, 210, 211, 212]. Using Equation 1.18, the scale range corresponding to D1-D3 was found to be ranging from 0.5-4 s, and that for D3-D6 and D6-D8 was found to be ranging from 4s-32s and 16s-128s respectively. ED plot for the initial one hour immersion is shown in Figure 3.9 a. From the figure, it is observed that the relative energy is defined on crystals D2, D3, D4, D5, D6, D7, D8 and the maximum contribution is on D5. The figure shows that the energy

contribution on D2, D3, D4 are 4%, 8%, 14% and that on D6, D7, D8 are 16%, 14%, 12% respectively. The maximum energy is deposited on D5 crystal which is around 19% of the total energy.

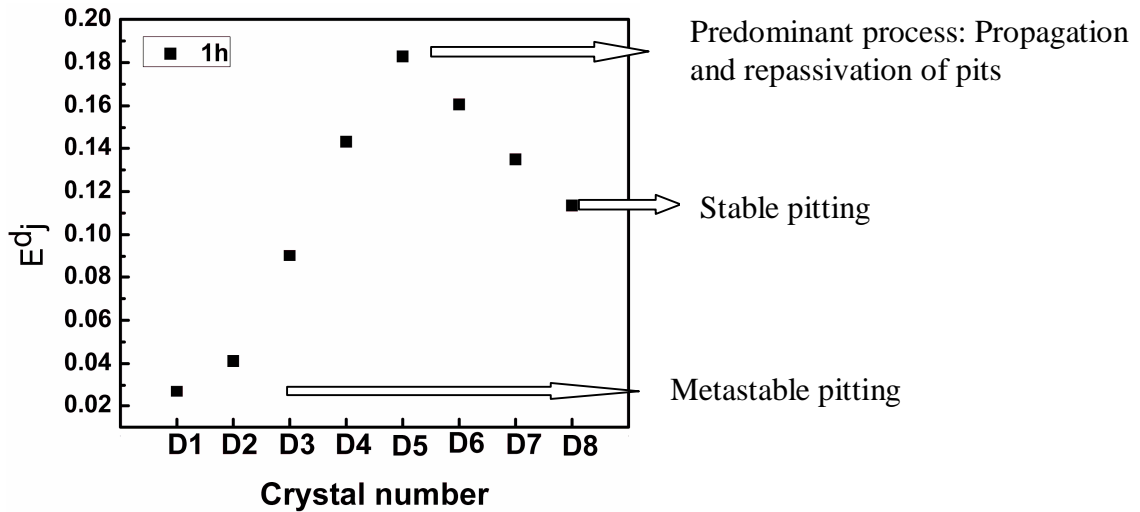


**Figure 3.9 a) EDP of current noise after 1h of immersion**

It could be inferred that during the initial immersion period three processes are occurring on the specimen surface, 1) small time scale process attributed to metastable pitting, 2) medium time scale process attributed to propagation and repassivation of pits and 3) large time scale process attributed to growth and stable pitting. Since the maximum energy is concentrated on D5 crystal it could be inferred that the predominant process occurring on the specimen surface is propagation/repassivation of pits.

The ED plots after 10 h and 14 h immersion shows energy distribution concentrated on D4, D5, D6, D7, D8 with the contribution of D<sub>j</sub> increasing with j, from D4 to D8. The energy distribution on the small time scale crystals, D1-D3, ranging from 0.5s to 4s, is negligible showing the absence of metastable pitting. It is observed that the energy

distribution on the larger time scale crystals, D6-D8, has prevailed over the medium time scale crystals (D4, D5). The scale range for D6-D8 varies from 16s-128s, which is associated with diffusion or growth of pits (stable pitting). Among the two processes occurring on the specimen surface which could be attributed to propagation/repassivation of pits and stable pitting, the dominant process is stable pitting.

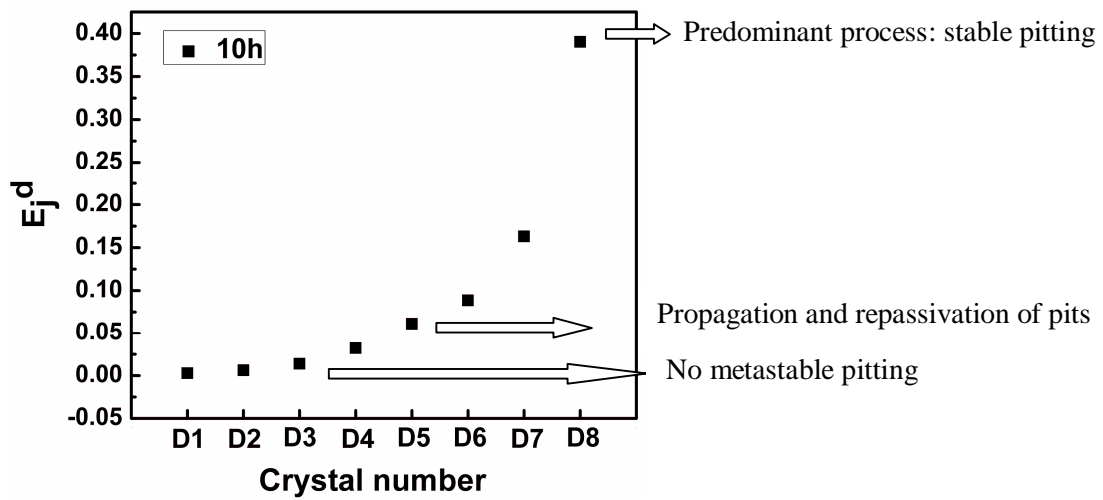


*Figure 3.9 b) EDP of current noise after 10h of immersion*

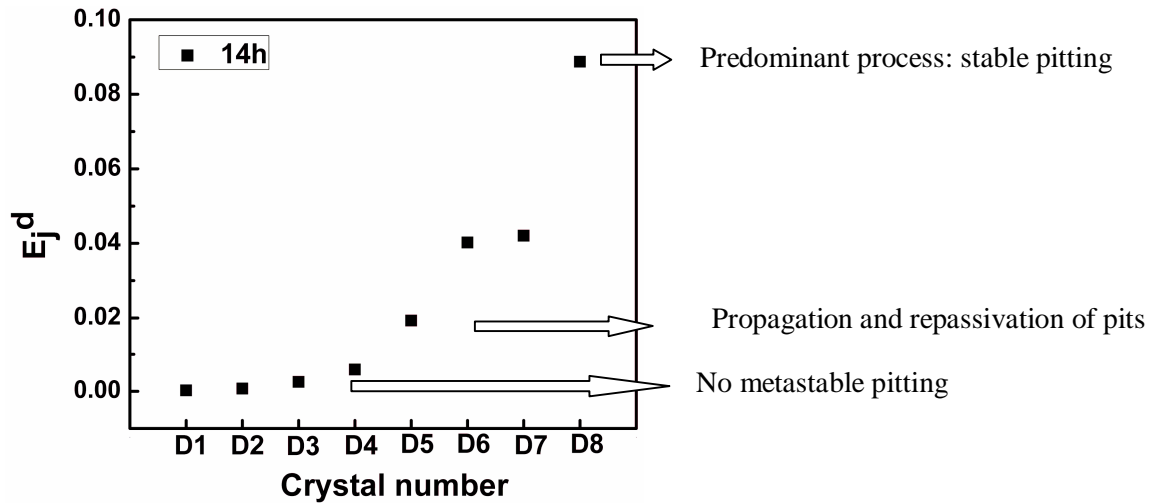


*Figure 3.9 c) EDP of current noise after 14h of immersion*

With further immersion, it is found that the energy concentration on D1-D3 is negligible, and that on D4, D5 has decreased. Most of the energy is concentrated on D6-D8 with maximum deposition on D8 crystal. It could be concluded that, during initial stages of immersion of the specimen in ferric chloride medium, the surface was undergoing metastable pitting, propagation/repassivation of pits and stable pitting. With time of immersion, it is seen that the relative energy on the small time scale (D1 – D3) continues to be negligible in the absence of metastable pitting and the energy contribution on medium time scale crystal (D4-D5) too is diminishing indicating that the propagation/repassivation events have got suppressed. Most of the energy is accumulated on the large time scale crystals, D6-D8, the contribution increasing with  $j$  and maximum concentration is in the D8 crystal which indicates that the dominant process occurring on the specimen surface is stable pitting.

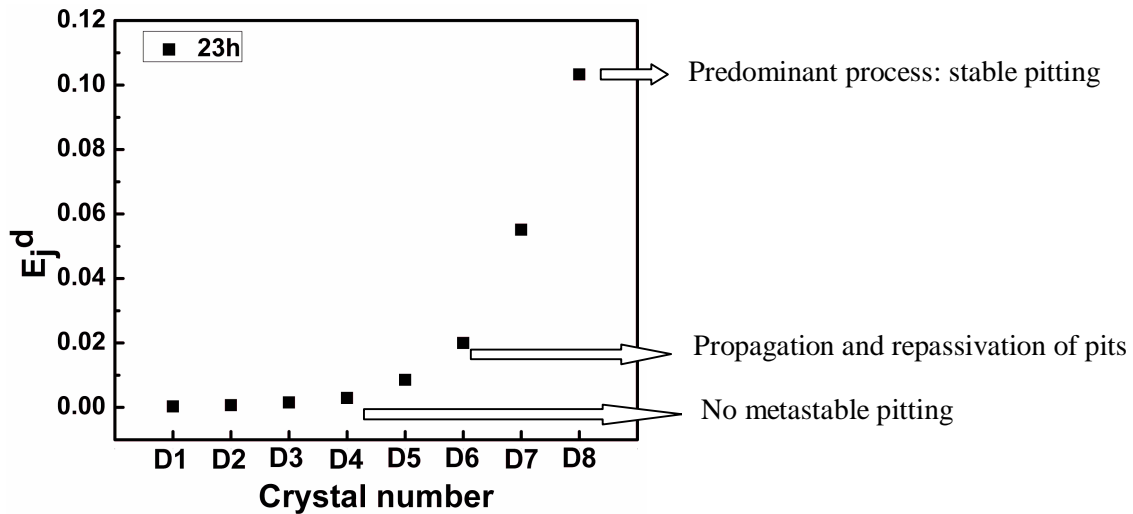


**Figure 3.9 d) EDP of current noise after 23 h of immersion**

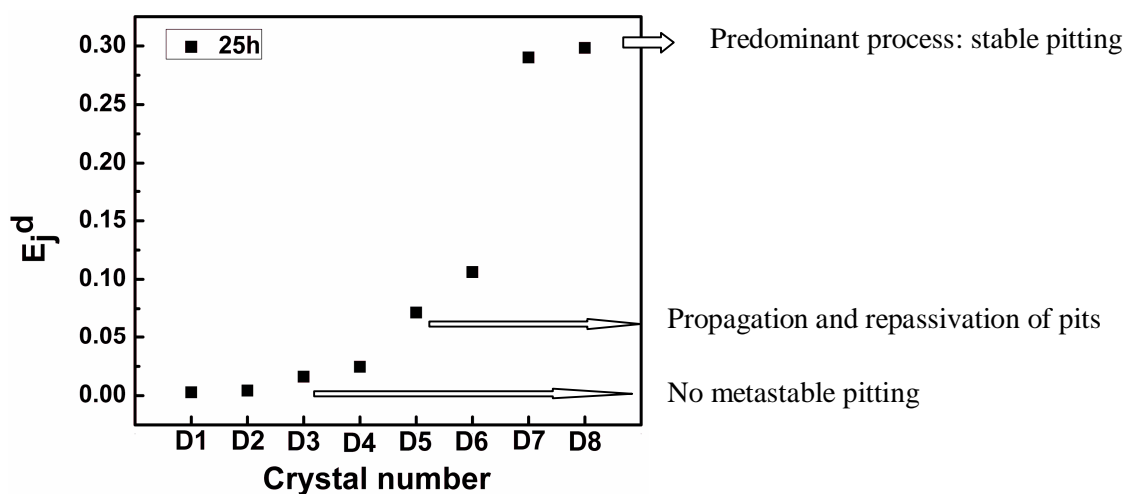


**Figure 3.9 e) EDP of current noise after 25h of immersion**

Time domain and power spectral analysis provided information on the corrosion phenomenon as a whole and the corrosion process was deduced to be pitting. From wavelet analysis, it was possible to infer mechanistic information about the various contributing corrosion processes occurring at every stage of corrosion of the specimen. The evolution of pitting process from metastable and propagation/repassivation to stable pitting could be well depicted by wavelet analysis.

### 3.3 Conclusions

The following conclusions were arrived from the electrochemical noise monitoring of 304L SS in 0.05 M  $\text{FeCl}_3$ :

The potential and current time record showed high amplitude fluctuations during the initial stages of immersion which is indicative of pitting attack. The random high amplitude fluctuations became more defined as corrosion progressed, and distinct potential and current spikes were obtained, which were indicative of pitting corrosion.

The corresponding power spectral plots exhibited  $1/f^n$  variation and the roll off slope corroborated with pitting attack. Statistical evaluation of the time record was carried out and parameters such as localization index, standard deviation of potential noise as well as the kurtosis of potential and current noise corroborated with pitting corrosion. However, useful information on the corrosion mechanism could not be obtained from the skewness. Energy distribution plots obtained from wavelet analysis was found to provide useful information on the mode of pitting attack. During initial stages of immersion, metastable pitting, propagation and repassivation of pits and stable pitting occurred on the specimen surface, the dominant process being propagation and repassivation of pits. With time of immersion, metastable pitting was completely absent and propagation/repassivation of pits got suppressed and the corrosion mechanism comprised of stable pitting as most predominantly occurring on the specimen surface. Although EN time domain and power spectral analysis provided an insight on the corrosion mechanism as a whole, wavelet analysis provided intrinsic details on the processes occurring on the specimen surface as corrosion progressed.

*ELECTROCHEMICAL NOISE MONITORING OF 304L SS IN NITRIC ACID  
AND SIMULATED NUCLEAR HIGH LEVEL WASTE MEDIUM*

---

The chapter demonstrates the application of electrochemical noise resistance (a parameter derived from the EN-time records) as a monitoring tool to reflect the corrosion activity of 304L SS in various environments, simulating reprocessing and waste storage conditions during the monitoring period. Electrochemical noise signals were acquired from AISI type 304L SS under solution annealed and sensitized microstructural conditions, in nitric acid medium of varying concentration (4 M, 8 M, 12 M) and temperature (298 K, 323 K) and in simulated HLW, under naturally corroding conditions, with respect to time of immersion. Double loop electrochemical potentiokinetic reactivation test was conducted to assess the degree of sensitization. EN records revealed passivation process during the monitoring period, under all conditions studied, except for the sensitized specimen in 4 M nitric acid (323 K) which showed localized attack. The results showed an inverse relation between EN resistance and corrosion activity. An increase in nitric acid concentration and temperature resulted in increase in corrosion activity. A profound increase in corrosion activity occurred for the sensitized specimen in nitric acid when compared to the solution annealed specimen, but the increase was marginal in simulated HLW. The results are detailed in the chapter.

---



#### ***4.1 Introduction***

In the interest to develop electrochemical noise probes for corrosion monitoring in nuclear reprocessing and waste storage applications, laboratory scale EN monitoring experiments were carried out on AISI type 304L SS in nitric acid and simulated high level waste (HLW) environments by simulating plant conditions. Type 304L SS exhibits excellent corrosion resistance in nitric acid medium owing to the spontaneous formation of protective  $\text{Cr}_2\text{O}_3$  passive film. But at nitric acid concentrations above 8 M and elevated temperatures, the corrosion potential of 304L SS approaches the transpassive region, where the stable and insoluble  $\text{Cr}_2\text{O}_3$  passive film transforms to soluble  $\text{Cr}_2\text{O}_7^{2-}$  rendering the steel to the external environment [13]. The concentration of nitric acid in HLW ranges from 1 M - 5 M acid, which maintains the corrosion potential of the steel in the passive region and hence passivates and protects 304L SS. However, the dynamic and complex chemistry combined with the radioactive heat generated in HLW can ennoble the corrosion potential, leading to corrosion initiation during long term storage. In nuclear waste tank infrastructure, problems of sensitization can occur in the heat affected zones near welds of thick components, at the time of fabrication. This could lead to corrosion problems in the sensitized zones, during long term exposure to nitric acid and HLW medium and hence requires corrosion monitoring. The corrosion property of 304L SS in nitric acid medium has been studied by various electrochemical investigations, but literature reports on electrochemical noise (EN) studies of such system is scanty. Except for the reports from the DOE sites [51-53] (explained in chapter 1), EN monitoring of 304L SS in nuclear waste medium is not reported. Among the various techniques

implemented in the waste tanks of the DOE sites, EN was found to give real time indication of the localized corrosion (pitting and SCC) in these tanks.

The need for corrosion monitoring in nuclear reprocessing and waste storage plants entails the implementation of suitable corrosion monitoring technique to give real time indication of the changes occurring in the plant conditions. The objective of the present work is to acquire electrochemical noise signals from the three identical electrode EN probe made of AISI type 304L SS under various microstructural conditions (solution annealed and sensitized). The electrolyte was nitric acid medium of varying concentration (4 M, 8 M, 12 M) and temperature (298 K, 323 K), and in simulated HLW, under naturally corroding conditions, with respect to time of immersion. Information on the corrosion processes as well as on the corrosion activity was derived, so as to understand similar phenomenon occurring in reprocessing and waste storage plants during monitoring. The current chapter demonstrates the usefulness of electrochemical noise-time records to depict the corrosion mechanism and the application of electrochemical noise resistance (a parameter derived from statistical evaluation of the EN time records) as a monitoring tool to reflect the corrosion activity of 304L SS in various environments, simulating nuclear reprocessing and waste storage conditions during the monitoring period.

---

#### ***4.2 Microstructure evaluation and DL-EPR test***

The optical micrographs of the specimens used for electrochemical noise investigation are shown in Figure 4.1, These are classified as step microstructure for the solution

annealed 304L SS specimen and ditch microstructure for the sensitized 304L SS specimen, as per ASTM A 262 [180].

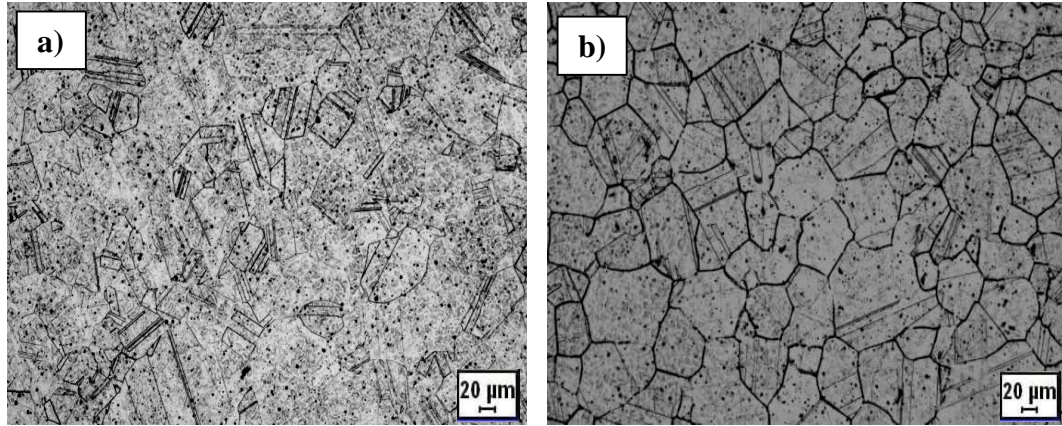


**Figure 4.1** Optical micrograph of 304 L SS used for EN measurements after oxalic acid etching a) solution annealed b) sensitized

The DL-EPR test plot for the sensitized 304L SS is given in Figure 4.2. For the solution annealed specimen, the % DOS was found to be 0.02% and that for the sensitized specimen was found to be 11.74 %.

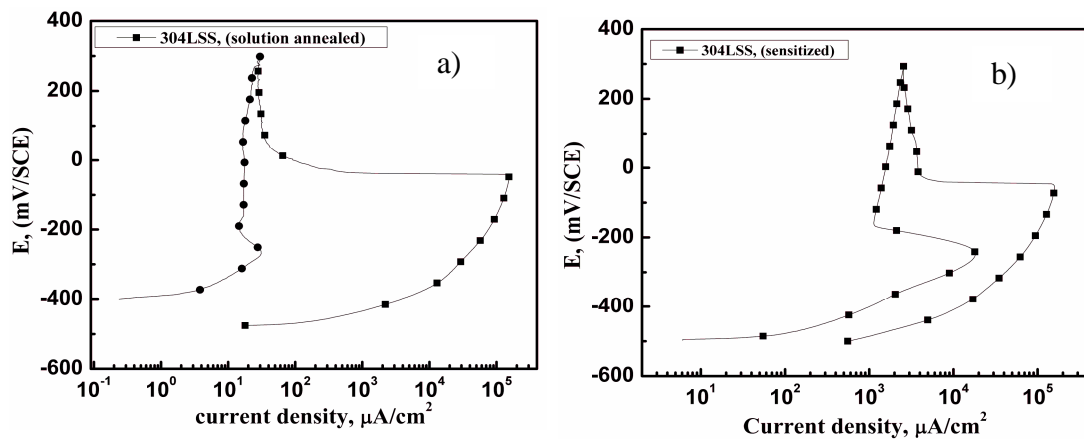


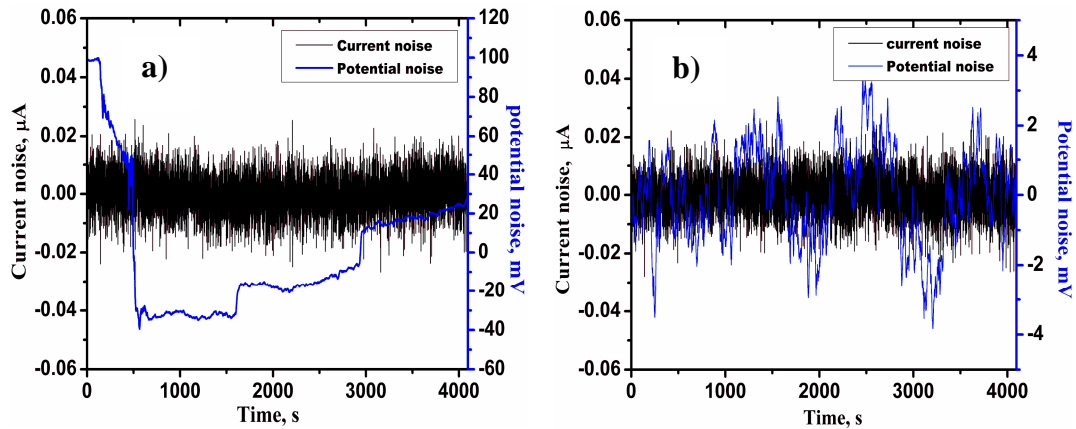
**Figure 4.2** DL-EPR test plots for 304L SS: a) solution annealed, b) sensitized

### 4.3 Electrochemical noise monitoring of 304L SS in nitric acid medium

Visual examination of EN time records has been found to be useful in predicting the processes taking place on a metal surface. Distinct features of current and potential fluctuations have been associated with various types of corrosion (uniform, pitting, crevice corrosion etc) [46, 57, 59, 78, 79, 80, 81]. Nevertheless, statistical and spectral evaluation of the time record is required for complete mechanistic information and rate determinations.

#### 4.3.1 Electrochemical noise-time record

Electrochemical current and potential noise-time record for solution annealed 304L SS in 4 M, 8 M and 12 M nitric acid at electrolyte temperature of 298 K, is shown in Figure 4.3 (a-c). In these concentrations, the electrochemical current noise-time record was characterized by low amplitude and highly repetitive current fluctuations in the range of 0.001 to 0.03  $\mu\text{A}$ , with the variations being marginal as concentration was increased. The potential fluctuations were low in 4 M nitric acid and some fluctuations occurred at higher concentrations.



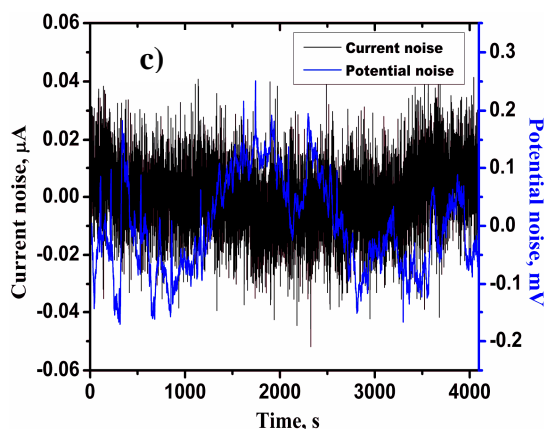
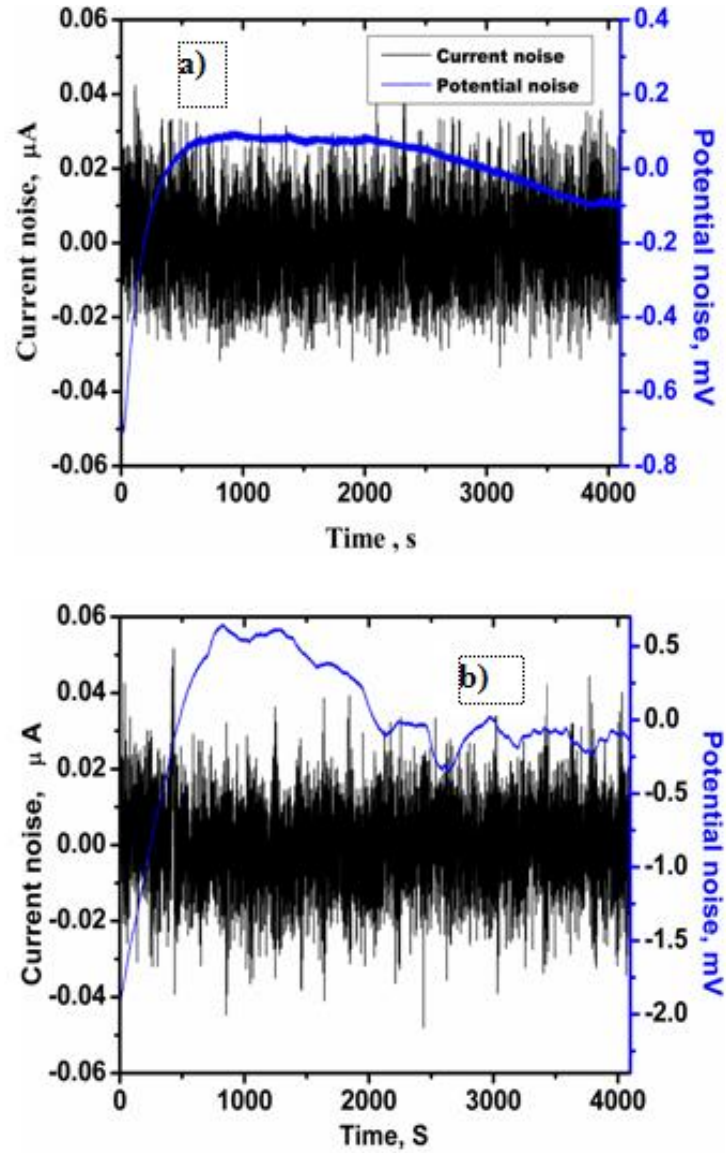


**Figure 4.3** *EN-time records taken after 150 h of immersion of solution annealed 304L SS in a) 4 M nitric acid (298 K) b) 8 M nitric acid (298 K) c) 12 M nitric acid (298 K)*

These features could be attributed to passivation process of the surface. Many investigators have reported very frequent current transients with amplitudes less than 2 nA, without detectable noise fluctuations, for passivated steels [57, 59, 138]. Cheng et al [138], obtained similar current transients, in the range of 4 nA for carbon steel passivated in chromate solution containing chloride ions until pitting occurred, where current time record showed stochastic, sharp fluctuations. For stainless steels in 0.1% NaOH, the highly repetitive and low amplitude current transients of the order of 0.01 – 0.02  $\mu\text{A}$  were associated with passivation process [81, 139].

A typical representation of EN potential and current noise - time record for the solution annealed 304L SS in 4 M and 8 M nitric acid, at electrolyte temperatures of 323 K, taken after 150 h of immersion is shown in Figure 4.4 (a & b). It is observed that the current-time records for the solution annealed 304L SS in 4 M and 8 M nitric acid, at electrolyte

temperatures of 323 K, are characterized by low amplitude, highly repetitive current fluctuations (0.02- 0.05  $\mu\text{A}$ ), depicting passivation process.



For the sensitized 304L SS, the current and potential noise time-record at 298 K and 323 K electrolyte temperature, showed features of passivation process throughout the

immersion period for all the concentrations studied except for 4 M nitric acid at 323 K electrolyte temperature. Typical plots are depicted in Figure 4.5 (a-d).

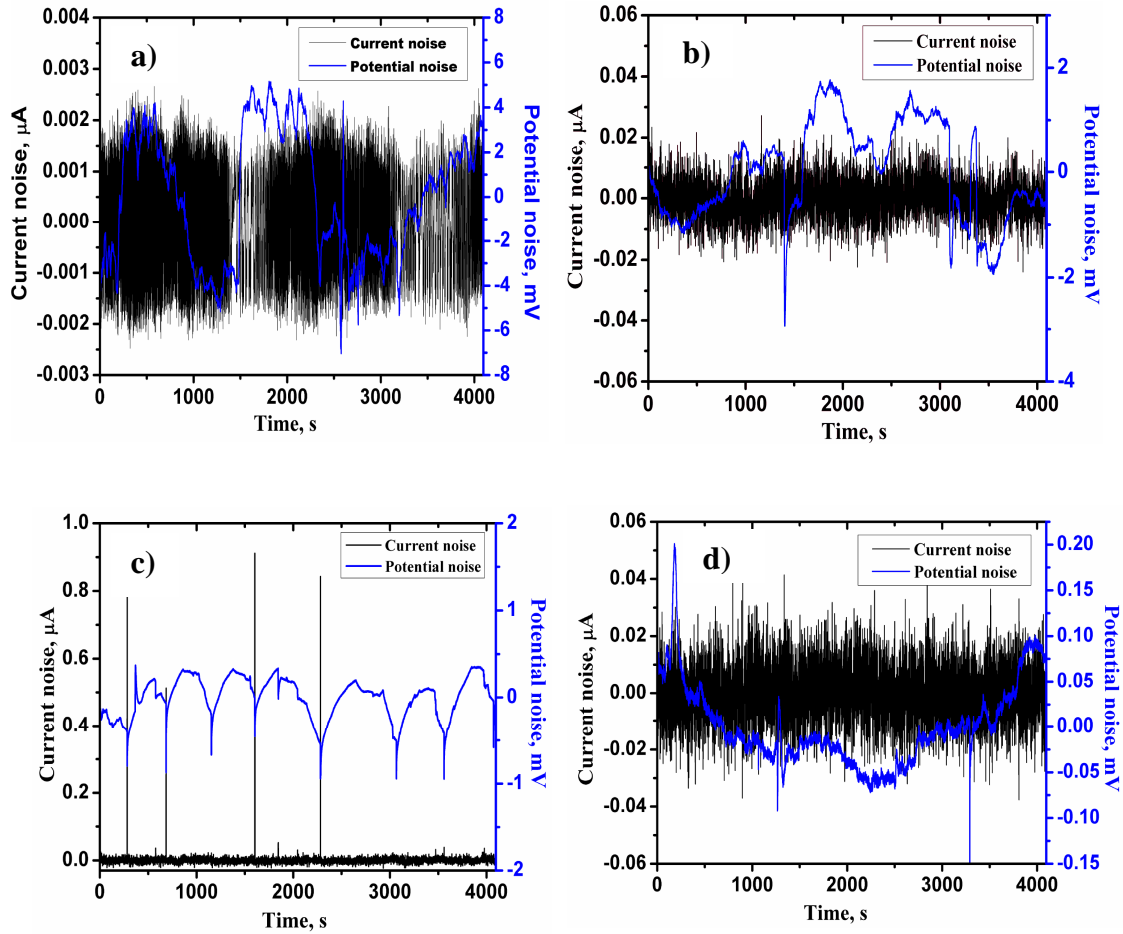


**Figure 4.5** EN-time records taken after 150 h of immersion of sensitized 304L SS in a) 4 M nitric acid (298 K), b) 8 M nitric acid (298 K), c) 4 M nitric acid (323 K), d) 8 M nitric acid (323 K)

As temperature increased, the passive film stability decreases, aiding slow dissolutions from the passive film which increases the corrosion activity, yet a defined passive range is maintained [13]. At concentrations greater than 8 M nitric acid and higher temperatures the corrosion potential shifts closer to transpassive region and corrosion rate increases.

The results show that in 4 M nitric acid, at electrolyte temperature of 323 K, the electrochemical current and potential noise-time record for sensitized 304L SS showed distinct current and potential spikes (Figure 4.5c), which could be attributed to localized attack. It is observed that current spikes are accompanied by potential drops. EN time records acquired from localized corrosion has been reported to be associated with distinct current and potential transients [81, 108]. The EN time record and the post experimental microstructure of the sensitized 304L SS in 4 M nitric acid (323 K) corroborated well with localized corrosion of the specimen. The passive film formed would be weak over sensitized zones depleted of chromium, where the chromium content is less than 11 %, and in addition, the passive film stability further decreases at elevated temperatures, making these zones less resistant to corrosion. Any local breakdown of the passive film at these zones exposes them to nitric acid attack. However, the attack has not completely propagated through the grain boundaries, and is confined to some regions of the grain boundary, as revealed by the post experimental microstructure, implying that there is a competition between passivation process and local breakdown and attack. This is expected, as 304L stainless steels exhibits excellent spontaneous passivation behavior in nitric acid medium, especially in the range of 1-6 M concentration. The breakdown has not led to complete dissolution of the passive film, in which case, the grain boundaries would have got attacked and also uniform corrosion too would have occurred. No such



evidence is observed in the EN-time record and the microstructure. This is because the measurements were made at open circuit conditions and the period of exposure was not sufficient to cause such effects. If measurements were carried out at ennobled potentials, the attack would have propagated through the grain boundaries. To the contrary, the annealed 304L SS, by virtue of its homogenous microstructure exhibited good passivation behavior in 4 M nitric acid (298 K and 323 K). This was well depicted in the EN-time record and post experimental microstructure. Nevertheless, the same localized breakdown did not occur in 8 M nitric acid at 323 K.

#### ***4.3.2 Electrochemical noise resistance***

Stainless steels showing passivation behaviour too, when continuously exposed to the medium can undergo dissolution from the film surface and on long term exposure, local or complete breakdown can occur leading to corrosion attack. A sensitive technique is thus required to monitor the changes happening at the material surface. Type 304L SS exhibits good passivation properties in nitric acid though, uniform dissolution from the film surface could contribute to low corrosion activity. An attempt is made to use electrochemical noise resistance to evaluate the corrosion activity during monitoring of 304L SS exposed to nitric acid medium of varying concentration and temperature, as mentioned above. Electrochemical noise resistance obtained from the statistical evaluation of the time record has been reported to be useful in determining the corrosion rates. Several investigators [75, 86, 87, 88, 89, 90, 101] have found that noise resistance ( $R_n$ ) from electrochemical noise analysis is equivalent to polarization resistance ( $R_p$ ) from linear polarization resistance method and hence  $R_n$  can replace  $R_p$  in Stearn - Geary equation to determine the corrosion rates. It has also been emphasized to remove the DC

components in potential and current noise record in the calculation of noise resistance. Riechert [188] found that the corrosion rates calculated from  $R_n$  are effective for systems exhibiting general corrosion rates below 1.3 mm/y and a good agreement between  $R_n$  and  $R_p$  was found for carbon steels and stainless steels in different environments. Zhang et al [214], Chen et al [88] also reported an inverse relationship between noise resistance and corrosion rate. However, Lumsden et al [215] found poor agreement between  $R_n$  from electrochemical noise analysis and  $R_p$  from electrochemical impedance spectroscopy in Fe / NaCl system. Though noise resistance is applied to systems that undergo uniform corrosion, low noise resistance have been obtained for systems with high corrosion activity and high noise resistance is reported for low active systems [74, 111]. Hence for systems that exhibit low corrosion rates, the term corrosion activity is more appropriately used in place of corrosion rate, by noise investigators [74,111]. In the present study, noise resistance was used to compare the corrosion activity during electrochemical noise monitoring of 304L SS (under solution annealed and sensitized conditions) in nitric acid at 298 K and 323 K electrolyte temperature and simulated HLW. The acquired time records were detrended by linear fit method to remove the DC component and subsequently noise resistance was determined from the detrended time record. Figure 4.6 shows electrochemical noise resistance versus time of immersion plots for 304L SS in the solution annealed and sensitized condition in nitric acid medium at 298 K and 323 K. The average noise resistance for 250 h of immersion is shown in Table 4.1. It is observed that at 298 K, the average noise resistance for the solution annealed 304L SS in 4 M, 8 M and 12 M nitric acid was  $8.4 \times 10^5 \text{ Ohm cm}^2$ ,  $6.1 \times 10^4 \text{ Ohm cm}^2$ ,  $3.8 \times 10^3 \text{ Ohm cm}^2$

respectively. The corrosion potential of 304L SS in nitric acid medium was found to be in the passive region and hence the material is in the passive state.

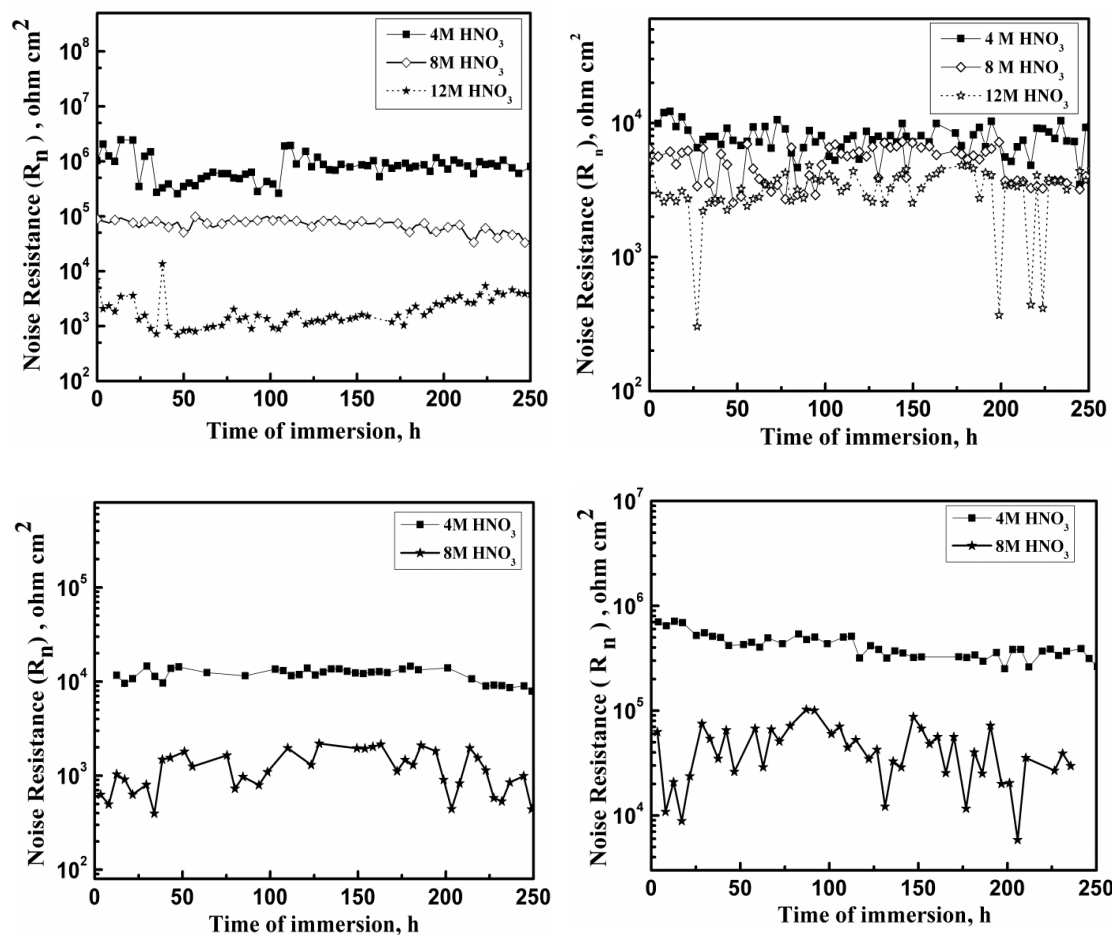


*Figure 4.6 Electrochemical noise resistance Vs Time plots for a) solution annealed 304L SS at 298 K , b) sensitized 304L SS at 298 K , c) solution annealed 304L SS at 323 K , d) sensitized 304L SS at 323 K .*

Heat treatment condition of 304 LSS	Electrolyte temperature	Electrolyte	Average noise resistance (ohm cm <sup>2</sup> )
Solution annealed	298K	4M HNO <sub>3</sub>	8.35 x 10 <sup>5</sup>
		8M HNO <sub>3</sub>	6.1 x 10 <sup>4</sup>
		12M HNO <sub>3</sub>	3.8 x 10 <sup>3</sup>
	323K	4M HNO <sub>3</sub>	4.21x10 <sup>5</sup>
		8M HNO <sub>3</sub>	4.5x10 <sup>4</sup>
Sensitized	298K	4M HNO <sub>3</sub>	9.1x 10 <sup>3</sup>
		8M HNO <sub>3</sub>	4.3 x 10 <sup>3</sup>
		12M HNO <sub>3</sub>	3.6x10 <sup>3</sup>
	323K	4M HNO <sub>3</sub>	1.1x10 <sup>4</sup>
		8M HNO <sub>3</sub>	1.2x10 <sup>3</sup>

*Table 4.1 Average electrochemical noise resistance of 304L SS in nitric acid medium for 250 h of immersion*

However, low rates of uniform dissolution from the passive film surface can occur which could differ depending on the passive film stability at different concentrations and temperatures and microstructure, which can be measured by electrochemical noise resistance. The results of the present investigation showed a decrease in noise resistance with increase in concentration which implies increase in corrosion activity with increase in concentration. The increase in corrosion activity could be attributed to increased uniform dissolution rate of passive film surface with increase in concentration. At 323 K, the average noise resistance of the solution annealed 304L SS in 4 M and 8 M nitric acid was found to be 4.21 x 10<sup>5</sup> Ohm cm<sup>2</sup> and 4.5 x 10<sup>4</sup> Ohm cm<sup>2</sup> respectively. Monitoring

results show that an increase in corrosion activity has occurred with increasing concentration. Increase in temperature has resulted in marginal increase in corrosion activity. For the sensitized 304L SS, the average noise resistance values at 298 K in 4 M, 8 M and 12 M nitric acid was found to be  $9.1 \times 10^3$ ,  $4.3 \times 10^3$ , and  $3.6 \times 10^3$  Ohm cm<sup>2</sup> respectively. With increase in concentration, the noise resistance of 304L SS (sensitized) was found to be decreasing indicating increase in corrosion activity during the monitoring period. At 323 K, noise resistance showed increase in corrosion activity for the sensitized 304L SS as concentration was increased from 4 M to 8 M nitric acid. In 4 M nitric acid, the corrosion activity of the sensitized specimen was comparable to that at 298 K. Although the sensitized specimen in 4 M (323 K) showed localized attack and no such attack occurred in 8 M (323 K), the higher corrosion activity exhibited by the latter could be attributed to higher uniform dissolution rate from the passive film surface. The corrosion potential of 304L SS in 8 M nitric acid at 323 K is very close to the transpassive region and in addition, the passive film stability at higher concentrations and temperature of nitric acid such as that at 8 M (323 K) decreases, providing increased dissolution and increasing corrosion activity. This has been well reflected in the lower noise resistance values in 8 M nitric acid (323 K). Whereas, in 4 M (323 K), 304L SS has a lower corrosion potential and a wider passive range and hence the dissolution rates are lower resulting in higher noise resistance than in 8 M (323 K). Further the post experimental morphology shows that the localized attack in 4 M (323 K) was not severe enough to contribute to higher rates. However, when compared to solution annealed specimen, the sensitized specimen showed higher corrosion activity in all the concentrations and temperatures, as inferred from the noise resistance values.

#### ***4.4 Electrochemical noise monitoring of 304L SS in simulated high level nuclear waste***

##### ***4.4.1 Electrochemical noise-time record***

Electrochemical noise monitoring was carried out for 304L SS under solution annealed condition in simulated HLW (prepared in 3 M nitric acid) and in the plain acid (3 M nitric acid) to see the effect of the ions (fission products, uranium, iron, chromium, nickel etc) present in simulated HLW on the passive film stability. Typical representation of the electrochemical noise-time records measured for AISI type 304L SS in the plain acid (3 M HNO<sub>3</sub>) at ambient conditions (298 K) is shown in Figure 4.7. For 304L SS in 3 M HNO<sub>3</sub>, the current fluctuations were of very low amplitude, in the range of about 0.015  $\mu$ A, appearing at high repetition rates and almost white type of noise throughout the measurement period was observed. The potential noise was very low, about 0.1 mV. These features are typical of passivation phenomenon. The noise monitoring for the entire period of measurement revealed the presence of a stable passive film on the surface. Figure 4.8 shows representations of electrochemical noise-time records taken after 85 h and 125 h of immersion of AISI type 304L SS in simulated HLW (prepared in 3 M nitric acid) at 298 K solution temperature. The electrochemical noise time record for 304L SS in simulated HLW solution showed low-level current and potential fluctuations with an amplitude of 0.01  $\mu$ A in the current noise.

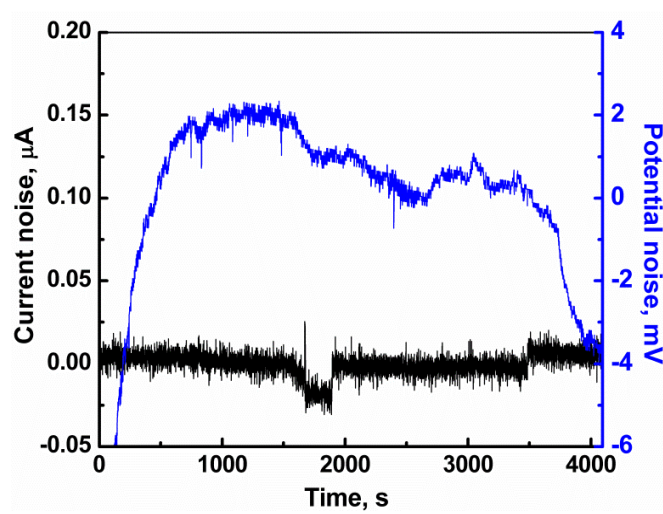
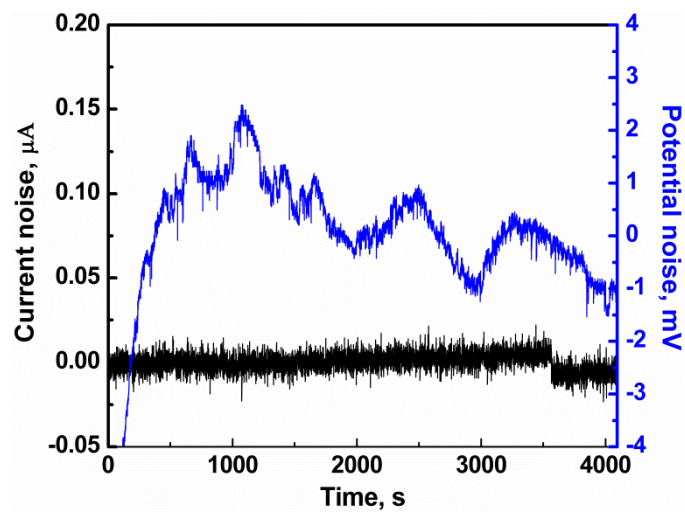


*Figure 4.7 EN -time record for 304L SS in 3 M nitric acid (298 K) taken after  
a) 85 h, b) 125 h of immersion*

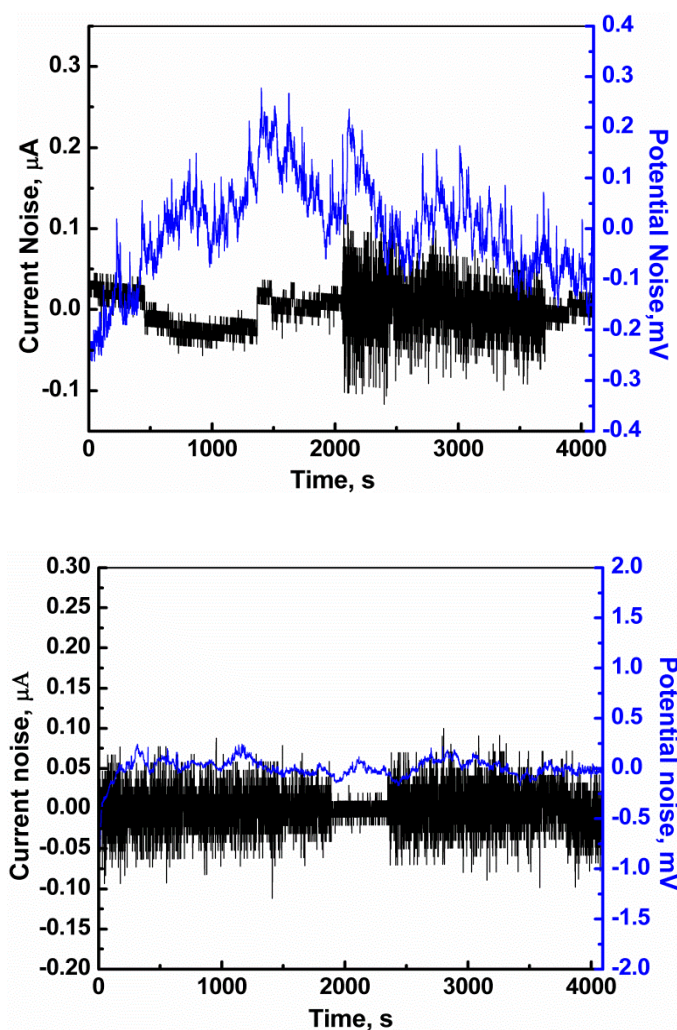


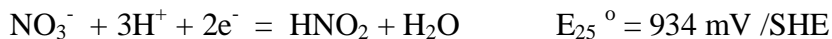
***Figure 4.8 EN-time record for 304L SS in simulated HLW (in 3 M nitric acid) (298 K) taken after a) 85 h b) 125 h of immersion***

A white noise feature was observed similar to that observed in 3 M HNO<sub>3</sub>, which depicts passivation process. At certain immersion times, the current noise time record for 304L SS in simulated HLW solution depicted low amplitude fluctuations followed by a sudden burst of current noise with the amplitude being almost ten times that during the passivation process. This could be attributed to two competent phenomenon. Nitric acid

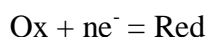


concentration of 3 M is a spontaneously passivating medium for stainless steels and therefore passivation of 304L SS has resulted in white noise feature in the current noise-time record. Sudden burst of current noise could be attributed to decrease in passive film stability by the cations present in simulated HLW. The instability of passive film observed in simulated HLW could be attributed to (i) presence of oxidizing ions in simulated HLW, (ii) possible adsorption of cations present in simulated HLW on the passive film surface.

(i) Instability of passive film of stainless steels in nitric acid containing oxidizing ions is well discussed in literature [14, 216, 217, 218, 219]. In nitric acid medium, the redox potential is imposed by the global reduction of nitric acid [216] which is given by



Nitrous acid generated doesn't accumulate, rather gets reduced to NO which combines with nitric acid to regenerate nitrous acid. The mechanism of reduction of nitric acid is detailed in chapter 5 (section 5.2.4). In nitric acid containing oxidizing ions, the redox potential is imposed by the reduction of the oxidizing ions present in the solution by metallic elements of the stainless steel [216].



The oxidizing ions in nitric acid medium undergo reduction at the stainless steel surface, enhancing the oxidation of the metal ions from the surface, which dissolves into the solution. The presence of oxidizing ions such as Fe(III) , Cr(VI) , Ce(IV) , Pr(IV) in simulated HLW enhances metal ion oxidation, thus destabilizing the passive film and increases the corrosion activity. In addition, the corrosion potential of the material is ennobled due to the redox couples formed from Fe(III)/Fe(II), Cr(VI)/Cr(III),

Ce(IV)/Ce(III), Pr(IV)/Pr(III), which increases the corrosion activity. Since the EN-time record in simulated HLW shows only passivation/depasivation signals and the post experimental micrographs showed no attack of the stainless steel surface, it is evident that the dissolution occurred from the passive film surface. A schematic of the mechanism of reduction in plain nitric acid and in simulated HLW containing oxidizing ions, showing passivation in 3M nitric acid and depassivation by oxidizing ions in simulated HLW is represented in Figure 4.9 and Figure 4.10 respectively.

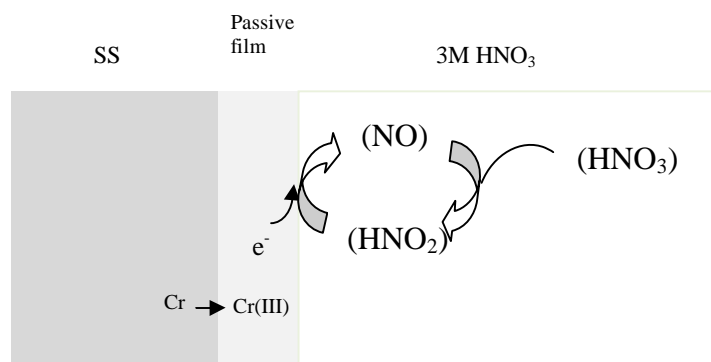


Figure 4.9 Passivation in 3M nitric acid

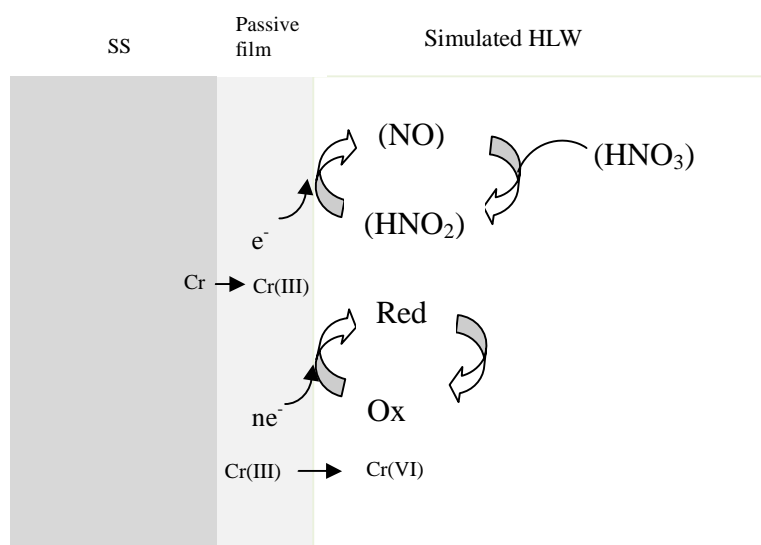


Figure 4.10 Passivation by 3 M nitric acid and decrease in passive film stability by oxidizing ions present in simulated HLW

(ii) Another contribution to the decrease in passive film stability is the adsorption of the cations present in simulated HLW (Table 2.3) into the passive film. The passive film contains three layers at the metal-solution interface. The first layer is the thin oxide film that contains charged oxide groups. A monolayer of hydroxides, strongly bound cations and adhered water molecules formed over the oxide is the inner Helmholtz layer. This is followed by the "Stern layer" or outer Helmholtz layer which contains hydrated ions. The third layer above the outer Helmholtz layer is the diffuse layer that contains adsorbed species and water. Ions in the diffuse layer act as countercharge to the other layers. Cations from the solution get attracted to the surface potential of the oxide layer by weak electrostatic forces or Vanderwaals forces and get adsorbed at the outer Helmholtz layer by physisorption. Cations also diffuse into the inner Helmholtz layer where they are chemisorbed, i.e. form a chemical bond with the metal oxide. A schematic representation [220] of cation adsorption in the inner and outer Helmholtz layer of the passive film is shown in Figure 4.11. The presence of several cations in simulated HLW (Table 2.3) makes it a complex subject to discuss the adsorption mechanism. Kadar et al [221] suggested that cation adsorption would occur in weakly acidic solutions. Ajlouni et al [222] reported the adsorption of cesium and strontium ions on stainless steel surface in reprocessing environments. Cations such as strontium and cesium can replace the  $H^+$  ion of the hydroxyl group by ion exchange [222, 223]. Takeuchi et al [224] have reported that the adhesive property of radionuclide on stainless steel surface in high level liquid waste occurs by (i) adhesion (ii) adsorption and ion exchange of ions and (iii) diffusion and penetration. The adsorption of the ions in the passive layer induces strain in the film which leads to the decrease in the stability.

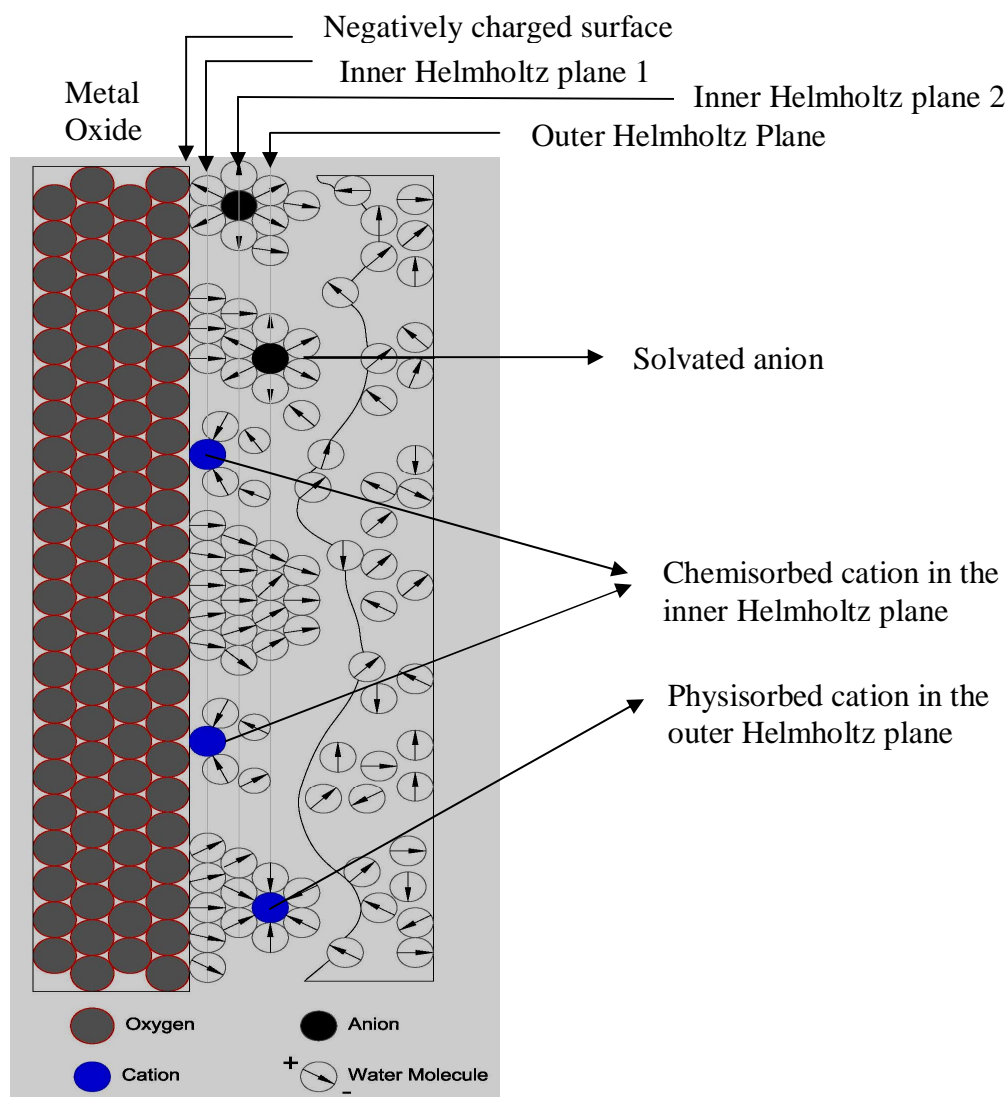
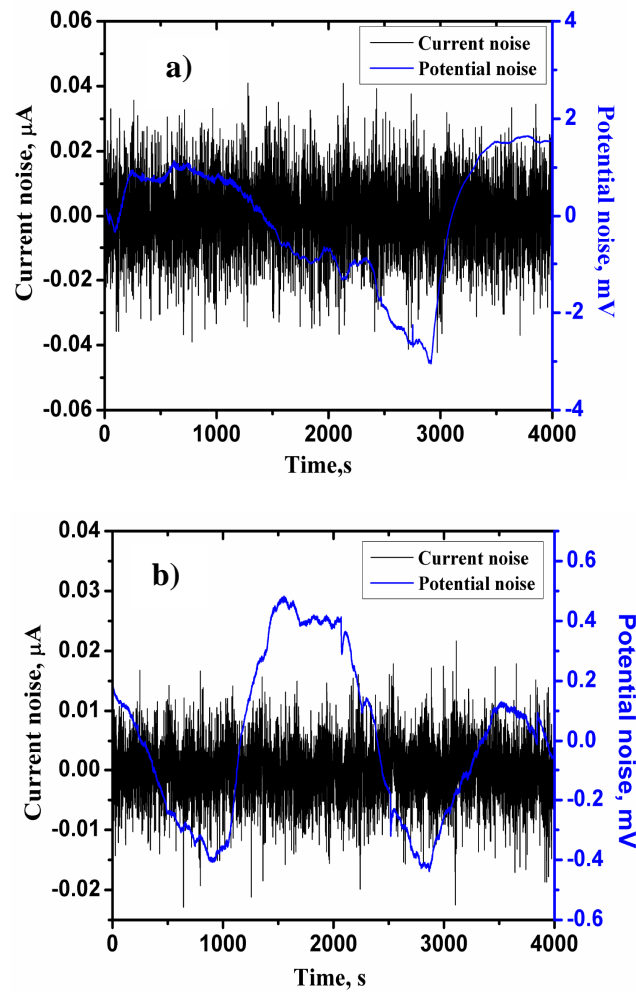


Figure 4.11 Schematic representation of cation adsorption into passive film [220]

Electrochemical noise monitoring experiments were carried out for 304L SS under solution annealed and sensitized conditions at 323 K, in simulating nuclear waste storage plant conditions where the high level waste solutions are at elevated temperatures, around 323 K due to radioactive decay heat. The EN-time records for 304L SS in simulated HLW (323 K) is shown in Figure 4.12. The figure depicts passivation process for the

solution annealed and sensitized specimen throughout the monitoring period. No features of depassivation were observed in the time records taken at 323 K. The probable reason could be that, at elevated temperatures, the kinetics of breakdown and repair of passive film is faster and hence the EN-time record doesn't distinguish regions of stability and instability of the passive film. The results show that EN-time record has been useful in depicting the corrosion mechanism of 304L SS in simulated high level waste medium.



*Figure 4.12 EN time record taken 150 h of immersion of 304L SS in simulated HLW (323 K) a) solution annealed, b) sensitized.*

#### ***4.4.2 Electrochemical noise resistance***

A plot of electrochemical noise resistance of 304L SS in 3 M nitric acid and simulated HLW (prepared in 3 M HNO<sub>3</sub>) at 298 K electrolyte temperature is represented in Figure 4.13. The experiment was carried out in plain acid and simulated high level waste medium in order to investigate the effect of the presence of ions present in high level waste medium on the corrosion resistance. It was observed that in 3 M HNO<sub>3</sub>, the average noise resistance for 304L SS for 150 h of immersion was in the range of  $7.4 \times 10^4$  Ohm cm<sup>2</sup>. The high noise resistance could be attributed to good passive behavior, which existed throughout the measurement period. Since noise resistance is inversely proportional to the corrosion activity, it could be noted that the corrosion resistance of 304L SS in 3 M HNO<sub>3</sub> remained high throughout the measurement time. For 304L SS in simulated HLW, the average noise resistance for 150 h of immersion was found to be in the range of  $2.7 \times 10^3$  Ohm cm<sup>2</sup>. A drop in noise resistance was observed for 304L in simulated HLW when compared to 304L in 3 M HNO<sub>3</sub>, which implies that corrosion activity of the material in simulated HLW is increased. Hence, it could be concluded that the presence of the ions in high level waste medium has a role in reducing the corrosion resistance of 304L SS. Further, the experiments were carried out in simulated HLW at 323 K in order to investigate the effect of radioactive heat on the corrosion resistance of 304L SS. The average noise resistance was found to be  $1.6 \times 10^4$  Ohm cm<sup>2</sup> (Table 4.2). As at higher temperature the kinetics is faster, the breakdown and repair of the passive film is faster. Hence, the EN response doesn't show the breakdown process in the time record at 323 K, whereas the time record at 298 K shows regions of depassivation caused

by the ions present in the waste medium, which has also reflected in the noise resistance values.

A plot of electrochemical noise resistance for sensitized 304L SS in simulated HLW at 323 K is given in Figure 4.14. The average noise resistance for 250 h of immersion was found to be  $9.7 \times 10^{-3} \text{ Ohm cm}^2$ . When compared to the solution annealed 304L SS, the

Heat Treatment condition	Electrolyte temperature	Electrolyte	Average noise resistance Ohm cm <sup>2</sup>
Solution annealed 304L SS	298 K	3 M HNO <sub>3</sub>	$7.4 \times 10^4$ (150 h immersion)
Solution annealed 304L SS	298 K	Simulated HLW	$2.7 \times 10^3$ (150 h immersion)
Solution annealed 304L SS	323 K	Simulated HLW	$1.6 \times 10^4$ (250 h immersion)
Sensitized 304L SS	323 K	Simulated HLW	$9.7 \times 10^{-3}$ (250 h immersion)

***Table 4.2 Average electrochemical noise resistance of 304L SS in simulated HLW***

sensitized 304L SS showed higher corrosion activity during the period of monitoring. From the results, it was found that noise resistance was useful to monitor variations in corrosion activity in low active systems like simulated high level waste medium.

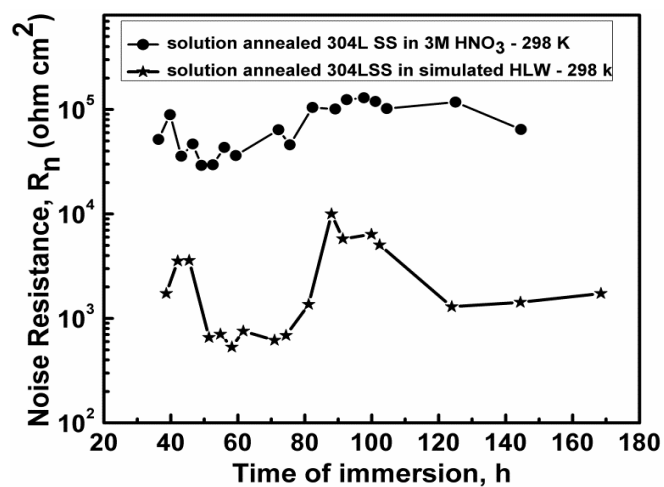


*Figure 4.13 Electrochemical noise resistance Vs time plots for solution annealed 304L SS in 3 M nitric acid and simulated HLW at 298 K*

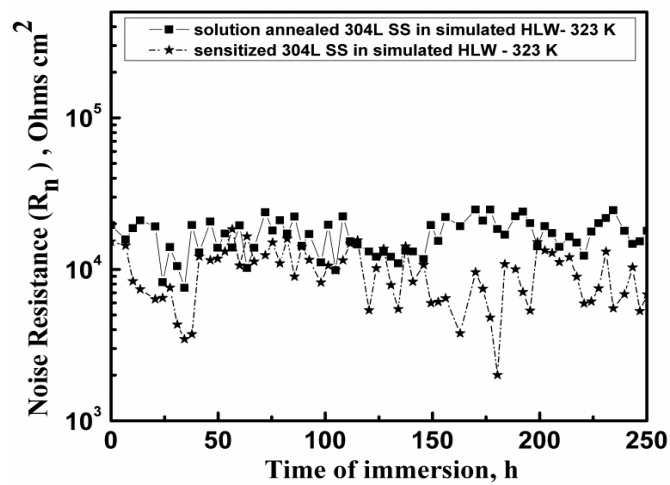


*Figure 4.14 Electrochemical noise resistance Vs time plots for solution annealed and sensitized 304L SS in simulated HLW at 323 K*



#### ***4.5 Post experimental optical microstructures***

Optical micrographs taken after electrochemical noise investigation showed no corrosion attack in 304L SS (solution annealed and sensitized) under all the experimental conditions, except for the sensitized material that underwent localized attack in 4 M nitric acid (323 K). The sensitized specimen in 12 M nitric acid showed some perforations in the microstructure. One probable reason could be that the measurements were made at open circuit potentials, where the corrosion potential of the stainless steel is in the passive region and the material is in the passive state. Surface attack would happen, subject to either a localized breakdown or passive film dissolution, which will expose the material surface. But the microstructures show no such evidences. Post experimental microstructures are shown in Figure 4.15 and Figure 4.16. The variations in the corrosion activities as inferred from variations in the noise resistance is attributed to variations in the dissolution rates from passive film surface in the different environmental conditions studied, but the exposure period was not sufficient enough to cause dissolution of the film for a surface attack to occur. During this exposure time period the stainless steel has exhibited good corrosion resistance.

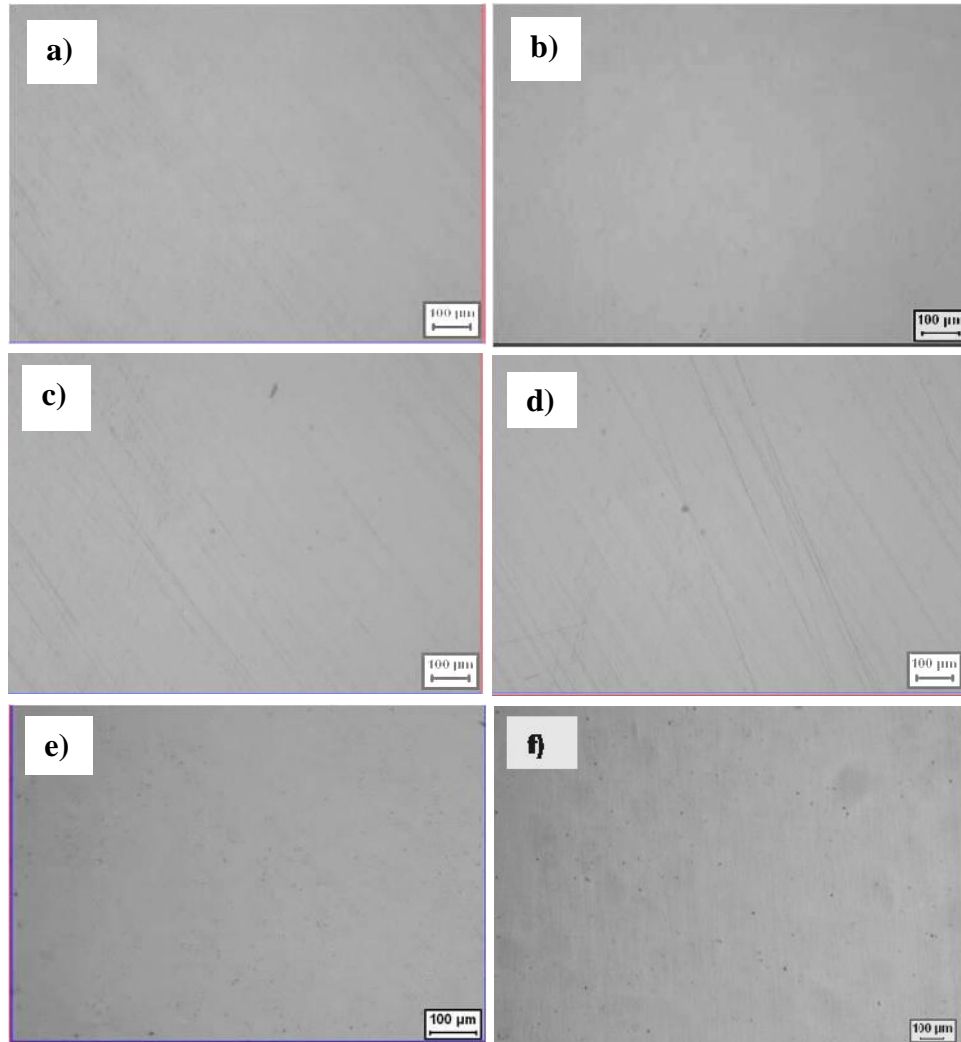


***Figure 4.15 Typical micrographs taken after EN experiments for 304 L SS at 298 K electrolyte temperature, showing no corrosion attack for a) solution annealed specimen in 4 M  $\text{HNO}_3$ , b) solution annealed specimen in 8 M  $\text{HNO}_3$ , c) solution annealed specimen in 12 M  $\text{HNO}_3$ , d) sensitized specimen in 4 M  $\text{HNO}_3$ , e) sensitized specimen in 8 M  $\text{HNO}_3$ , f) sensitized specimen in 12 M  $\text{HNO}_3$***

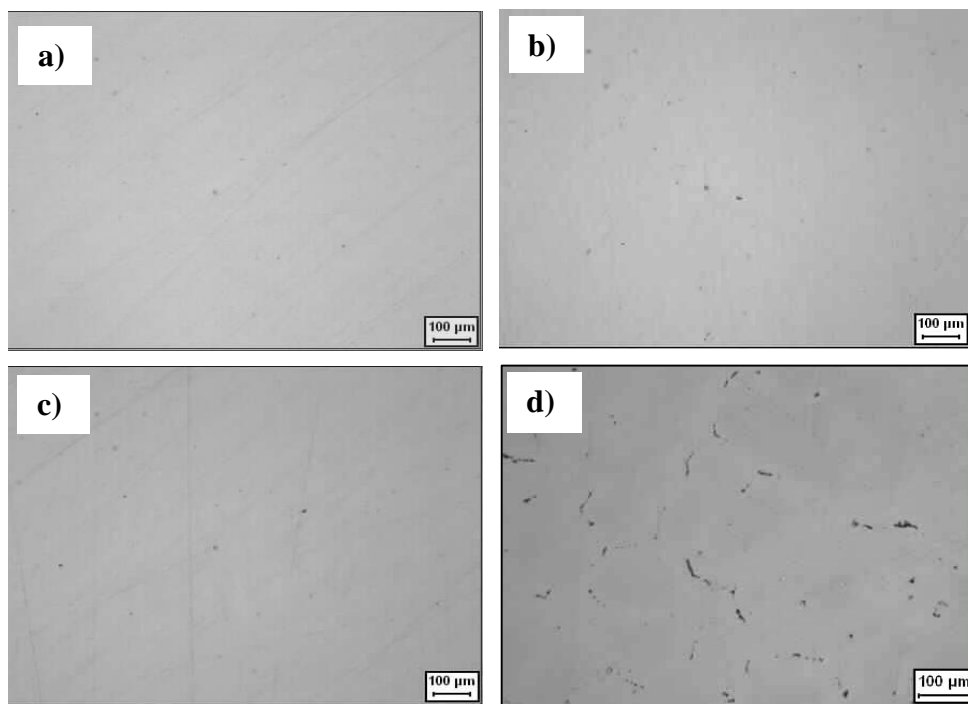


**Figure 4.16** Typical micrographs taken after EN experiments for 304 L SS at 323 K electrolyte temperature, showing no corrosion attack for a) solution annealed specimen in 4 M  $\text{HNO}_3$ , b) solution annealed specimen in 8 M  $\text{HNO}_3$ , c) sensitized specimen in 8 M  $\text{HNO}_3$ , d) Localized attack seen in sensitized 304L SS in 4 M  $\text{HNO}_3$

#### 4.6 Conclusions

EN-time record of 304L SS (solution annealed and sensitized) showed passivation process in nitric acid at electrolyte temperature of 298 K and 323 K and in simulated HLW (323 K). Only in 4 M nitric acid (323 K), the sensitized specimen showed distinct potential and current spikes which could be attributed to localized attack. Optical micrograph confirmed localized attack for sensitized 304L SS in 4 M nitric acid at 323 K

electrolyte temperature. No surface attack was observed in other specimens. An attempt was made to apply EN resistance to monitor the corrosion activity of 304L SS in nitric acid medium. EN resistance decreased with increase in concentration of nitric acid for solution annealed 304L SS at 298 K and 323 K implying higher corrosion activity at higher concentration. For the same concentration of the acid, increase in temperature resulted in increase in the corrosion activity of 304L SS. For the sensitized 304L SS, the corrosion activity was found to increase with increase in concentration of nitric acid from 4 M to 8 M and 12 M nitric acid, at 298 K. An appreciable increase in corrosion activity occurred in 8 M nitric acid when the electrolyte temperature was increased to 323 K. The corrosion activity was found to be higher for sensitized specimen when compared to solution annealed 304L SS. From the EN-time record and noise resistance evaluation, it was found that the corrosion activity of 304L SS in simulated HLW (in 3 M nitric acid) was greater than that in the plain 3 M nitric acid at 298 K, indicating that the ions (fission products, uranium, iron, chromium etc) present in the waste medium facilitates increased dissolution from the passive film surface of the material. The time record showed regions of passivation and depassivation in simulated HLW medium at 298 K. Further, the effect of radioactive heat on the corrosion activity was studied by increasing the temperature of simulated HLW to 323 K. At this temperature, EN-time record did not show regions of depassivation. This could be because the kinetics of breakdown and repair of passive film is faster at elevated temperature. The EN resistance for the sensitized specimen in simulated HLW (323 K) decreased when compared to that of the solution annealed specimen implying higher corrosion activity for the sensitized specimen compared to the solution annealed specimen during the period of measurement. EN resistance was found

to be useful in discerning the variations in the corrosion activity even for systems that exhibited low corrosion activity. The high EN resistance for these systems could be attributed to passive state which the system exhibited throughout the monitoring period, nevertheless the variations in the EN resistance in the environments is because of variations in the dissolution rates from the passive film surface. However, it could be stated that more insight into the system behavior could be achieved if the exposure period is further increased to longer durations.

*EFFECT OF NITROGEN ON THE CORROSION BEHAVIOR OF NITROGEN  
CONTAINING 304L SS IN NITRIC ACID AND SIMULATED HIGH LEVEL WASTE MEDIUM*

---

Under Indo-Bulgarian collaboration programme, three nitrogen containing 304L SS (0.132 % N, 0.193 % N, 0.406 % N) were prepared at Bulgarian Academy of sciences, in the forged and rolled conditions. They were assessed for their application in nuclear reprocessing and waste storage plants by assessing their corrosion behavior using potentiodynamic anodic polarization and electrochemical noise investigations. The objective of the research work was to investigate the effect of nitrogen on the corrosion property of 304 L SS in nitric acid and simulated high level waste medium. The chapter comprises of two parts. The first part presents the results from the potentiodynamic anodic polarization investigations and the second part presents the results from the electrochemical noise studies. Potentiodynamic anodic polarization investigations were carried out in 1 M, 4 M, 6 M nitric acid and simulated HLW, using forged and rolled nitrogen containing 304L SS. Since nitric acid reduction mechanism below and above 6 M concentration are different, concentrations below 6M nitric acid was used for the polarization studies. The pitting corrosion resistance of the three nitrogen containing 304L SS under forged and rolled conditions in 0.5 M NaCl is also discussed. Scanning electron micrographs, optical micrographs and energy dispersive spectra were used for microstructural evaluation. In the second part of the work, an attempt was made to establish the electrochemical noise probe made of the nitrogen containing 304L SS to monitor the corrosion activity in nuclear reprocessing and waste storage medium. For

this purpose, electrochemical current and potential noise was acquired from the three nitrogen containing 304L SS in 1 M, 4 M, 8 M nitric acid and simulated high level waste under ambient conditions. For design convenience, rod specimens were used for electrochemical noise studies. The acquired signals were analyzed by statistical, spectral, shot noise and wavelet methods to derive electrochemical noise parameters which were used to obtain mechanistic information as well as the extent of corrosion activity.

---

### ***5.1 Introduction***

Towards developing materials for nuclear reprocessing and high level liquid waste storage plants, nitrogen containing austenitic stainless steels have drawn considerable attention, due to its well balanced combination of excellent mechanical and corrosion properties. The role of nitrogen in improving the corrosion resistance of stainless steels is well documented in literature [22, 28, 225, 226, 227, 228, 229], nevertheless, most studies focus on localized corrosion and fewer reports are available in acidic medium. In certain specific environments such as hydrochloric acid, the effect of nitrogen content in the steel has been found to have no influence on the polarization behavior of steels [230]. Janik-Czachor et al [231] proposed that nitrogen bearing stainless steels, without Mo, do not show any influence on the polarization behavior of the austenitic stainless steels. It has also been reported that nitrogen does not have an influence on the anodic dissolution and passivation of highly alloyed stainless steels [230]. Padhy et al [16] reported an ennoblement in the corrosion potential, decrease in corrosion current density and passive current density for nitrogen implanted 304L SS in  $\text{HNO}_3$  medium using potentiodynamic polarization technique. Sadough Vanini, et al. [232], in their study on

the role of nitrogen on the passivity of austenitic stainless steel in sulphuric acid medium using the potentiodynamic polarization technique, found no influence of nitrogen on the general corrosion and passivation behavior of the alloy. Olefjord and Wegrelius [31] noted that the addition of nitrogen had no influence on the passivation behavior of the Fe-Cr-Ni-Mo-based alloys in acid – chloride medium. Park et al [233] studied the repassivation behaviour of 304L and 304LN in NaCl medium using polarization technique. They found that the electrochemical parameters were not affected by the addition of nitrogen in the stainless steel. Similar observations were reported by some other researchers [234, 235]. Since literature reports on corrosion property of nitrogen containing 304L SS in nitric acid and simulated HLW is seldom reported, an attempt was made to investigate the same using potentiodynamic anodic polarization and electrochemical noise techniques.

---

## ***5.2 Effect of nitrogen on corrosion behavior of nitrogen containing 304L SS in nitric acid and chloride medium by potentiodynamic anodic polarization***

### ***5.2.1 Microstructure***

Optical and scanning electron micrographs (SEM) of the three nitrogen containing 304L stainless steels under forged conditions (namely 304LN1F, 304LN2F and 304LN3F) and hot rolled condition (namely 304LN1R, 304LN2R and 304LN3R) are given in Figure 5.1 to 5.4.



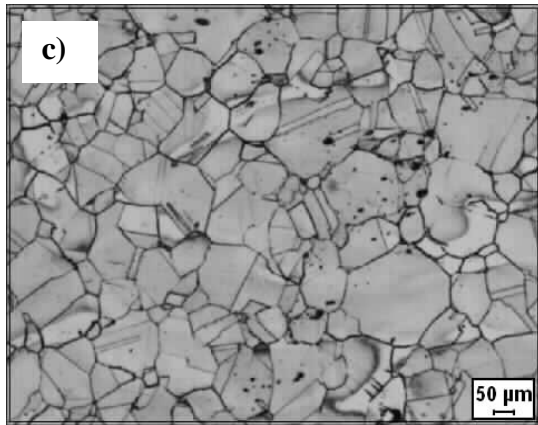
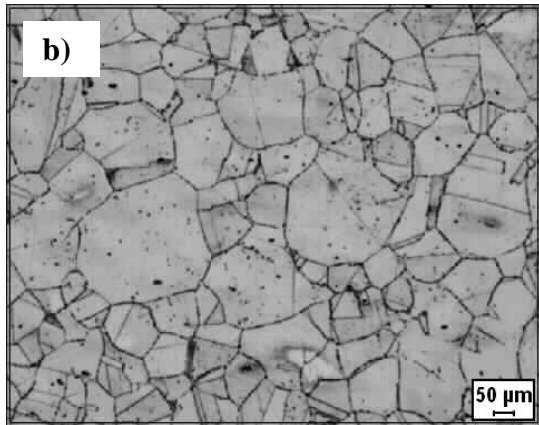
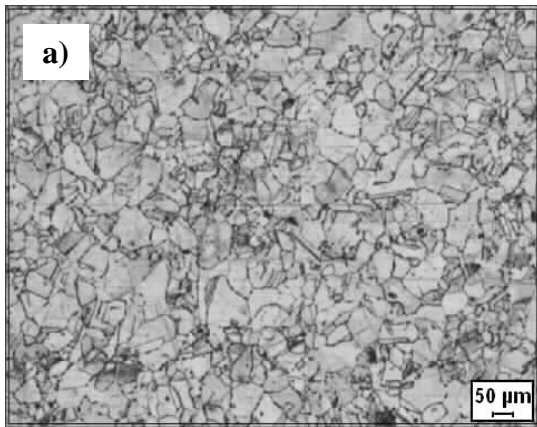


**Figure 5.1** Optical micrographs of the as forged a) 304LN1F SS, b) 304LN2F SS c) 304LN3F SS

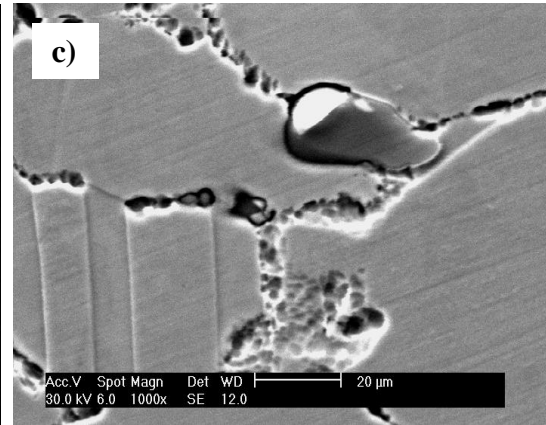
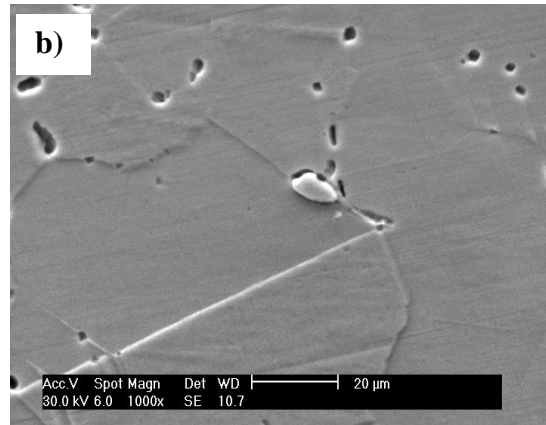
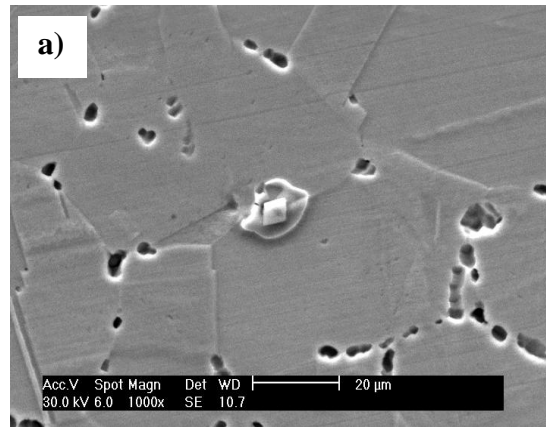


**Figure 5.2** SEM of the as forged a) 304LN1F SS, b) 304LN2F SS c) 304LN3F SS

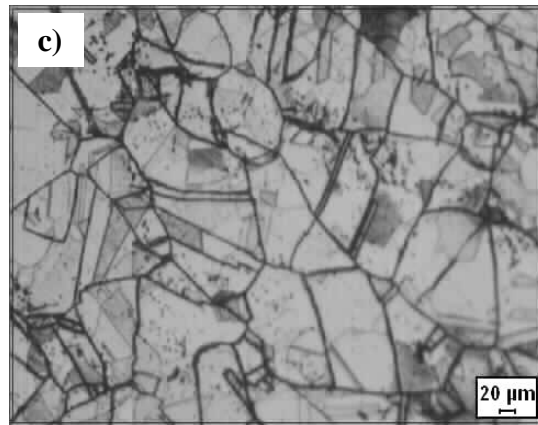
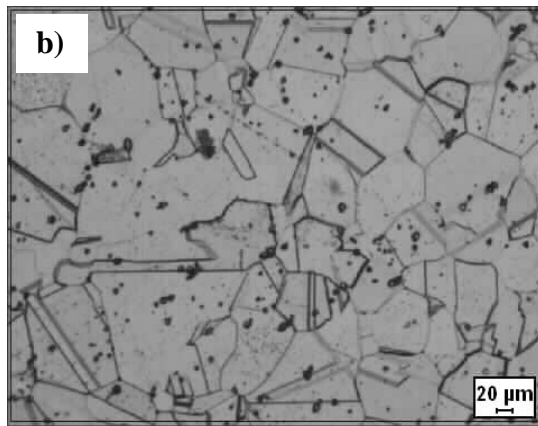
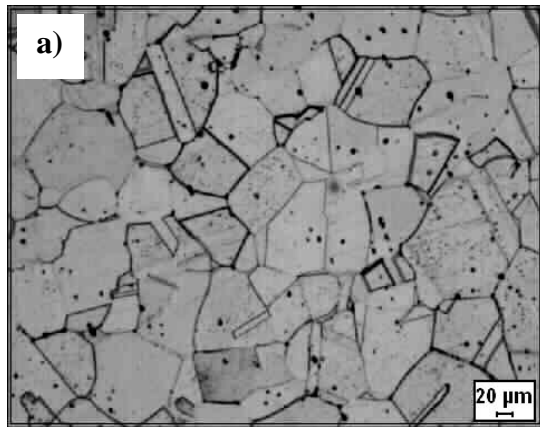


*Figure 5.3 Optical micrographs of the rolled a) 304LN1R SS b) 304LN2R SS c) 304LN3R SS*

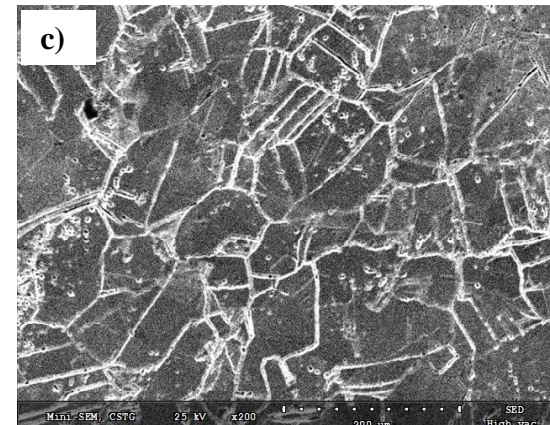
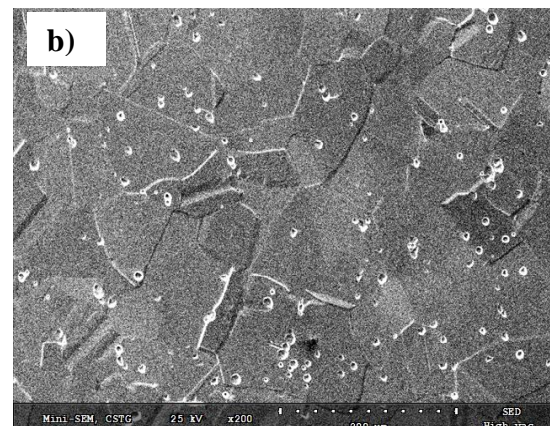
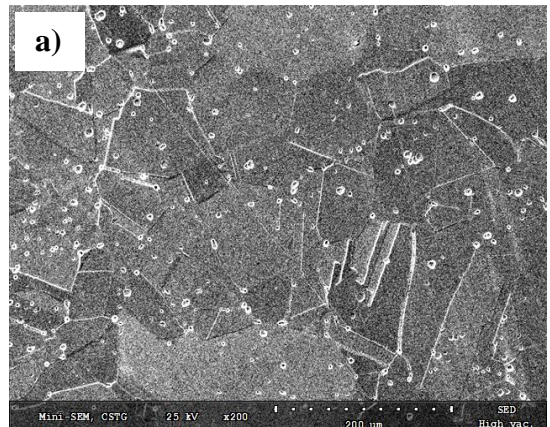


*Figure 5.4 SEM of the rolled a) 304LN1R SS b) 304LN2R SS c) 304LN3R SS*

The microstructures showed mainly homogenized distribution of austenite grains containing twin structures. An increase in twin structures with increase in nitrogen content is observed for both forged as well as rolled conditions. The microstructure in Figure 5.2 reveals continuous precipitation along grain boundaries in 304LN3F stainless steel, whereas in 304LN1F and 304LN2F stainless steels, precipitation is discontinuous. The microstructures of the hot rolled stainless steels show more intragranular precipitates and only a few intergranular precipitates in all the three nitrogen containing stainless steels. The continuous network of precipitates observed in the forged 304LN3F stainless steel is not observed in the rolled (304LN3R) stainless steel.

#### ***5.2.2 Energy dispersive spectra of the nitrogen containing 304L SS***

Energy dispersive spectra (EDS) of the etched stainless steel alloys for the matrix and precipitate is depicted in Figures (5.5 to 5.7). Only iron, chromium, nickel, and manganese, which show the pronounced peaks, were identified. The EDS spectra were found to be identical for both forged and rolled nitrogen containing stainless steels. Hence, only a single representation of the EDS spectra is given in the figures depicting the elemental composition of both forged and rolled nitrogen containing stainless steels. In 304LN1F(R) stainless steel, the precipitate consisted of chromium, iron, and manganese. Chromium and manganese enrichment has occurred in the precipitate, compared to the matrix. In 304LN2F(R) stainless steel, the precipitate contained chromium, iron, and manganese. Chromium and manganese enrichment and reduction in iron content was noticed in the precipitate, compared to the matrix. Also, 304LN3F(R) stainless steel contained chromium- and manganese-rich precipitate and iron is almost negligible in the precipitate when compared to the matrix.

Manganese enrichment is more in 304LN3F(R) SS compared to 304LN2F(R) SS.

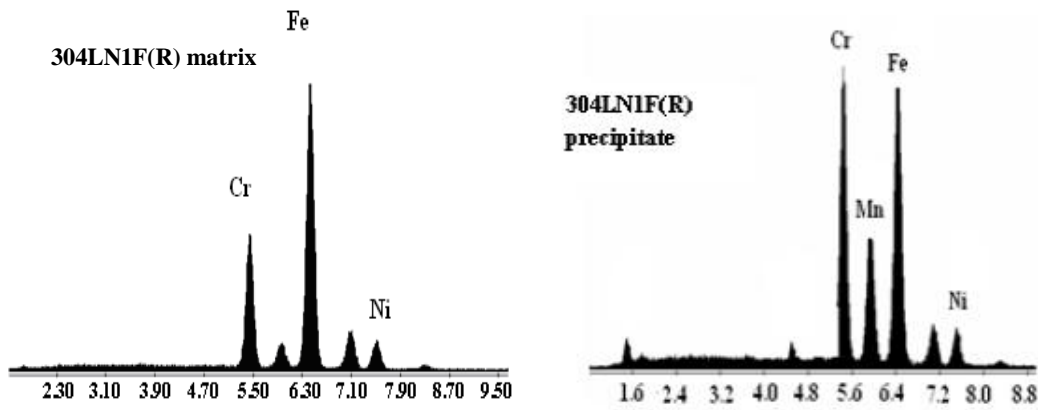


*Figure 5.5 EDS of the matrix and precipitate of the forged and rolled nitrogen containing 304LN1 stainless steel, showing chromium and manganese enrichment in the precipitate compared to matrix.*

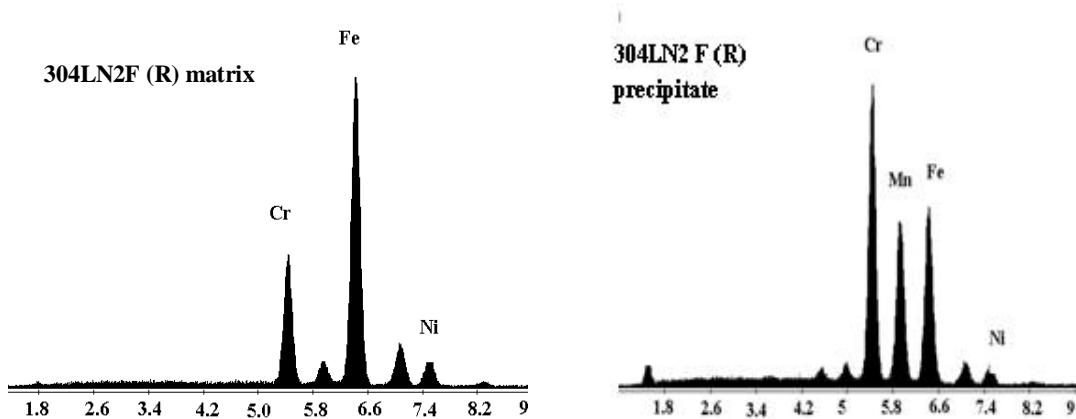


*Figure 5.6 EDS of the matrix and precipitate of the forged and rolled nitrogen containing 304LN2 stainless steel, showing chromium and manganese enrichment in the precipitate compared to matrix, and a decline in Fe content in the precipitate compared to matrix.*

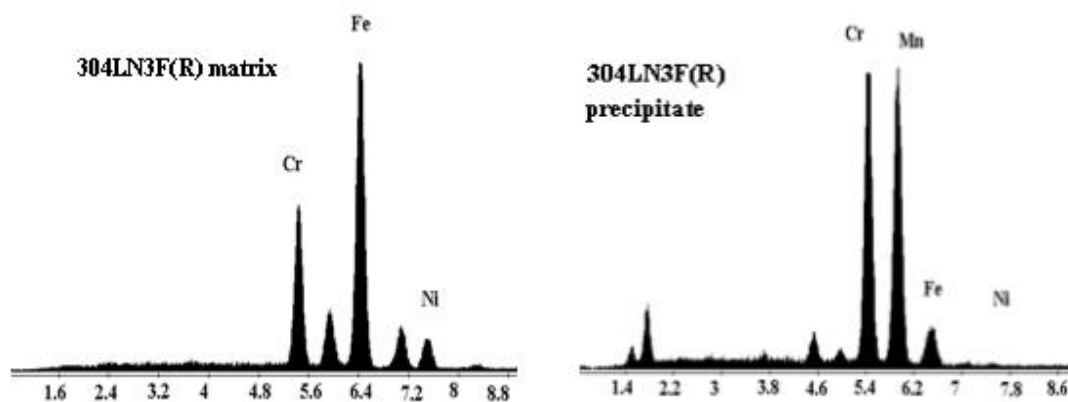


*Figure 5.7 EDS of the matrix and precipitate of the forged and rolled, nitrogen containing 304LN3 stainless steel, showing chromium and maximum manganese enrichment in the precipitate compared to matrix, and a substantial decline in Fe content in the precipitate compared to matrix.*

### *5.2.3 Potentiodynamic anodic polarization behavior of as-forged and rolled nitrogen containing 304L SS in nitric acid medium*

Figures (5.8 and 5.9) represent potentiodynamic anodic polarization curves of the forged and rolled nitrogen containing stainless steels in 1 M, 4 M, and 6 M HNO<sub>3</sub> at 298 K electrolyte temperature. Similarly, Figures (5.10 and 5.11) represent the corresponding potentiodynamic anodic polarization curves at elevated temperature (323 K) of nitric acid, for the forged as well as rolled steels.

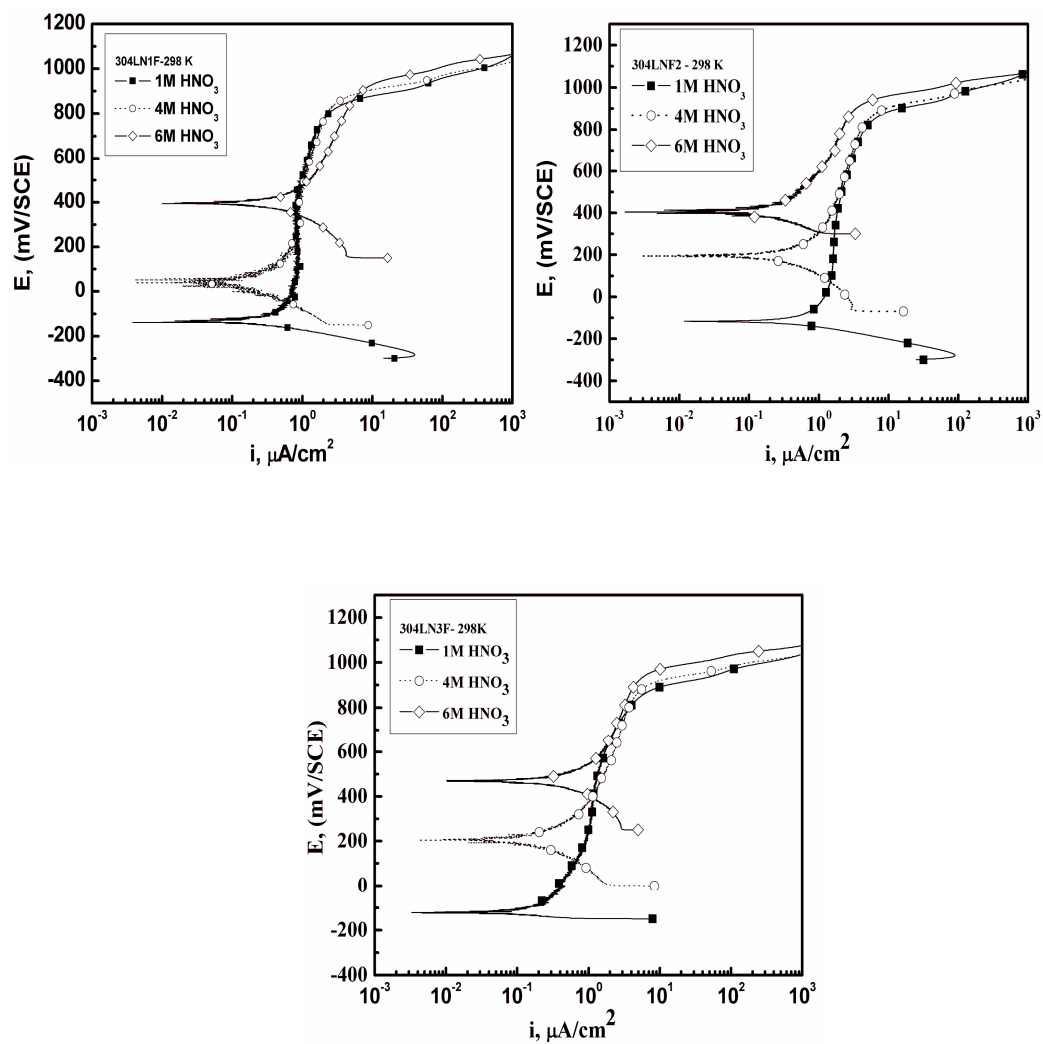


*Figure 5.8 Potentiodynamic anodic polarization curves in 1 M, 4 M, and 6 M  $\text{HNO}_3$  (298 K) for the forged nitrogen containing stainless steels*

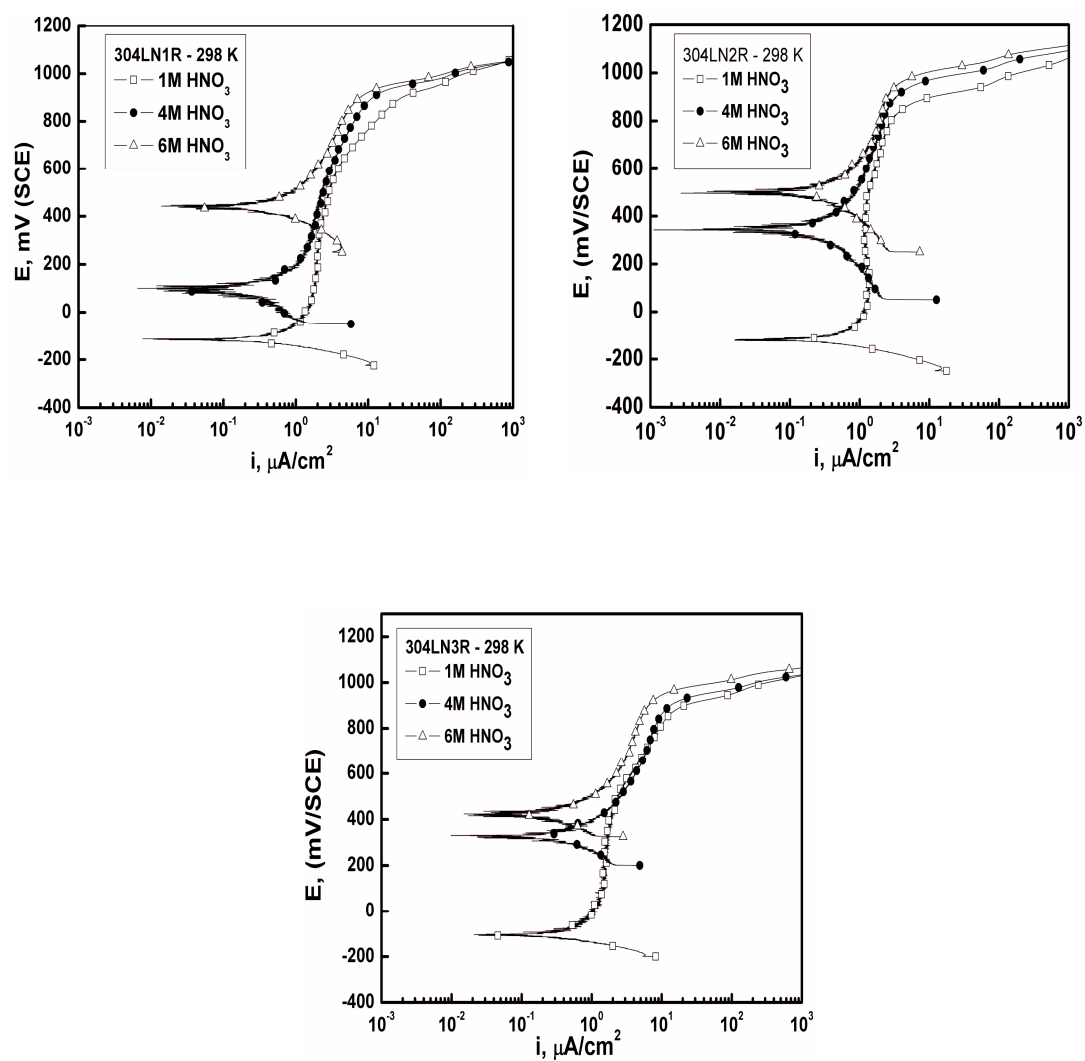


**Figure 5.9** Potentiodynamic anodic polarization curves in 1 M, 4 M, and 6 M  $\text{HNO}_3$  (298 K) for the rolled nitrogen containing stainless steels



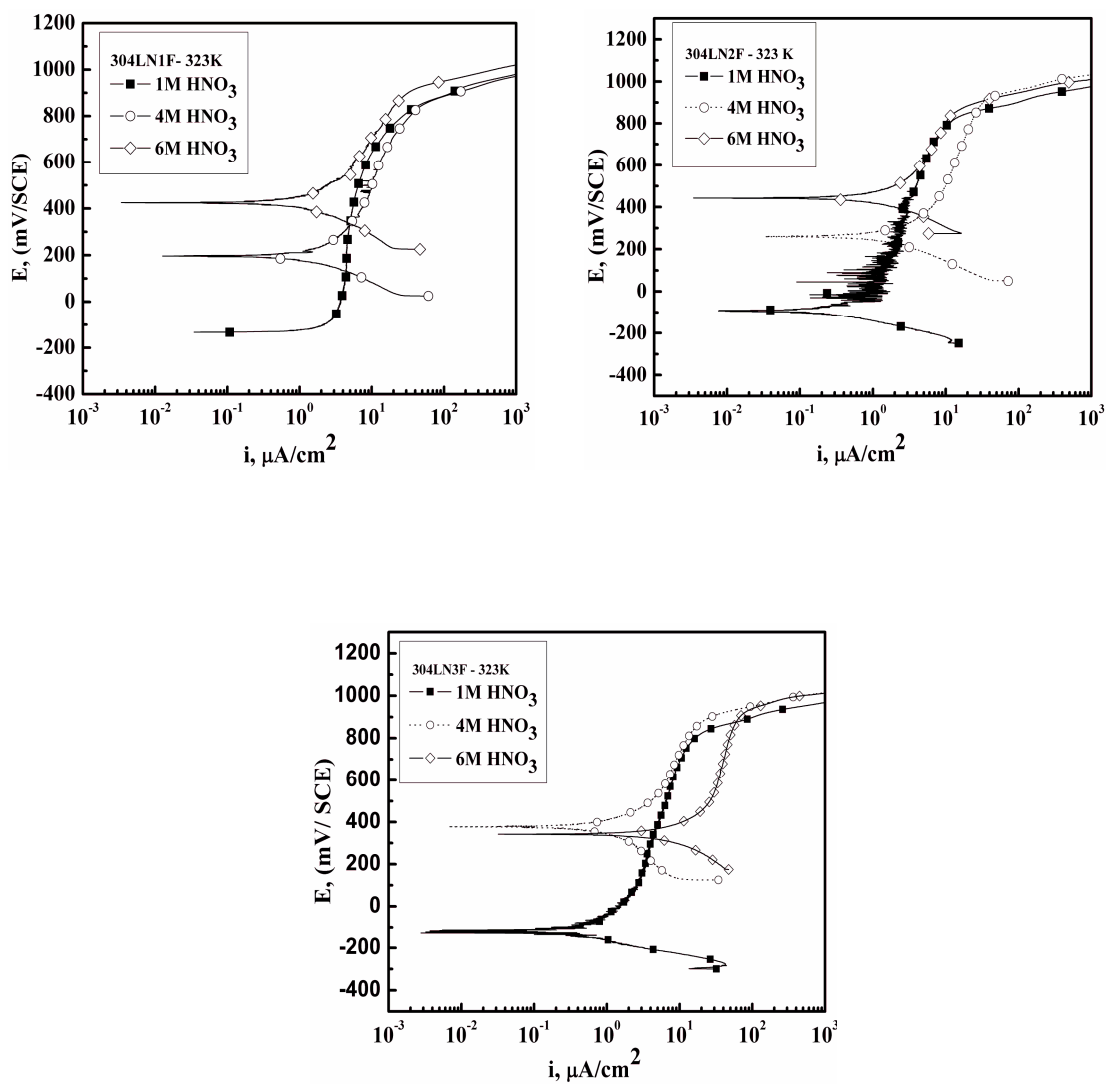


**Figure 5.10** Potentiodynamic anodic polarization curves in 1 M, 4 M, and 6 M  $\text{HNO}_3$  (323 K) for the as forged nitrogen containing stainless steels



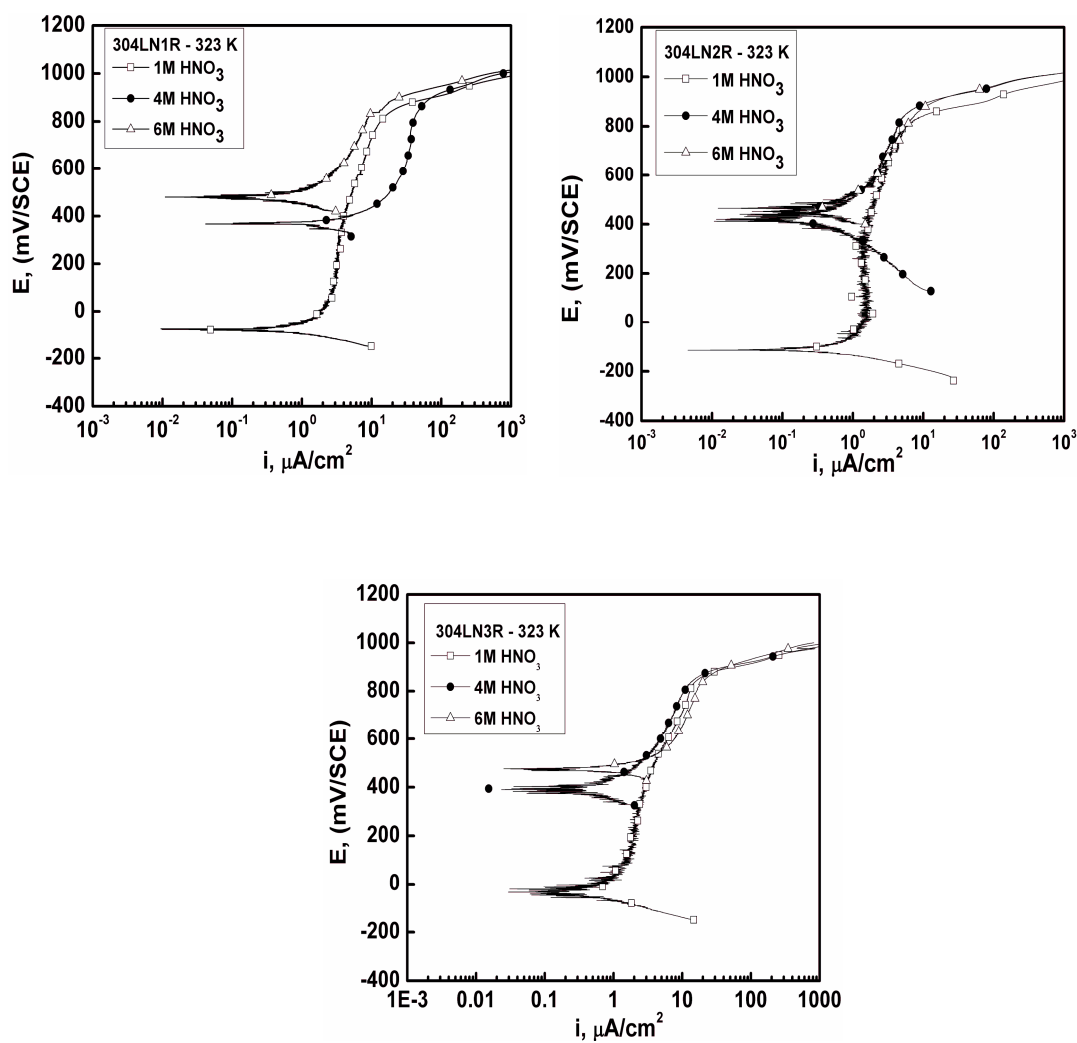


**Figure 5.11** Potentiodynamic anodic polarization curves in 1 M, 4 M, and 6 M HNO<sub>3</sub> (323 K) for the rolled nitrogen containing stainless steels

The electrochemical parameters are collectively presented in Table 5.1 and Table 5.2. From the results, it was observed that the polarization curves of the alloys, both in forged and rolled conditions showed spontaneous passivation in 1 M, 4 M and 6 M nitric acid.

The passive range varied depending on the concentration of the  $\text{HNO}_3$  used for the study. The potential at which the anodic current density monotonically increased beyond the passive range was inferred as transpassive potential. From the polarization curve, it is clear that the anodic current density increased after minor potential increase beyond the  $E_{\text{corr}}$ . For further increase in potential in the noble direction, the current remained constant until transpassive potential. The passive region begins at the potential noble to the  $E_{\text{corr}}$ , till the transpassive potential. The stainless steel alloys under forged and rolled conditions exhibited high transpassive potentials, wide passive range, and low passive current densities. It is observed that the corrosion potential,  $E_{\text{corr}}$ , increased with increase in concentration of nitric acid and the passive range decreased. All the hot rolled nitrogen containing stainless steel alloys exhibited a marginal increase in transpassive potentials and passive range, at ambient conditions. At higher temperature (323 K), the rolled steel exhibited a nobler corrosion potential compared to the forged steel, thereby, causing a marginal reduction in the passive range. However, the transpassive potentials were almost similar for both conditions. In general, both the forged and rolled conditions exhibited good corrosion resistance in nitric acid medium, however, the rolled steel showed a marginal improvement in corrosion resistance when compared to the forged alloy of the same composition under ambient conditions.

**Table 5.1 Electrochemical parameters for the forged nitrogen containing stainless steels in nitric acid medium**

Material	Conc. of HNO <sub>3</sub>	Corrosion potential, mV(SCE)		Passivation current density, $\mu\text{A}/\text{cm}^2$		Transpassive Potential, mV(SCE)		Passive range mV(SCE)	
		298K	323K	298K	323K	298K	323K	298K	323K
304LN1F	1 M	-130	-133	0.9	5.8	839	820	873	882
	4 M	46	198	1	11	853	849	700	542
	6 M	398	425.6	2	9.6	890	876	390	361
304LN2F	1 M	-116	-95	1.9	3.2	871	846	897	877
	4 M	194	259	2.3	6.7	890	877	609	521
	6 M	405	442	1.5	7.2	888	871	411	332
304LN3F	1 M	-122	-120	1.2	5	861	804	873	807
	4 M	209	376	2.3	8.5	890	868	574	379
	6 M	472	342	2.6	39	938	910	403	464

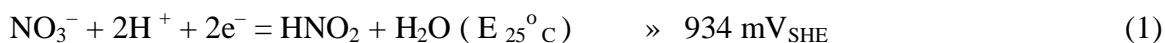
**Table 5.2 Electrochemical parameters for the rolled nitrogen containing stainless steels in nitric acid medium**

Material	Conc. of HNO <sub>3</sub>	Corrosion Potential mV(SCE)		Passivation current density $\mu\text{A}/\text{cm}^2$		Transpassive Potential mV(SCE)		Passive range mV(SCE)	
		298K	323K	298K	323K	298K	323K	298K	323K
304LN1R	1M	-116	-77	2.5	4.5	869	861	854	872
	4M	96	371	2.5	6.6	918	892	730	467
	6M	439	480	3.3	6.4	917	888	401	334
304LN2R	1M	-120	-112	1.92	1.85	862	809	902	860
	4M	338.9	430	1.52	2.78	925	858	517	357
	6M	501	461	1.8	4	963	884	396	373
304LN3R	1M	-106	-35	2.2	3.3	888	855	929	326
	4M	322	385	5	6.4	900	841	504	372
	6M	421	469	3.4	11.6	937	855	463	326

#### ***5.2.4 Effect of concentration and temperature of nitric acid on corrosion behavior of the stainless steels***

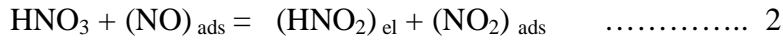
The potentiodynamic polarization curves of the nitrogen-containing stainless steels in HNO<sub>3</sub> showed spontaneous passivation in 1 M, 4 M and 6 M nitric acid under forged and rolled conditions, which could be attributed to the formation of stable chromium (III) oxide (Cr<sub>2</sub>O<sub>3</sub>) passive film. From the polarization curves of forged and rolled nitrogen containing stainless steels, it is evident that, as the HNO<sub>3</sub> concentration was increased from 1 M to 4 M to 6 M, the corrosion potential (E<sub>corr</sub>) increased.

The increase in corrosion potential with an increase in HNO<sub>3</sub> concentration could be attributed to the reduction of nitrate, which could be represented as [216, 218, 219, 236, 237, 238, 239, 240] :

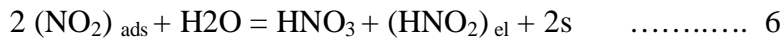
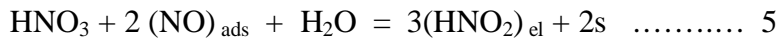
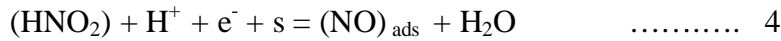


From the above equation, it is understood that the redox potential increases with an increase in NO<sub>3</sub><sup>-</sup> and H<sup>+</sup> concentration and temperature. The cathodic reduction generates nitrous acid (HNO<sub>2</sub>), and at concentrations below 6 M nitric acid, HNO<sub>2</sub> does not accumulate, but rather gets reduced to nitric oxide (NO). Electrochemical studies carried out on the reduction of HNO<sub>3</sub> [219], revealed that the final reduction product of the reduction is NO, at concentrations below 6 M HNO<sub>3</sub>. The reduction is autocatalytic, a mechanism well established by many investigators [216, 218, 219, 236, 237, 238, 239, 240]. According to Balbaud et al [27, 216], the reduction of nitric acid occurs indirectly through an autocatalytic mechanism where the final reduction product is NO at nitric acid concentrations below 6M. The generalized mechanism operative at all concentrations could be summarized as follows. Here, the electroactive species is nitrous acid, which is

reduced to nitric oxide. Nitrous acid is then regenerated at the electrode by a chemical reaction between nitric acid and nitric oxide. A third reaction occurs between nitrous acid and nitric acid.



At the concentrations below 6M, regeneration of  $\text{HNO}_2$  is slow as a result of which nitric oxide accumulates and as  $\text{NO}_2$  is unstable at low concentrations, the third reaction favours backward reaction. Therefore, the reduction mechanism could be explained as



Where,  $(\text{HNO}_2)_{\text{el}}$  and  $(\text{HNO}_2)_{\text{sol}}$  represent the nitrous acid concentration at the electrode and solution, respectively, “s” represents a free adsorption site at the electrode surface. From a thermodynamic point of view, the redox potential of the medium increases with an increase in concentration of  $\text{HNO}_3$  and hence increases the  $E_{\text{corr}}$ . From a kinetic point of view, the reduction is catalyzed by the reduction products, increasing the reduction rate. Hence, the cathodic part of the current-potential curve shifts toward higher potentials; consequently, the  $E_{\text{corr}}$  of the steel increases. The corresponding oxidation reaction is that of metal dissolution ( $\text{Fe} = \text{Fe} [\text{III}] + 3 \text{e}^-$ ,  $\text{Cr} = \text{Cr} [\text{III}] + 3 \text{e}^-$ ,  $\text{Ni} = \text{Ni} [\text{II}] + 2 \text{e}^-$ ) [238].

As the equilibrium potential shifts to higher values, the cathodic curve will meet the anodic curve of the stainless steel in the passive region and hence the steel spontaneously passivates in nitric acid medium. Temperature has been found to have a deleterious effect on the corrosion resistance of the nitrogen containing stainless steel. An increase in solution temperature was found to result in an increase in  $E_{\text{corr}}$  and  $i_{\text{pass}}$  and a marginal decrease in transpassive potential. Increase in  $E_{\text{corr}}$  with an increase in temperature could be attributed to the increase in the redox potential of the  $\text{HNO}_2/\text{HNO}_3$  system. Increase in temperature increases the oxidizing power of  $\text{HNO}_3$  [181]. The effect of temperature is to increase both the current from  $\text{HNO}_3$  reduction and the currents from passive/transpassive metal dissolution. Another contribution of temperature is that it aids the dissolution of ions from the passive film surface as evident from an increase in passive current density. Studies of earlier research have shown that the corrosion rate of type 304 stainless steel increases with both temperature and  $\text{HNO}_3$  concentrations, particularly at higher temperature solution [235]. In addition, it is observed that the rolled alloy exhibited a marginal increase in corrosion resistance in nitric acid medium.

#### ***5.2.5 Effect of nitrogen on corrosion behavior of the nitrogen-containing stainless steel alloys in nitric acid***

Nitrogen as an alloying element in steels and stainless steels is known to enhance passivity in chloride-containing environments. From the present study, it was observed that the nitrogen-containing stainless steel alloys in forged as well as rolled conditions have exhibited similar corrosion resistance for a given concentration of  $\text{HNO}_3$  and temperature, irrespective of the nitrogen content. A wide passive region in all three alloys

was observed; however, an increase in nitrogen content in the stainless steel did not show any discernible difference in the passive range. The present investigation reveals that increasing nitrogen content of the stainless steel, though, has led to precipitation of chromium nitride along the grain boundaries, it did not show any deleterious effect on the corrosion resistance of the alloy. Though precipitation of chromium nitride leads to Cr depleted zones which are prone to nitric acid attack, no such evidences were found. This could be attributed to the spontaneous passivation property of stainless steels in nitric acid medium by the formation of stable  $\text{Cr}_2\text{O}_3$  passive film, particularly in the concentration range of 1-6 M nitric acid.

#### ***5.2.6 Effect of nitrogen on pitting corrosion of high-nitrogen stainless steel alloys in***

##### ***0.5 M NaCl***

The potentiodynamic polarization curves for the forged and rolled nitrogen containing stainless steels in 0.5 M NaCl is represented in Figure 5.12 (a and b) respectively. The pitting potentials obtained from the polarization curves are given in Table 5.3. Pitting corrosion experiments were repeated three times. As a deviation of  $\pm 10$  mV was observed in each set of experiments, the average was taken to represent the pitting potential. From the polarization curves, the pitting potentials for 304LN1F, 304LN2F, and 304LN3F stainless steels in 0.5 M NaCl were found to be 435 mV(SCE), 530 mV(SCE), and 275 mV(SCE), respectively and that for the rolled stainless steels were found to be 550 mV(SCE) for 304LN1R and 304LN2R, and 710 mV (SCE) for 304LN3R respectively . All the three nitrogen containing rolled stainless steels showed superior pitting resistance than the forged stainless steels with the same nitrogen content.

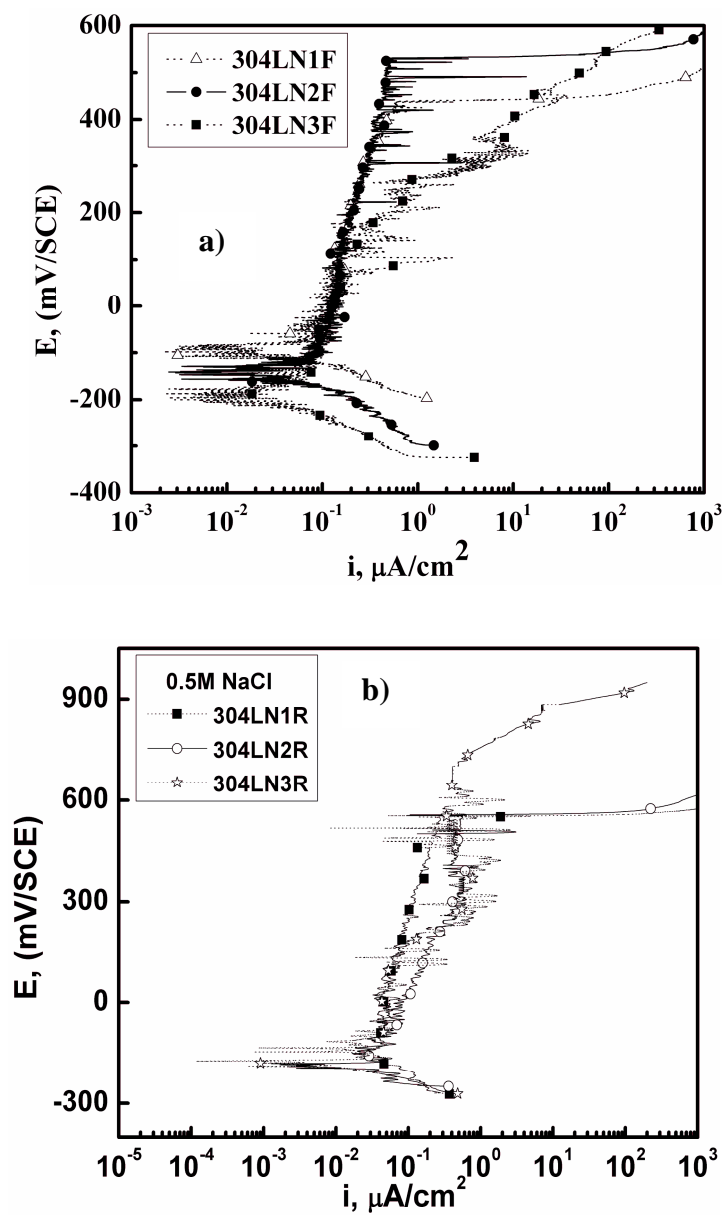


**Figure 5.12** Potentiodynamic anodic polarization curves for the a) forged and b) rolled nitrogen containing stainless steels containing three different nitrogen contents in 0.5 M NaCl



Material	N Content (wt%)	Pitting Potential mV(SCE)	
		As Forged	Rolled
304LN1	0.132	435	550
304LN2	0.193	530	550
304LN3	0.406	275	710

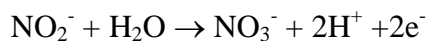
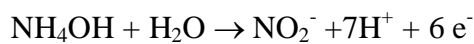
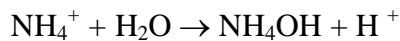
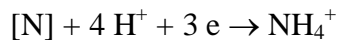
***Table 5.3 Pitting Potential of the as-forged and hot rolled nitrogen containing stainless steel alloy in 0.5 M NaCl***

From the results of the investigation of the pitting corrosion resistance of the three alloys in 0.5 M NaCl, it was observed that as the nitrogen content is increased from 0.132 wt% N (304LN1F SS) to 0.193 wt% N (304LN2F SS), the pitting potential increased, implying an increase in pitting corrosion resistance. However, the pitting potential of 304LN3F stainless steel was found to be lower than 304LN1F and 304LN2F stainless steels. An increase in nitrogen content of upto 0.193% was beneficial in enhancing the pitting resistance in the forged stainless steel. Further increase in nitrogen caused the decrease in pitting resistance. This could be attributed to the presence of continuous network of chromium rich precipitate and manganese-rich precipitates along the grain boundary of the 304LN3F steel. EDS analysis of 304LN3F stainless steel showed significant enrichment in chromium when compared to 304LN1F and 304LN2F stainless steels. Chromium enrichment in the precipitate could have led to the depletion of

chromium in the adjacent zones where the passive film formation would be weak, thus forming sites for pitting attack.

The pitting potentials for 304LN1R and 304LN2R stainless steel were found to be similar while 304LN3R alloy exhibited a profound increase in the pitting potential. An increase of nitrogen upto 0.406% was found to be beneficial in enhancing the pitting resistance of the rolled stainless steels. From the present investigation, it was found that the hot rolled stainless steel alloys exhibited superior pitting resistance when compared to the forged alloys [19]. A significant improvement in the pitting resistance was observed in the forged alloy [19] when the nitrogen content was increased from 0.132 wt% to 0.193 wt%, but the hot rolled alloys containing these compositions of nitrogen were found to be exhibiting similar pitting resistance. A beneficial effect of nitrogen in enhancing the pitting resistance was found in the hot rolled 304LN3R alloy, which exhibited a substantial improvement in the pitting resistance, in comparison to the inferior pitting resistance exhibited by the forged 304LN3F alloy [19]. The improvement in the pitting resistance of the hot rolled high nitrogen stainless steel could be attributed to various aspects. One aspect is that the continuous network of precipitates found along the grain boundary in the forged specimens are absent in the rolled steels. Hot rolling and annealing has resulted in partial dissolution of precipitates leading to a more homogeneous matrix, as observed in the optical and SEM micrographs, consequently reducing the number of pit initiation sites. In addition, dissolution of chromium nitride precipitates results in enrichment of the stainless steel matrix with nitrogen. Nitrogen in solid solution is known to enhance corrosion property of stainless steel, in particular pitting corrosion resistance. The susceptibility of stainless steel to pitting corrosion is

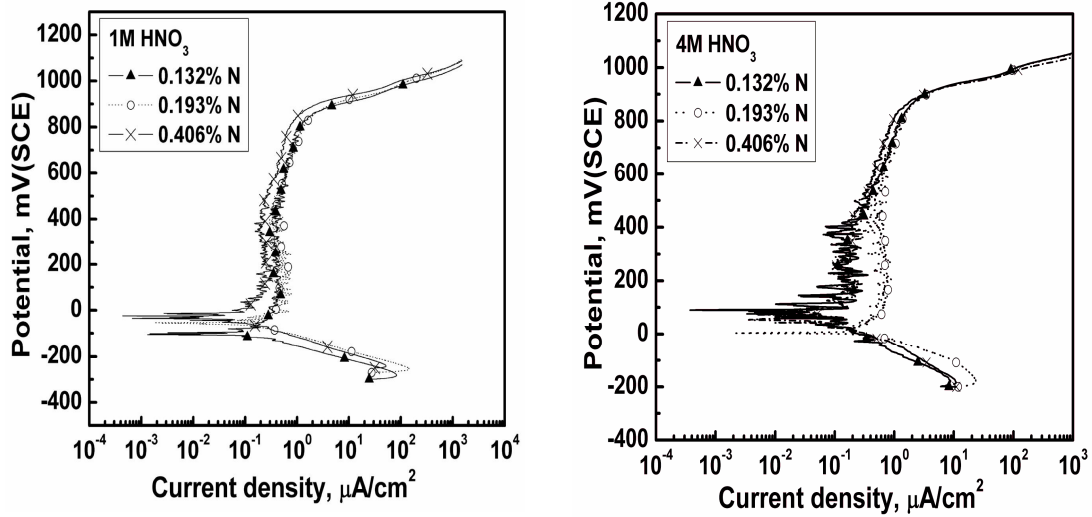
represented by their chemical composition as  $PREN = \% Cr + 3.3 \times \% Mo + 16 \times \% N$ , where PREN represents the pitting resistance equivalent number [181]. The measure of alloying for resistance to corrosion (MARC) relates the alloy content of austenitic stainless steels to their localized corrosion resistance in chloride solutions ( $MARC = \% Cr + 3.3\% Mo + 20 C + 20 N - 0.5 Mn - 0.25 Ni$ ) [244]. Since the chromium, nickel, molybdenum, and carbon contents of 304LN1F and 304LN2F stainless steels are similar, PREN and MARC for the alloy are governed by the nitrogen content. Hence, nitrogen content of the alloys plays an important role in influencing the pitting corrosion resistance. The beneficial role of nitrogen to pitting corrosion resistance has been well established by many investigators. According to Newman, et al [245], Clayton and Martin [228], during active dissolution, nitrogen gets enriched at the metal-film interface which then provides an inactive surface to the attack by chloride ion during film breakdown. According to Osozawa, et al [246], the nitrogen at the pit surfaces dissolves to form ammonium ions, which, according to Mudali, et al [28] later transforms to nitrate and nitrite ions to develop a stable and protective repassivation layer at the pit site by “local inhibition effect”. The increase in the pH at the pit site retards the pit growth kinetics.  $NH_4^+$  ions further get hydrolyzed to form nitrite and nitrate film, which favors repassivation. The entire process could be represented by the following set of equations:



### 5.3 Effect of nitrogen on corrosion behavior of nitrogen containing 304L SS in nitric acid and simulated HLW by electrochemical noise

#### 5.3.1 Evaluation of Stern - Geary coefficient

Potentiodynamic anodic polarization experiments were carried out for the three nitrogen containing alloys (as received hot rolled specimens) in 1M, 4M, 8M and simulated HLW medium in order to obtain the Stern Geary coefficient (B). A typical representation of the polarization graphs in 1M and 8M nitric acid are shown in Figure 5.13.



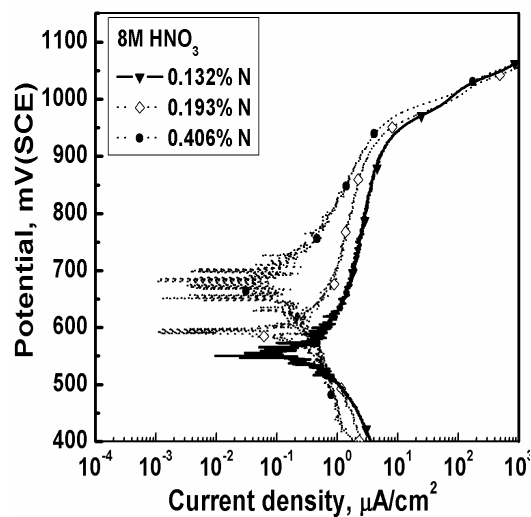


**Figure 5.13 Typical Polarization curves for the nitrogen containing stainless steels in 1 M, 4 M and 8 M HNO<sub>3</sub>**

From the polarization graphs, the anodic ( $\beta_a$ ) and cathodic ( $\beta_c$ ) Tafel slopes were extracted and used in the well known Stern Geary equation (17) to deduce the Stern Geary coefficients for the stainless steels in the respective medium.

$$B = \frac{(\beta_a \beta_c)}{2.303(\beta_a + \beta_c)} \quad (17)$$

These values were further used for the shot noise analysis. The values of B are listed in Table 5.4.

<b>Nitrogen content</b>	<b>1 M HNO<sub>3</sub></b>	<b>4 M HNO<sub>3</sub></b>	<b>8 M HNO<sub>3</sub></b>	<b>Simulated HLW (in 3M HNO<sub>3</sub>)</b>
<b>0.132% N</b>	<b>0.02</b>	<b>0.03</b>	<b>0.063</b>	<b>0.03</b>
<b>0.193% N</b>	<b>0.02</b>	<b>0.03</b>	<b>0.059</b>	<b>0.028</b>
<b>0.406% N</b>	<b>0.023</b>	<b>0.032</b>	<b>0.05</b>	<b>0.033</b>

*Table 5.4 Stern Geary coefficients in V/decade, for the nitrogen containing stainless steels*

### **5.3.2 Time record and noise resistance**

The potential and current noise-time record for the three nitrogen containing 304L SS depicted passivation process [21,81,143] in 1M, 4M, 8M and simulated HLW solution. The current noise- time record was characterized by low amplitude rapid transients typical of white noise and the potential noise comprised of slow rise and slow fall of potential. Typical representation of the current noise and potential noise – time record for the stainless steel containing 0.132 % N is shown in Figure 5.14.

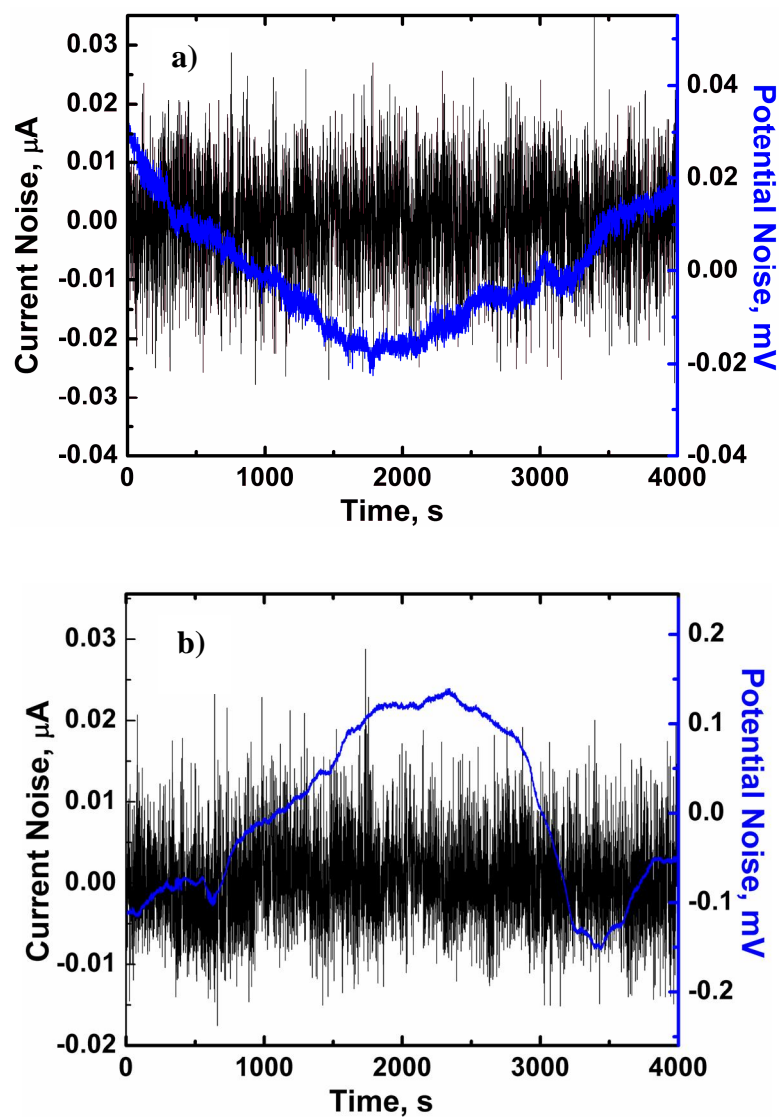


*Figure 5.14 Typical representation of electrochemical current and potential noise time record for 304L SS containing a) 0.132% N b) 0.193% N in 4 M  $\text{HNO}_3$  taken after 8 h of immersion*

Electrochemical noise resistance was evaluated from the time record as the ratio of the standard deviation of potential noise to that of the current noise. Electrochemical noise resistance has been well established by several investigators, to be inversely related to

corrosion rates, under conditions when both working electrodes have the same activity and the corrosion process is uniform under activation control [74, 111]. However, even for systems that do not undergo uniform corrosion, high noise resistance has been obtained for systems that show low corrosion activity and vice versa [21, 81, 111]. It could thus be accepted that even for low active systems such as that for a passivation process, a comparatively high noise resistance implies low corrosion activity and low noise resistance implies high corrosion activity and hence corrosion activity would be more appropriately used than corrosion rates. The plot of noise resistance with time of immersion for the three nitrogen containing 304L SS in 1 M, 4 M, 8 M  $\text{HNO}_3$  and simulated HLW is represented in Figure 5.15 and the average noise resistance for 24 h of immersion is given in Table 5.5. It was observed that the nitrogen containing stainless steels in the environments studied, exhibited high noise resistance which is generally known to be associated with passive systems [21, 108, 110]. Further, a profound increase was observed in the noise resistance with increase in nitrogen content of the stainless steel. It is evident from the results that nitrogen has a major role to play in decreasing the corrosion activity with its increase in the alloy. From the noise resistance plots it is found that with increase in time of immersion, there is an increase in passive film stability in 1M acid, a decrease in 8M acid and almost a constant stability in 4M acid. The reasons for the mentioned observations could be explained as follows. In 1M  $\text{HNO}_3$ , the corrosion potential of 304L SS is in the passive region closer to the active region and hence the stability increases with time of immersion [34].



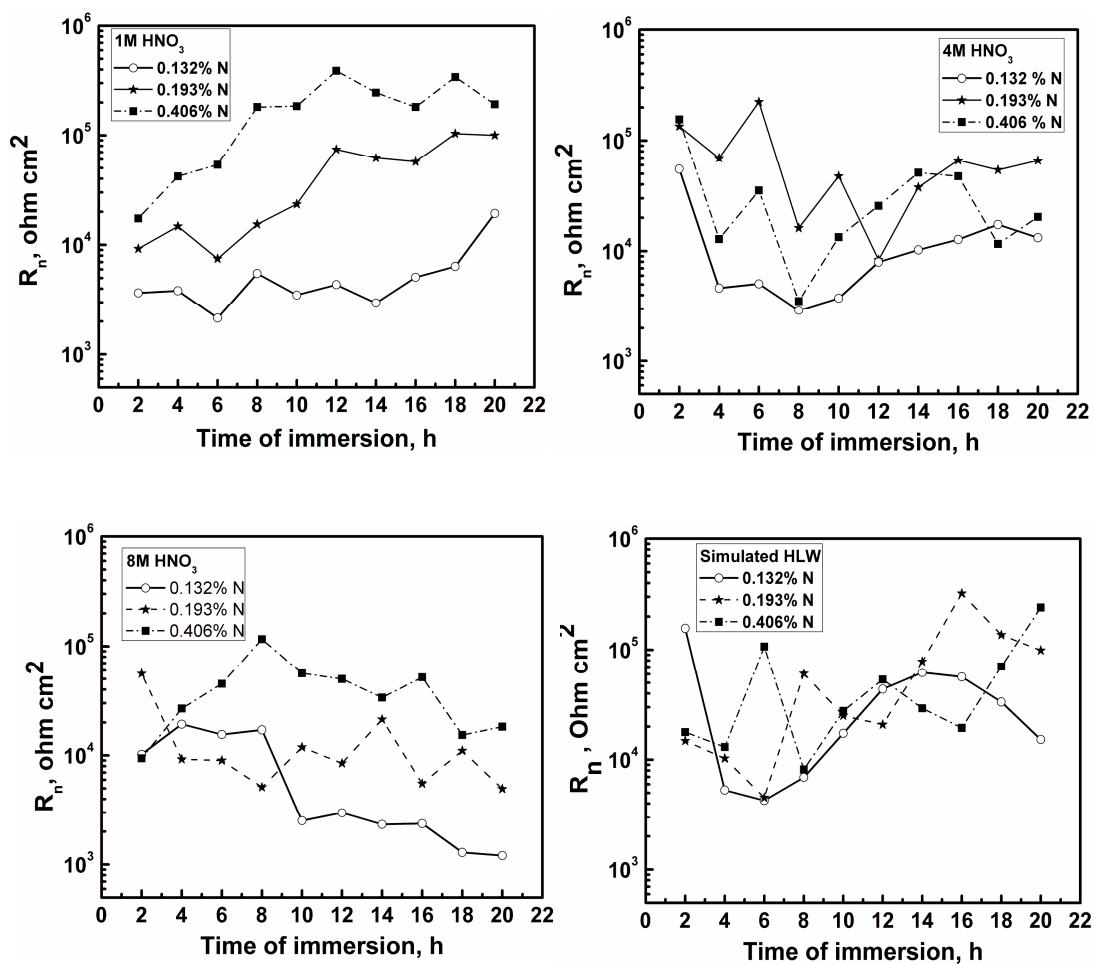


Figure 5.15 Electrochemical noise resistance of the three nitrogen containing 304L SS in 1 M, 4 M, 8 M  $\text{HNO}_3$  and simulated HLW medium.

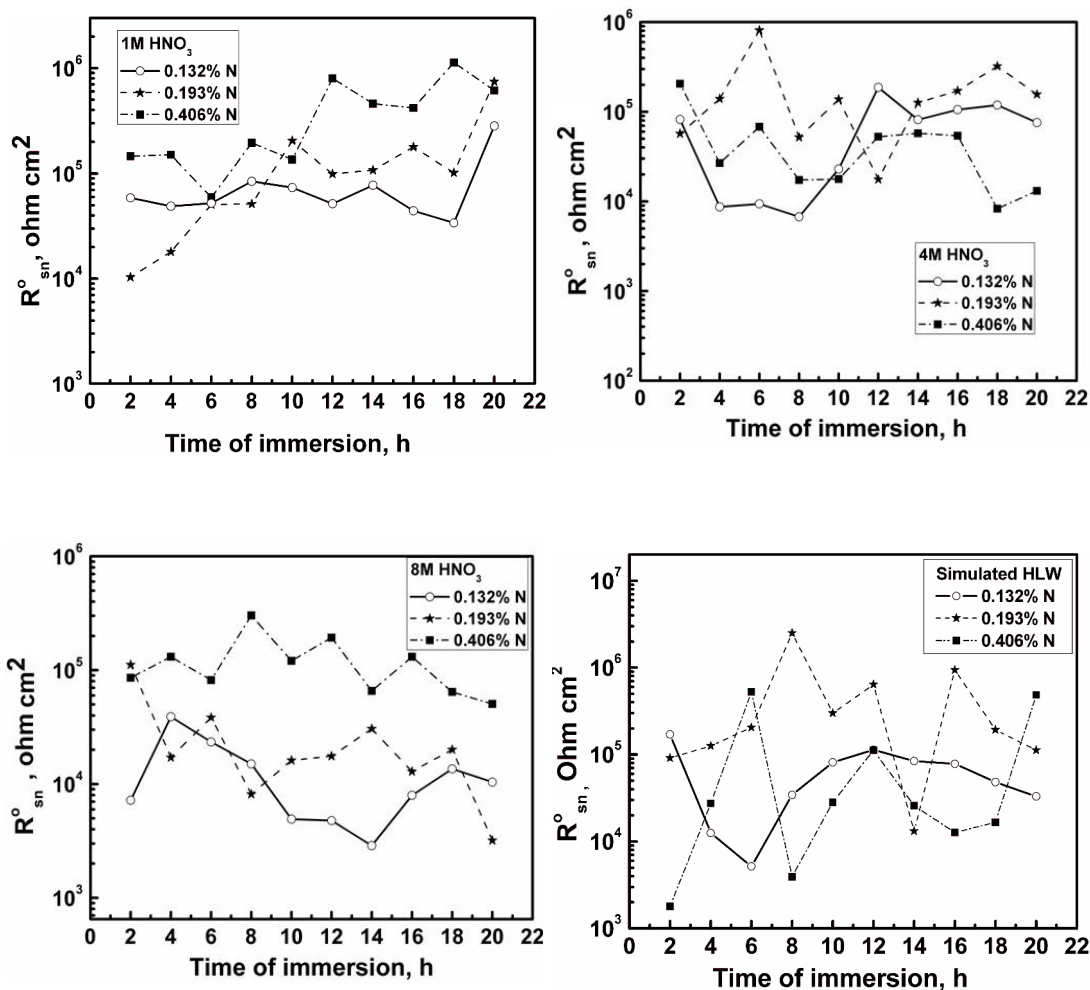
<b>Nitrogen content</b>	<b>1M HNO<sub>3</sub></b>	<b>4M HNO<sub>3</sub></b>	<b>8M HNO<sub>3</sub></b>	<b>Simulated HLW (in 3M HNO<sub>3</sub>)</b>
0.132% N	5667	13132	7435	40111
0.193% N	46717	72351	14248	77325
0.406% N	182872	37616	42299	58728

***Table 5.5 The average noise resistance for 24 h of immersion***

In 8 M HNO<sub>3</sub>, the corrosion potential of the steel is in the passive region closer to transpassive potentials and hence a decrease in stability is reflected with time of immersion and in 4 M acid, the corrosion potential is in the passive region between active region and transpassive potentials and hence the steel exhibits almost constant passive film stability with time of immersion [34]. In simulated HLW solution containing 3 M HNO<sub>3</sub>, the noise resistance was found to be in close range, with marginal increase in the higher nitrogen stainless steels. This result could be attributed to the complex chemistry of simulated HLW which contains 3 M HNO<sub>3</sub>, a well known passivating medium for stainless steels and the presence of cations, which could get adsorbed on the passive film. The competition between passivation by 3 M HNO<sub>3</sub> and the instability of the film caused by adsorption of cations appears to have subdued the effect of nitrogen and hence only a marginal increase in the resistance was observed with increase in nitrogen content of the stainless steels. The fluctuations in the noise resistance with time of immersion reflect a disturbed passive film in simulated high level waste medium.

### 5.3.3 Spectral noise resistance

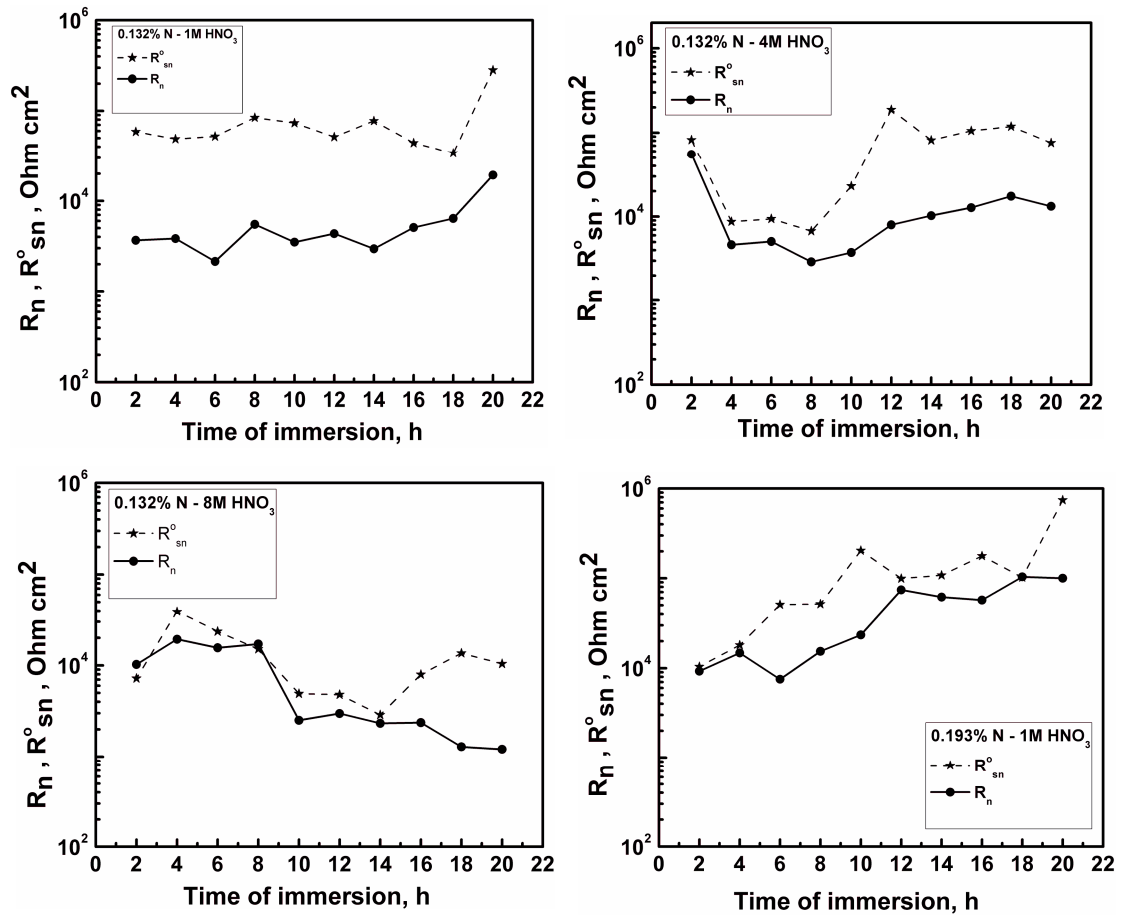
Spectral noise resistance was evaluated as the ratio of the square root of power spectral density of potential noise to that of the current noise at each frequency. Mansfeld et al [106] introduced the parameter called “the spectral noise impedance”  $R_{sn}(f)$  in their studies on coating systems by EN method. The spectral noise plots have been extrapolated to the dc limit to obtain the spectral noise resistance,  $R_{sn}^0$  which has the unit of resistance and has been compared with  $R_n$ . A plot of  $R_{sn}^0$  as a function of time of immersion is shown in Figure 5.16.  $R_{sn}^0$  for the nitrogen containing steels in  $HNO_3$  and simulated HLW has been found to be high, which could be attributed to passivation process, as observed in our earlier investigations also [21, 108]. In recent literature, Cottis et al [109, 111] have associated high noise impedance for passive systems and low noise impedance for uniform and localized corrosion of carbon steel [109] and aluminum alloys [111]. In the present work,  $R_{sn}^0$  in 1 M, 4 M and 8 M  $HNO_3$  was found to increase with increase in nitrogen content, after 8 h of immersion.  $R_{sn}^0$  plots also indicated better passive film stability in 4 M  $HNO_3$  when compared to 1 M and 8 M acid. In simulated HLW,  $R_{sn}^0$  was high for all the three alloys with nitrogen which could be attributed to passivation process.  $R_{sn}^0$  increased as the nitrogen content of the steel increased from 0.132% to 0.193%. For further increase in nitrogen,  $R_{sn}^0$  was comparable to the lower nitrogen steels. The fluctuations in the spectral noise resistance reflect an unstable passive film in simulated high level waste medium.

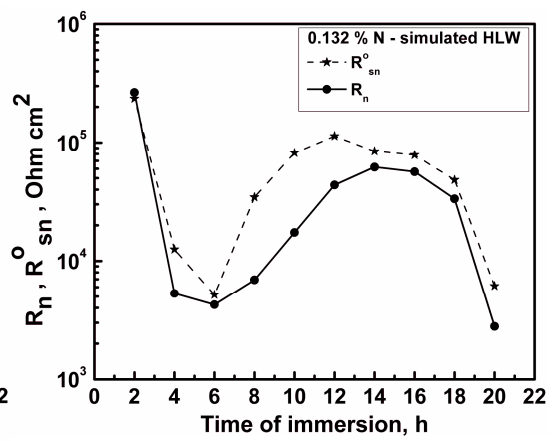
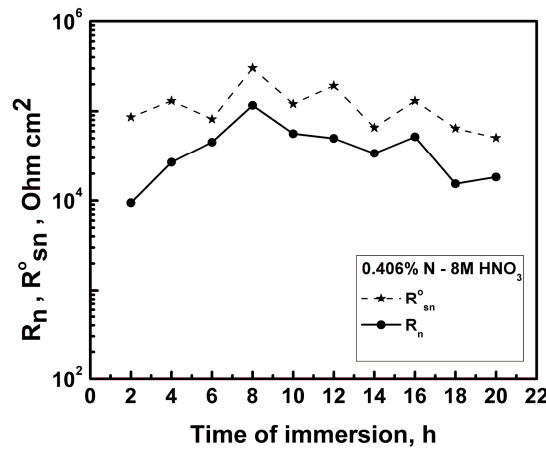
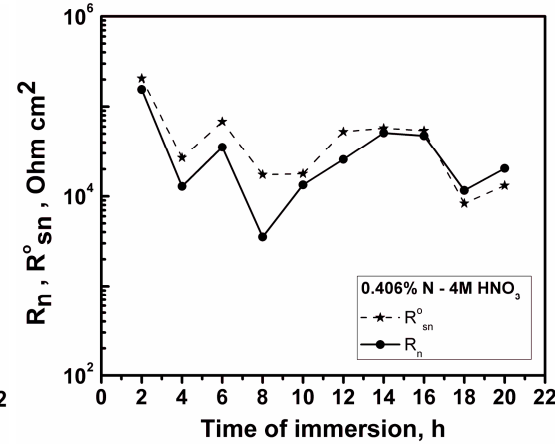
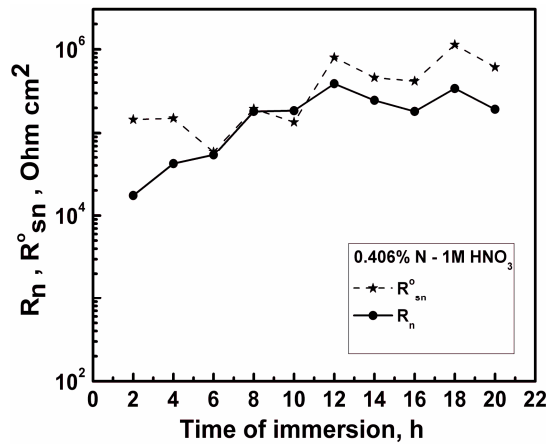
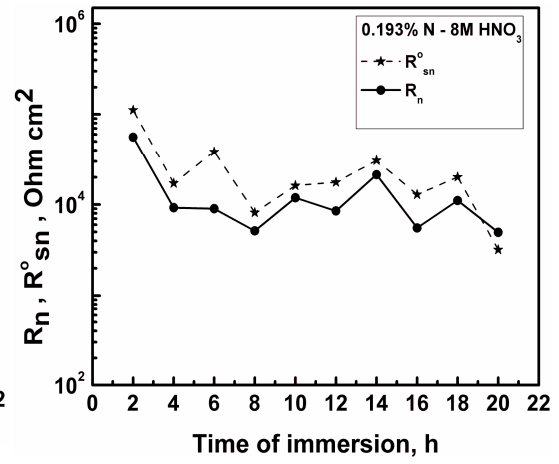
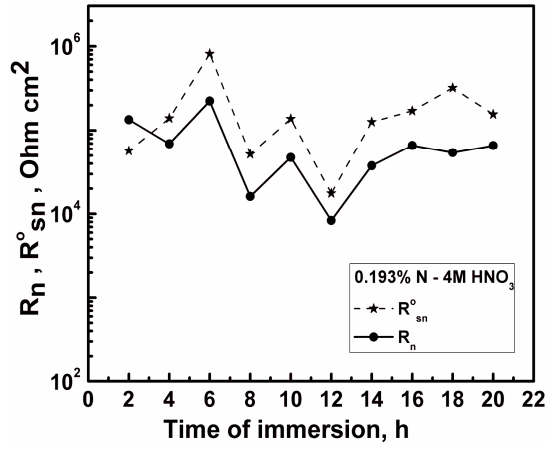


**Figure 5.16** Spectral noise resistance of the three nitrogen containing 304L SS in 1 M, 4 M, 8 M  $\text{HNO}_3$  and simulated HLW medium.

In Figure 5.17,  $R_{sn}^0$  and  $R_n$  have been plotted for the nitrogen containing stainless steels in order to check the validity of the correlations between the two parameters for systems exhibiting low corrosion activity. It has been reported in literature [106,107,50,46] that  $R_{sn}^0$  obtained from power spectral density plots compares well with  $R_n$  from statistical

analysis and polarization resistance ( $R_p$ ) obtained from linear polarization technique. Cottis et al [111] has reported equivalence between  $R_{sn}^o$  and  $R_n$  for corrosion of aluminum in various environments. In several other studies, the above relationship was not found to be satisfied [143]. In the present investigation, it was found that  $R_{sn}^o$  followed  $R_n$  in  $HNO_3$  as well as simulated HLW medium. A good equivalence existed between the two parameters. It could be well appreciated that even for passive systems where the corrosion activity is low, noise resistance and spectral noise resistance could discern the variations in the corrosion activity.





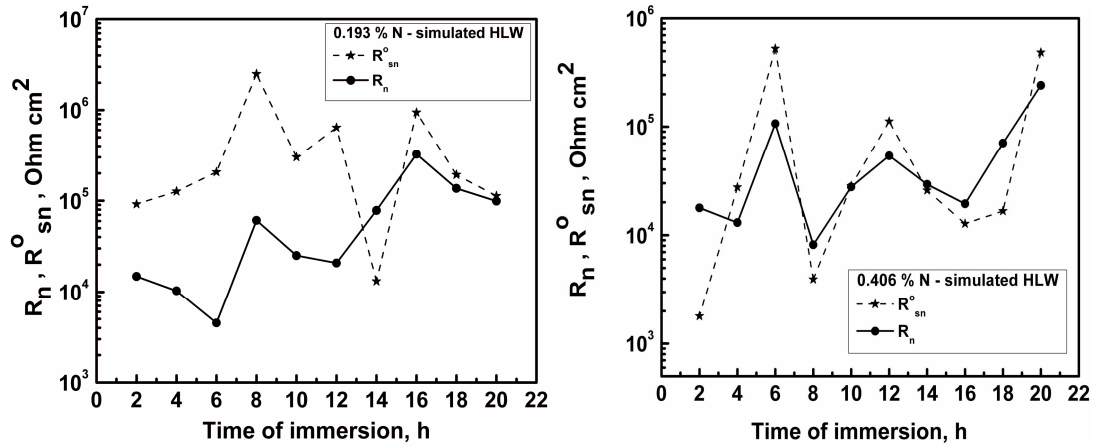


**Figure 5.17** Plots showing correlations between noise resistance and spectral noise resistance for the nitrogen containing stainless steels in  $\text{HNO}_3$  and simulated HLW medium.  $R_{sn}^o$  is found to follow  $R_n$

### 5.3.4 Shot noise analysis

#### 5.3.4.1 Characteristic frequency plots

Characteristic frequency is the frequency of events divided by the area of the specimen exposed to the medium. The characteristic frequency ( $f_n$ ) and charge ( $q$ ) have been established to provide information about the nature of the corrosion process [74, 46, 75, 112]. The characteristic charge gives information about the amount of metal lost in each event occurring in the corrosion process and characteristic frequency is associated with the rate at which these events occur [109, 111]. For a uniform corrosion process which is associated with high frequency of corrosion at the surface,  $f_n$  and  $q$  are high. In localized corrosion such as pitting and intergranular corrosion, where transients are large and the number of events or frequency of events is small,  $f_n$  is small and  $q$  is large. For passive systems,  $q$  is expected to be low and  $f_n$  may be low or high depending on the processes

occurring on the passive film [109]. The shot noise theory is based on the assumption that the power spectrum of an individual transient is constant at low frequencies and it is expected that the PSD should show a plateau at the low frequency range and the lowest possible frequency is taken for analysis. In cases where the low frequency plateau is absent, the PSD values corresponding to lowest frequency is used to estimate  $f_n$ , and  $R_{sn}^o$  [75, 109]. In the present investigation, the PSD was taken corresponding to the lowest frequency of  $5 \times 10^{-4}$  Hz. The nitrogen containing stainless steels showed low characteristics frequency, which remained almost steady with time of immersion. The low characteristic frequency which implies low rate of events or low corrosion activity could be attributed to good passivation behaviour of stainless steels in  $HNO_3$  medium. Cottis et al [109, 111] reported high  $f_n$  for inhibited and passive systems of carbon steels<sup>109</sup> and variable values of  $f_n$  for aluminum alloys [111]. Further, it was observed that  $f_n$  decreased with increase in nitrogen content implying low corrosion activity with increase in nitrogen content. A plot of characteristics frequency or the frequency of events per unit area as a function of time is shown in Figure 5.18. The characteristic frequency plots also reflect better passive film stability in 4 M  $HNO_3$  when compared to 1 M and 8 M  $HNO_3$ . The characteristic charge associated with these events were found to increase with increase in nitrogen content, the reasons being absurd and hence is not further discussed.



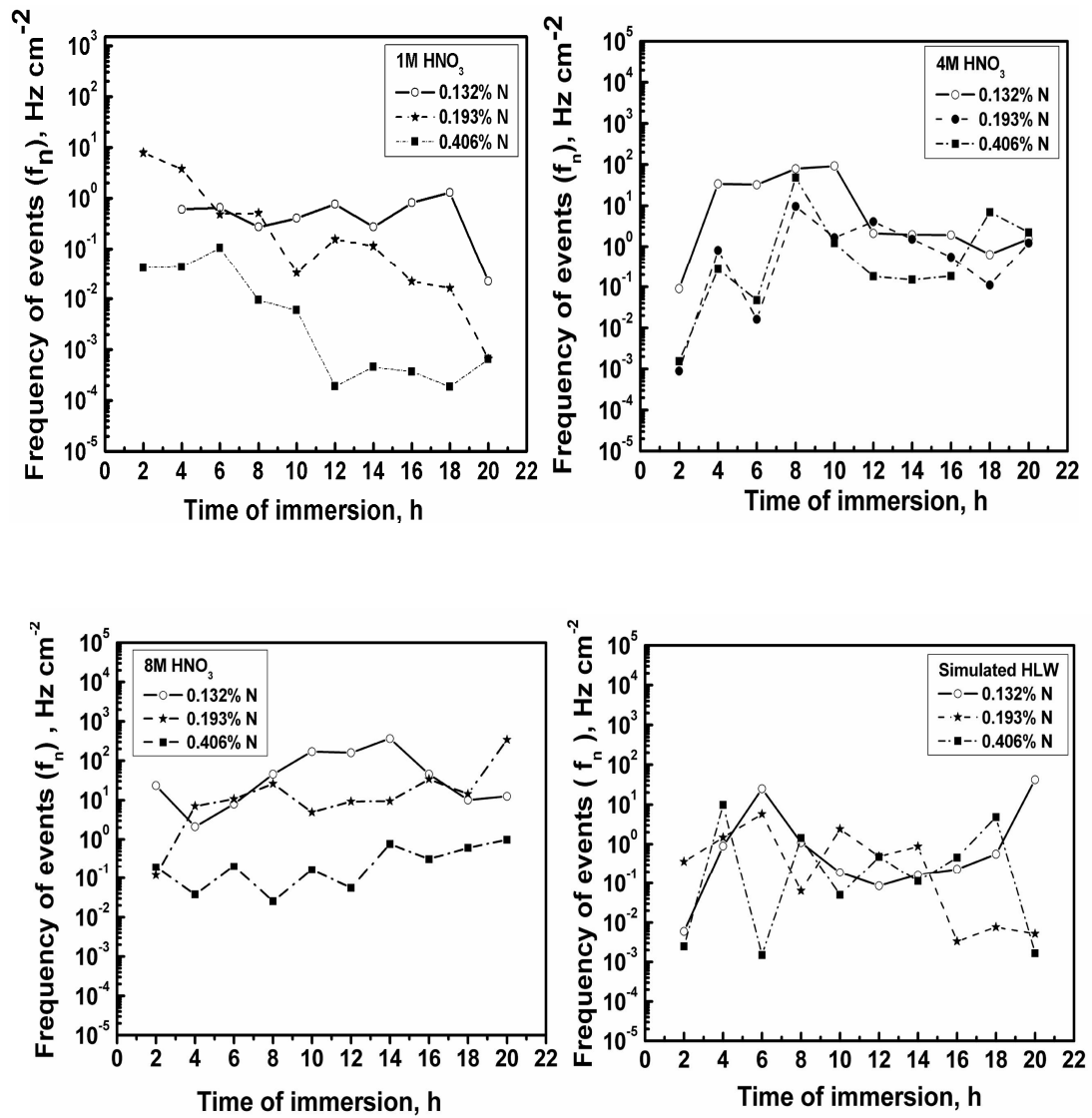


*Figure 5.18 Characteristic frequency as a function of time of immersion for the three nitrogen containing stainless steels in  $\text{HNO}_3$  and simulated HLW medium.*

One probable cause could be that these low frequency occurrences could be arising from dissolution near the vicinity of chromium nitride precipitates where there would be chromium depleted zones, contributing to higher charge in the higher nitrogen content stainless steel.

#### ***5.3.4.2 Cumulative probability plots***

The cumulative probability  $F(f_n)$  is plotted against the frequency of events,  $f_n$ , in Figure 5.19, for the nitrogen containing 304L SS in 1 M, 4 M, 8 M, and simulated HLW. The frequency of distribution was found to shift towards lower frequency with increase in nitrogen content of the steels in 1 M, 4 M and 8 M  $\text{HNO}_3$ , implying a decrease in the corrosion activity with increase in nitrogen content. This could be attributed to improved passivation behavior of the steels as the nitrogen content is increased. In 1 M  $\text{HNO}_3$ , the frequency of events was found to range between  $0.02 \text{ Hz/cm}^2$  to  $1.2 \text{ Hz/cm}^2$  for 0.132 % N,  $7 \times 10^{-4} \text{ Hz/cm}^2$  –  $8 \text{ Hz/cm}^2$  for 0.193 % N and  $1.9 \times 10^{-4} \text{ Hz/cm}^2$  –  $4 \times 10^{-2} \text{ Hz/cm}^2$  for 0.406 % N. In addition, it was observed that as the nitrogen content is increased from 0.132 % to 0.193 % to 0.406 %, there is a corresponding decrease in the frequency of events in the cumulative probability range of 0.2 to 0.6. Similar correspondence in the frequency of events and nitrogen content was observed in 8 M  $\text{HNO}_3$  for the cumulative probability range above 0.9. A direct correlation between nitrogen content and corrosion activity has been observed in 1 M and 8 M  $\text{HNO}_3$ . In 4 M  $\text{HNO}_3$  too, a direct correlation exist between nitrogen content and corrosion activity in the cumulative probability regime of 0.35-0.6 as there is a decrease in the frequency of events with increase in nitrogen content. In the lower and higher cumulative probability region, the steel containing 0.193 % N showed least corrosion activity. The cumulative probability –

frequency of events plots also confirmed an increase in corrosion activity with increase in concentration of  $\text{HNO}_3$  as it was observed that the cumulative probability shifted towards higher frequency of events with increase in nitrogen content.

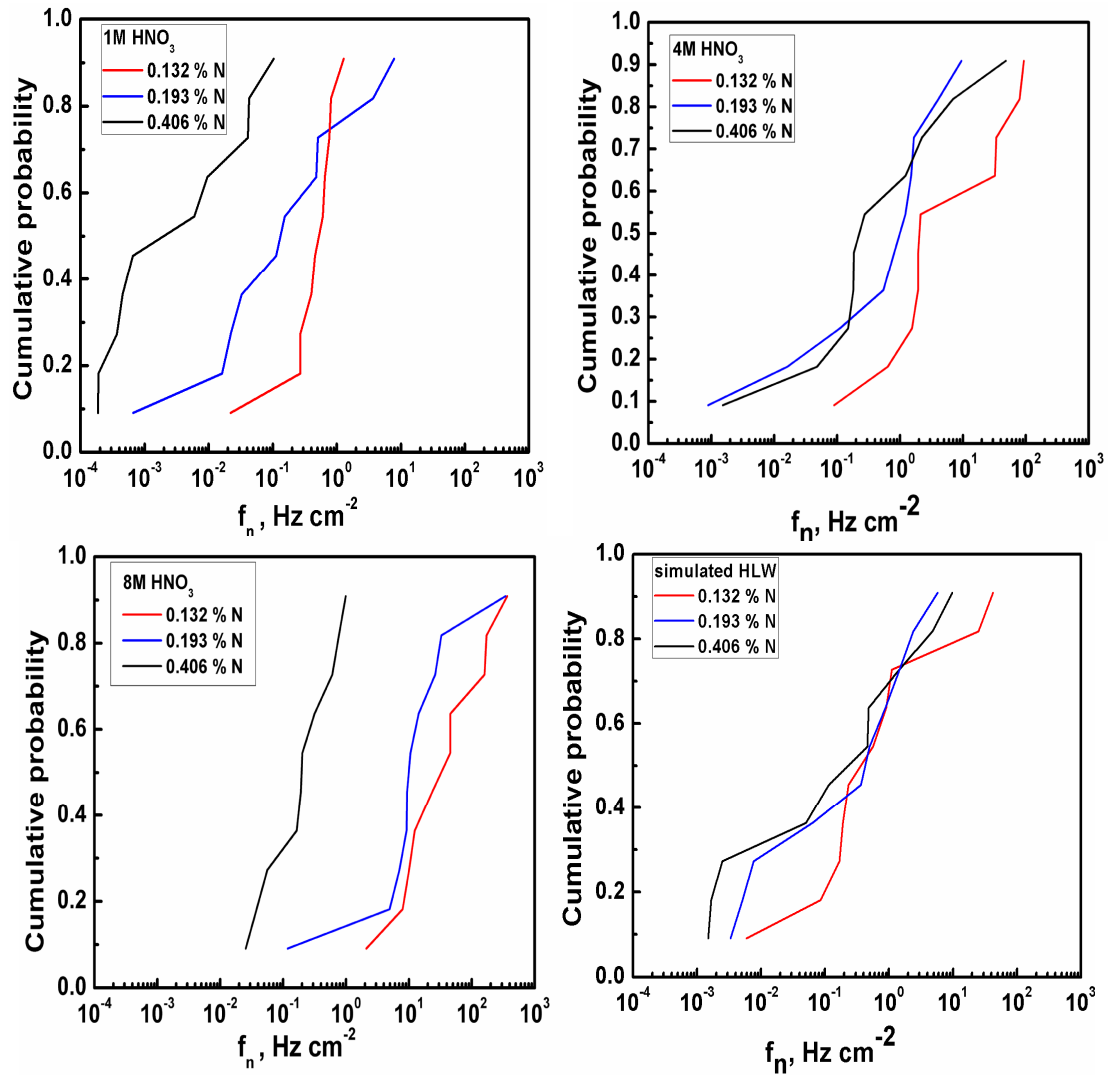


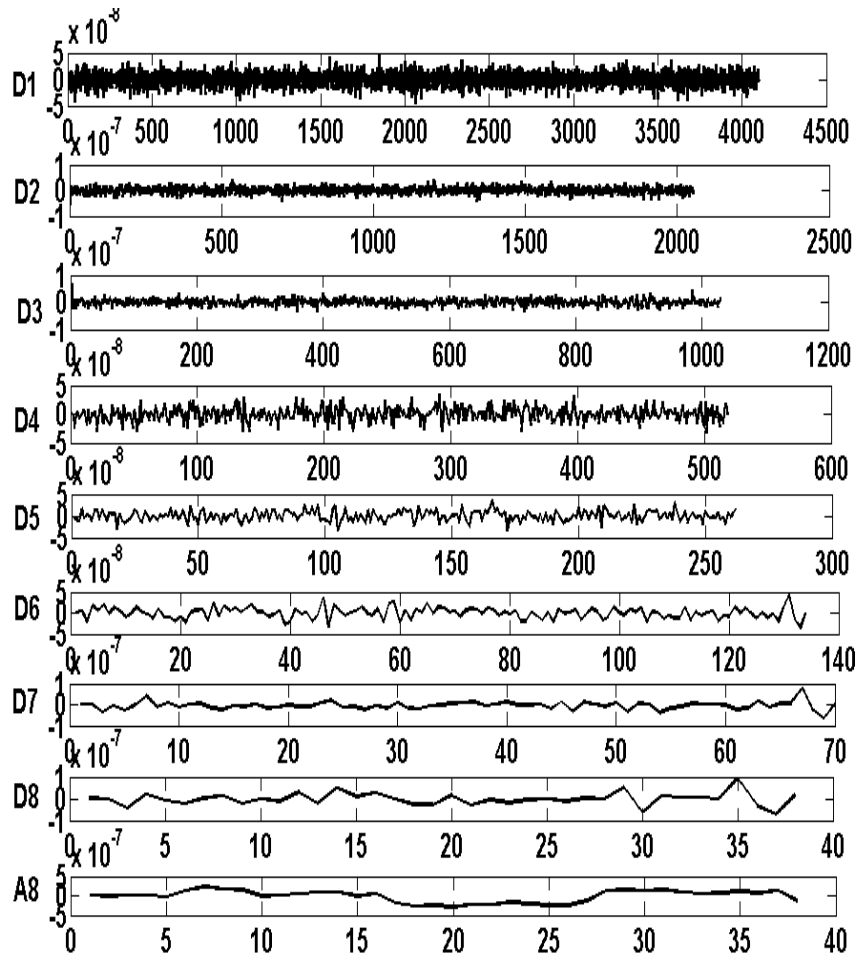
**Figure 5.19** Cumulative probability plots representing the distribution of frequencies for the three nitrogen containing stainless steels in  $\text{HNO}_3$  and simulated HLW medium.

The frequency of distribution was found to range from 0.09 - 93 Hz/cm<sup>2</sup> , 0.0009 – 9.5 Hz/cm<sup>2</sup> and 0.0016 – 48 Hz/cm<sup>2</sup> for 0.132 % N, 0.193% N and 0.406 % N in 4M HNO<sub>3</sub> respectively and from 2-366 Hz/cm<sup>2</sup>, 0.12 Hz-342 Hz/cm<sup>2</sup> and 0.02-1 Hz/cm<sup>2</sup> in 8M HNO<sub>3</sub>. In simulated HLW solution, the frequency of events and hence the corrosion activity were found to decrease with increase in nitrogen content, in the lower cumulative probability region, until a value of 0.5. In the intermediate cumulative probability regime (0.5-0.7), the frequency of events showed lowest corrosion activity for the stainless steel with highest nitrogen content, while the two lower nitrogen stainless steels show similar corrosion activity. In the higher cumulative probability regime of 0.7 and above, the corrosion activity was found to decrease as nitrogen content increased from 0.132 % to 0.406 % , nevertheless the corrosion activity of the stainless steel with 0.193 %N was found to be the least. From the results of the shot noise analysis, it can be appreciated that except for minimal discrepancies, a direct correlation could be explained between nitrogen content and corrosion activity. Although noise resistance and noise impedance well explained the decrease in corrosion activity with increase in nitrogen content, a direct correlation between nitrogen content and corrosion activity was obtained from shot noise analysis.

### ***5.3.5 Wavelet analysis***

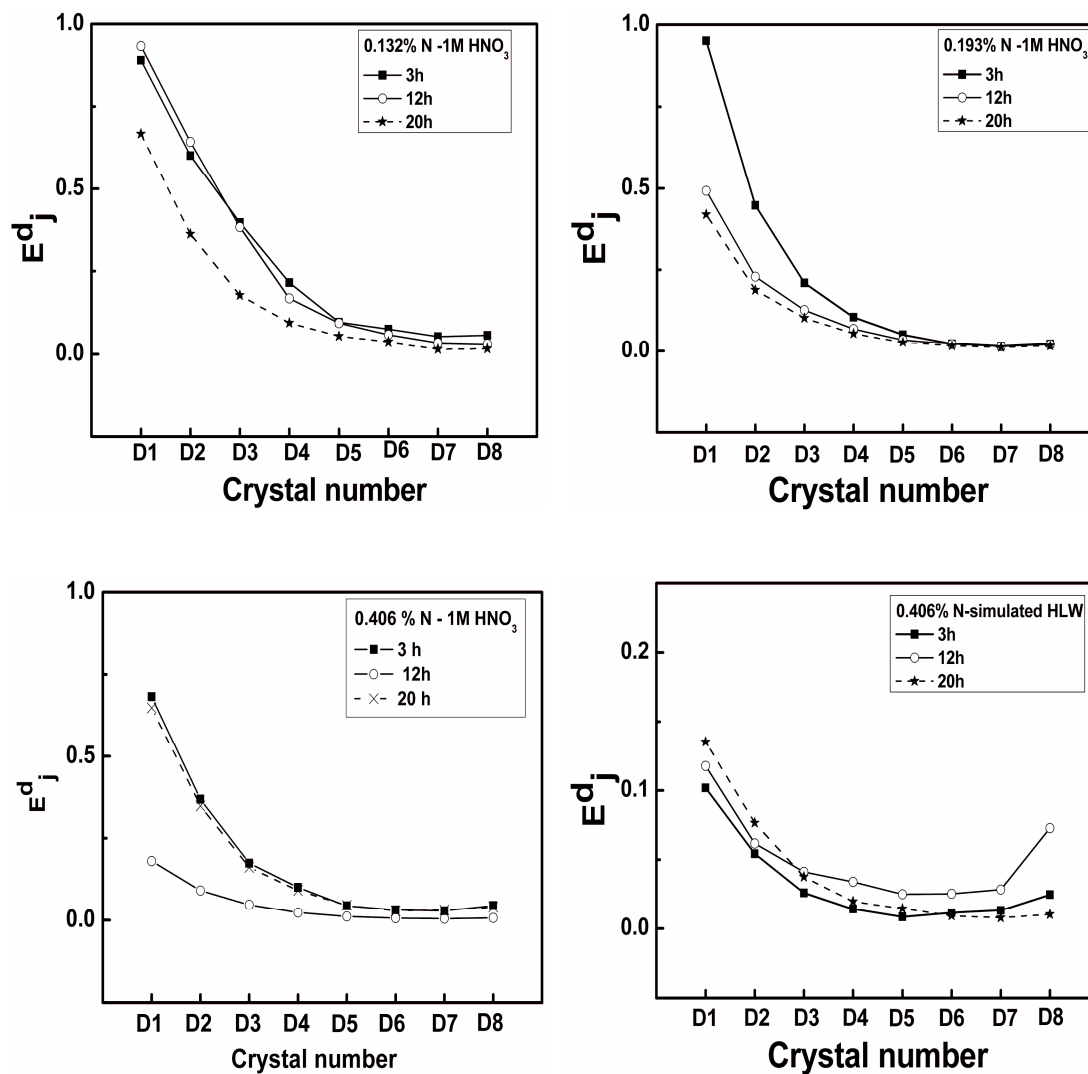
Wavelet analysis was used to derive mechanistic information about the processes occurring on the surfaces of the nitrogen containing stainless steels. Figure 5.20 represents a typical representation of the decomposition of the current – time record of the stainless steel containing 0.406% N into the details (or crystals, D1 to D8) and smoothed signal (A8), using Daubechies (db4) wavelet. The position of the maximum

relative energy distribution of a crystal has been associated with dominant process contributing to the signal. The energy distribution plots for an eight level decomposition can be described by three regions [115, 117, 169].



*Figure 5.20 Typical representation of eight level decomposition using Daubechies 4 wavelet, of the current noise-time record of the stainless steel containing 0.406% N in 1 M HNO<sub>3</sub>, 20 h after immersion.*

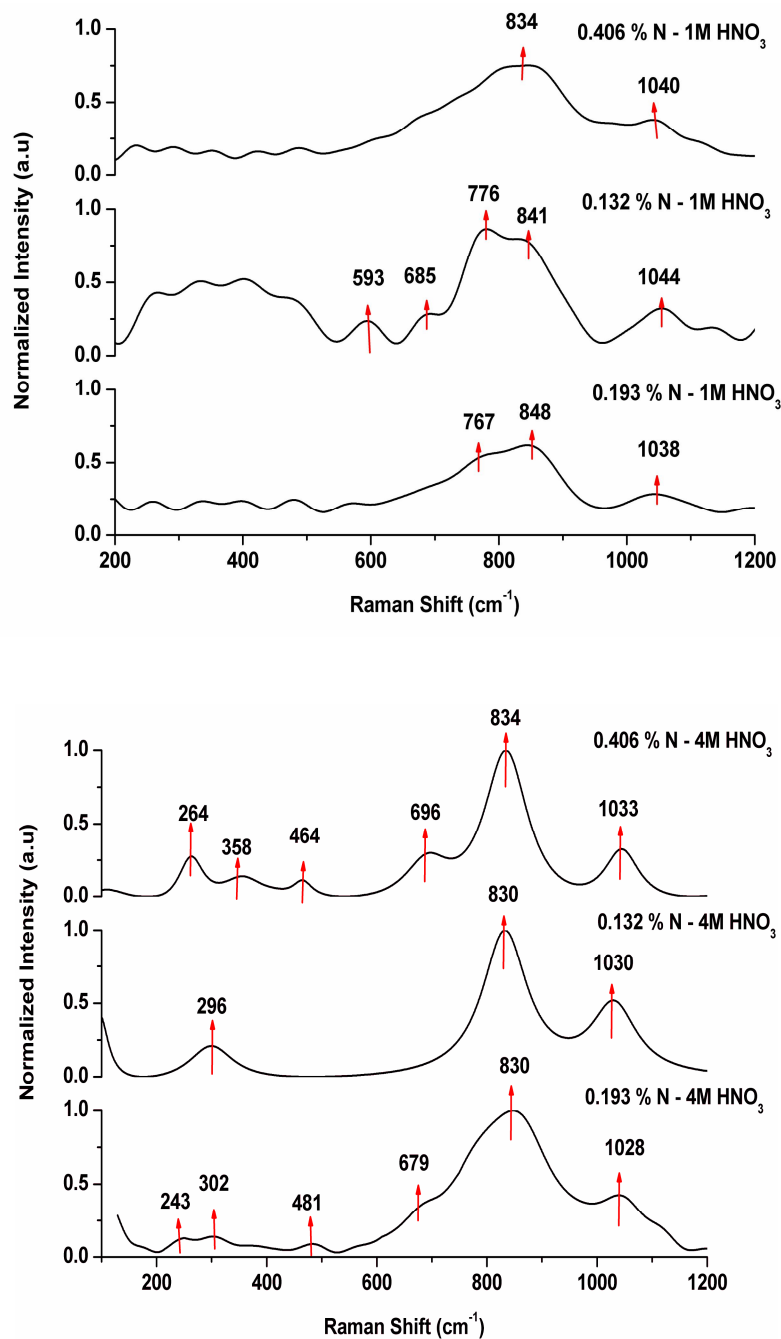
D1-D3 are the smaller time scale crystals, D3-D6 are the medium time scales and D6-D8 crystal are the large time scale crystals. Processes such as metastable pitting have the energy deposited on D1-D3, while repassivation/growth of pits are associated with D3-D6 and stable pitting have the energy on D7-D8. Lafront et al [120] in their study on copper anode passivation in sulphuric acid medium by EN measurements have demonstrated that the electrode passivation is dominated by short time scale process and the energy accumulated mainly on D3 crystals. Li Jian et al [67] have reported maximum energy deposition on D3-D5 crystal, for passivation process. The energy distribution plots of the current noise for the nitrogen containing stainless steels in  $\text{HNO}_3$  and simulated HLW were found to have the energy accumulated on crystals D1, D2, D3, D4 and the maximum contribution is located on D1 crystal, which is the shortest time scale crystal. This is in agreement with the time record of current transients obtained during passivation of austenitic stainless steels [21, 108, 81, 143] as also explained in section 5.3.2. A typical representation of the EDP of current noise for the three nitrogen containing 304L SS in 1M  $\text{HNO}_3$  is represented in Figure 5.21. Similar plots were obtained for the nitrogen containing stainless steels in all concentrations of the acid and in simulated HLW medium. The wavelet analysis indicated that the process occurring on the surface of the investigated nitrogen containing 304L SS in  $\text{HNO}_3$  and simulated HLW throughout the immersion period was predominantly passivation.



*Figure 5.21 Typical representation of energy distribution plots of current noise for the nitrogen containing stainless steel in 1 M  $\text{HNO}_3$ , showing maximum deposition of energy at D1 crystal, which is attributed to rapid current transients during passivation.*

#### 5.4 Passive film analysis by laser Raman spectroscopy

The Raman spectra of passive films formed on different nitrogen containing 304L SS in 1 M, 4 M, 8 M and simulated HLW are shown in Figure 5.22.





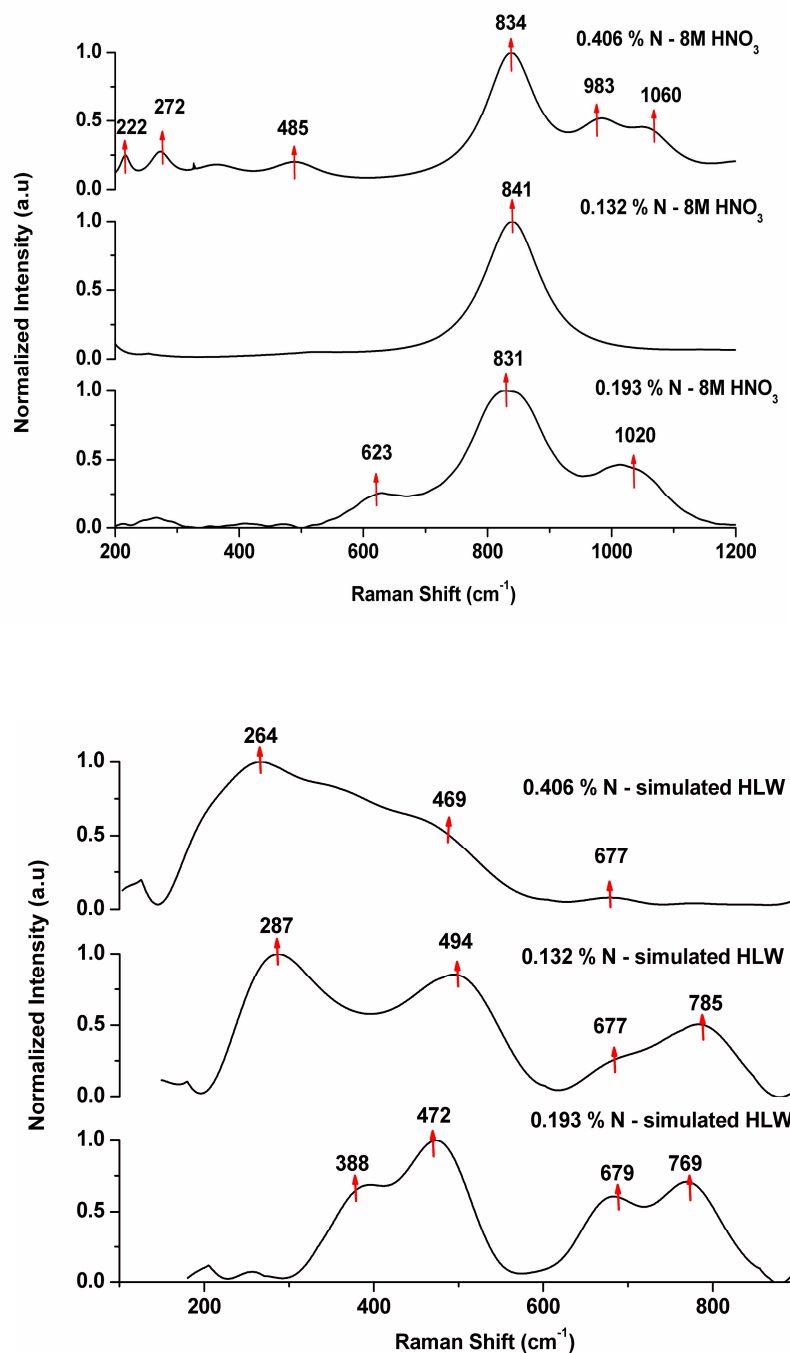


**Figure 5.22** Laser Raman spectra of passive films formed on the three nitrogen containing 304L SS in 1 M, 4 M, 8 M HNO<sub>3</sub> and simulated HLW. excitation wavelength = 488 nm, laser power = 10 mw, laser exposure time = 5s, Acquisitions = 20.

Laser Raman spectroscopic studies confirmed that the passive film mainly consisted of mixed oxides of iron and chromium. Frequencies were identified based on the literature [14,187]. The Raman assignments of the various peaks are shown in the Table 5.6.

<b>Band (cm<sup>-1</sup>)</b>	<b>Assignments</b>
Around 250-310	Fe-O stretching
Around 350	Cr <sub>2</sub> O <sub>3</sub>
450-490	Fe(OH) <sub>2</sub>
665-680	Fe <sub>3</sub> O <sub>4</sub> or $\gamma$ -Fe <sub>2</sub> O <sub>3</sub>
750-840	Fe –Cr Spinel
860-870	Cr (III) and Cr(VI) mixed oxides
900-970	CrO <sub>3</sub>
Around 1030-1050	Surface mono and poly chromates

***Table 5.6 Raman assignments corresponding to the various peaks***

The composition of passive film should consists of oxides, hydroxides, oxy hydroxides of Fe, Cr. All the Raman spectrum showed the presence of iron oxides, hydroxides, Fe-Cr spinel and chromium (VI) oxides. However, distinct peaks around 750-850 cm<sup>-1</sup> were obtained due to the formation of stable spinel oxides irrespective of their passivation in

different concentrations of  $\text{HNO}_3$  medium. Shifts in spectral positions were observed due to surface stresses and heterogeneities. The film contained mainly Fe-Cr spinel oxides. In 4 M  $\text{HNO}_3$  passivated specimens, Fe-O stretching and  $\text{Fe}(\text{OH})_2$  were observed. From the Raman analysis, it was observed that the oxide film formed on 4 M  $\text{HNO}_3$  passivated specimen was stable when compared to other specimens. The films of 1 M  $\text{HNO}_3$  passivated samples were found to be amorphous and the spectra obtained were broad due to the overlapping of various frequencies and intensities were also lesser than that of 4M  $\text{HNO}_3$  passivated specimens. The intensity of the Raman features of 8 M  $\text{HNO}_3$  passivated samples was lesser in their magnitude when compared to 4 M  $\text{HNO}_3$  passivated samples. One common aspect in 1 M, 4 M and 8 M  $\text{HNO}_3$  passivated specimens is the presence of spinel oxide phase around  $750\text{-}840\text{ cm}^{-1}$ . This phase was completely disturbed in HLW samples. However, dominant Fe-O stretching due to  $\gamma\text{-Fe}_2\text{O}_3$ ,  $\text{Fe}_3\text{O}_4$  and  $\text{Fe}(\text{OH})_2$  were obtained. Also, the intensities of those peaks were remarkably lesser than those obtained in 1 M, 4 M and 8 M  $\text{HNO}_3$  concentrations. This was probably due to the destruction of passive film and formation of iron corrosion products. The presence of aggressive ions in HLW might have stimulated the corrosion process and damaged the passive film structure.

### ***5.5 Conclusions***

Potentiodynamic anodic polarization experiments carried out on forged and rolled nitrogen containing stainless steels in nitric acid medium showed that the steels possessed good corrosion resistance (1 M, 4 M, 6 M) under ambient and elevated temperatures of the acid. All the hot rolled nitrogen containing stainless steel alloys exhibited a marginal improvement in corrosion resistance in nitric acid medium when compared to the forged

stainless steel alloys of the same composition. Increase in nitrogen content of the alloys showed no discernable difference in the corrosion property in nitric acid medium owing to the spontaneous formation of chromium oxide passive film in nitric acid medium.

Increasing the nitrogen content upto 0.193% was found to be beneficial in enhancing the pitting resistance of the forged stainless steels, beyond which the pitting resistance deteriorated. To the contrary, an increase of nitrogen content till 0.406% substantially improved the pitting resistance of the rolled stainless steels. Hot rolling and annealing resulted in partial dissolution of the primary precipitates such as manganese rich and chromium nitride precipitates, thereby, reducing the number of pit initiation sites, as well as, enriching the stainless steel matrix with nitrogen.

As the influence of nitrogen on the corrosion property of the three stainless steels in nitric acid medium could not be evidenced by potentiodynamic polarization technique, an attempt was made to derive information on the same aspect by electrochemical noise technique. From the results of the investigations carried out on the nitrogen containing stainless steels in nitric acid and simulated high level waste medium, the following inferences could be derived. The stainless steels were found to exhibit good corrosion resistance in  $\text{HNO}_3$  and simulated HLW medium, as evidenced by the high noise resistance and spectral noise resistance. In addition, the two parameters were found to show an inverse relation with corrosion activity and an increase in nitrogen content of the stainless steels was found to decrease the corrosion activity in  $\text{HNO}_3$  and simulated HLW medium as well. It was further found that  $R_{\text{sn}}^0$  obtained from spectral analysis tracked  $R_n$  obtained from statistical analysis. From shot noise analysis, it was found that the characteristic frequency decreased with increase in nitrogen content and the frequency of

distribution shifted towards lower frequency as nitrogen content increased. Except for a couple of disagreements, a direct correlation between nitrogen content and corrosion activity was established by shot noise analysis. In addition, the frequency of distribution was found to shift towards higher frequency with increase in concentration implying higher corrosion activity at higher concentration. EN analysis indicated better passive film stability in 4 M  $\text{HNO}_3$  compared to 1 M and 8 M  $\text{HNO}_3$ . The energy distribution plots of current noise were found to be useful in deriving mechanistic information about the processes happening on the electrode surface. LRS results inferred a stable passive film in 4 M  $\text{HNO}_3$  when compared to 1 M and 8 M  $\text{HNO}_3$  and an unstable structure in simulated HLW. LRS results were found to be in agreement with EN results. From the results of the investigation, it could be inferred that the three identical electrode configuration electrochemical noise probe could monitor the corrosion activity of the nitrogen containing stainless steels in reprocessing and waste storage conditions. The effect of nitrogen on the corrosion property of the nitrogen containing stainless steels in reprocessing and waste storage medium could be established by the three electrode probe. Increase in nitrogen content of the steel resulted in improved passivation behavior of 304L SS in these environments as inferred from an increase in the noise resistance and spectral noise resistance and decrease in the characteristics frequency.

Austenitic stainless steel of type 304L SS is the major structural material for nuclear reprocessing and waste storage plants. Type 304L SS is continuously exposed to the process medium under operational conditions. During long term service, the process medium containing nitric acid, corrosion products, fission products together with radioactive heat, can elevate the corrosion potential of the most resistant 304L SS material towards transpassive region, where the highly tenacious and protective chromium oxide passive film ruptures, subjecting the material to corrosive environment leading to corrosion degradation. In this regard, towards developing electrochemical noise as useful corrosion monitoring technique for Indian nuclear reprocessing and high level waste storage plant applications, a three identical electrochemical noise monitoring probe fabricated from the structural material was designed. The implementations of online monitoring for applications in these areas require establishing the technique offline. Hence, laboratory scale experiments were carried out using the electrochemical noise probe to monitor the corrosion activity of 304L SS in environments simulating reprocessing and waste storage plant conditions. The forthcoming section presents the summary and conclusions of the investigations carried towards meeting the theme of the work.

---

### ***6.1 Electrochemical noise monitoring during pitting corrosion of 304L SS***

The study comprised of electrochemical noise monitoring of 304L SS during pitting corrosion using the three identical electrode configuration. The presence of chloride ions in reprocessing medium or high level waste, by ingress of chloride from the water or acid, is detrimental, as adsorption and penetration of these ions through the protective

passive film could lead to local breakdown of passive film, promoting the formation of pits, the propagation and growth of which is catastrophic. The objective of the study was to obtain electrochemical noise data using the three identical electrode probe made of 304L SS, and derive mechanistic information of the processes occurring on the material surface exposed to environments conducive for pitting to occur. The three identical electrochemical noise probe made of 304L SS was immersed in 0.05M FeCl<sub>3</sub> for 24h of immersion and electrochemical current and potential noise was monitored. The acquired data was visually examined and then analyzed by statistical, spectral and wavelet analysis.

***The following conclusions were derived from the study:*** The random high amplitude fluctuations observed during initial immersion period became more defined as corrosion progressed, and distinct potential and current spikes indicative of pitting attack were obtained. The roll off slope evaluated from the corresponding power spectral plots corroborated with pitting attack. Statistical evaluation of the time record was carried out and parameters such as localization index, standard deviation of potential noise as well as the kurtosis of potential and current noise corroborated with pitting attack. Energy distribution plot (EDP) obtained from wavelet analysis was found to provide useful information on the progress of corrosion. From the EDP, it was observed that metastable pitting, propagation and repassivation of pits and stable pitting occurred on the specimen surface, during initial stages of immersion and the dominant process was propagation and repassivation of pits. With time of immersion, metastable pitting was suppressed. The corrosion mechanism comprised of propagation / repassivation of pits and stable pitting, the latter being most predominant and the former becoming insignificant with time.

Although electrochemical noise time domain and power spectral analysis provided an insight on the corrosion mechanism as a whole, wavelet analysis provided intrinsic details on the processes occurring on the specimen surface as corrosion progressed. The three electrode EN probe was established to monitor the progress of pitting corrosion of 304L SS.

## ***6.2 Electrochemical noise monitoring of 304L SS in nitric acid and simulated nuclear high level waste medium :***

The objective of the study is to establish electrochemical noise resistance (a parameter derived from the EN-time records) as a monitoring tool to reflect the corrosion activity of 304L SS in various environments simulating reprocessing and waste storage conditions. For this purpose, electrochemical noise signals were acquired from 304L SS under various microstructural conditions (solution annealed and sensitized) in nitric acid medium of varying concentration ( 4 M, 8 M, 12 M ) and temperature (298 K, 323 K), and in simulated HLW, under naturally corroding conditions, for 250 h of immersion.. The EN records were visually examined for mechanistic information and statistically evaluated to obtain noise resistance which was used to determine the corrosion activity.

***The following conclusions were derived from the study:*** EN-time records of 304L SS in nitric acid medium revealed passivation process during the monitoring period, under all conditions studied, except for the sensitized specimen in 4M nitric acid (323 K) that showed localized attack. The observations were confirmed by post experimental optical micrographs. The noise resistance showed an increase with increase in concentration of nitric acid for solution annealed 304L SS at 298 K and 323 K electrolyte temperature implying higher corrosion activity at higher concentration. Increase in temperature did



not appreciably increase the corrosion activity. For the sensitized 304L SS, the corrosion activity was found to be comparable in 4 M, 8 M and 12 M nitric acid at 298 K. An appreciable increase in corrosion activity occurred in 8M nitric acid when the electrolyte temperature was increased to 323 K. The corrosion activity was found to be higher for sensitized specimen when compared to solution annealed 304L SS. In simulated HLW under ambient conditions, the EN time records of the solution annealed 304L SS showed regions of depassivation by the ions present in the waste solution. The decrease in noise resistance for the sensitized specimen in simulated HLW (323K) was found to be marginal when compared to that of the solution annealed specimen implying comparable corrosion activity for the solution annealed and sensitized specimen during the period of measurement. The high noise resistance for these systems could be attributed to passive state which the system exhibited throughout the monitoring period, nevertheless the variations in the noise resistance in the environments is because of variations in the dissolution rates from the passive film surface. Electrochemical noise resistance was found to be useful in discerning the variations in the corrosion activity even for systems that exhibited low corrosion activity. From the results of the present study, it was found that an inverse relationship between EN resistance and corrosion activity could be established for 304L SS in nitric acid and simulated high level waste.

### ***6.3 Effect of nitrogen on corrosion behaviour of nitrogen containing 304L SS in nitric acid medium:***

Towards developing materials for nuclear reprocessing and waste storage applications, nitrogen containing austenitic stainless steels stand as candidate materials by virtue of their high mechanical property and corrosion resistance. Three 304L SS containing

0.132% N, 0.193% N , 0.406% N received from Bulgarian Academy of Science under the Indo-Bulgarian collaboration programme were tested for its corrosion resistance in nitric acid and simulated high level waste medium by potentiodynamic anodic polarization and electrochemical noise technique. The objective was also to establish the three electrode electrochemical noise probe made of these materials to monitor the corrosion activity in reprocessing and waste storage medium and also to obtain information on the effect of nitrogen on the corrosion property by electrochemical noise. *The following are the conclusions derived from the study:* Corrosion studies on three nitrogen containing stainless steels (under forged and rolled conditions) in nitric acid and simulated HLW medium inferred superior resistance for the rolled steels compared to the forged steel in acid and chloride medium, but no inferior influence of nitrogen on the corrosion property was noticed from potentiodynamic anodic polarization studies in acid medium.

It was possible to establish the three identical electrode noise probe to monitor the surface activity of the nitrogen containing 304L SS in nitric acid and simulated HLW medium. The positive effect of nitrogen in acid medium was evidenced by electrochemical noise analysis. Electrochemical noise time record reflected passivation process for these steels in these environments, which was substantiated by statistical, spectral, wavelet and shot noise analysis. Noise resistance, spectral noise resistance increased while the frequency of events decreased with increase in nitrogen content. The energy distribution plots from wavelet analysis were useful in determining the corrosion mechanism.

#### ***6.4 Scope for future work***

1. The EN probe has been established in reprocessing and simulated HLW medium under static conditions, the implementation of the same under plant operating conditions would be one of the scope for future studies.
2. To establish electrochemical noise monitoring of 304L SS welds in reprocessing and waste storage medium. Type 304L SS welds are subjected to sensitization in the heat affected zone, during fabrication. During long term exposure in reprocessing and waste storage medium, the sensitized regions are prone to intergranular corrosion. Electrochemical noise technique could be used to monitor intergranular corrosion of 304L SS welds. It would be of interest to establish correlation between various degree of sensitization using electrochemical noise measurements (in nitric acid medium) and electrochemical potentiokinetic reactivation studies.
3. To establish the role of various inclusions like MnS and Al<sub>2</sub>O<sub>3</sub> on the electrochemical noise behavior to understand the tunnel corrosion effect.
4. To establish electrochemical noise measurements to study the variations of porosity and other defects of coated 304L SS.
5. To study the effect of different compositions of HLW generated for different burn up, under prolonged storage conditions.

## ***References***

1. J Homi Bhabha, N B Prasad, A Study of the Contribution of Atomic Energy to a Power Programme in India, in: Proceedings of the Second United Nations International Conference on the Peaceful Uses of Atomic Energy, Geneva, September, 1958, pp.89.
2. Rajamani Natarajan, Baldev Raj, Journal of Nuclear Science and Technology 44 (3) (2007) 393.
3. Baldev Raj, U.Kamachi Mudali, Progress in Nuclear Energy 48 (2006) 283.
4. K. Raj, K.K. Prasad, N.K. Bansal, Nuclear Engineering and Design 236 (2006) 914.
5. S.D. Misra, Energy Procedia 7 (2011) 474.
6. H.A.C McKay, J.H Miles, J.L Swanson, The Purex process, in: Science and Technology of Tributyl Phosphate, W.W Schulz, L.L Burger, J.D Navratil , K.P Bender (Eds.), CRC Press: Boca Raton, Florida, USA, 1990, Vol. 3, pp. 1 - 9.
7. D.D Sood, S.K Patil, Journal of Radio Analytical Nuclear Chemistry Articles 203 (2) (1996) 547.
8. Baldev Raj, H.S. Kamath, R. Natarajan, P.R. Vasudeva Rao, Progress in Nuclear Energy 471 (4) (2005) 369.
9. K Raj, M.T Samuel, Modified pot glass process for vitrification of high level liquid waste-process engineering aspects, in: Proceedings of the XIV International Congress on Glass, Vol. 2, New Delhi, India, 1986, pp.399.
10. A.Palamalai, G.R.Balasubramanian, Trans. SAEST 19 (1984) 89.
11. U. Kamachi Mudali, R.K.Dayal, J.B.Gnanamoorthy, Journal of Nuclear Materials 203 (1993) 73.

12. U. Kamachi Mudali, A. Ravishankar, S. Ningshen, Girija Suresh, Ravikumar Sole, K. Thyagarajan, *Energy Procedia* 7 (2011) 468.
13. Girija Suresh, V.R.Raju, U.Kamachi Mudali, R.K.Dayal, *Corrosion Engineering Science and Technology* 38 (4) (2003) 309.
14. S.Ningshen, U.Kamachi Mudali, S. Ramya, Baldev Raj, *Corrosion Science* 53 (1) (2011) 64.
15. Girija Suresh, T.Nandakumar, C.Mallika, U.Kamachi Mudali, L.Nenova, C.Andreev, Corrosion resistance of nitrogen containing hot rolled 304LN in nitric acid medium, *Transactions of the Indian Institute of Metals* (in press).
16. N.Padhy, S.Ningshen, B.K.Panigrahi, U.Kamachi Mudali, *Corrosion Science*, 52 (2010) 104.
17. Girija Suresh, N.Parvathavarthini, U.Kamachi Mudali, Baldev Raj, Ch Andreev, L Nenova, *Steel Tech* 4 (4) (2010) 77.
18. Pradeep Samantaroy, Girija Suresh, Ranita Paul, U. Kamachi Mudali, Baldev Raj, *Journal of Nuclear Materials* 418 (2011) 27.
19. Pradeep Kumar Samantaroy, Girija Suresh, U. Kamachi Mudali, *Corrosion* 68 (2012) 046001-1-046001-13.
20. Pradeep Kumar Samantaroy, Girija Suresh, N. G. Krishna, U. Kamachi Mudali, *Journal of Materials Engineering and Performance* 22 (4) (2013) 1041.
21. Girija Suresh, U.Kamachi Mudali, Baldev Raj, *Journal of Applied Electrochemistry* 41, (2011) 973.

22. U.Kamachi Mudali, Baldev Raj, High Nitrogen Steel and Stainless Steels: Manufacturing properties and Applications, Narosa Publication, New Delhi, India, 2004.
23. M.O. Speidel, in: Proceedings of the 1<sup>st</sup> International Conference of High Nitrogen Steels, The Institute of Metals, J.Foct, A.Hendry (Eds.), London, 1989, pp. 92.
24. J.Foct, Future Developments and Applications of Nitrogen-Bearing Steels and Stainless Steels, in: High Nitrogen Steels and Stainless steels: Manufacturing properties and Applications, U.Kamachi Mudali, Baldev Raj (Eds.), Narosa Publications, New Delhi, India, 2004, pp. 256.
25. J.H.Andrew, "Nitrogen in iron", Carnegie Scholarship Memories 11 (1912) 236.
26. H.H Uhlig, Trans Am Soc. Met 30 (1942) 947.
27. U.Kamachi Mudali, R.K.Dayal, J.B.Gnanamoorthy, P.Rodriquez, Material Transactions JIM, 37 (1996) 1568.
28. U.Kamachi Mudali, R.K.Dayal, T.P.S.Gill, J.B.Gnanamoorthy, Werkstoffe and Korrosion 37 (1986) 637.
29. Girija Suresh, U.Kamachi Mudali, V.Shankar, R.K.Dayal, Transactions of Indian Institute of Metals 55 (5) (2002) 439.
30. N.Parvathavarthini, R.K.Dayal, J.B.Gnanamoorthy, Journal of Nuclear Materials 208 (1994) 251.
31. I.Olefjord, L.Wegrelius, Corrosion Science 38 (1996) 1203.
32. U.Kamachi Mudali, S.Ningshen, Nitrogen addition and localized corrosion behavior of austenitic stainless steels, in: Advances in Stainless Steel, Baldev Raj et al. (Eds.), Universities press (India) Pvt.Ltd., India, 2010, pp.561.

33. N.Parvathavarthini, U.kamachi Mudali, Liliyana Nenova, Chavdar Andreev, Baldev Raj, Metallurgical and Materials Transaction A 43 (2012) 2069.
34. S.Girija, U.Kamachi Mudali, C.Andreev, L.Ninova, Baldev Raj, Corrosion (2012) 922.
35. <https://www.honeywellprocess.com/library/support/Public/Documents/ChemEngJune07.pdf>
36. Ha-Won Song, Velu Saraswathy, International Journal of Electrochemical Science 2 (2007)1.
37. <http://corrosion-doctors.org/MonitorBasics/Types.htm>.
38. Fei Kuang , Jinna Zhang , Changjun Zou, Taihe Shi, Yang Wang, Shihong Zhang, Haiying Xu, Recent Patents on Corrosion Science 2 (2010) 34.
39. A.J.Sedriks, in: Corrosion of Stainless steels, 2<sup>nd</sup> ed, Wiley-Interscience publication, New York.
40. S. Ningshen, U. Kamachi Mudali, Baldev Raj, Corrosion Reviews 27 (2009) 493.
41. F.Mansfeld, H.ShilGreene, C.H.Tsai, Analysis of EIS Data for Common Corrosion Processes, Electrochemical impedance analysis and interpretation, ASTM STP 1188, 1993.
42. H. Chen, "Evaluation of Commercial Coating by EIS", CORROSION /94, (Houston, TX: NACE, 1994) Paper no.437.
43. W.P.Iverson, Journal of Electrochemical Society 115 (6), 617 (1968).
44. J. L. Dawson, Electrochemical Noise Measurement: The Definitive In-Situ Technique for Corrosion Applications, in: Electrochemical Noise Measurement for Corrosion

- Applications, J.R. Kearns, J. R. Scully, P. R. Roberge, D. L. Reichert, J. L. Dawson (Eds.), ASTM, Philadelphia, 1996, pp. 3.
45. J.R. Kearns, J. R. Scully, P. R. Roberge, D. L. Reichert, J. L. Dawson, in: Electrochemical Noise Measurements for Corrosion Applications, ASTM STP 1277 ASTM, Philadelphia, 1996.
  46. R. A. Cottis, Corrosion 57 (2001) 265.
  47. U. Bertocci, J. Kruger, Surface Science 101 (1980) 608.
  48. M.G. Pujar, Girija Suresh, U. Kamachi Mudali, Workshop on Advances in Corrosion Testing, Indian Institute of Metals, Kalpakam Chapter, India, 2000, pp. 4.1
  49. S. Girija, U. Kamachi Mudali, V.R. Raju, Baldev Raj, Corrosion Reviews 23 (2-3) (2005) 107.
  50. F. Mansfeld, H. Xiao, Electrochemical Noise and Impedance Analysis of Iron in Chloride Media, in: Electrochemical Noise Measurement for Corrosion Application, J.R. Kearns, J. R. Scully, P. R. Roberge, D. L. Reichert, J. L. Dawson (Eds.), ASTM, Philadelphia, 1996, pp. 59.
  51. Michael T. Terry, Glenn L. Edgemon, Ronald E. Mizia, Development and Deployment of Advanced Corrosion Monitoring Systems for High-Level Waste Tanks, in: WM'02 Conference, February 24-28, 2002, Tucson, AZ- pg. 1.
  52. Patrick J. Pinhero, Tedd E. Lister, Ronald E. Mizia, Development of an Electrochemical Noise Surveillance System for Determining Compliance of INEEL High Level Waste Tanks to Corrosion Standards, Idaho National Engineering & Environmental Laboratory, CORROSION 2003, NACE International, March, 2003, San Diego Ca (Doc ID 03406).



53. G. L. Edgemon, Electrochemical Noise Based Corrosion Monitoring at the Hanford Site: Third Generation System Development, Design and Data, CORROSION/2001, paper 01282.
54. G.L.Edgemon, M.J.Danielson, G.E.C.Bell, Journal of Nuclear Materials 245 (1997) 201.
55. C.A.Loto, International Journal of Electrochemical Science 7 (2012) 9248.
56. D.D. Macdonald, Journal of Electrochemical Society 139 (1992) 3434.
57. P.R.Roberge, R.Beaudoin, V.S.Sastri, Corrosion Science 29 (10) (1989) 1231.
58. G.T.Burstein, P.C.Pistorious, S.P.Mattin, Corrosion Science 35 (1993) 57.
59. Hladky, J.L.Dawson, Corrosion Science 21 (4) (1981) 317.
60. ASTM G5-94-(Reapproved 2004), Standard Reference Test Method for Making Potentiostatic and Potentiodynamic Anodic Polarization Measurements, ASTM International.
61. R.A.Cottis, C.A.Loto, Corrosion 46 (1990) 12.
62. N.Bastos, F.Huet, R.P.Nogueira, P.Rousseau, Journal of Electrochemical Society 147 (2) (2000) 671.
63. U.Bertocci, J.Frydman, C.Gabrielli, F.Huet, M.Keddam, Journal of Electrochemical Society 145 (9) (1998) 2780.
64. F.Huet, U.Bertocci, C.Gabrielli, M.Keddam, Proc.Topical Research Symp.NACE, 1997, pp.11.
65. U.Bertocci, F.Huet, R.P.Nogueira, P.Rousseau, Corrosion 58 (2002) 337.
66. A.M.Homborg, T.Tinga, X.Zhang, E.P.M Van Westing, P.J.Oonincx, J.H.W. de Wit, J.M.C.Mol, Electrochimica Acta 70 (2012) 199.

67. Li Jian, Kong Weikang, Shi Jiangbo, Wang Ke, Wang Weikui, Zhao Weipu, Zeng Zhoumo, International Journal of Electrochemical Science 8 (2013) 2365.
68. Milton Martinez Luaces, Victor Martinez Luaces, Mauricio Ohanian, Trend-removal in Corrosion Processes using Neural Networks, in: Proceedings of the 5th WSEAS International Conference on Artificial Intelligence, Knowledge Engineering and Data Bases, Madrid, Spain, February 15-17, 2006, pp.248.
69. J. Y Huang, Y. B Qiu, X. P Guo, Corrosion Engineering, Science and Technology 45 (4) (2010) 288.
70. Y.J.Tan, S.Bailey, B.Kinsella, Corrosion Science 38 (1996) L286.
71. M. Ohanian, V. Martinez, G Guineo-Cobs, The Journal of Corrosion Science and Engineering 7 (2004).
72. F.Mansfeld, Z.Sun, C.H.Hsu, A.Nagiub, Corrosion Science 43 (2001) 341.
73. H. Ashassi-Sorkhabi, D. Seifzadeh, Journal of Applied Electrochemistry 38 (11) (2008) 1545.
74. R.A.Cottis, S.Turgoose, in: B.C.Syrett (Eds.), Corrosion Testing Made Easy- Electrochemical Impedance and Noise, (Houston, TX: NACE 1999).
75. R.A.Cottis, S.Turgoose, Material Science Forum 192-194 (1995) 663.
76. F.Mansfeld, Z.Sun, C.H.Hsu, Electrochimica Acta 46 (2001) 3651.
77. A.A.El-Moneim, Corrosion Science 46 (2004) 2517.
78. T.Okada, Journal Electrochemical Society 297 (1991) 349.
79. C. Gabrielli, M.Keddam Corrosion 48 (1992) 794.
80. Y.Cheng, J.Luo, M.Wilmott, Electrochimica Acta 45 (2000) 1763.

81. S.Girija, U.Kamachi Mudali, V.R.Raju, R.K.Dayal, H.S.Khatak, Baldev Raj, Material Science and Engineering A 407 (2005) 188.
82. D.A.Eden, D.G.John, J.L.Dawson, International Patent WO 87/07022, World intellectual property Organization, 1987.
83. D.A.Eden, K.Hladky, D.G. John, J.L.Dawson, CORROSION / 86, (Houston, TX: NACE, 1986) paper no. 274.
84. J.L. Dawson, D. M. Farrell, P.J.Aylott, K. Hladky, CORROSION / 89 (Houston, TX: NACE, 1989).
85. Yong-Jun Tan, Journal of Corrosion Science and Engineering vol 1, paper 11 (1999).
86. U.Bertocci, C.Gabrielli, F.Huet, M.Keddam, P.Rousseau, Journal of Electrochemical Society 144 (1997) 37.
87. G.P.Bierwagen, Journal of Electrochemical Society 141(1994) L 155.
88. J.F.Chen, W.F.Bogaerts, Corrosion Science 37(1995) 1839.
89. V. Brusamarello, A.Lago, C.V.Franco, Corrosion 56 (3) (2000) 273.
90. D.A.Eden, A.N.Rothwell, CORROSION / 92 (Houston, TX: NACE, 1992) Paper 292.
91. R.G.Kelly, M.E.Inman, J.L.Hudson, Analysis of Electrochemical Noise for Type 410 Stainless Steel in Chloride, in: Electrochemical Noise Measurements for Corrosion Applications, J.R. Kearns, J. R. Scully, P. R. Roberge, D. L. Reichert, J. L. Dawson (Eds.), ASTM STP 1277, ASTM, Philadelphia, 1996, pp.101.
92. D. Eden, "Electrochemical Noise - The first two octaves" CORROSION / 98 (Houston, TX: NACE, 1998) paper 386.
93. G Montespereelli, G Gusmano, Fluctuations and Noise Letters 4 (3) (2004) R39.

94. Y. Y. S h i, Z. Zhang, F.H. Cao, J.Q. Zhang, *Electrochimica Acta* 53 (2008) 2688.
95. S. Reid, G.E.C. Bell, G. L Edgemon, The use of Skewness, Kurtosis, and Neural networks for Determining Corrosion Mechanism from Electrochemical Noise Data,” *CORROSION / 98*, (Houston, TX: NACE, 1998) Paper 176.
96. K.Hladky, J.L.Dawson, *Corrosion Science* 22 (3) (1982) 231.
97. U.Bertocci, Y.Yang-Xiang, *Journal of Electrochemical Society* 131 (1984) 1011.
98. T.Fukuda, T.Mizuno, *Corrosion Science* 38 (1996) 1085.
99. M.G.Pujar, T.Anita, H.Shaikh, R.K.Dayal, H.S.Khatak, *International Journal of Electrochemical Sciences* 2 (2007) 301.
100. G. Bagley, The measurement and the analysis of electrochemical noise, Ph.D. thesis, Umist, 1998.
101. F. Mansfeld, H. Xiao, *Journal Electrochemical Society* 140 (1993) 2205.
102. P. Searson, J.L. Dawson, *Journal of Electrochemical Society* 135 (1988) 1908.
103. A.Legat, V.Dolecek, *Corrosion* 51 (4) (1995) 295.
104. P.R.Roberge, *Journal of Applied Electrochemistry* 23 (1993) 1223.
105. J.P. Burg, Maximum Entropy Spectral Analysis, in: proceedings of the 37<sup>th</sup> International SEG Meeting, 1967.
106. F.Mansfeld, L.T.Han, C.C.Lee, *Journal of Electrochemical Society* 143 (12) (1996) L286.
107. H.Xiao, F.Mansfeld, *Journal of Electrochemical Society* 141 (1994) 2332.
108. S.Girija, U.Kamachi Mudali, H.S.Khatak, Baldev Raj, *Corrosion Science* 49 (11) (2007) 4051.

109. R.A.Cottis, M.A.A.Al-Awadhi, H.Al-Mazeedi, S.Turgoose, *Electrochimica Acta* 46 (2001) 3665.
110. H.A.A.Al-Mazeedi, R.A.Cottis, *Electrochimica Acta* 49 (2004) 2787.
111. J.M.Sanchez-Amaya, R.A.Cottis, F.J.Botana, *Corrosion Science* 47 (2005) 3280.
112. U. Bertocci, F. Huet, *Corrosion* 51 (2) (1995) 131.
113. J.A.Wharton, R.J.K.Wood, B.G.Mellor, *Corrosion Science* 45 (2003) 97.
114. A.Abelle, M.Bethencourt, F.J.Botana, M.Marcos, J.M.Sanchez-Amaya, *Electrochimica Acta* 46 (2001) 2353.
115. A.Aballe, M. Bethencourt, F.J. Botana, M. Marcos, *Electrochimica Acta* 44 (1999) 4805.
116. A.Aballe, M. Bethencourt, F. J. Botana, M. Marcos, *Electrochemical Communication* 1 (1999) 266.
117. M. Shahidi, S. M. A. Hosseini, A. H. Jafari, *Electrochimica Acta* 56 (2011) 9986.
118. B.D.Malamud, D.L.Turcotte, *Journal of Statistical Planning and Inference* 80 (1999) 173.
119. <http://www.mathworks.in/help/wavelet/ref/wavedec.html>, (Mar.12, 2013)
120. A. M. Lafront, W. Zhang, E. Ghali, G. Houlachi, *Electrochimica Acta* 55 (2010) 2505.
121. M.T Smith, D.D.Macdonald, *Corrosion* 65 (7) (2009) 438.
122. MATLAB, WaveletToolbox™ 4 User's Guide, in *Wavelets: A new tool for signal analysis*, M.Misiti, Y.Misiti, G.Oppenheim, and J.-M.Poggi, Editors. 2008, The MathWork,Inc
123. V.A.Tyagi, *Electrochimica* 3 (1967) 1331.

124. V.A.Tyagi, *Electrochimica Acta* 16 (1971) 1674.
125. V.A.Tyagi, N.B.Lukjanchikova, *Surface Science* 12 (1968) 331.
126. G.C.Barker, *Journal of Electroanalytical Chemistry* 21 (1969) 127.
127. G.C.Barker, *Journal of Electroanalytical Chemistry* 39 (1972) 484.
128. M.Fleischmann, J.W.Oldfield, *Journal of Electroanalytical Chemistry* 27 (1970) 207.
129. G.Okamoto, T.Sugita, S.Nishiyama, K.Tachibana, T.Takaishi, *Proceedings of the 6<sup>th</sup> International Congress on Metal Corrosion, Australia, 1975.*
130. G. Blanc, C. Gabrielli, M. Keddam, *C.R. Hebd. Seances Acad. Sci.* 283C, 4 (1976) 107.
131. G. Blanc, C. Gabrielli, M. Ksouri, R. Wiart, *Electrochimica Acta* 23 (4) (1978) 337.
132. K.Hladky, *European Patent* 084404A3, *USA Patent* 455709, *Canadian Patent* 418938.
133. J.L.Dawson, K.Hladky, D.A.Eden, *Electrochemical Noise - Some New Developments in Corrosion Monitoring*, in: *Proceedings of the Conference UK Corrosion '83*, held Nov. 16-17, 1983 (Birmingham,UK: Institute of Corrosion, 1983) pp. 99.
134. U. Bertocci, J.L. Mullen, Y.-X. Ye, *Electrochemical Noise Measurements for the Study of Localized Corrosion and Passivity Breakdown*, in: *Proceedings. Passivity of Metals and Semiconductors*, held May 30-June 3, 1983 (Bombannes, France:Elsevier Science Publishers, 1983) pp. 229.
135. C. Gabrielli, F. Huet, M. Keddam, H. Takenouti, *Application of Electrochemical Noise Measurements to the Study of Localized and Uniform Corrosions*, in:

- Proceedings of the 8th European Congress on Corrosion, vol. 2, November. 19-21, 1985 (Paris, France: Centre Francais de la Corrosion, 1985) paper no. 37
136. G.Montesperelli, G.Gusmano, F.Marchioni, Corrosion 51 (8) (2000) 551.
137. Girija Suresh, U.Kamachi Mudali, Baldev Raj, Journal of Electrochemical Society India 57 (3/4) (2008) 77.
138. Y.F.Cheng, B.R.Rairdan J.L.Luo, Journal of Applied Electrochemistry 28 (1998) 1371.
139. A.Legat, V.Dolecek, Journal of Electrochemical Society 142 (6) (1995) 1851.
140. J.S.Stewart, D.B.Wells, P.M.Scott, D.E.Williams, Corrosion Science 33 (1) (1992) 73
141. T.Anita, M.G.Pujar, H.Shaikh, R.K.Dayal, H.S.Khatak, Corrosion Science 48 (2006) 2689-2710.
142. C.A.Loto, R.A.Cottis, Corrosion 45 (2) (1989) 136.
143. G.Gusmano, G.Montespareli, S.Pacetti, A.Petitti, A.Damco, Corrosion 53 (1997) 860.
144. M.Metikis-Hukovic, E.Stupnisek Lisac and M.Loncar, Journal of Electrochemistry 7 (3) (1991) 128.
145. W.P Iverson, L.F Heverly , Electrochemical Noise as an indicator of Anaerobic Corrosion, in: Corrosion Monitoring in Industrial Plants using Nondestructive Testing and Electrochemical Methods, G.C.Moran and P.Labine (Eds.), ASTM STP 908, American Society for Testing and Materials, Philadelphia, 1986, pp. 459.
146. Shinichi Magaino, Ryuichi Yamazaki, Journal of Electroanalytical Chemistry 305 (1991) 141.

147. C.Monticelli, F.Zucchi, F.Bonalla, G.Brunoro, A.Frignani, G.Trabanelli, Journal of Electrochemical Society 142 (1995) 405.
148. C.Monticelli, G.Brunoro, A.Frignani, G.Trabanelli, Journal of Electrochemical Society 139 (1992) 706.
149. S.Martinet, R.Durand, P.Ozil, P.Lebance, P. Blanchard, Journal of power sources 83 (1999) 93.
150. P.R.Roberge, E.Halliop, D.R.Lenard, J.G.Moores, Corrosion Science 35 (1-4) (1993) 213.
151. M.Stephenson, "Electrochemical Detection of sensitization in 5000 Series Aluminum Alloys" (MSc diss, UMIST, 2000).
152. F. Cappeln, N. J. Bjerrum, I. M. Petrushina, Journal of the Electrochemical Society 152 (7) (2005) B228.
153. K.Hladky, D.G.John, S.E.Worthington, D.Herbert, "corrosion monitoring of stainless steels under condensing nitric acid conditions", <http://www.khdesign.co.uk/acrobat/bnfl.pdf>.
154. L.H.Wang, J.J.Kai, C.H.Tsai, C. Fong, Journal of Nuclear Materials 258-263 (1998) 2046.
155. R.Van Nieuwenhove, Corrosion 56 (2) (2000) 161.
156. S.A.Reid, G.P.Quirk, M.Hadfield, Corrosion 99, San Antonio, TX, USA, April 25-30, NACE, pp.9.
157. R.J.K.Wood, J.A.Wharton, A.J.Steyer, K.S.Tan, Tribol.Internal. 36 (10) (2002) 631.



158. Gordon R. Holcomb, Bernard S Covino, David Eden, “State of Art review of electrochemical noise sensors, technical report US (DOE/ARC-TR-2001-16 ) 2001-09-01.
159. J.M. Sanchez-Amaya, M.Bethencourt, Gonzalez-Rovira, F.J.Botana, *Electrochimica Acta* 52 (2007) 6569.
160. Kyung-Hwan Na, Su-II Pyun, *Corrosion Science* 50 (2008) 248.
161. M.G.Pujar, N.Parvathavarthini, R.K.Dayal, S.Thirunavukarasu, *Corrosion Science* 51 (2009) 1707.
162. M.G.Pujar, R.P.George, P.Muralidharan, U.Kamachi Mudali, 67 (11) *Corrosion* (2011) 115004-1 - 115004-11.
163. E.Lewis, in: *Introduction to Reliability Engineering*, John Wiley and Sons (Eds.), New York, 1987.
164. Kyung-Hwan Na, Su-II Pyun, Hong-Pyo Kim, *Corrosion Science* 49 (2007) 220.
165. Sung-Woo Kim and Hong-Pyo Kim, *Electrochimica Acta* August 2009.
166. Tao Zhang, Xiaolan Liu, Guozhe Meng, Fuhui Wang, *Corrosion Science* 50 (2008) 3500.
167. J.J.Kim, *Materials Letters* 61 (18) (2007) 4000.
168. S.V.Muniandy, W.X.Chew, C.S.Kan, *Corrosion Science* 53(1) (2011) 188.
169. Chao Cai, Zhao Zhang, Fahe Cao, Zuoning Gao, Jianqing Zhang, Chunan Cao, *Journal of Electroanalytical Chemistry* 578 (2005) 143.
170. Bing Zhao, Jian – Hua Li, Rong-Gang Hu, Rong-Gui Du, Chang-Jian Lin, *Electrochimica Acta* 52 (2007) 3976.

171. A. Legat, J. Osredkar, V. Kuhar, M. Leban, Materials Science Forum, 289 – 292 (2) (1998) 807.
172. A. Legat, E. Govekar, Fractals 2 (1994) 241.
173. G. Corcoran, K. Sieradzki, Journal of the Electrochemical Society 139 (6) (1992) 1568.
174. D. Sazou, M. Pagitsas, C. Georgolios, Electrochimica Acta 37 (11) (1992) 2067.
175. M. Keddam, M. Krarti, C. Pallotta, Corrosion 43 (8) (1987) 454.
176. J. Stringer A. J. Markworth, Corrosion Science 35 (1–4) (1993) 751.
177. D. Bahena, I. Rosales, O. Sarmiento, R. Guardi, C. Menchaca, J. Uruchurtu, International Journal of Corrosion (volume 2011) doi:10.1155/2011/491564.
178. Anna Chen, Fahe Cao, Xiaining Liao, Wenjuan Liu, Liyun Zheng, Jianqing Zhang, Chunan Cao, Corrosion Science 66 (2013) 183.
179. M. Leban, V. Dolecek, A. Legat, Corrosion 56 (9) (2000) 921.
180. ASTM A262, “Standard Practice for Detecting Susceptibility to Intergranular Attack in Austenitic Stainless Steel,” (West Conshohocken, PA: ASTM International, 2002).
181. M. G. Fontana, in: Corrosion Engineering, 3<sup>rd</sup> ed, McGraw Hill publications, New Delhi, 1986.
182. U. Kamachi Mudali, R. K. Dayal, T. P. S. Gill, J. B. Gnanamoorthy, Corrosion NACE, 46 (1990) 454-460.
183. ASTM G108-94, Standard Test Method for Electrochemical Reactivation (EPR) for Detecting Sensitization of AISI Type 304 and 304L Stainless Steels.
184. A. P. Majidi, M. A. Streicher, Corrosion 40 (1984) 584.

185. N.Parvathavarthini, R.K.Dayal, Sensitization and testing for intergranular corrosion, in: H.S.Khatak, B.Raj (Eds.), Corrosion of Austenitic Stainless Steels. Mechanism, Mitigation and Monitoring, Narosa Publishing House, New Delhi, pp. 117-138.
186. Mojtaba Momeni, Mohammad Hadi Moayed, Ali Davoodi, Corrosion Science 52 (2010) 2653.
187. S. Ramya, T. Anita, H. Shaikh, R.K. Dayal, Corrosion Science 52 (2010) 2114.
188. D.L. Reichert, Electrochemical Noise Measurements for Determining Corrosion Rates, in: Electrochemical Noise Measurements for Corrosion Applications, J.R. Kearns, J. R. Scully, P. R. Roberge, D. L. Reichert, J. L. Dawson (Eds.), ASTM STP 1277, ASTM, Philadelphia, 1996, pp.79
189. U. Bertocci, F.Huet, R.P.Nogueira, Corrosion 59 (2003) 629.
190. B.M. Grafov, Russian Journal of Electrochemistry 41(2005) 113.
191. J. Smulko, K. J Darowicki, Journal Electroanalytical Chemistry 545 (2003) 59.
192. S. A. Reid, D. A. Eden, Assessment of Corrosion, A method and apparatus for using EN to assess corrosion, preferably with skewness and kurtosis analysis using neural nets, US 6, 264, 824 B1, 2001.
193. D.E. Williams, C. Westcott, M. Fleischmann, Journal of Electrochemical Society 132 (1985) 1796.
194. Mehdi Attarchi, Majid S.Roshan, Saleh Norouzi, S. K. Sadrnezhad, Journal of Electroanalytical Chemistry 633 (2009) 240.
195. A. M. P. Simoes, M. G. S. Ferreira, British Corrosion Journal 27 (1987) 21.
196. C.C.Shih, Flow assisted corrosion-laboratory studies and models, Ph.D. thesis, University of Manchester, 1991.

197. D.A.Eden, A.N.Rothwell, J.L.Dawson, Electrochemical Noise for Detection of Susceptibility to Stress Corrosion cracking, CORROSION / 91, (Houston, TX: NACE, 1991), paper 444.
198. D. E. Williams, Dechema Monograph 101(1986) 253.
199. Y. Tan, Sensors and Actuators B. 139(2009) 688.
200. P. R. Roberge, S. Wang, R. Roberge, Corrosion 52 (1996) 733.
201. H. Lin Ch Cao, Journal of Chinese Society Corrosion Protection 6 (1986) 141.
202. P. C. Pistorious, R. G Kelly, M. E Inman, J.L. Hudson, Analysis of Electrochemical Noise for Type 410 Stainless Steel in Chloride Solutions, in: Electrochemical Noise Measurement for Corrosion Applications, J.R. Kearns, J. R. Scully, P. R. Roberge, D. L. Reichert, J. L. Dawson (Eds.), ASTM, Philadelphia, 1996, pp.101.
203. A.M. Brennenstuhl, G. Palumbo, F. S. Gonzalez, G. P. Quirk, The Use Of Electrochemical Noise to Investigate the Corrosion Resistance of UNS Alloy N04400 Nuclear Heat Exchanger Tubes, in: Electrochemical Noise Measurement for Corrosion Applications, J.R. Kearns, J. R. Scully, P. R. Roberge, D. L. Reichert, J. L. Dawson (Eds.), ASTM, Philadelphia, 1996, pp.266.
204. A. Padilla Viveros, E. Gacia Ochao D. Alazard, Electrochimica Acta 51(2006) 3841.
205. S. Webster, L. Nathanson, A.G.Green, B.V.Johnson, The use of Electrochemical Noise to assess inhibitor film stability, UK Corrosion, 1992.

206. A.N. Rothwell, G.L. Edgemon, G.E.C. Bell, Data Processing for Current and Potential Logging Field Monitoring Systems, CORROSION / 99, ( Houston, TX : NACE, 1999) Paper 192.
207. E.E Barr, R. Goodfellow, L.M. Rosenthal, Noise Monitoring at Canada's Simonette Sour Oil Processing Facility, CORROSION / 2000 (Houston, TX: NACE, 2000) Paper 414.
208. A. Davoodi, J. Pan, C. Leygraf, S. Norgren, *Electrochimica Acta* 52 (2007) 7697.
209. L. Li, Y. Li, F. Wang, *Electrochimica Acta* 54 (2008) 768.
210. C. Cai, Z. Zhang, F. Cao , Z. Gao , J. Zhang, C. Cao, *Journal Electroanalytical Chemistry* 578 (1) (2005) 357.
211. F. H. Cao, Z. Zhang, J. X. Su, Y. Y. Shi, J. Q. Zhang, *Electrochimica Acta* 51(2006) 1359.
212. Z. Zhang, W. H. Leng, Q. Y. Cai, F. H. Cao, J. Q. Zhang, *Journal of Electroanalytical Chemistry* 578 (2005) 357.
213. G.L.Edgemon, M.J.Danielson, G.E.C.Bell, *Journal of Nuclear Materails* 245 (1997) 201.
214. Tao Zang, Yawei Shao, Guozhe Meng, Fuhui, Wang, *Electrochemical Acta* 53 (2007) 561-568.
215. J.B. Lumsden, M.Kendig, S.Jeanjaquet, CORROSION / 92, (Houston, TX: NACE, 1992) Paper 224.
216. P.Fauvet, F.balbaud, R.Robin, Q.-T.Tran, A. Mugnier, D.Espinoux, *Journal of Nuclear Materials* 375 (2008) 52.
217. M.Ozawa, *Journal of Nuclear Science and Technology* 22 (1985) 68.

218. F.Balbaud, G.Sanchez, G.Santarini, G. Picard, European Journal of Inorganic Chemistry 4 (2000) 665.
219. F. Balbaud, G. Sanchez, P. Fauvet, G. Santarini, G. Picard, Corrosion Science 42 (2000) 1685.
220. A. Nilsson, L.G.M. Pettersson, J.K.N. Orskov, Chemical bonding at surfaces and interfaces, 2008, Amsterdam, Oxford, Elsevier. xii, p.520.
221. P. Kadar, K. Varga, Z. Nemeth, N. Vajda, T. Pinter, J. Schunk , Journal of Radioanalytical and Nuclear Chemistry 284 (2010) 303.
222. A.W Ajlouni, Y.S Almasa'efah, M Abdelsalam, Journal of Environmental Science and Technology, 3(4) (2010) 182.
223. P. Kadar, K. Varga, B. Baja , Nemeth , N. Vajda , L S. Zs Kover, I Cserny , J Toth, T Pinter, J Schunk , Journal of Radioanalytical and Nuclear Chemistry 288 (2011) 943.
224. Masayuki Takeuchi, Takayuki Nagai, Seiichiro Takeda, Tsutomu Koizumi, Atushi Aoshima, Journal of Nuclear Science and Technology 37 (1) (2000) 107.
225. U.Kamachi Mudali, R.K.Dayal, Journal of Material Science 35 (2000) 1799.
226. T.A.Mozhi, W.H.S.Betrabet, V.Jagannathan, B.E.Wilde, W.A.T.Clark, Scripta Metallurgica 20 (1986) 723.
227. R.C.Newman, T.Shahrabi, Corrosion Science 27 (1987) 827.
228. C.R. Clayton, K.G. Martin, Evidence of Anodic Segregation of Nitrogen in High Nitrogen Stainless Steels of Anodic Segregation and Its Influence on Passivity, Proceedings of the Internal Conference on High Nitrogen Steels, HNS 88, London, U.K, The Institute of Metals, 1988, pp. 256.

229. R.F.A. Jargelius Pettersson, Corrosion Science 41 (1999) 639.
230. L. Wagrelus, I.Olefjord, Material Science Forum 185 (1995) 347.
231. M.Janik-Czachor, E.Lunarska, Z.Szklaraska-Smialowska, Corrosion 31 (1975) 394.
232. S. Vanini, J.P. Audouard, P. Marcus, Corrosion Science 36 (1994) 1825.
233. J.W. Park, V. Shankar Rao, H.S. Kwon, Corrosion 60 (12) (2004) 1099.
234. H. Baba, T. Kodama, Y. Katada, Corrosion Science 44 (2002) 2393.
235. Y.S. Lim, J.S. Kim, S.J. Ahn, H.S. Kwon, Y. Katada, Corrosion Science 43 (2001) 53.
236. F.Balbaud, G.Sanchez, G.Santarini, G.Picard, European Journal of Inorganic Chemistry 2 (1999) 277.
237. U.R.Evans, The corrosion and oxidation of metals, Edward Arnold, London, 1960.
238. D. G. Kolman, D. K. Ford, D. P. Butt, T. O. Nelson, Corrosion Science 39 (1997) 2067.
239. V.P. Razygraev, R.S.Balovneva, E.Yu.Panomareva, M.V.Lebedeva, Protection of Metals 26 (1990) 43.
240. O.W.J.S.Rutten, A.Van Sandwijk, G.Van Weert, Journal of Applied Electrochemistry 29 (1999) 87.
241. E.N.Mirolubov, A.P.Kazakov, M.M.Kurtepov, in: Corrosion of Metals and Alloys, N.D.Tomashov and E.N.Mirolubov (Eds.), Israel Program for Scientific Translation Jerusalem, 1966, pp.102.

242. Girija Suresh, U.Kamachi Mudali, R.K.Dayal, Baldev Raj, Materials Performance (Jan 2009) 70.
243. J S Noh, N J Laycock, W Gao, D B Wells, Corrosion Science 42 (2000) 2069.
244. M.O. Speidel, Materialwiss Werkstofftech 37 (2006) 875.
245. R.C. Newman, Y.C. Lu, R. Bandy, C.R. Clayton, Proceedings of the 9th International Congress on Metallic Corrosion, vol. 4, Toronto, Canada: National Research Council, 1984, pp. 394.
246. K. Osozawa, N. Okada, Passivity and Its Breakdown on Iron and Iron-Base Alloys (Houston, TX: NACE, 1976), pp. 135.



## **PUBLICATIONS**

### **I. Journals**

1. Girija Suresh, U.Kamachi Mudali, Baldev Raj, “Corrosion monitoring of type 304L stainless steel in nuclear near high level waste by electrochemical noise”, Journal of Applied Electrochemistry 41 (2011) 973-981.
2. Girija Suresh, U.Kamachi Mudali, Chavdar Andreev, Lili Ninova, Baldev Raj, “Corrosion behavior of high nitrogen stainless steel in nitric acid and chloride environment”, Corrosion 68 (10) (October 2012) 922-931.
3. Girija Suresh, U.Kamachi Mudali, “Electrochemical noise analysis of pitting corrosion of 304L stainless steel”, Corrosion 17 (3) (2014) 283-293.
4. Girija Suresh, U. Kamachi Mudali, “Electrochemical noise resistance evaluation of 304L SS in nitric acid and simulated nuclear high level waste”, Corrosion Engineering Science and Technology, 49 (5) (2014)
5. Girija Suresh, T.Nandakumar, C.Mallika, U.Kamachi Mudali, L.Nenova, C.Andreev, “Corrosion resistance of nitrogen containing hot rolled 304LN in nitric acid medium”, Transactions of the Indian Institute of Metals 67 (3 ) (2014) 367-374.
6. Girija Suresh, T.Nandakumar, U.Kamachi Mudali , “Electrochemical noise investigation of nitrogen containing 304L SS in nitric acid and simulated high level waste medium.” , Corrosion science engineering and technology (in press)

### **II. Conference Proceedings**

1. Girija Suresh, U.Kamachi Mudali, Baldev Raj, Electrochemical noise monitoring of 304L SS in nuclear reprocessing and waste storage medium, in proceedings of “9th

- Spring Meeting of the International Society of Electrochemistry” May 8 – May 11, 2011, Turku, Finland, pp 216.
2. Girija Suresh, T.Nandakumar, C.Mallika, U.Kamachi Mudali, L.Nenova, C.Andreev, Effect of nitrogen on the corrosion behaviour of nitrogen containing Rolled 304L SS in nitric acid and simulated high level waste , in: Proceedings of the Eleventh International Conference on High Nitrogen Steels and Interstitial Alloys, Chennai, India, September 27-29, 2012, pp. 283-292.